BONE MARROW FAT – A NOVEL QUANTIFICATION METHOD AND POTENTIAL CLINICAL APPLICATIONS

BY

ODDOM S DEMONTIERO

MBBS, FRACP

A THESIS IN SATISFACTION OF THE REQUIREMENT FOR THE DEGREE OF DOCTOR OF PHILOSOPHY (MEDICINE)

MUSCULOSKELETAL AGEING RESEARCH PROGRAM DEPARTMENT

OF MEDICINE

FACULTY OF MEDICINE, THE UNIVERSITY OF SYDNEY

APRIL, 2018

Statement of Originality

This thesis is submitted to the University of Sydney in fulfilment of the requirement for the degree of Doctor of Philosophy.

I declare that this submission is my own work and that it contains no material previously published or written by another person except where acknowledged in the text. Nor does it contain material that has been submitted, either in full or in part, for a degree at this or any other institution.

I understand that if I am awarded a higher degree for my thesis entitled "Bone Marrow Fat- A Novel Quantification Method and Potential Clinical Applications" being lodged herewith for examination, the thesis will be lodged in the University of Sydney Library and be available for immediate use. I agree that the University Librarian (or in the case of a department, the Head of the Department) may supply a copy of the thesis to an individual for research or study, or to a library.

Oddom Samban Demontiero

April 2018

Ethics Approval

This research was approved by the Human Research Ethics Committee of the University of Sydney, and the Research Ethics Committee of Nepean Blue Mountains Local Health District.

Contents

Acknowledgements

I acknowledge that my supervisor, Professor Gustavo Duque, has contributed significantly to the work presented in this thesis- including study concepts, data analysis, data interpretation and the review of resulting manuscripts. I am in debt to Gustavo for his unconditional support and guidance in pursuing this doctorate. I thank him for his encouragement as a supervisor, colleague and a friend. His dedication to support and promote clinician scientists is inspiring.

I am also thankful to Professor Richard Lindley for his guidance with this thesis in his role as co-supervisor.

A number of colleagues and collaborators were involved in the design, implementation and data collection in the studies described in this thesis. I would like to acknowledge their important contribution, as well as describe my role, in the following chapters. My principal role was to study concepts, in particular, marrow fat quantification method, data analysis, interpretation and writing manuscripts.

Chapter 3

The study described in this chapter, validation of non-invasive quantification of marrow fat in aging LOU rats, was designed by Professor Gustavo Duque. The research program's senior scientist, Wei Li, conducted all laboratory procedures involving animal specimens, including animal procurement; euthanasia; dissection; histomorphometry and micro CT imaging. Miss Emma Thembani provided research assistance support.

My role included the design of the study; performing all the image analysis; completing all statistical analysis; data interpretation; and preparing and writing the published manuscript.

Professor Gustavo Duque also provided guidance in writing this chapter.

Chapter 4

The study "The Effect of Dietary Fatty Acids on Bone Marrow Fat in a Murine Model of Senile Osteoporosis" in this chapter is a sub-study of a previously published study by Dr Yohann Wittrant (Clermont Université, Université d'Auvergne, Unité de Nutrition Humaine, BP 10448, F-63000 Clermont-Ferrand, France, INRA, UMR 1019, UNH, CRNH Auvergne, F-63009 Clermont-Ferrand, France, and Equipe Alimentation, Squelette et Métabolismes, France) and his group.

I am grateful for Dr Yohann Wittrant's collaboration. Tasks in the study design, including animal procurement and care; specimen preparation; imaging; data measurement; and collection, were carried out by his team of researchers. I thank him for access to the data-base of μCT images and associated clinical data.

My role involved examining all the μCT images manually and completing analysis of these images; completing all statistical analysis; data interpretation; preparing and writing this chapter. Professor Gustavo Duque provided feedback in writing this chapter.

Chapter 5

I am thankful to Dr Alvin C Ng (Department of Endocrinology, Singapore General Hospital, Outram Road, Singapore) and his team for their collaboration. I thank Dr Ng for allowing us access to his data-base, making the study "Anatomical Differences in Marrow Fat in a Cohort of Older Men: Correlation with Body Composition and Calciotropic Hormones" possible.

Dr Ng and his team were responsible for patient recruitment and data collection, including CT images. My role included performing all the image analyses; completing all statistical analysis and data interpretation; preparing and writing this chapter. Professor Gustavo Duque provided guidance in writing this chapter.

Chapter 6

The study "Effects of Calcium-Vitamin D3 and Exercise on Marrow Fat in Older men: an 18- Month Randomized Controlled Trial" in this chapter is a sub-study of a previously published trial by Professor Robin M. Daly (Department of Medicine, The University of Melbourne, Western Hospital, Footscray, Melbourne 3011, Australia) and his group. I am grateful for Professor Daly's collaboration. The study design, including participant recruitment and retention; conduct of the trial; and data collection were carried out by Professor Daly's research team. I thank him for access to the data- base of CT images and clinical data. In addition, his feedback for the analysis of the data has been invaluable.

My role involved examining the thousands of CT images manually and completing analysis of these images; completing all statistical analysis; data interpretation; preparing and writing this chapter. Professor Gustavo Duque provided feedback in writing this chapter.

I would also like to acknowledge the support of my family (wife and best friend Minh Xuan, and my two angels Joranai and Apsara) and extended family for their love and patience, and my work colleagues for their encouragement during the chaos of work.

Thank you all for your encouragement and support.

Publications Resulting During the Course of This Thesis

Peer reviewed papers

1. Marrow Adipose Tissue in Older Men: Association with Visceral and Subcutaneous Fat, Bone Volume, Metabolism, and Inflammation. Bani Hassan E, **Demontiero O**, Vogrin S, Ng A, Duque G. Calcif Tissue Int. 2018 Mar 26.

2. Association Between Circulating Osteogenic Progenitor Cells and Disability and Frailty in Older Persons: The Nepean Osteoporosis and Frailty Study. Gunawardene P, Bermeo S, Vidal C, Al-Saedi A, Chung P, Boersma D, Phu S, Pokorski I, Suriyaarachchi P**, Demontiero O**, Duque G. J Gerontol A Biol Sci Med Sci. 2016 Sep;71(9):1124-30.

3. Yield and cost-effectiveness of laboratory testing to identify metabolic contributors to falls and fractures in older persons. Johnson K, Suriyaarachchi P, Kakkat M, Boersma D, Gunawardene P, **Demontiero O**, Tannenbaum C, Duque G. Arch Osteoporos. 2015; 10:226. doi: 10.1007/s11657-015-0226-3. Epub 2015 Jul 21.

4. Comprehensive nutritional status in sarco-osteoporotic older fallers. Huo YR, Suriyaarachchi P, Gomez F, Curcio CL, Boersma D, Gunawardene P, **Demontiero O**, Duque G. J Nutr Health Aging. 2015 Apr; 19(4):474-80.

5. Phenotype of osteosarcopenia in older individuals with a history of falling. Huo YR, Suriyaarachchi P, Gomez F, Curcio CL, Boersma D, Muir SW, Montero-Odasso M, Gunawardene P, **Demontiero O**, Duque G. J Am Med Dir Assoc. 2015 Apr;16(4):290-5.

6. Clinical Outcomes of Impaired Muscle and Bone Interactions. **Demontiero O**., Boersma D., Suriyaarachchi P., Duque G. Clinic Rev Bone Miner Metab. 2014; 12:86–92.

7. Postoperative prevention of falls in older adults with fragility fractures. **Demontiero O**, Gunawardene P, Duque G. Clin Geriatr Med. 2014 May; 30(2):333-47.

8. Evaluation of a blended learning model in geriatric medicine: a successful learning experience for medical students. Duque G, **Demontiero O**, Whereat S, Gunawardene P, Leung O, Webster P, Sardinha L, Boersma D, Sharma A. Australas J Ageing. 2013 Jun;

32(2):103-9.

9. Effects of balance training using a virtual-reality system in older fallers. Duque G, Boersma D, Loza-Diaz G, Hassan S, Suarez H, Geisinger D, Suriyaarachchi P, Sharma A, **Demontiero O**. Clin Interv Aging. 2013; 8:257-63. doi: 10.2147/CIA.S41453. Epub 2013 Feb 28.

10. Differing approaches to falls and fracture prevention between Australia and Colombia. Gomez F, Curcio CL, Suriyaarachchi P, **Demontiero O**, Duque G. Clin Interv Aging. 2013; 8:61-7. doi: 10.2147/CIA.S40221. Epub 2013 Jan 20. Review.

11. Aging and bone loss: new insights for the clinician. **Demontiero O**, Vidal C, Duque G. Ther Adv Musculoskelet Dis. 2012 Apr; 4(2):61-76.

12. Vitamin D status in relation to postural stability in the elderly. Boersma D, **Demontiero O**, Mohtasham Amiri Z, Hassan S, Suarez H, Geisinger D, Suriyaarachchi P, Sharma A, Duque G. J Nutr Health Aging. 2012 Mar; 16(3):270-5.

13. Supplementation with vitamin D and calcium in long-term care residents. **Demontiero O**, Herrmann M, Duque G. J Am Med Dir Assoc. 2011 Mar;12(3):190-4.

14. Validation of non-invasive quantification of bone marrow fat volume with micro CT in aging rats. **Demontiero O**, Li W, Thembani E, Duque G. Exp Gerontol. 2011 Jun; 46(6):435- 40.

15. Once-yearly zoledronic acid in hip fracture prevention. **Demontiero O**, Duque G. Clin Interv Aging. 2009; 4:153-64.

16. Prevention and treatment of senile osteoporosis and hip fractures. Duque G, **Demontiero O**, Troen BR. Minerva Med. 2009 Feb; 100(1):79-94.

Presentations and Abstracts

Poster presentation at The **2010 Annual Scientific Meeting of The American Geriatrics Society** (May, Orlando Florida) "***Increasing Levels of Marrow Fat are site specific: The Fat Against Trabeculae (FAT) Study***"

Poster presentation at **American Society of Bone Mineral Research Conference** (September, Denver Colorado) ***"Validation of Non-invasive Marrow Fat Measurement by Micro CT in Aging LOU Rats"***

Awards and Scholarships

2012 American Geriatric Society Annual Scientific Meeting **- Merck New Investigator Award**

2012 **Best Poster Award** at The **2012 Annual Scientific Meeting of The American Geriatrics Society** (Seattle, WA) "***Fat infiltration of the pancreas is associated with vitamin D deficiency in older men***"

2011 Nepean Medical Research Foundation Research Grant Award

2011 Nepean Medical Research Foundation Equipment Grant Award

2010 Nepean Medical Research Foundation Isobel Corin Travel Award

2009 **Award** – Nepean Scientific Day: Best Oral Presentation by Medical Registrar

2009 **Scholarship** – Rebecca Cooper Medical Research Foundation

ABSTRACT

Ageing bone is characterised by increased marrow fat infiltration altering its composition and microstructure, thus predisposing the person to osteoporosis. Yet to date, non-invasive quantifications of marrow fat are limited to special MRI techniques, and clinical studies examining marrow fat in the ageing skeleton are scarce.

Thus, the key aims of this thesis are to:

- Validate a new non-invasive technique of marrow fat quantification using CT technology
- Determine the effects of dietary fatty acids on marrow fat
- Measure marrow fat content in different skeletal regions in healthy older men
- Determine the effect of exercise and calcium on marrow fat.

The imaging techniques employed in our animal and human studies were micro CT (μCT) and quantitative CT (QCT) respectively. All images were analysed with the imaging software Slice O Matic version 4.1 (Tomovision). Regions of interest [ROIs] were Volumes of interests (VOIs) of bone, fat and blood measured in μm^3 or mm^3. Individual tissue volumes, expressed as percentages of the total marrow volume, and ratios of tissue volumes were also used in the analysis.

Global and local thresholds for individual tissue volumes were determined separately for μCT and QCT. Thresholds for μCT were those derived from the initial validation study, whereas those for QCT were based on previous published data. To account for partial volume averaging effects, further manual refinement of threshold ranges were undertaken by inspection of individual pixels and their neighbours. This manual process was carried out for both μCT and QCT to derive local thresholds for use in manual segmentation and computation of volumes.

Our validation study showed that quantification of marrow fat using μCT was reliable and accurate compared to the gold standard technique- histology- when reliably definedthresholds were used. Good agreement between tissue volumes measured by histology and those computed by the imaging software was demonstrated. We applied this technique to quantify marrow fat in an animal model of senile osteoporosis, and showed that fatty acids (ω- 3 and ω-6) had dual effects on bone. With QCT studies, we confirmed the age related increase in marrow adiposity, and more significantly, different ratios between fat and bone in common fracture regions. Similarly, exercise affects marrow fat differently in different regions, and there was a trend to statistically significant changes to marrow fat with exercise.

In conclusion, this body of work showed that quantification of marrow fat using CT is promising, and has future clinical implications. However, significantly more clinical studies are needed to confirm these findings and refine shortfalls in quantification capabilities.

1.0 Chapter 1: Introduction and Background

1.1 Osteoporosis in the older population

Osteoporosis has been defined as a decline in bone mass and altered micro-architecture, associated with a preponderance to fragility fractures.[1] In clinical practice, it is defined as a T score of -2.5 measured by DXA as recommended by the World Health Organisation (WHO) or by the occurrence of a fragility fracture.

There are a number of risk factors that interact overtime to reduce bone mass and negatively impact bone quality. Bone quality has been operationally defined as the combination of characteristics of bone that allow it to resist fracture. These characteristics include microarchitecture, accumulated microscopic damage, the quality of collagen, the size of mineral crystals and the rate of bone turnover. Risk factors that impact these qualities and bone mass range from unmodifiable factors such as gender, age, race, family history and body built to modifiable factors including hormone levels (sex hormone levels and hormone levels from the thyroid, adrenal and parathyroid), dietary factors (low calcium intake, eating disorders, gastrointestinal surgery), medications (steroids, anticonvulsants, PPIs, immunosuppressants in setting of cancer treatments and transplant rejections), medical comorbidities (celiac disease, inflammatory bowel disease, kidney or liver disease, cancer, lupus, multiple myeloma, rheumatoid arthritis) and life style factors (sedentary lifestyle, excessive alcohol and tobacco consumption).

Among these risk factors for osteoporosis, aging is the most important.[2, 3] For Caucasian women in the United States, the prevalence is 15% at age 50-59 years and 70% at age 80 years or older.[4] In Australia, 5.9% of men and 22.8% of women aged 50 years and over have osteoporosis. The incidence of osteoporosis increases to 12.9% of men and 42.5% of women in those aged 70 years and above.[5] However, in both countries the prevalence is expected to increase significantly with the aging population. In Australia, 1.2 million people are currently

affected by osteoporosis and 6.3 million people have low bone density (osteopenia).[5] The prevalence is expected to reach 3 million people by 2021 as a result of the ageing population.[6] This high prevalence may be explained by the combination of pathophysiological changes with ageing and the silent nature of the disease where the processes evolve unchecked. Unfortunately, a diagnosis of osteoporosis typically only becomes evident after fragility fractures occur.

The rates for fragility fractures in people above the age of 60 years is up to 1 in 2 and 1 in 3 in postmenopausal women and older men respectively.[6] More importantly, a fragility fracture, especially the hip, predicts new fractures[7-10] increases mortality[10-12] and results in greater disability.[13] The increased risk in all-cause mortality is greatest with a hip fracture during the first three months. The risk is estimated to be 5-8 fold higher in older adults. In fact, in the first 6 months after hip fractures, the 20% to 30% of deaths that occur in this period may be causally linked to the hip fracture itself.[11]

Over time, the increased mortality rates persist but they are higher for men at any given age after a hip fracture.[14] More than 25% of people will die within a year of having suffered a hip fracture and less than 30% of people will regain their previous ability to ambulate.[15] Unfortunately, the prediction for the number of Australians who will suffer hip fractures remains bleak for the immediate and intermediate future. Over the next decade until 2026, it is projected to rise at a rate of 15% per five years. By 2051, when the projected population of Australians age 65 and over and 85 years and over reach 23% and 8% respectively, the hip fracture rates are predicted to quadruple.[16]

Thus, it is evident that osteoporosis remains a major burden in the older population due to significant gaps in our knowledge with respect to the evaluation of overall bone health and effective therapies. Despite significant advancement in the understanding of the pathophysiology of osteoporosis over the last two decades, the underlying biology at both the cellular and molecular level remains a work in progress. The following section summarizes

the mechanisms of age related bone loss and highlights the gaps in our knowledge.

1.2 Age related bone loss

Bone tissue is dynamic, as it has a mechanical function as a structural support for soft tissues, muscles and nervous systems, plus a homeostatic function in storing and releasing calcium and haematopoiesis. To carry out its functions throughout the lifespan, bone continually regenerates itself by removing old bone (resorption) and replacing it with new bone (formation) (Figure 1). This active process takes place in dedicated areas or pits termed *"bone metabolic units (BMUs)*".[18] Each cycle of the process within each BMU is coordinated such that bone resorption is followed by bone formation. These cycles of new bone production (undertaken by osteoblasts) and bone destruction (carried out by osteoclasts) are connected and balanced tightly to preserve net bone mass and structural integrity. However, with increasing age this tight coordination and delicate balance is lost, resulting in a deficit in net bone formation relative to bone resorption. Ultimately, the deficiency in bone mass and strength reduction results in osteoporosis and propensity to fractures.

Bone remodelling occurs throughout life. The bone formation phase is coupled firmly with the resorption phase in a relatively steady state for approximately the first thirty years of life. With some variances in bone turnover rates, women achieve maximum bone mass and size approximately by the ages of 15–20 whereas men achieve it later.[19] Beyond the third decade however, predating any deficiency in sex steroids, bone loss starts to emerge. [20]

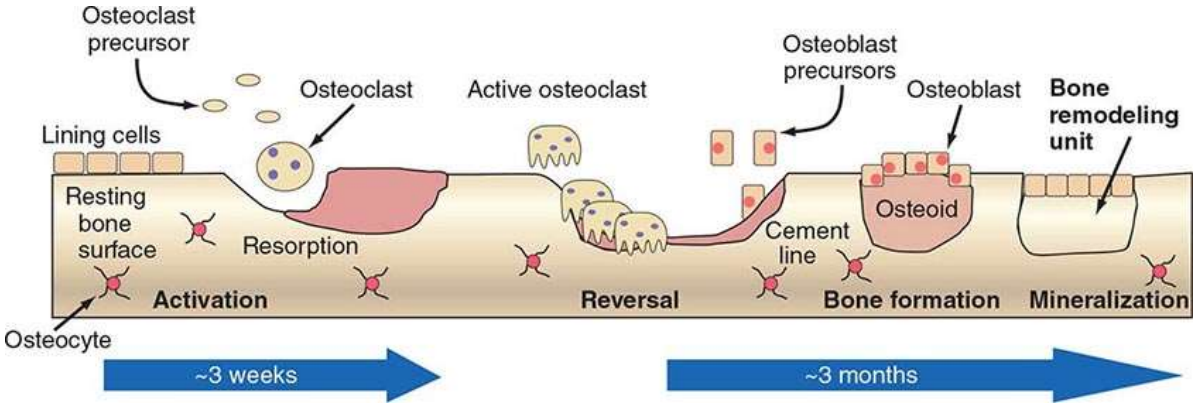

Figure 1. Bone remodeling process. In the resting state, the bone surface is covered with bone-lining cells intercalated with preosteoblasts. B-cells are present in the bone marrow and secrete OPG, which suppresses osteoclastogenesis.The cycle of bone remodeling is carried by a group of osteoclasts and osteoblasts arranged within temporary anatomical structures known as "basic multicellular units" (BMUs). ***Activation*** – remodeling initiation signal is detected. Osteoclast precursors are recruited to the site and upon activation by receptor activator of NF-κB ligand (RANKL), secreted from osteoblasts, they fuse together to form multinucleated, active osteoclasts. Meanwhile, lining cells retract and underlying membrane is removed. ***Resorption*** - the mature osteoclasts attach to the bone surface by adhering to hydroxyapatite crystals. Subsequently, a sealing mechanism is formed and a ruffled border is created. Osteoclasts then begin resorbing bone by secreting collagenases and proteinases to solubilize the bone matrix. Osteoclasts diminish when the resorption is complete. ***Reversal*** – the resorbed surface remains covered with undigested demineralized collagen matrix. Mononuclear cells of undetermined lineage, also called "reversal cells", remove these collagen remnants and prepare the bone surface for the subsequent bone formation phase. A sugar-rich cement line is produced to help with bonding old bone and new bone. *Formation* - precursors of osteoblasts appear along the cavities and undergo mitosis and proliferate to become mature osteoblasts. These osteoblasts then deposit an unmineralized bone matrix called osteoid at the cavities. As osteoblasts become embedded within the matrix, they synthesize, become inactivated and differentiate into osteocytes on the surface and regulate bone remodeling processes. ***Mineralization*** – this calcification process begins a few days after the osteoid is deposited. Over several months, the osteoid becomes mineralized with calcium and phosphorus forming the new bone. Finally, the bone surface is restored and covered by the protective lining cells, and remains quiescent till the next cycle.[17]

Once "*peak bone mass"* is reached, the bone remodelling rate slows down with predominant phases of bone resorption and over bone formation, as demonstrated by studies showing a rapid reduction in bone turnover markers.[19] Later, in the post-menopausal state, oestrogen deficiency in women markedly increases *"bone resorption"* further accelerating *"age related bone loss."*

Compared to menopausal related bone loss, the mechanisms responsible for the shift from a balanced bone turnover state to a net bone mass deficit state during ageing

remain not well understood.

Macroscopically, *"age related bone loss"* is evident at surfaces of bone due to two simultaneous yet opposing processes. At individual *"BMU"* sites, resorption occurs inside surfaces of the bone (endosteal) and formation occurs on outside surfaces of the bone (periosteal apposition). Overall, bone losses from endosteal resorption are compensated adequately by concurrent steady periosteal apposition prior to the fourth decade. In both sexes, beyond the fourth decade bone turnover rates slow down, resulting in net bone loss at individual BMU sites. From the fourth decade onwards, periosteal apposition can no longer keep up with escalating bone resorption associated with greater concentration of remodelling units at endosteal surfaces. "*Although men and women have a similar decline in endosteal bone resorption, periosteal apposition is less affected in men*."[21] Overall, ageing leads to *"cortical thinning, increased cortical porosity, thinning of the trabeculae and loss of trabecular connectivity, all of which reduce bone quality and consequently bone strength."*[22]

Other mechanisms proposed to contribute to bone loss with ageing include: secondary hyperparathyroidism; gonadal sex steroid deficiency; increasing bone marrow fat; leptin; serotonin; fat and muscle interactions; bone formation decline; cathepsin K and comorbidities

1.2.1 Secondary hyperparathyroidism

Deficiencies in either calcium or vitamin D can lead to secondary hyperparathyroidism.[23] Globally, vitamin D deficiency is prevalent in older people.[22] A low serum level of 25 Hydroxyl Vitamin D (25-(OH) D) concentration results in a low active form of vitamin D (1,25-$(OH)_2$D), and reduced calcium absorption subsequently stimulates an parathyroid hormone (PTH) secretion. The *"increased serum PTH subsequently increases osteoclastic activity and bone resorption, resulting in primarily cortical bone*

loss."[23] Further bone loss also occurs due to impaired osteoblastogenesis and reduced bone formation as a direct consequence of vitamin D deficiency.

A chronic net negative calcium balance can also occur independently of vitamin D. Low dietary intake, which commonly occurs with ageing, leads to reduced calcium absorption.[24] Subsequently, secondary hyperparathyroidism results when this deficiency is not adequately compensated through dietary intake or calcium supplements.

Other factors that are associated with aging can also cause elevated levels of PTH. Common factors include impaired renal function; the use of loop diuretics, such as furosemide and estrogen deficiency. In women, the rapid bone loss occurring in the early phase of menopause is associated with some suppression of PTH secretion. However, PTH secretion gradually rises and increases bone turnover in the later stages.[25] In men, a similar increase in PTH secretion is also seen with ageing.[26,27] However, their effects on bone resorption may be tempered by normal circulating testosterone and other gonadal sex steroids. Thus, a direct role of PTH causing bone loss in ageing men is less certain.[28]

1.2.2 Gonadal sex steroid deficiency

Approaching menopause, ovarian function ceases, leading to reduced oestrogen levels and the beginning of rapid bone loss. During this menopausal phase, "*serum 17b-estradiol levels decrease by 85–90% and serum estrone levels decrease by 65–75% from mean pre- menopausal levels."* [29] Of greater significance, there are marked reductions in the levels of free sex steroids associated with aging. In fact, it has been shown that the start of bone loss may be associated with a serum bioavailable (non-sex hormone binding globulin [non-SHBG]-bound) oestradiol threshold of below 40 pmol/L.[30] For most women, this period of rapid bone loss may continue for up to a decade after menopause.

The mechanisms by which oestrogen deficiency induce bone loss are multiple and are relatively well elucidated. In general, oestrogen deficiency is associated with the loss of control and restraint over the mediators of bone resorption.[31] Increasing "*osteoprotegerin*

(OPG)", or "*transforming growth factor β(TGF-β"* production, and thus inhibiting the formation and reducing osteoclasts activity are usually the mechanisms by which oestrogen affects the resorption process.[32,33] Oestrogen also suppresses "*osteoblastic cells"* and "*T and B lymphocytes"* production of RANKL as shown by both in-vitro and in-vivo studies.[34,35]

The Receptor activator of nuclear factor kappa-B (RANK)/ Receptor activator of nuclear factor kappa-B Ligand (RANKL) signalling system plays a critical role in bone remodelling. RANK is a transmembrane protein member of the Tumor Necrosis Factor (TNF) receptor superfamily. It is expressed on osteoclast precursors, mature osteoclasts and other cells including dendritic cells, mammary gland cells and some cancer cells, including breast and prostate. RANKL is a membrane-bound homotrimeric protein secreted by osteoblastic and activated T cells. The coupling of RANK and its ligand (RANKL), expressed by osteoblasts in the local bone micro-environment, recruits osteoclast precursors to the site of resorption and promotes osteoclastogenesis from progenitor cells and activates mature osteoclasts.

Directly by dampening "*c-jun"* activity and blocking "*RANKL/macrophage colony-stimulating factor (M-CSF)"*-induced "*activator protein-1-dependent transcription"*, oestrogen enhances apoptosis and reduces differentiation of "*osteoclast"* precursor cells.[36,37] In addition, the production of cytokines that favour "*bone resorption"*, such as *TNF-α, M-CSF, prostaglandins* and *interleukin (IL)-1 and IL-6*, may be suppressed indirectly by oestrogen.[38] Finally, the actions of mature "*osteoclasts"* may also be directly inhibited through receptor-mediated mechanisms by oestrogen.[39] Concurrently with declining oestrogen levels, low ovarian "*inhibin B"* and elevated follicle-stimulating hormones (FSH) during this menopause transition also escalate bone turnover.[40]

In men, the generally accepted assumption was that low serum testosterone primarily contributed to bone loss associated with ageing. However, similar to women, a dominant role played by oestrogen has also been shown. Better correlations between

serum oestradiol and BMD, compared with testosterone and BMD at different skeletal sites, have been demonstrated in cross- sectional and observational studies involving ageing men.[41-45] In fact, further studies investigating contrasting effects of testosterone and oestrogen confirmed that deficiency of the latter was more important in causing bone deterioration in ageing men[46,47] and that these skeletal effects of "o*estrogen"* were not dependent on FSH.[48] More significantly, a recent large prospective study of older men showed that low bio-available oestradiol levels correlated with a marked increase in fracture risk. Furthermore, after adjusting for "*oestradiol"* levels and in the presence of high "*SHBG*", low levels of testosterone correlated with an elevated fracture risk.[49] Nevertheless, testosterone does contribute to reducing men's fracture risk due to its positive influence on bone size during the growth and development phase in men.[50]

1.2.3 Bone marrow fat

A prominent feature of age-related bone loss is the accumulation of bone marrow fat at the expense of bone tissue.[51] This is evident from the 30s and 40s and it is an active process that is not dependent on oestrogen.[52] Significant increases in marrow fat have been shown consistently in both ageing bone and osteoporotic bone from animal model biopsy studies[53] and human studies.[54, 55]

More recently, studies using MRI have also shown correlation between the amount of marrow fat (measured as marrow fat fraction) and increasing age.[56,57] Furthermore, in osteoporotic men and women the relationship between marrow fat, volume tissue fraction and bone volume tissue fraction was inversed and independent of sex.[58] These observations suggest that mesenchymal stem cells (MSCs) predominantly differentiate into adipocytes, rather than osteoblasts as we age.[59] However, optimal conditions are needed for MSCs to be stimulated to differentiate into osteoblasts, including the recruitment of appropriate number of MSCs to adequate density and confluence, release of appropriate amount of growth factors, activation of lineage-specific transcription factors,[59,60,62] and a good blood

supply within the bone marrow to achieve adequate oxygen tension.[63] Ageing can alter these conditions and facilitate MSCs differentiation into adipocytes instead.[62]

Furthermore, the expressions of transcription factors specific for osteoblastic lineage and adipocyte lineages (*runt-related transcription factor 2 (Runx2)*, Dlx5 and *peroxisome proliferator-activator gamma 2 (PPAR-γ2) respectively),*are affected by ageing.[51,64] In aged MSCs, the expression of Runx2 and Dlx5 are decreased, as are osteoblast markers such as collagen and osteocalcin. Conversely, the expression of PPAR-γ2 is increased, as is a gene marker of adipocyte phenotype- fatty acid binding protein aP2.[65]

Recently, there has been some evidence suggesting that lamin A/C, a nuclear envelope protein, could have an important role in MSCs differentiation. Lamins are intermediate filament proteins that make up the major components of the nuclear lamina. There are three types of lamins, which are classified into 2 classes in adult mammalian somatic cells: "*A type (A, AΔ10 and C) and B type (B1 and B2).*"[66] Both A- and B-type lamins appear to be expressed in all cells, with the exception of T-cells and B-cells, which express only B-type lamins. The B-type lamins (lamins B1, B 2 and B3) are the initial building blocks of the lamina,[67] and at least one B-type lamin must be expressed in a cell to ensure its viability.[68] Lamin A and C are type V filament proteins located in the matrix and nuclear lamina, and they regulate the differentiation processes of stem cells.[69] Both proteins are encoded by the *LMNA* gene and are produced by alternative splicing. Lamin C is directly translated into its mature form. In contrast, lamin A undergoes post-translational modifications. Lamin A/C serves several functions- including stabilization of the nuclear membrane; regulation of gene expression; and cell cycle control. Mice carrying mutations in the lamin A/C gene or in genes encoding for lamin A/C–processing proteins had lower BMD; thinning of trabeculae and cortices, and they suffered from spontaneous fractures.[68,70] Aged mice have been shown to display lower lamin A/C expression levels in osteoblasts and decreased numbers of lamin A/C–expressing osteoblasts in bone.[71]

With increasing age, normal osteoblasts expression of "*lamin A"* is decreased with direct effects on osteoblastogenesis.[72] The degree to which lamins deficiency affect bone mass can be seen in those who suffer "*Hutchinson Gilford Progeria Syndrome (HGPS)"*. In HGPS, mutations in the "*lamin A/C"* gene[73] cause significant bone changes such as "*severe osteoporosis, osteolysis, bone deformities and spontaneous fracture*."[70] Similarly in mice, abnormalities in "*type A lamins"* cause low "*lamin A/C"* levels and low BMD,[71] and deficiency of the "*lamin A/C"* processing enzyme (Zmpste24−/−) accelerates bone loss typical of "*age related osteoporosis*." [74] The role "*lamin A/C"* has in osteoblastogenesis was further illustrated in a recent in vivo knockout "*lamin A/C"* mice study. "*MAN-1"* protein which co localizes with "*Runx2"* is expressed uninhibited in the absence of "*lamin A/C"* and this impairs the "*Runx2"* ability to promote osteogenesis.[66]

Because ageing on its own is a potent stimulator of marrow adipogenesis, age related osteoporosis can be considered a form of lipotoxic disease[22] and in fact marrow adipocytes have shown direct toxicity on osteoblasts.[75] When adipocytes are co-cultured with osteoblasts, adipocytes proliferate and release adipokines and fatty acids into the bone marrow milieu,[76] limiting osteoblasts' survival and inhibiting their activity. Illustrating this lipotoxicity effect is the use of thiazolidenediones in diabetes. Thiazolidenediones induce *PPARγ* and they are linked to increased bone loss and risk of fractures.[77] This is consistent with the suggestion that elevated levels of PPARγ within the bone marrow affect bone formation, and also stimulate bone resorption.[78] In fact, in a mice model, "PPARγ was observed to directly regulate osteoclastogenesis"[79] and PPARγ knockout mice showed significantly increased bone formation.[80] Thus, it was considered that the inhibition of PPARγ could present a potential therapeutic pathway for osteoporosis. However, results from animal studies so far have been inconclusive. In one study, blocking *PPARγ* with the antagonist *bisphenol-A-diglycidyl ether (BADGE)* decreased marrow fat but did not increase bone mass in type 1 diabetic mice.[81] Similarly,

in human MSCs subjected to antagonists of *PPARλ, bisphenol-A-diglycidyl ether (BADGE), GW9662,* and *lentivirus*- mediated knockdown of *PPARγ,* adipogenesis was inhibited with no significant effect on osteogenesis.[82] This contrasts with another study using mature male mice, whose phenotypes were shown to be appropriate models for use in studying endogenous, age-related osteopenia and senile osteoporosis.[83] In this study, nine-month-old *C57BL/6* mice treated with a *PPARγ* antagonist, *bisphenol-A-diglycidyl ether (BADGE),* alone or in combination with active Vitamin D ($1,25[OH]_2$ D_3) for 6 weeks, had significantly increased bone volume relative to total tissue volume and improved bone quality compared with controls as reflected in the increased number and thickness of trabeculae and higher mineral apposition rate in cortical and trabecular bone.[84] This anabolic response occurred with a significant increase in circulating levels of bone formation markers without changes in bone resorption markers, with higher levels of expression of vitamin D receptor within the bone marrow and in the absence of alterations in osteoclast number.

1.2.4 Systemic fat distribution

The role of body fat and its influence on bone has been intensely researched over the last two decades. Ample evidence has supported the belief that obesity conferred protection against osteoporosis after menopause.[85,86] Some studies have shown a positive correlation between increased body weight (or body mass index) and BMD, and an association between a decreased body weight and bone loss.[87-90] Other studies also showed that fat mass, the main index of obesity, was independently and positively related to BMD.[91-95] Furthermore, the changes in fat mass also showed positive correlations with changes in BMD over time.[89,96] However, observations that fat mass may not be protective to bone in contrast to the studies above have also been reported.[97 -99] Fat mass and bone mass were positively correlated when the impact of mechanical loading due to total body weight had not been factored in. However, when this was controlled, fat mass was inversely correlated with bone mass.[100]

Furthermore, when subjects were matched by BMI, significant negative associations ($p <$ 0.001) between fat mass (%) and bone mass were demonstrated in all BMI groups for both sexes. In addition, another study not only showed that fat mass was negatively related to bone mass, but that subjects with higher body fat content (%), independent of weight, had much higher risks of osteopenia, osteoporosis, and non-spine fractures.[97] A number of exercise and drug intervention studies have also demonstrated this negative association between fat and bone. In one study, bone mass increased while fat mass reduced with physical exercise [101] and bone mass decreased while central obesity increased with glucocorticoids.[10,103]

Clearly, the relationship between fat and bone is complex and given the conflicting data, several mechanisms are thought to play a role .[105] One mechanism suggests that biologically active molecules secreted from adipocytes, such as oestrogen, resistin, leptin, adiponectin, and interleukin-6 (IL-6), affect human energy homeostasis and indirectly, bone and fat. Another potential mechanism involves the effects of bone-active hormones secreted from the pancreas (including insulin, amylin, and preptin). However, the net effect of fat mass on bone ultimately depends on the fate of MSCs. Pluripotent MSCs, which have equal potential to differentiate into adipocytes or osteoblasts, are regulated by several competing pathways and the balance of these interactions determine the net effect of fat mass on bone.

Another important factor that contributes to bone loss seen with aging is the attainment of peak bone mass. The likelihood of developing osteoporosis at later stages of life is less in those who achieve higher peak bone mass, whereas the risk is greater in those with low levels of bone mass.[105] Nevertheless, a myriad number of factors, such as corticosteroids usage; chronic diseases including malabsorption, anorexia nervosa and idiopathic hypercalciuria; and behaviours, such as smoking, excess alcohol consumption and physical inactivity, also contribute to fracture risk in 40% of men and 20% of women in the older population.[106] Finally, *"although controversial still, sarcopenia, probably through reduced muscle loading*

on bone, may also contribute to age-related bone loss."[105,93]

1.2.5 The role of exercise

With ageing, mechanical loading declines with physical activity levels. Less mechanical loading diminishes the downstream stimulus upon osteoblasts to secrete OPG while increasing signals to express and secrete more RANKL, IL-1, IL-6, IL-11, and TNF-α. Consequently, these molecules directly enhance osteoclast activity and trigger an increase in osteoclast formation. Furthermore, lower levels of OPG increase availability of RANKL to bind RANK, further promoting osteoclastogenesis and bone resorption.[22] These cellular and molecular events are also consistent with observations from animal studies investigating the effects of complete immobility on bone. These animal studies showed a striking imbalance in bone remodelling characterized by a transient but rapid increase in bone resorption phase that is followed by a persistent lower rate of bone formation.[107]

Recently, lamin A/C an was shown to play a role in the anabolic response to exercise.[108] Relative to their non-exercised counterparts, when *"Lamin A/C haploinsufficient mice"* undergo strenuous exercise, there is a depletion of osteoblasts, as well as osteocytes, leading to significant thinning of cortical and trabecular bone; whereas, with wild types, exercise exposure increased bone volume and bone cellularity. Similarly, it has been shown that functional loading in humans improves bone mass[109] and *"exercise training programs can prevent or reverse almost 1% of bone loss per year in both lumbar spine (LS) and femoral neck (FN) for both premenopausal and postmenopausal women."*[110]

1.2.6 Bone loss due to decreased bone formation

Although reduced levels of sex steroids play a key role in the age-related decrease in bone formation, deficiencies in essential growth factors critical for osteoblast

differentiation/function may equally contribute. With ageing, the anterior pituitary secretes growth hormone less frequently and with decreased amplitude.[111] Growth hormone levels may decline by 1.4% annually in both men and women,[112] resulting in a reduction in hepatic synthesis of insulin-like growth factor (IGF)-1[113]and IGF-2 (its major role is as a growth promoting hormone during gestation).[114] Other than decreases in the skeletal production of IGF-1 and IGF-2 locally and systemically, growth factor binding proteins may also play a role in the pathophysiology of age- related bone loss. Higher serum levels of IGF binding protein (IGFBP)-2 not only predicted lower BMD, but increased bone resorption, as evident by elevated markers independently of sex hormones, age and body weight.[115]

Changes in essential proteins, such as sclerostin, may also contribute to impaired bone formation. Predominantly secreted by osteocytes, the glycoprotein Sclerostin (SOST) inhibits osteoblastogenesis vigorously. By binding to "*LRP5"* and "*LRP6"*, SOST prevents the co-localization of these co-receptors with "*frizzled protein"* and "*Wnt"* signalling, thus impeding osteoblastogenesis and reducing bone formation.[116] Furthermore, abnormalities of SOST at a gene level are associated with uninhibited bone formation. In the autosomal-recessive disorder, "*sclerosteosis"*, a loss-of-function of the "*SOST gene"* causes progressive and excessive bone growth.[117] Whereas, a deletion downstream from this gene causes reduced "*SOST"* expression and results in "*van Buchem disease"*, a milder form of "*sclerosteosis,"*[118] and in animal studies, the phenotype of SOST-null mice is characterized by a high bone mass.[119] Consistent with the above observations, pharmacologically inhibiting SOST produces significant anabolic effects. Animal model studies of postmenopausal osteoporosis aged ovariectomized rats treated with SOST neutralizing monoclonal antibody showed significant new bone formed in the trabecular region and at periosteal, endocortical and intracortical surfaces.[110] More importantly, this antisclerostin antibody- induced bone formation is not accompanied by increases in bone resorption.[120] SOST seem to mediate bone signals by responding to mechanical unloading.

Mechanical unloading in SOST knockout mice did not induce bone loss.[113] Promising results were also seen in humans with a recent phase I study, in which healthy men and postmenopausal women were administered a single dose of a SOST monoclonal antibody (AMG 785). Bone formation markers, such as procollagen type 1 N-propeptide (P1NP), bone-specific alkaline phosphatase (BAP) and osteocalcin, increased in a dose-related manner. Conversely, with the bone-resorption marker serum C- telopeptide (sCTx), a dose-related decrease was seen.[121]

1.2.7 Cathepsin K

The synthesis and release of cathepsin K (CTSK) from osteoclasts is the critical step during normal bone remodelling processes; in particular, the resorption phase.[122-124] Bone resorption is initiated when osteoclasts avidly bind bone surfaces to form resorption pits. The acid medium that is produced inside these pits then dissolves the bone mineral component, revealing the organic matrix. Metalloproteinases and CTSK enzymes then degrade the exposed matrix. In human osteoclasts, RANKL plays a central role in activating and driving the differentiation of osteoclasts by stimulating CTSK mRNA and protein expression.[125] Indeed, any agent that induces formation and activation or inhibits activity of osteoclasts will enhance CTSK gene expression or suppress it respectively.[126]

Osteoclasts can be stimulated by a number of agents to increase CTSK production, including transcription factors (NFAT) cytokines (TNF, IL-1), nuclear receptors (PPARΔ/β), stretching, and proteins (extracellular matrix proteins (ECM)). Likewise, CTSK expression can be inhibited by agents, such as oestrogen, interferon-γ (IFN- γ), and OPG.[122]

In a phase I study, odanacatib (ODN), a CTSK inhibitor, was well tolerated; had a long half-life; plus it showed marked and sustained suppression of bone resorption markers when administered weekly and daily with no influence on bone formation markers.[127] In a follow up phase II study, postmenopausal women [128] administered ODN achieved dose dependent gain in BMD at all sites. The highest dose produced the greatest increase. In

addition, there were dose-dependent reductions in resorption markers in the first 6 months, which then increased and resembled placebo levels. Markers of bone formation increased significantly and at 12 and 24 months remained significantly different compared to a placebo.

When this phase II was extended for another year to 3 years,[129] 50 mg of ODN treatment resulted in marked increases in BMD from baseline and from year 2 at the spine (7.9% and 2.3% respectively) and total hip (5.8% and 2.4% respectively). Urine cross-linked *N*-telopeptide of type I collagen (NTx) was suppressed up to 3 years (−50.5%), but bone-specific alkaline phosphatase (BSAP) did not change from baseline. When treatment ceased, bone loss resulted at all sites, however, BMD persisted at or above baseline. Twenty- four months after discontinuation, there was a transient increase of bone turnover markers above baseline, but it was resolved 12 months later. There were no significant differences with adverse event rates between treatment groups.

Observations were further extended to 5 years.[130] Consistent increases in spine and hip BMD were seen in women continuously treated with Odanacatib (10-50mg) for 5 years. Those treated with 50mg of Odanacatib (n=13) showed the largest percentage change from baseline in spine and hip BMD (11.9%) compared to women who were switched to a placebo after 2 years (0.4%, n=14). At 5 years, bone resorption markers (NTX/creatinine and CTX) reduced by 55% with continuous ODN treatment (10-50 mg, n = 26-29) but bone formation markers (BSAP and P1NP) remained near baseline.

A small phase III trial evaluated the effects of odanacatib at the hip and lumbar spine with QCT[131, 132] distal radius and tibia with high resolution peripheral (HRp) QCT[129] , bone turnover markers and areal BMD with DXA in 214 postmenopausal women with low bone density. After one year, there was a greater percentage change in BMD from baseline of 3.5% with odanacatib compared with a placebo.[131] After 6 months, greater increases in trabecular volumetric BMD and estimated compressive strength at the spine and hip ($P < .001$) were shown in the treated women. At 2 years, bone mineral content, thickness, volume, and cross-

sectional area also increased from baseline with odanacatib vs a placebo (P < .001) at the cortical envelope of the femoral neck. Bone-resorption marker C-telopeptide of type 1 collagen was significantly lower with odanacatib vs a placebo at 6 months and 2 years (P < .001). Bone-formation marker procollagen I N-terminal peptide initially decreased with odanacatib but did not differ from a placebo by 2 years.

At the proximal femur, QCT analyses[132] showed significant gains in total hip integral (5.4%), trabecular volumetric BMD (vBMD) (12.2%), and cortical vBMD (2.5%) at 2 years with comparable gains also in bone mineral content (BMC) for integral and trabecular compartments but smaller differential increases in cortical volume (1.0% to 1.3%) and thickness (1.4% to 1.9%).

Cortical geometry and bone strength analysis using HRp QCT[133] showed significant increases in total, trabecular, and cortical volumetric BMD with treatment compared with a placebo (3.84% and 2.63% difference for radius and tibia, respectively). Similar improvements were seen with cortical thickness, cortical area, and strength (failure load) (2.64% at radius and 2.66% at tibia). In addition, trabecular thickness improved at the distal radius; attenuation of cortical porosity at a more proximal radial site; and significantly improved trabecular number and separation at the distal tibia. Safety and tolerability were similar between treatment groups.

The usefulness of any anti-osteoporosis agents requires the demonstration of its anti-fracture efficacy and tolerability in a large phase III study. The LOFT[134] (long-term odanacatib fracture trial) study was a large international, randomized, blinded, placebo-controlled study that included 16 713 postmenopausal women aged ≥ 65 years with a BMD T-score of -2.5 or worse at the total hip, or femoral neck, or a history of vertebral fracture and a T-score at the total hip or femoral neck of -1.5 or worse. Primary analysis showed 50 mg of odanacatib once a week for 3 years reduced the relative risk of new and worsening morphometric vertebral fractures by 54%, clinical hip fractures by 47%, clinical vertebral fractures by 72% and 23%

for clinical nonvertebral fractures.[135] These risk reductions were evident across subgroups including age; race; bisphosphonate intolerance; pre-existing radiographic vertebral fracture and BMD at baseline.[136] In a small sample of women (164), a second subgroup analysis[137] showed that compared to a placebo, odanacatib treatment (n=78) led to significant increases in trabecular, cortical, and integral volumetric BMD at the spine and total hip. In addition, finite element analysis showed associated increases in whole bone-estimated strength at both sites. In the pre-plan double blind extension study, which included 8257 women for a mean follow-up period of 44 months, continual odanacatib treatment resulted in relative risk reductions of 48% for hip fractures, 67% for clinical vertebral fractures, 52% for morphometric vertebral fractures and 26% for nonvertebral fractures. Associated with these risk reductions were mean increases in BMD at the lumbar spine and hip (10.9% and 10.3% respectively).[13]

Although odanacatib seemed generally well tolerated, there were some safety concerns noted in phase II studies, and because of adverse events with other cathepsin inhibitors and significant adverse events associated with other osteoporosis agents, a number of categories of adverse events were assigned for further examination by external independent clinical adjudication committees.

One category consisting of significant dermatologic (morphea-like skin lesions and systemic sclerosis) and serious respiratory infections was included, because these had been noted from phase II studies of another cathepsin inhibitor, balicatib. A skeletal category- given major skeletal adverse events, such as delayed fracture union; osteonecrosis of the jaw; and atypical femoral shaft fractures, which have been known to occur with antiresorptives- was included In addition, the category of major adverse cardiovascular events was included due to increased incidence of atrial fibrillation associated with Zoledronic acid and observations of atheroma stabilization in a murine genetic cathepsin K-null model of dyslipidaemia.

Despite reports of similar adverse events between odanacatib- and placebo-treated groups[139-140] in the major phase III study of the LOFT research, some adverse events were adjudicated to be more common with odanacatib. Diarrhoea and extreme pain were seen more frequently with odanacatib treatment, as was morphea-like lesions (13 cases with odanacatib (0.1%) compared with 3 cases with a placebo].[135, 140] Incidence of serious respiratory infections systemic sclerosis, and delayed fracture union were similar to placebo groups. Osteonecrosis was not evident with either group although atypical femoral fractures were more common with odanacatib 10 subjects vs none in placebo (0.1% incidence).[140-141]

The most concerning result, however, was the adjudicated difference in major cardiovascular events compared with a placebo.[142] Although atrial fibrillation and atrial flutter events were more common in patients treated with odanacatib, the difference did not reach statistical significance (hazard ratio, 1.22; 95% confidence interval, 0.99 to 1.55). Similarly, incidence of major adverse cardiovascular events was greater with the odanacatib group vs the placebo group, but the difference also did not reach statistical significance. However, relative to treatment with a placebo, odanacatib treatment was associated with a statistically significantly increased risk of cerebrovascular accidents (hazard ratio, 1.37; 95% confidence interval, 1.10 to 1.71; $P < 0.01$), most of which were ischemic rather than haemorrhagic. This independent analysis further noted that the earlier trend towards an increased risk of cerebrovascular accidents appeared to be further increased during the extension phase of LOFT. Subsequently, the study sponsor withdrew odanacatib from regulatory consideration by the U.S. Food and Drug Administration (FDA).

Finally, another important and common extrinsic factor seen with ageing that reduces bone formation is the use of glucocorticoids. Glucocorticoids used in the treatment of common diseases such as COPD and RA affect bone directly and indirectly, plus they affect bone formation and to a lesser extent, resorption. On histomorphometry, the most prominent feature seen is reduced bone mass, which is seen more in cancellous bone than cortical. The

bone loss occurs in two stages- a rapid phase of bone loss due to resorption and a later phase of bone loss through reduced bone formation. In a study of healthy volunteers prescribed 5mg of prednisone, markers of bone formation serum P1NP and osteocalcin rapidly and significantly decreased. These changes reversed upon cessation of prednisone. [143] High concentrations of steroids reduced osteoblast numbers due to decreased formation of osteoblasts and increased osteoblast apoptosis. A similar picture is seen with osteocyte numbers and activity.[144] Glucocorticoids induce the differentiation of MSCs into adipocytes and osteoblasts, but fail to induce terminal osteoblast differentiation. The transcription factors for adipocytes CCAAT/enhancer-binding proteins (C/EBPs), such as C/EBPα, C/EBPβ and C/EBPδ and PPARγ2, are upregulated whereas the expression of an osteoblast transcriptor such as osterix, responsible for terminal osteoblast differentiation, is diminished.[145-147] Glucocorticoids increase the expression of cytokines, including receptor of activator of NF-kappa b ligand (RANKL), that are involved in differentiation of osteoclasts and conversely decrease those involved in inhibition of osteoclasts, resulting in a net increase in bone resorption.[148] Indirectly, glucocorticoids contribute to bone loss through decreases in calcium resorption; suppression of sex hormones and growth hormones; and changes in parathyroid hormone pulsatility.[148] The secondary hyperparathyroidism is subclinical and is considered a minor pathway for bone loss in glucocorticoid induced osteoporosis.

1.3 Bone Marrow Fat

Bone marrow fat (BMF) is composed of adipocytes and their products, which make part of the bone marrow milieu. These adipocytes contain a large lipid vacuole containing triglycerides made of a combination of saturated, mono or polyunsaturated fatty acid. The amount of BMF varies with age[58,149], sex[150,151] and disease states.[56,58,152-155]

Bone cavities are predominantly filled with red hematopoietic marrow at birth and the red marrow is then gradually converted to yellow (fat marrow) during childhood. How this

transition occurs is not fully elucidated. Earlier thoughts were that adipocytes are metabolically inert under most physiological conditions and that this transition was a default pathway where mesenchymal cells, which could not differentiate into various tissue lineages such as muscle, bone or chondrocytes, enter fat lineage.[156] However, studies emerging since have demonstrated an active role of adipocytes. Adipocytes can self-promote such that existing marrow adipocytes can induce differentiation of more MSCs into adipocytes[156-157] by secreting paracrine, and autocrine factors such as adipokines, steroids, and cytokines[158-159] that can sustain or suppress adjacent marrow cells' ability to carry out haematopoiesis and osteogenesis.[160]

The conversion of bone marrow begins distally in peripheral bones then up to the axial skeleton. Then, by the age of 25, red marrow is limited to the axial skeleton, ribs and breastbone.[161] In adults, the appendicular skeleton is the primary location for yellow bone marrow. However, quantities vary according to anatomical location (BMF is higher in long bones diaphysis than in the epiphyses); age (increases with age); and sex (BMF is higher in men than in women).[55,58,161] Moreover, quantitative variations of BMF have been observed in several diseases, especially in osteoporosis.[54,55,58]

Marrow fat's actions differs from other types of fat. Earlier animal model studies[162,163] and more recent studies of anorexia nervosa patients[164,165] showed that marrow fat did not have a role in energy metabolism during periods of severe calorie restriction. In addition, higher marrow fat content was not associated with higher body mass index or with increased cholesterol or triglycerides levels, indicating that BMF possess different characteristics that separate it from other adipose tissue and explains why it has a negligible metabolic role. In a mice model examining adipokine expression, compared with adipocytes from subcutaneous tissue, marrow adipocytes from ageing bone displayed a more *"proadipogenic, anti-osteoblastogenic and proapoptotic phenotype"*. Furthermore, marrow adipocytes derived from ageing mice demonstrated

higher toxic adipokine levels that have been linked to the stimulation of lipoapoptosis in other tissues.[166] Lipoapoptosis describes a variety of deleterious effects resulting from ectopic fat deposits. Fatty acids and other metabolites released by adipocytes in these deposits affect the survival and function of surrounding cells.[167] An example of an organ well known to be affected by lipotoxicity is the pancreas. Progressive fat infiltration of the pancreas leads to the release of fatty acids and production of ceramide,[175] in addition to activation of apoptotic pathways in β cells resulting in cell death and affecting the total population of β cells and inducing pancreatic failure.[168,169]

Another study compared fatty acid compositions of marrow fat with that of subcutaneous tissues from human subjects having varied bone densities. Concordant with the data from mice studies, fatty acid composition of marrow fat in this study differed from the composition of subcutaneous fat, and varied between marrow sites that are predominantly erythropoietic or fatty. Subcutaneous fat showed significantly higher monounsaturated fat and significantly lower saturated fatty acid concentration. This difference was reflected by a significant difference in the amount of many fatty acids between marrow and subcutaneous fat. Marrow fat obtained from the proximal femur had a higher saturated fat content than marrow obtained from the proximal tibia. More than half of the fatty acids differed between the two sites. The content of all fatty acids, except for cis-7-hexadecenoic acid [C16:1 (n-9)] and docosanoic acid [C22:0], was similar in all subjects irrespective of BMD. The marrow fat content of cis-7-hexadecenoic acid [C16:1 (n-9)] was significantly less in osteoporotic subjects compared to low bone mass subjects and normal subjects, while docosanoic acid [C22:0] was significantly lower in osteopaenic subjects compared to osteoporotic subjects.[177]

1.3.1 Bone marrow adipocytes

In the skeleton, mesenchymal stem cells (MSCs), erythrocytes, leukocytes, thrombocyte and their precursors constitute the bone marrow, which surrounds the skeletal

lattice elements called trabecular bone. A complex interplay of extracellular mediators such as growth factors, hormones, nutrients and certain physiologic and pathologic states then affect the expression and activation of lineage-specific transcription factors that determines the fate of MSCs. Differentiation of MSCs to a specific lineage in the bone marrow comprises two processes: cellular commitment to a specific lineage and the proliferation of these lineage-committed cells. A number of events involving extracellular and intracellular signalling are involved throughout both phases.

Wnt gene transcription factors CCAAT/enhancer binding protein (C/EBPα) and PPAR-*γ* are important for initiating adipocyte differentiation.[171] Wnt signalling and activation of β-catenin through the canonical pathway inhibits adipogenesis primarily by blocking the generation of critical adipogenic transcription factors C/EBPα and PPAR-*γ* and restrict preadipocytes to remain undifferentiated.[171] Conversely, PPAR-γ induction is known to suppress the β-catenin signalling during adipogenesis.[172] Deviation of MSCs down the adipogenesis pathway occurs after activation of the nuclear receptor PPAR-γ2 by fatty acids or exogenous ligands[173] and a number of other essential intermediary adipogenic transcription factors such as sterol regulatory element binding protein-1c (SREBP1c); phosphorylated cAMP response element-binding protein (pCREB); the zinc finger transcription factor KROX-20; Kruppel-like factor 5 (KLF5); CEBPβ and CEBPδ.[153]

PPARλ is part of the nuclear hormone receptor gene superfamily of ligand-activated transcription factors and is expressed as two isoforms: PPAR-λ1 and PPAR-λ2. PPAR-λ2 is the predominant isoform found in adipose tissue whilst PPAR-λ1is expressed at lower levels but is found in many other cell types and tissues as well. All PPAR-λ isoforms play an important role in adipocyte differentiation, energy balance and lipid biosynthesis. Thus PPAR-λ is commonly referred to as the master regulator of adipogenesis, because no factor has yet been identified that can induce normal

adipogenesis in its absence. In addition, PPAR-λ is the focal point of adipogenesis, which all involved key cell signalling pathways converge on and factors that stimulate adipogenesis largely produce their effect by regulating this transcription factor.[153,174]

As bone marrow ages, PPAR-λ2 expression on bone marrow cells increases.[175] The increases in PPAR-λ2 levels are accompanied by higher levels of fatty acids,[183] as well as impairment of osteogenesis, because cyclooxygenase-2 and inducible nitric oxide expressions have been down regulated.[176] In vivo, forced expression of PPAR-λ is insufficient to induce adipogenesis of satellite cells, implying that some other factors besides PPAR-λ expressions are needed to initiate adipogenesis in vivo.[177] However, the presence of a ligand does not appear to be a requisite to maintain the differentiation of mature adipocytes, but rather for commitment of cells to the adipocyte lineage. This was made evident with the observation that differentiation of non-adipogenic fibroblasts with forced expression of PPAR-λ, required PPAR-λ activation via exposure to exogenous ligand, whereas the adipogenic differentiation of preadipocytes occurred in the absence of a ligand.[64,177]Exogenous ligands for PPAR-λ include derivatives of long-chain polyunsaturated acids, as well as thiazolidenediones (TZD). Indeed, treatment with rosiglitazone has been shown to inhibit osteoblastogenesis, while simultaneously stimulating marrow adipogenesis and markedly decreasing bone mineral density (BMD), bone volume and bone microarchitecture changes.[178]

A number of other extracellular ligands that modulate adipocyte differentiation of bone marrow-derived MSCs, along with potential interactions on osteoblastogenic differentiation pathways, have been identified, such as members of the hedgehog, delta/jagged, FGF, and IGF families of proteins.[179] Among these, the role of hedgehog and its transcriptional effectors (members of the Ci/Gli family of zinc-finger proteins) has been the best described. Adipocyte differentiation of human MSCs is characterized by a decrease in hedgehog signalling, primarily as a consequence of decreased Gli expression.

Conversely, hedgehog activation was shown to interfere with adipocyte differentiation by reducing the adipogenic induction of C/EBPa and PPARγ, as well as lipid accumulation.[180] The delta and jagged family of proteins are the extracellular ligands for the notch receptors. The role of notch signalling in the adipogenic differentiation is highly complex, and remains poorly elucidated. Existing evidence provides support for both an inhibitory role and, alternatively, an absolute requirement for notch signalling in adipogenic differentiation.[181]

Several hormones and growth factors have also been identified as important extracellular regulators of adipocytes. Commitment to adipocyte differentiation involves the cooperation of C/EBPs with PPARγ2. C/EBPβ and C/EBPδ are induced in response to hormonal stimuli and, together, directly activate transcription of the PPARγ2 gene[182,183] and other genes linked to adipogenesis.[184] Activation of PPARγ2 transcription and transcriptional activation by ligand results in further activation of adipocyte marker genes. C/EBPβ and -δ are down-regulated as differentiation proceeds, and their transcription functions are thought to be replaced by C/EBPα.[185]C/EBPα cooperates with PPARγ2 to activate adipocyte gene expression, and both factors are required for adipocyte differentiation.[186] Thus, any of these transcription factors could represent targets for regulation by signalling pathways that affect adipogenesis. One signalling pathway that affects adipocyte differentiation is initiated by TGF-β. TGF-β regulates mesenchymal differentiation, inhibiting osteoblast[189], myoblast[190], and adipocyte differentiation.[189,190]

TGF-β signals through two types of transmembrane serine threonine kinase receptors- Ligand binding to the type II TGF-β receptor stabilizes complex formation with the type I TGF-β receptor and induces activation of the type I receptor (TβRI) by the type II receptor (TβRII) kinase.[192] Smads then act as signalling effectors.[192,193]C-terminal phosphorylation of Smad2 or Smad3 by TβRI results in a conformational change that promotes

heteromerization with Smad4, and stimulates nuclear translocation of Smad complexes, leading to inhibition of adipocyte differentiation by TGF-β.[190] It was then shown that TGF-β directly targeted either C/EBPβ or C/EBPδ, inhibiting them without affecting C/EBP protein levels. C/EBPβ and C/EBPδ physically interacted with Smad3 and Smad4, and Smad3 cooperated with Smad4 and TGF-β signalling to repress the transcriptional activity of C/EBPs. Ultimately, the suppression of the activity of C/EBPs by Smad3/4 at C/EBP binding sites inhibited transcription from the PPARγ2 and leptin promoters.[194] In contrast, BMP2/4 cytokines, the largest member of the TGF-β super family of growth factors, commit MSCs to adipocyte lineage and/or enhance their differentiations via Smad-dependent mechanisms, as well as p38 kinase.[195] GH affects both proliferation and differentiation of preadipocytes. Both preadipocytes and mature adipocytes possess specific GH receptors. GH may mediate its actions via these receptors, but some effects are indirectly mediated through GH secretion of insulin-like growth factor-I (IGF-I) within adipose tissue.[196]

Apart from the switching that occurs through specific signalling pathways as describe in the previous sections, the number and size of adipocytes increase, resulting in higher marrow fat volume, paralleling advancing age.[197] In humans, by the thirties, fat predominantly occupies the femoral cavity and the vertebral marrow is heavily infiltrated with fat, so much so that it can be visualized and quantified by magnetic resonance imaging scans.[198] With increasing age, the microenvironment of the bone marrow changes to favour committing MSCs to differentiate into adipocytes. Despite the mechanisms underlying this switch remaining relatively unclear, it is thought to involve both intrinsic (occurring inside MSCs) and extrinsic mechanisms.

Among numerous intrinsic factors underlying the switch of MSCs to favour adipogenesis telomerase and lamin A/C, are important determinants. Lifespan is prolonged and osteogeneic differentiation potential is maintained when telomerase is

stabilized.[199] Furthermore, evidence from long-term culture showed that telomerized clones of human stromal cells displayed physical characteristics of hematopoietic-supporting osteoblastic and myofibroblastic cells.[200] Similarly, Lamin A/C plays a critical role in osteoblast differentiation,[190,201] and where lamin A/C expression is reduced, for example, aging osteoblasts,[72] MSCs predominantly differentiate into adipocytes[74,201] and osteoblastogenesis is inhibited.[74] Indeed, it has been demonstrated in mice deficient of lamin A/C, that agents capable of inducing lamin A/C activity- for example, zoledronic acid combined with statins- can correct osteoporotic phenotypes.[202]

As for extrinsic factors, associations have been shown between reduced marrow perfusion and increased oxidative stress levels;[203] lower oestrogens levels;[149] and declining osteogenic factors.[65] A magnetic resonance imaging study in men (mean age = 73 years)[56] showed reduced vertebral marrow perfusion and higher marrow fat content in osteoporotic subjects compared to counterparts with osteopenia. In turn, osteopaenic subjects relative to those with normal BMD have reduced marrow perfusion and higher marrow fat content. *In vitro* studies have shown a direct association between hypoxia and increasing adipocyte differentiation,[204] whereas oestrogen inhibits adipogenesis.[205] Consistent with this, one study showed that oestrogen administration to postmenopausal women could mitigate rising marrow fat volume.[206] The mechanism for the abating effect of oestrogen on marrow fat possibly relates to circulating MSCs, preserving their capacity to differentiate into osteoblasts in an oestrogen rich environment. This was demonstrated in a study comparing old and young oophorectomized mice. The old mice receiving supplemental oestrogen showed much lower marrow fat levels.[149]

1.3.2 Pathophysiology in osteoporosis

The role of adipocytes (direct and indirect) in the pathogenesis of osteoporosis has been interpreted as a type of lipotoxic disease (Figure 2).[207]The indirect role lies in the fact

that the fate of MSCs, whether it differentiates into adipocyte or osteoblast, is in a competitive balance, where the fate of one cell is promoted by the same mechanisms that inhibit the stimulation of the alternative lineage. Complex signalling pathways achieve this through "cross talking," including those related to "*bone morphogenic proteins (BMPs), wingless type mouse mammary tumour virus (MMTV) integration site (Wnt) proteins, hedgehogs, delta/jagged proteins, fibroblastic growth factors (FGF), insulin, insulin-like growth factors (IGF), and transcriptional regulators of adipocyte and PPARg and Runx2*."[219] This reciprocal regulation is supported by numerous in-vitro experiments performed with bone marrow-derived MSCs, which have demonstrated that factors which induce adipogenesis inhibit osteoblast formation[209,210] and, likewise, factors which induce osteoblastogenesis hinder adipocyte formation.[211] Furthermore, the majority of conditions associated with accelerated bone loss, including ageing; glucocorticoid treatment;[212,213] increased cortisol production; osteoporosis and post- ovariectomy state;[214,215]also show increased adipogenesis in the marrow and decreased osteogenesis.[216]

As for direct effects, one example is their stimulatory effect on osteoclasts. An in vitro study showed that bone marrow adipocytes co-cultured with osteoclast precursor cells supported osteoclast differentiation.[217] This effect of adipocytes is mediated through RANKL expressions.[21] Furthermore, PPAR-λ and its ligands may also stimulate osteoclast differentiation and resorption.[79]

Adipocytes may further impact bone remodelling by releasing fatty acids (lipotoxicity) and adipokines (adipotoxicity), that could influence the development and function of stem cell precursors and mature osteoblasts and mature osteoclasts.[219]To what extent the degree of fat infiltration affects bone is still not clear; however, sufficient evidence exists to indicate that within the bone marrow microenvironment, fat and bone maintain an inverse relationship. Co- culture experiments showing adipocytes inhibiting the proliferation of human osteoblasts confirmed this inverse relationship.[75]This inhibition

was shown to be due to polyunsaturated fatty acids[220] in the marrow milieu; Runx2 expression and induced osteoblast apoptosis.[221] Subsequent analysis demonstrated two fatty acids, stearate and palmitate, to be responsible for this lipotoxicity and indeed, when adipocytes were subjected to the fatty acid synthase inhibitor, "*cerulenin"*, the detrimental effects of fatty acids on osteoblast function and survival were negated.[221]

The adipokine, *"Leptin"*, is secreted from fat cells and is well known for its regulatory role of appetite, reproduction, and energy use. With respect to bone, after traversing the blood–brain barrier, it binds to a receptor in the "*ventromedial nucleus"* of the "*hypothalamus"* and induces activation of the sympathetic nervous system, reducing osteoblast activity and stimulating bone resorption. On the contrary, peripherally, leptin signalling increases cortical bone growth and triggers MSC to differentiate down the osteoblast lineage over adipocytes.[222] Animal studies have shown that high bone mass associated with leptin deficiency is a result from decreased sympathetic tone innervating β2 adrenergic receptors in osteoblasts. However, the link between serum leptin and BMD remains uncertain, given that studies have equally reported positive and negative associations, especially after adjustments for body compositions.[223]

Given the increasing body of evidence that bone marrow adipogenesis is detrimental to bone formation, it would seem pertinent to consider the possibility of utilizing the degree of bone marrow adiposity as another correlate of bone quality. Although there is no consensus definition for "Bone quality", it has been defined operationally as *"the totality of features and characteristics that influence a bone's ability to resist fracture."*[224]As such, it encompasses abnormalities in bone size; cortical thickness; porosity; trabecular number; thickness and connectivity; bone tissue mineral content; micro damage production; progression; cessation and removal; rate of remodelling; extent of resorption and formation in each BMU; osteocyte number and distribution; and periosteal apposition.[225] Since we now know that the "pores" contain marrow fat and that marrow fat has a physiological role, it is plausible to argue that

the amount of marrow fat may reflect the level of activity of adipocytes within that bone region. Furthermore, it is plausible to imagine that the greater the amount of marrow fat within a volume of bone would proportionately affect the number, thickness and connectivity of trabecular bone. Thus, given that that the propensity to fracture results from a number of components failing, the addition of marrow fat volume, as another quantifiable component or risk factor, may improve the ability to predict fracture risk.

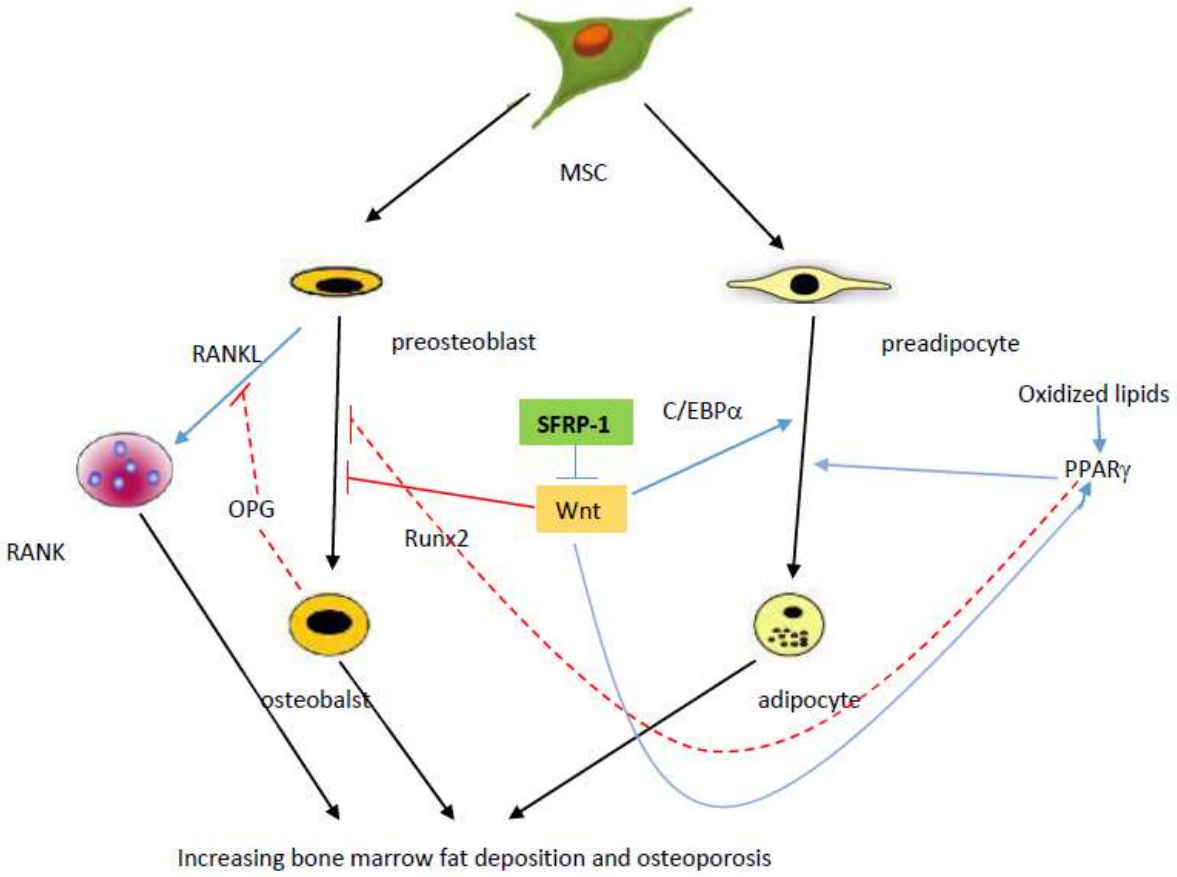

Figure 2.[207] Cross- communication within a network of extracellular stimuli, receptors and transcription factors affecting the differentiation of osteoblasts and adipocytes. The net outcome of the bone marrow milieu is determined by the result of the cross talk. sFFRP-1, secreted frizzled related protein 1, OPG, osteoprotegerin.

1.4 Quantification of Bone and Bone Marrow Fat

As illustrated above, a weight of evidence has shown that marrow fat plays an active and integral role in the pathophysiology of osteoporosis. Just like the amount of bone tissue, whether quantified as density or volume, reflects the net result of formation versus

resorption, so does the amount of marrow fat tissue. Thus, it makes physiological and clinical sense that quantification of this tissue would also reflect bone health. In fact, the rationale for the quantification of marrow fat is twofold.

Firstly, the amount of fat tissue in the marrow cavities is determined by the commitment of MSCs entry into the adipogenesis pathway. This level of commitment has, in turn, been determined by the net outcome of the interactions of several pathways that lead to differentiation of MSCs into adipocytes. Thus, the degree of marrow adiposity would indicate whether the bone state is in one of predominant formation or resorption phase. In addition, the degree of adiposity would also indicate the lipotoxic state of the bone marrow milieu.

Ultimately, the amount or degree of adiposity may be a clinical surrogate of bone health. Secondly, current therapeutics for osteoporosis mainly affect osteoblasts and osteoclasts. Considering the significant direct and indirect effects adipocytes have in the bone marrow milieu, therapeutics targeting adipocytes or precursors of adipocytes could increase the osteoporosis armament. Below is a review of the advances that have been made with marrow fat quantification thus far.

1.4.1 Invasive methods

Histomorphometry has been the primary method of evaluating the bone marrow-quantitatively (the amount of bone, haematopoietic and adipocytic tissue) and qualitatively (the cellularity).

An early pathological association between bone marrow adipogenesis and osteoporosis came from the work of Meunier,[55]who reported a marked accumulation of adipocytes in iliac crest biopsies prepared from osteoporotic patients. In this study, 84 subjects, comprising of those with clinical osteoporosis and those who were healthy, underwent iliac crest biopsies. Decalcified sections were stained in haematoxylin-eosin-

safranin and undecalcified sections in osteochrome of Villa-neuva of Frost. All were analysed quantitatively using integrating Zeiss I eyepieces. Trabecular bone and marrow adipose tissue volumes were calculated. In the healthy group, trabecular bone volume ranged from 26% to 16% between the age of 20 and 65. In contrast, in the osteoporotic group, the trabecular bone volume was consistently below 16% irrespective of age. In the same age range, marrow adipose tissue volume increased from 15% to about 60% of the marrow cavity in the healthy group compared to an adipose tissue volume of greater than 35% in all osteoporotic individuals. More importantly, for the first time, a significant inverse relationship between trabecular bone volume and adipose tissue volume was demonstrated.

This inverse relationship between bone and fat subsequently drove the "clonal switch' hypothesis. Indeed, a number of in vitro studies using various animal models demonstrated an inverse relationship between osteoblastic and adipocytic differentiation of bone marrow stromal cell cultures.[216, 217,226,227] One of the first in vivo studies to investigate this clonal switch and address a further question resulting from Meunier's study was conducted by Hirano et al.[228] They made histomorphometric measurements of the ratio of haemopoietic tissue to adipose tissue in osteoporotic women. A gradual decrease in hematopoietic tissue of the bone marrow was proportionate to the decrease in cancellous bone, regardless of age. On the other hand, the ratio of eroded perimeter/bone perimeter remained almost steady until hematopoietic tissue decreased significantly. The findings of this study suggested that decrease in hematopoietic tissue causes an imbalance in bone formation and resorption, and leads to bone loss.

However, a number of other in vivo studies subsequently confirmed increased bone marrow adiposity in osteoporotic postmenopausal women, and an inverse relationship between bone formation and marrow adiposity.[54,58, 149,213,229,230]

Justesen et al[58] compared healthy individuals of different ages (age 30 -100) with those who have osteoporosis (age 52 -92). Fat and bone tissues were obtained through biopsies of the

iliac crests. Individual tissue volume of interest, namely adipose (AV), haemopoietic (HV) and trabecular (TV), were quantified as a percentage fraction of the total tissue volume (calculated as BV + AV + HV) using the point-counting method. This was in contrast to findings from previous studies, which found an increase in AV in osteoporotic patients only; thus, there was an age-related increase in AV and HV but a decline in BV was demonstrated. As well, there was an age-related inverse correlation between BV and AV that was independent of BMI. Osteoporotic patients, relative to their age-matched healthy counterparts, demonstrated increased AV, decreased BV and no significant difference in HV. Verma et al[54] examined the ratio of adipose tissue to haemopoietic/stromal tissue in a sample of osteoporotic patients to investigate the differentiation of stromal cells from an osteoblastic to an adipocytic lineage. Bicortical iliac crest biopsies from 127 patients with established osteoporosis (47 male, 80 female) were examined. Patients ranged in age 5 to 80 with a mean age of 55. Primary osteoporosis accounted for sixty -seven patients; the remaining 60 cases were secondary osteoporosis, including 36 postmenopausal; 10 steroid induced cases; 12 involving other endocrine dysfunction and two post gastrectomy cases. The control group consisted of 14 patients (nine female, five male), with an age range of 21 to 70 years (mean age 48). The ratio of adipocytic to haemopoietic/stromal tissue (A/H) was higher in OP bone than in the normal controls (OP mean 43.06% v normal mean 22.4%; $p < 0.001$). Age and several measures of bone formation (primarily cancellous apposition rate and osteoid volume) largely accounted for the variability in the A/H ratio.

More recent studies performed on iliac crest bone biopsies also demonstrate that marrow adipose tissue volume increases with age. Burkhardt et al[229] carried out a retrospective study, comparing fat and bone volume of normal persons of different age groups with age- and sex-matched groups of patients with primary osteoporosis and aplastic anaemia. Bone biopsies and post mortem samples were analysed by histology in both populations. Higher adipose tissue volume was demonstrated only in younger patients with

osteoporosis aged 27–52 years. However, the inverse relationship between percentage bone volume and fat volume in osteoporotic individuals was evident, and was similarly demonstrated with ageing. This age-related increase in fat tissue fraction was shown to be related to an increase in both the size of individual adipocytes and their number in another study.[149]

Since increasing age in women parallel decreasing levels of oestrogen, Syed et al[213] examined the possibility that the observed increase in marrow adiposity associated with ageing would be in part due to oestrogen deficiency. They examined trans iliac bone biopsies of 56 postmenopausal osteoporotic women (mean age, 64 years) from an earlier randomized, placebo-controlled trial involving treatment either with a placebo (n = 27) or transdermal oestradiol (0.1 mg/d, n = 29) for 1 year. Adipocyte volumes/tissue volumes (AV/TV), and adipocyte numbers increased by about 20% in the placebo group. In contrast, the adipocyte numbers did not change, and the AV/TV decreased by 24% in the oestrogen group. Treatment with oestrogen also prevented increases in mean adipocyte size over 1 year.
However, a more recent study examining the marrow fat bone relationship did not find an inverse relationship, as prior studies have found. Cohen et al[230] compared marrow adiposity and bone formation; volume and microstructure measures quantified from tetracycline-labelled trans iliac biopsy specimens in 64 premenopausal women with idiopathic osteoporosis (IOP) or idiopathic low bone mineral density (ILBMD), and 40 controls. Those with IOP and ILBMD had significantly higher adipocyte number, size, and volume than controls; independent of age, body mass index, and bone volume. However, an inverse relationship between adiposity and bone parameters was not observed. Interestingly, controls did show expected direct associations between marrow adiposity and age, and inverse relationships between marrow adiposity and bone formation; volume; and microstructure measures.

1.4.2 Non-invasive methods

Over the last two decades, great advances have been made into the understanding of the ways in which bone responds to phenomena, such as aging, weightlessness, and treatment from a physiological and micro architectural perspective. Much of this has been achieved by a number of imaging techniques. Macro and micro-architectural parameters, such as bone size and geometry; fine cortical and trabecular structural detail; and marrow content have been assessed with techniques such as radiography; Dual-energy X-ray Absorptiometry (DEXA); Quantitative ultrasound (QUS); high resolution peripheral quantitative computed tomography (HR-pQCT); Quantitative Computed Tomography (QCT); micro CT (μCT) and Magnetic Resonance Imaging (MRI).

1.4.2.1 Computed Tomography (CT) and Quantitative Computed Tomography (QCT)

CT's ability to delineate one tissue from another is based on the differential absorption of ionizing radiation by different tissues within an organ. The projections through objects generate the linear attenuation profile. The linear attenuation profile from each X-ray projection passing through the object is unique and combined to form a 3D reconstruction. For bone quantification, standard QCT is generally performed at the lumbar spine using routine clinical CT scanners with a mineral reference phantom scanned in the same field for calibration. The calibration phantom contains known different concentrations of hydroxyapatite equivalent material. The resultant attenuation of the lumbar vertebrae measured in Hounsfield Units (HU) is then transformed into bone mineral equivalents (mg/cm^3) using standardized software.[231] QCT can provide separate measurements of BMD for each voxel of the scanned volume of interest (VOI) in the cortical and trabecular compartments. The bone mineral content (BMC) can then be derived from the product of BMD and volume. Analogous to T-scores derived from DEXA BMD, QCT T-scores can be calculated based on appropriate normal reference data, but their relevance to clinical

care is limited by the considerable discordance from DXAT-scores.[232-234]

Quantitative Computed Tomography (QCT) has been utilized extensively to characterize and quantify bone structure. Main uses have been to characterize the trabecular bone structure of vertebrae two-dimensionally and at a three-dimensional level; enable quantification of bone tissue content as mass (BMC); or density (volumetric BMD, vBMD) of a sub region of bone or the whole anatomical area. More recent applications include finite element modelling (FEM) - an engineering technique enabling estimation of bone strength based on bone geometry; vBMD values and clinically relevant loading conditions;[235] and the accurate quantification of cortical bone thickness.[236]

Despite its widespread use, particularly in research settings, QCT cannot provide high-spatial resolution images to quantify individual trabeculae, due to the high exposure time and thus, high radiation dose that would be needed to achieve the required spatial resolution. The trabecular structure is compromised by the effects of partial-voluming, so the actual CT images represent a projection or pattern instead of a true image of the trabecular structure. For instance, a high-resolution CT with in- plane spatial resolution of 400 × 400 μm is only able to characterise a structure as rough or smooth in texture; homogeneous or heterogeneous in content; or high rather than low orientation with respect to trabecular distribution. Partial volume also affects newer higher resolution CTs, such as spiral CT and Multidetector row CT (MDCT). However, these scanners, particularly MDCT, have significantly improved the capacity to assess the structure of trabecular bone.

Relevant to this thesis, standard clinical computed tomography (CT) has been used to measure BMD and was found to be useful. Data from both in vitro experiments and in vivo studies showed strong correlation between BMD measured on routine clinical CT and BMD derived from standard QCT.[237] A reference phantom was used in this study to standardize measurements and to calibrate mineral reference. In contrast, a phantom in daily clinical

practice is typically absent. More interestingly, a study of menopausal women having coronary CT showed strong correlations between BMD measurements of the thoracic spine, regardless of whether a reference phantom was used or not.[238]

Similarly, in a study of adults age 50 years and older, simple attenuation measurements without a reference phantom and obtained directly from images on CT colonography compared to DEXA derived BMD measurements were effective in screening for osteoporosis.[239] A board-certified radiologist performed formal QCT on a dedicated phantomless QCT software package (BMAP, Philips Healthcare). The procedure entails placing oval regions of interests (ROIs) on the vertebral body, paraspinal musculature and subcutaneous fat at each level from T12 through L5. A sagittal reconstruction is used to angle the transverse plane of section to make it parallel with the end plate at each level. The vertebral body ROI is placed in the anterior trabecular region, avoiding the basi-vertebral venous plexus posteriorly, the surrounding cortical bone and any focal lytic or sclerotic lesion. A BMD measurement (in gm/cc) is derived by the software program, which was used as the main QCT outcome measure for comparison against the DEXA T-score. The radiologist was unaware of the DEXA results at the time of QCT interpretation. With the simple attenuation measurements, vertebral body attenuation at individual levels was obtained using a trabecular ROI technique similar to QCT, but without the initial step of plane angulation. A single ROI measurement of mean attenuation (in HU) at an individual spinal level was carried out on a standard PACS workstation (McKesson), as would be used for routine CT interpretation, with images viewed in a bone window setting (W:1200, L:350). Individual ROI measurements were performed from T12 through L5. The interpreting radiologist was again blinded to DXA results. The diagnostic ability of phantomless QCT and simple ROI approaches, with respect to the DXA T-score reference standard, was assessed using ROC curve analysis, as well as threshold analysis to determine relevant cut-off values for osteoporosis detection. The results showed that simple mean attenuation measurements of

trabecular ROIs of the lumbar spine, without formal derivation of BMD values, yielded results that were similar to phantomless QCT. At L1, a trabecular ROI attenuation cut-off of 160 HU was 100% sensitive for osteoporosis, with a specificity of 46.4%. Below this threshold, 84% had low BMD and 58% above this threshold had normal BMD at DEXA. ROI performance was similar at all individual T12-L5 levels. At ROC analysis, AUC for osteoporosis was 0.888 for phantomless QCT, compared with 0.825–0.853 using trabecular ROIs at single lumbar levels at multivariate analysis. However, marrow fat was not determined.

More recently, another group employed similar attenuation measurements of thoracic vertebrae on routine clinical chest CTs to assess skeletal health of COPD patients. They measured the average attenuation of thoracic vertebrae 4, 7, and 10 on routine chest CTs of COPD patients and correlated these measurements with the lowest BMD of the hip and lumbar spine (L1 to L4) on DEXA.[240] The average attenuation for bone in COPD patients with osteoporosis (on DXA) was 152.3 ± 56.5 HU. This mean bone attenuation was about 50% lower compared to the mean bone attenuation in COPD patients with normal BMD ($p<0.001$). The correlation between CT-measured bone attenuation and the lowest BMD assessed on DXA was high ($r = 0.827$, $p<0.001$). The correlation between bone attenuation and BMD of the hip and lumbar spine were 0.775 ($p<0.001$) and 0.767 ($p<0.001$) respectively. At the highest sensitivity (93%) and specificity (97%) for detection of osteoporosis, the mean bone attenuation threshold was 147 HU.

Other studies that have used simple attenuation measurements from clinical CTs employing the same techniques have also found similar high correlations between mean bone attenuation; age and presence of fractures;[241] and osteoporosis with acceptable specificity and sensitivity.[242]

Although high degrees of interrater reliability have been demonstrated in the above studies, suggesting that it could be a reliable method for that particular machine and

institution, the technique is limited in its generalizability and diagnostic utility for a number of reasons. Many of the studies that have been done are retrospective in nature and thus are limited by referral and spectrum biases. Hence, the applicability of the results to the general population is limited. The associations and correlations between bone attenuation and BMD have been derived differently- for example, using the attenuation of the individual vertebra, rather than the average attenuation of the thoracic vertebrae; and correlated BMD of the lumbar spine, rather than the lowest BMD of the lumbar spine and hip.

Also, the use of simple attenuation as a screening and diagnostic tool is limited by the fact that there is a lack of CT-attenuation data for the hip, a region associated with high incidence of fractures. Indeed, data for the use of CT attenuation in the prediction of fracture risk has been based largely on the values derived from attenuation at the level of L1. Furthermore, there has not been cross validation of different scanners across different settings to confirm whether current cut-offs apply to other CT scanner configurations and acquisition techniques. In contrast to its utilization in quantifying the bone compartment of the marrow, the use of QCT and other CTs to quantify marrow fat is limited.[243-249]

Earlier studies have measured the amount of bone marrow fat in patients with Gauchers disease, [243-245] anorexia and Cushing's disease,[246] using a combination of single energy and dual energy QCT. The methods employed to quantify marrow fat in these studies, however, involved complicated post processing techniques.[243]

More recently, Di Iorgi et al[247] examined the relationship between marrow fat and bone mass at the time of peak bone mass using clinical CTs. The first three lumbar vertebrae and mid shafts of femurs of 255 healthy teenagers and young adults (126 females, 129 males, 15–24.9 yrs. of age) were scanned using a General Electric Hilite Advantage scanner (General Electric Healthcare, Milwaukee, WI) and a standardized mineral reference phantom for simultaneous calibration (CT bone densitometry package; General Electric). They showed that for both men and women, the inverse association between cancellous bone in the

vertebrae and femoral cortical bone in the femur with bone marrow fat was independent of anthropometric measurements, bone dimensions and total body fat. The technique of marrow fat quantification employed by these researchers resembles the technique that we use for this body of work that comprises the thesis. In their study, simple CT attenuations of ROIs in HU (average attenuation of first three lumbar vertebrae and mid shaft of femur) were obtained, then converted to established density values for analyses.

1.4.2.2 Peripheral QCT (pQCT) and High Resolution Peripheral QCT (hr-pQCT)

Given the difficulties of assessing the structure of trabecular bone in vivo, peripheral CT scanners (pQCT) were specially developed to characterize extremities of the skeleton where trabecular thickness (Tb.Th) ranges from 60 to 150 μm and trabecular separation (Tb.Sp) from 300 to 1000μm, such as the tibia and distal forearm.[248] Once the bone volume fraction derived by pQCT has been calibrated with that from μCT, a range of segmentation thresholds can be determined. Despite lower resolution, in vitro structure measurements with pQCT can correlate highly with measurements by μCT.[249] More recently, higher resolution hr-pQCT, which produces 3D images with an isotropic voxel size of 62 μm or 82 μm and provides isotropic spatial resolution of about 130–150 μm, has been used to evaluate peripheral skeletons, in particular the distal forearm and tibia.[250] A number of microarchitecture parameters within trabecular bones can be determined including BV/TV, Tb.Th, Tb.Sp, and trabecular number (Tb.N) in addition to BMD, and in cortical bones, parameters such as BMD, thickness and porosity can also be calculated.[251] pQCT and hr-pQCT have been used extensively in clinical studies for microstructure assessment,[252,253] fracture discrimination[254-257] and prediction of bone strength.[258] To date, two studies have quantified marrow fat, and both have used different approaches. Rantalainen et[236] al employed a threshold-based edge

detection method from the BoneJ software to measure bone marrow density (MaD) as an estimate of marrow adiposity in a small sample of young female athletes, and found acceptable precision error. In this study, marrow density (milligrams per cubic centimetre) at the mid tibia was analysed and used as an estimate of bone marrow adiposity. A custom made Java software was used for the segmentation procedure. Using established CT number (in HU) and physical density of various human tissues, a threshold density of 80 mg/cm3, corresponding to 1.05 times the physical density of red marrow, was used to separate marrow fat from bone. A recalibration of the equivalent coefficient of water for the device used in the study was determined first, then the marrow density was computed according to previously published equations relating these coefficients and Hounsfield measurements.[259] The range of marrow density considered to be marrow fat, (0.928 g/cm3 (91.9% fat) to 1.08 g/cm3 (3.3% fat), were taken from previously calculated densities based on chemical composition derived from human tissue samples.[260]

More recently, Gibbs et al[237] compared the test-retest precision error for pQCT derived marrow density and marrow area segmentation at the tibia in younger and older adults, and in individuals with spinal cord injury using 3 software packages (Stratec, BoneJ, and SliceOmatic). Test-retest precision errors for marrow density (mg/cm^3) and marrow area (mm^2) were calculated for the watershed-guided manual segmentation technique for SliceOmatic version 4.3 and 2 threshold-based edge detection technique for Stratec version 6.0 and BoneJ version 1.3.14. Precision error for pQCT-derived marrow density segmentation exceeded 5% for all methods of analysis across a range of bone mineral densities and fat infiltration, whereas precision error for marrow area segmentation ranged from 2% to 5%. The researchers concluded that in the current format, all three software packages are limited in their utility for clinical and research applications.

1.4.2.3 Microquantitative Computed Tomography (μ-CT)

μ-CT is a CT technique that uses X ray tube as the radiation source, or more recently,

tight collimation synchrotron as the radiation source to allow either faster scanning or higher spatial resolution in imaging bone specimens. Standard μ-CT enables in vitro assessment of bone microstructure at an ultra-high spatial resolution of 1–100μm non-invasively and non-destructively. The system employs a cone-beam X-Ray geometry and reconstruction algorithm. A spatial resolution as high as ≈60 μm is typically achievable and can clearly visualize individual trabecula. These cross sections can then be reconstructed to form a 3D model of trabecular network for intensive analysis.[261] It has largely replaced the traditional labour intensive histomorphometry technique that was used to analyse fine bone sections of small animals, typically mice and rats.[262-265] Human clinical studies have also extensively used this technique to investigate effects of osteoporosis drug therapy on the microarchitecture of trabecular bone obtained from biopsies of human iliac crest.[266-270] Overall, μ-CT enables highly accurate and precise assessment of three-dimensional structural components of cortical as well as trabecular bone, permitting 3D modelling for finite-element analysis as used in virtual biomechanics to enable the prediction of mechanical properties.[271] However, marrow fat quantification is yet to be explored.

1.4.2.4 Magnetic Resonance Imaging (MRI)

MRI is an imaging technique that does not involve ionizing radiation, but electromagnetic wave frequency (radiofrequency range), which is found all around us. The images result from the interaction between an atom, an external magnetic field and radio waves. Atoms, the smallest constituents of living tissues in the body, are made up of protons, electrons and neutrons. Atoms with an odd number of protons and/or an odd number of neutrons spin on their own axes, behaving like bar magnets and under normal circumstances, their axes randomly align.[272]

Hydrogen is the most abundant element in existence, particularly in water and fat, and thus for MR imaging the hydrogen nucleus (a single proton) is used. As the body

enters the MRI scanner and its magnetic field, all axes of the protons line up along the axis of the MRI scanner, producing magnetic vectors. These magnetic vectors are deflected when radio wave (additional energy) is then added to the magnetic field. The energy (radio wave frequency (RF)) that causes the hydrogen nuclei to create magnetic vectors is proportional to the element and the magnetic field's strength. The magnetic field strength is altered in small increments using multiple gradient electric coils and multiple different transmitted radiofrequency pulses applied in sequence. Once the radiofrequency source is switched off, the magnetic vector returns to its resting state (Longitudinal or T1 relaxation) then afterwards, the axial spin returns to its resting state (Transverse or T2 relaxation). These relaxation times cause signals (forms of radio waves also) to be emitted. The intensity of these signals are then collected in k-space and Fourrier transformed into the spatial domain from frequency. Axial images are finally reconstructed to create MR images. Among all the non-invasive imaging modalities, MRI has been extensively applied to the study of bone quality in particular marrow fat content, marrow diffusion and marrow perfusion. MRI methods that have been mainly used to quantify bone marrow fat fraction have been T1-weighted imaging (T1WI), magnetic resonance spectroscopy (MRS), and chemical shift encoding-based water–fat imaging (Dixon method). Among these techniques, marrow adipose tissue (MAT) has been quantified reliably using single-voxel proton magnetic resonance spectroscopy (MRS).[273-275] The physics and mechanics of MR spectroscopy (MRS) are the same as standard MRI, however, it does not generate images- instead, it quantifies the relative amount of fat within tissues by measuring the fat to water ratio (Figure 1).

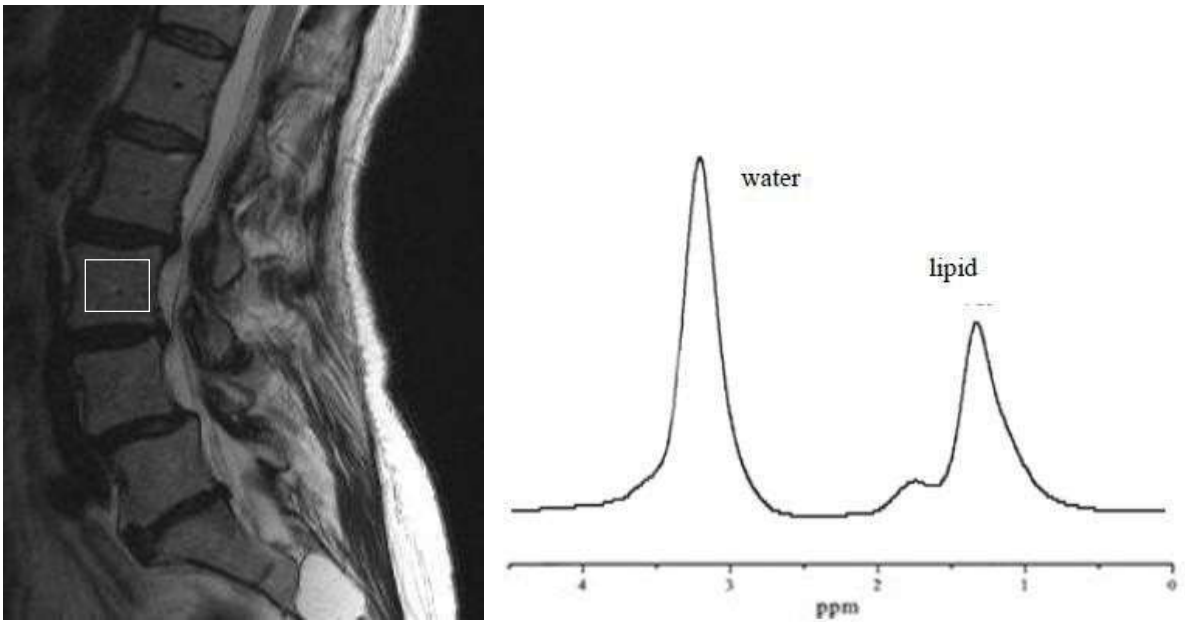

Figure 1. MRS of L3 vertebral body. MRS assesses the fat peak: water peak ratio. Relatively higher water peak compared to fat peak is consistent with red marrow.

Two main MRS pulse sequence acquisition methods have been used, either point-resolved spectroscopy (PRESS) or stimulated echo acquisition mode (STEAM). The STEAM mode has two advantages over PRESS mode- firstly, it has reduced sensitivity to J-coupling effects of the fat peaks and thus, reduced errors when performing an echo time (TE) series to correct for T2 decay effects in proton density fat fraction quantification. Secondly, the bone marrow water peak has short T2. STEAM allows shorter minimum echo times compared to PRESS, and despite its 50% signal loss compared to PRESS, can reduce the T2-weighted signal loss for the short T2 water peak. Although quantification of marrow fat by MRI is considered the gold standard non-invasive technique, MRS has some limitations. The marrow water content is not constant but is assumed to be so in MRS; volumes of interest (VOI) may only be studied one at a time; and density (g/cm3) is not calculated but rather the amount of fat expressed as % fat content (semi-quantitative measurement) is obtained. Alternative MRI techniques have recently been proposed, which allow multiple skeletal regions to be studied concurrently. These techniques use alternative pulse sequencing to generate images of either fat measurements only or water measurements only pixel by pixel. However, proton MRS has

been the primary technique used in clinical investigations to determine the status of marrow fat with age, [150,276,279,281] sex[276,279] and disease states.[277,278,280].

Another MR method is chemical shift encoding-based water–fat imaging. This technique overcomes the spatial resolution requirements of single voxel MRS and enables the spatially resolved assessment of bone marrow fat fraction, especially in regions with heterogeneous red marrow distribution (e.g., proximal femur, spine). The technical aspects of this technique have been reviewed in detail previously.[282]

Finally, T1-weighted imaging is the least technically demanding, and has been mostly used for the pelvis, hip and spine. The technique calculates bone marrow fat volume by applying a set threshold at the same gray-scale level as subcutaneous adipose. Thresholds are then applied on T1WI to extract bone marrow fat voxels.[283] The main error source for the quantification of bone marrow fat volume based on T1WI results from partial volume effects and threshold selection, especially in regions with red marrow.[284]

Recently, the measurements of bone marrow fat among T1-weighted MRI, modified Dixon method and MRS were compared.[284] Good correlations were demonstrated among the three MR methods for bone marrow fat quantification. There was a correlation among the three MR methods measuring bone marrow fat fraction and bone marrow adipose tissue, with (BMAT) ranging from 0.78 to 0.88 in the L3 vertebra. There was also a correlation between BMAT measured by T1-weighted MRI and bone marrow fat fraction measured by modified Dixon- the result was 0.86 in femoral necks.

Despite MRI methods being the gold standard, their use in clinical practice is limited by availability, technical demand and cost.

1.4.2.5 Dual X-ray Absorptiometry (DXA)

Dual Energy X-ray Absorptiometry (DXA) is an imaging technique that employs

low levels of radiation and is widely available. However, because the X-Ray attenuations of bone are projected in 2-dimensions (2D) and DXA calculates density by dividing this by the scanned areas, areal bone mineral density is quantified rather than true density. Other limitations are its use in children, men and different ethnic groups. Even in the setting of post-menopausal females, over and under-estimations of BMD may occur in taller and shorter individuals respectively.

Nevertheless, calculated T scores that are derived from areal BMD remain the universally accepted bone density indices used for screening and defining *"the diagnosis"* of osteoporosis by The World Health Organisation (WHO). It is also used in serial monitoring of the response to therapy. However, DXA has limitations in its ability to measure the mass distribution in cortical bone and trabecular bone region, and in the analysis of bone geometry and microstructure.[285]

1.4.2.6 Quantitative ultrasound (QUS)

QUS has been used for measuring BMD at peripheral sites such as the heel, tibia and phalanges. It is not suitable for central sites such as the spine or hip because of poor tissue penetration. QUS uses sound waves to measure broadband ultrasound attenuation (BUA) and speed of sound (SOS). Ultrasound waves are attenuated by bone as they travel from the transmitting transducer to the receiving transducer. Normal bones or bones of higher density attenuate greater sound waves, allowing sound to travel from one transducer to the other at a higher speed than osteoporotic bone.

Presently, QUS is considered a much inferior imaging modality compared to DXA and QCT for measuring BMD. It is not the approved modality to diagnose or to monitor responses to osteoporosis treatment. It is used to screen at-risk individuals, particularly older Caucasian women, with confirmation by DXA. It has not been utilised in the quantification of marrow fat.

1.5 Summary of marrow fat and the aging skeleton

One of the aims of this thesis is to validate a new technique of quantifying bone marrow fat noninvasively and utilising an imaging technique that is readily available; easily accessible; inexpensive and well tolerated in the older population- CT.

The following chapters of this thesis will present the methodology and results of studies:

1.4.2.1 Validating our new technique using μ-CT and an imaging software.

1.4.2.2 Exploring further the distribution of marrow fat in different areas of the ageing skeleton.

1.4.2.3 Assessing the effects of dietary lipids on marrow fat distribution in animal model of senile osteoporosis.

1.4.2.4 Exploring the effects of exercise and its interaction with calcium on bone and marrow fat in older men.

2.0 Chapter 2 -Methodology

Details of subjects, image acquisition, image analysis and statistical analyses specific for each study are described under relevant sections within individual studies. Here the method of fat and bone parameters quantification are described for each imaging method used in the studies.

2.1 Computed Tomography (Chapters 5 and 6)

2.1.1 CT Acquisition Protocol

Subjects were placed in a supine position with their arms extended above their head for the duration of the measurement. Axial images of the abdomen at the level of the T4– proximal femur were performed with no angulation, using a lateral pilot for location. Single- slice CT images were acquired at all these levels. Axial images of the mid femur and mid tibia were obtained at the level of the mid-thigh and mid lower leg respectively. All scans were performed using dual energy CT scanners and saved as DICOM images for analysis. Standard CT procedures of 120 kV with 5 mm thickness and a 512 x 512 matrix were used for all subjects.

2.1.2 CT Image Analysis Protocol

The physical density of a material as an X-Ray beam of a CT scan passes through it is expressed as a CT number. CT numbers describe the linear attenuations of x-ray beams, measured as they pass through a medium occupying that space (a volume element, or voxel), and is the sum of the attenuation of all the different materials contained in that voxel. The numbers are called Hounsfield units (HU), and the densities of water and air have been established as reference density points (linear attenuation coefficient of 0 and -1000 respectively, i.e. HU = 0 and -1000 respectively).) Using these reference densities,

Hounsfield units describing fat lie in a range of negative values (Figure 2).[286]

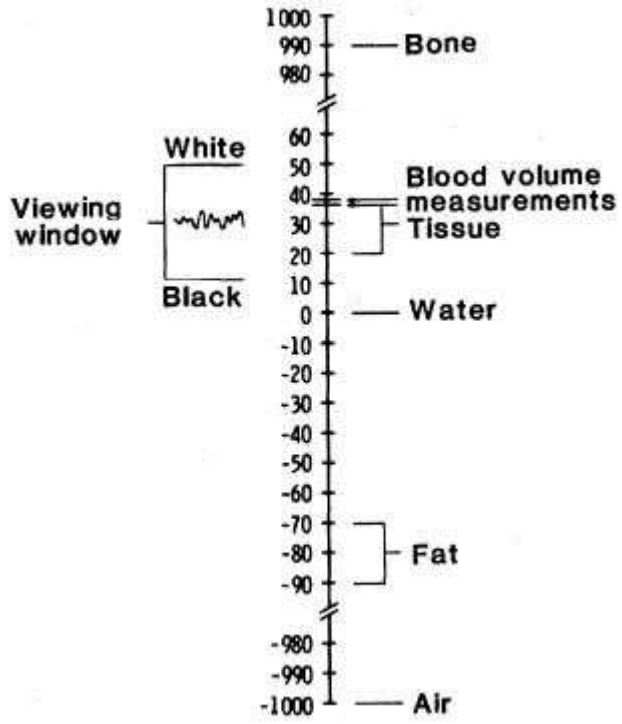

Figure 2.[286] Accuracy to which absorption values can be ascertained on a CT picture. The whole range of a machine from air (-1000) to bone (1000) describing 1000 absorption on either side of water, which has been chosen to be zero. The range of tones between black and white (viewing window) can be restricted to a small part of the scale and be raised or lowered depending on the tissues being compared or contrasted.

Previous published work on mass densities and elemental weights of human tissues and their correlation with CT numbers in Hounsfield units has shown that CT numbers of soft tissues are situated within the range between −100 and +100 Hounsfield units, whereas the CT numbers of skeletal tissues take values from 100 up to 1524.[259,287--289] Relevant to this thesis, calculated CT numbers for yellow marrow, red marrow, yellow and red marrow mixture of 1:1 and whole blood were -49, 11, -22 and 56 respectively.[259] These calculated CT numbers came about through a series of related equations that took into account the properties of the scanner (spectral function, Klein–Nishina coefficients),[287] and established mass densities and elemental weights of 71 types of human tissues[287,288] derived through bone models and calibration with phantoms. In vivo studies have shown variable normal distribution of both yellow and red marrow, and CT images of marrow from different regions within a bone have different appearances and

absolute Hounsfield values are location dependent. Given that both hematopoietic tissue, which has a density of 1.06 g/cm^3, and adipose tissue, which has a density of 0.92 g/cm^3, make up the marrow space, a higher density of the marrow tissue would suggest a lower fat fraction and vice versa.[259] Changes in marrow fat fraction do not occur during growth, but throughout life depending on age, bone type and skeletal regions.[289,290] With growth, hematopoietic tissue converts to fatty marrow in the vertebral bodies and metaphyses of the long bones. The conversion persists throughout life at a slow steady rate generally, but varies greatly. Thus, by adulthood, the metaphyseal and epiphyseal regions generally have positive Hounsfield values, at times reaching100 HU. Whereas, by the age of 15 years, the diaphyses of the long bones reach their adult pattern and comprise of fat mostly. Therefore, even in early adulthood, the CT marrow density values at this site of negative Hounsfield values predominantly as low as -100 HU, essentially reflect fat tissue density due to negligible influence of the haemopoietic component.[291] Furthermore, Hounsfield values at similar locations in long bones are generally comparable, such that a difference of up to 20 HU between sides would be considered acceptable,[291] and given accurate positioning, Hounsfield readings from the two sides should be similar.[292] The same, however, cannot be said for the vertebrae.

CT has also been used extensively as a research tool for the differentiation and quantification of various soft tissue depots investigating the impact of ageing, obesity and physical inactivity on clinical outcomes.[293-296] In these studies, the threshold, which separates adipose from muscle, was found by taking the average of their peaks from an image histogram. For the purpose of the studies reported in this thesis, CT Hounsfield values for bone (trabecular and cortical), marrow fat and haematopoietic volume are based on previous published studies described above, and final threshold ranges used for quantification of these parameters are derived through similar approaches to previous techniques for delineating tissues of overlapping densities with an image histogram.[293]

Even though different scanners were used in our two CT studies, scanning settings were at similar levels. All images were analysed with the same imaging software (Slice O Matic version 4.1, Tomovision), and global and local thresholds for bone, haemopoietic and fat tissues were determined manually by the following procedure: Thirty randomly selected CT images in axial slices of vertebrae and proximal femur from different subjects were manually inspected. Images that contain artefacts, such as movements and over or under exposure, were excluded from the analysis. The maximum Hounsfield unit of bone tissue applied in the whole analysis was the maximum Hounsfield unit encountered in cortical bone from any anatomical region- for example. the vertebrae or femur. The maximum density of cortical bone in any image was consistently the same as the maximum CT number in the threshold setting in the region growing painting mode (Figure 3A). Thus, for the maximum density of cortical bone, the threshold was set as the maximum for each individual analysis. This maximum threshold was then gradually lowered to find the lowest threshold at which the resolution would still enable auto-segmentation of the region of interest (Figure 3B-3C). The cortical bone surfaces, which were thin or were adjacent to trabecular bone, were not detected by this threshold limit. Segmentation of these regions of cortical bone required the lowest threshold limit, which accounted for partial volume effects. Partial volume effects significantly affect the CT numbers of cortical bone. Thus, to account for this, the image was viewed in zoom mode, and densities were determined pixel by pixel. Pixels that had lower CT numbers, but were bright in appearance and contiguous with cortical bone surface, were counted as cortical bone (Figure 3D-3F). Pixels that were not contiguous, but were bright and had lower CT numbers, were counted as trabecular bone. These pixels were presumed to be thin or broken trabecular whose thicknesses were beyond the resolution of the CT scanner.

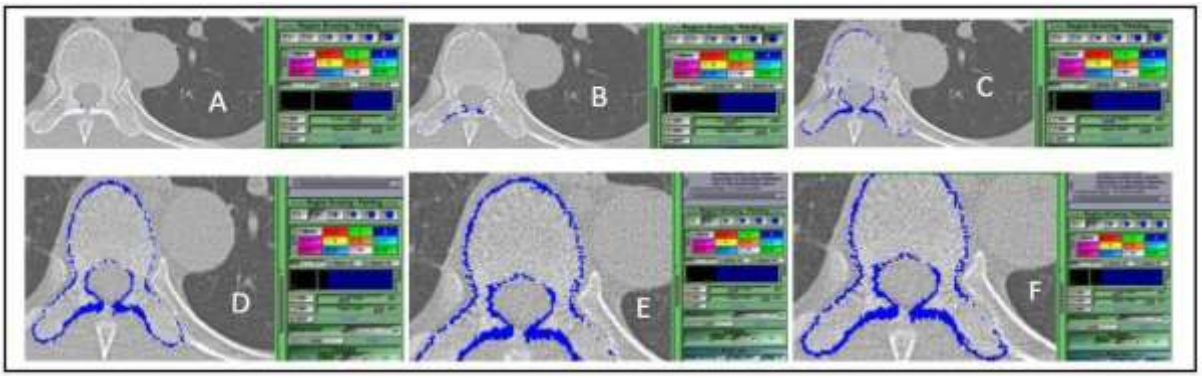

Figure 3. [A-C] Maximum threshold limit gradually decreased until auto-segmentation no longer possible [A] is maximum global threshold for cortical bone (i.e. at gray scale value of 1600 few pixels detected). [B] Greater volume of cortical bone detected by auto-segmentation at limit of 1000. [C] is the lowest gray scale value (600) that auto-segmentation is able to be carried out i.e. lower limit for global threshold. [D-F] are zoomed images to determine the lower limit of cortical bone for local thresholds.

The thirty values were then plotted on a histogram, and the average CT number was considered to be the lower threshold for cortical bone tissue in all the analyses. However, to derive final threshold ranges specific to each study set of images and the CT scanner used to obtain those images, during segmentation of the region of interest (ROI), CT numbers up to 2 standard deviations lower than this average were accepted if the ROI was deemed to be bone on visual inspection.

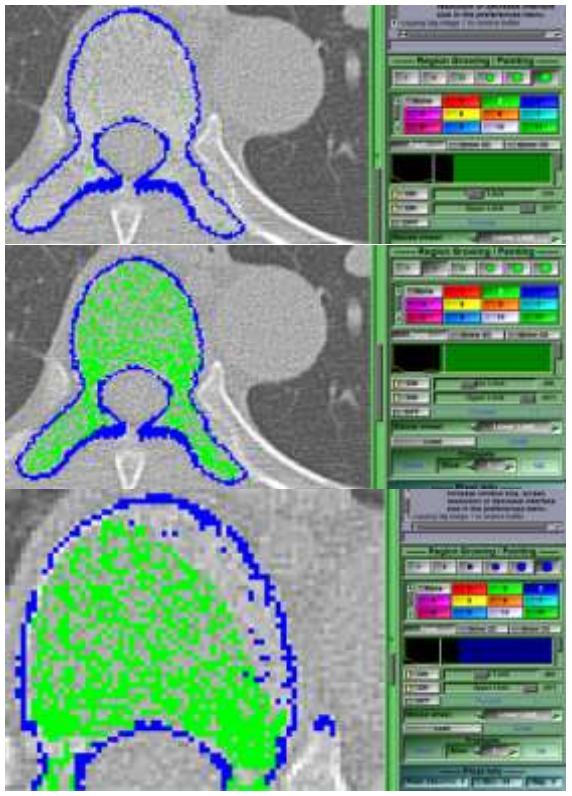

Figure 4. Segmentation procedure to determine the range of thresholds for trabecular bone. [A] Upper limit of threshold is 1 HU below lowest threshold for cortical bone. [B] - [D] threshold decreasing to capture trabecular bone pixels. [E] = Pixels with low CT numbers but appear bright and pixels adjacent to cortex that appear bright but have low CT numbers or appear disconnected from cortical surface are counted as trabecular bone by visual inspection.

For trabecular bone, the maximum setting is 1 HU less than the lower threshold for cortical bone, and the lower limit was the average CT number of trabecular bone tissue at the interface with fat and haemopoietic tissue. Delineating trabecular bone from surrounding stromal tissues or haemopoietic tissue was carried out in the same way as delineating cortical bone from trabecular bone. To account for the presence of thin trabecular bone whose thickness was smaller than the voxel size, the principle of partial volume effects were applied to the surrounding pixels of visually obvious pixels representing bone tissue (Figure. 4). Partial volume effects occur when tissues of different absorption are encompassed on the same CT voxel, producing a beam attenuation, proportional to the average value of these tissues. Hence, the surrounding pixels with lower CT numbers, regardless of whether they were contiguous with a trabeculum or not, but bright in appearance, were counted as trabecular bone. The CT numbers were then plotted on a histogram (Figure. 5).

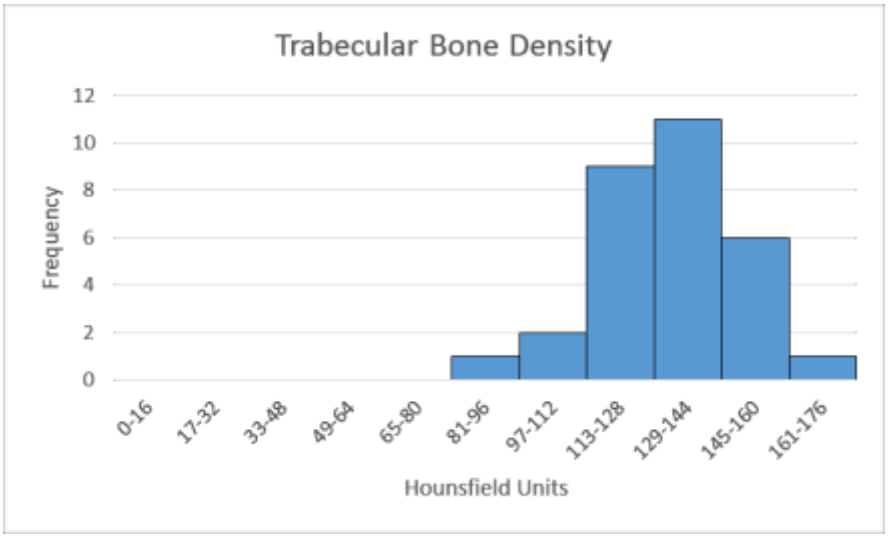

Figure 5. Distribution of HUs for lower limits of trabecular bone in 30 random images.

Threshold ranges of grey scale values for fat were derived through the same process as above. The lower limit was set at a maximum negative value for each and every analysis. This was done for convenience, but also on the rationale that within a closed cavity, as in a vertebral body or proximal femur, all negative values represent fat rather than air. The upper limit was the average CT number of adipose tissue pixels adjacent to non-adipose neighbouring pixels.

Here we considered previous published data, showing that CT numbers for red marrow, yellow and red marrow mixture of 1:1 and whole blood were 11, -22 and 56 respectively,[259] but we further examined grey scale values pixel by pixel. Pixels that had low positive CT numbers, but had darker appearance resembling adipose pixels, were counted as adipose tissue. Pixels with low positive CT numbers, but appeared less dark, resembling haematopoietic tissue, were counted as haematopoietic tissue. The values were then plotted on a histogram (Figure 6).

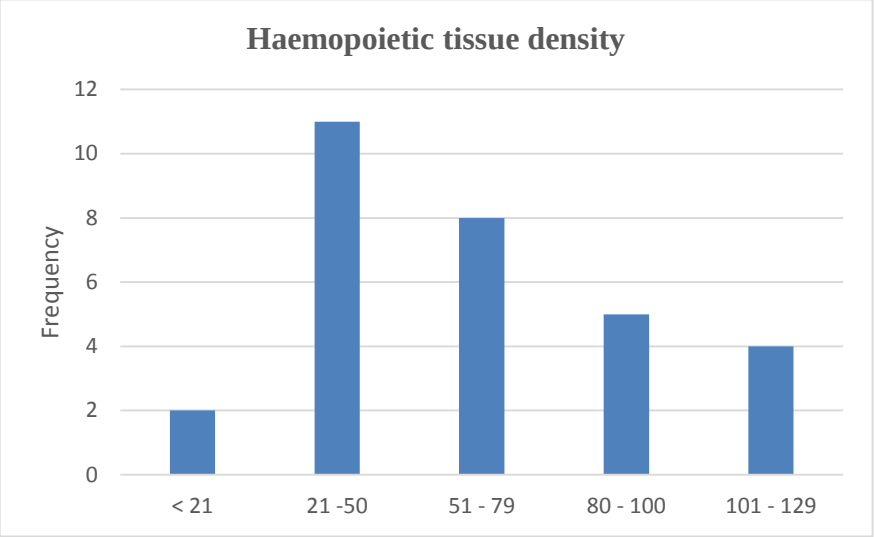

Figure 6. Distribution of HUs for lower and upper limits of haemopoietic tissue density in 30 random images.

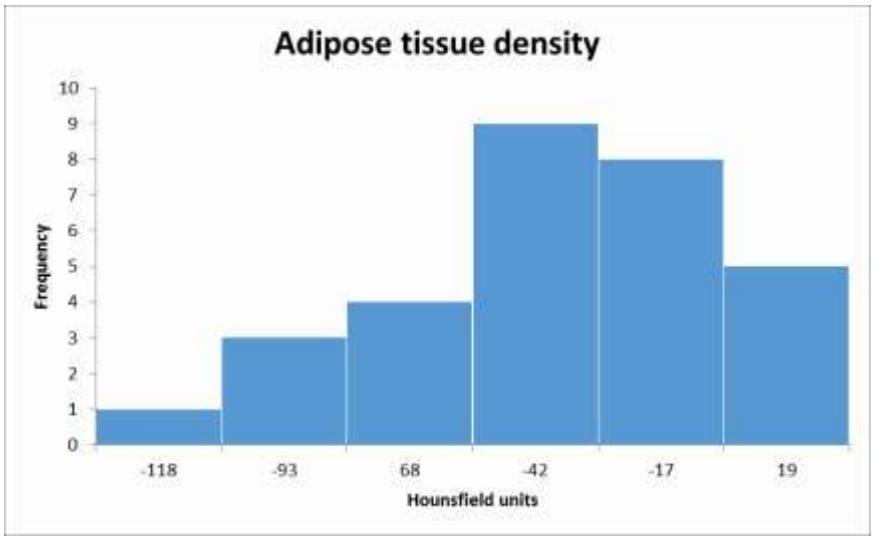

Figure 7. Distribution of HUs for upper limit of marrow fat in 30 random images.

Thus, the following CT numbers were applied for global thresholding algorithms in all CT image segmentation (semi-automated): bone (trabecular 130-600, cortical ≥ 601), marrow fat ≤ 10, and 21 ≥ haematopoietic tissue ≤ 129. For manual segmentation to include pixels that were not captured in the semi-automated segmentation procedure, local threshold for fat (≤ 20) and lower limit of trabecular bone (≥ 100) were applied.

2.1.2.1 Slice-O-Matic Volume Quantification Protocol

Each axial CT scan image was examined for inclusion suitability. Images with any presence of artefacts, resulting in reduced image quality, were excluded from the analysis. Artefacts were deemed to be present if the image had been affected by movements, acquisition techniques or associated with hardware issues (Table 1), or the borders were poorly defined or the image was not complete with all ROIs intact.

The size of the tissue volume of interest (VOI) was defined by the total number of pixels, with Hounsfield units in the range, as defined above for that tissue. For the purpose of the quantification of volumes, each depot was assigned the following colours arbitrarily: marrow fat (yellow), bone (dark blue for cortical, green for trabecular) and red for haemopoietic volume.

The global threshold ranges for bone, marrow fat and blood volume were set consecutively using the thresholding function- this is the autosegmentation process based on previously published values. The global thresholded regions were edited manually. The region-growing function was then used to segment the volume compartment individually and sequentially using values obtained from the 30 individual pixels within cross sectional areas, which were not accounted for in the initial global segmentation. These were visually inspected and allocated as most likely blood or fat, and a local threshold was manually applied. The painting function was used to segmentate these pixels. The volume function was then used to compute the segmented VOIs. All absolute volumes were expressed in mm^3.

Note: Each CT scanner's daily performance is checked in accordance with manufacturer's recommendations and specifications. This is carried out as per local quality control procedure protocols. Cross calibrations of the CT scanners would be ideal but were not possible due to locations of each research centres and the retrospective nature of the studies. Previously published and validated CT numbers for various tissues were applied to both scanners for the auto and semi-autosegmentation procedures. Nevertheless, the final thresholds for

segmentations of volumes were determined individually for each scanner.

Types of Artifacts	Examples
Patient related - motion	blurring, streaking, or shading
Physics based	Beam hardening - cupping artifact - streak and darks bands - metal artifact/high-density foreign material artifact Noise Photon starvation – streaks
Hardware based	ring artifact tube arcing out of field artifact

Table 1. Sources of image artifacts and types of artifacts excluded from study.

2.2 Micro-CT (chapters 3 and 4)

Micro-computed tomography (μCT) is an imaging technique possessing ultra-high resolution. It utilizes cone-beam X-ray geometry and a reconstruction algorithm to form 3D models and achieve high spatial resolution. Very high-spatial resolution images can be achieved, approaching 10 μm or better.[261] With spatial resolution as high as ≈60 μm, individual trabeculae can be visualized clearly, allowing three-dimensional modelling and detailed bone microstructure analysis. Further advances in more recent times have seen the use of synchrotron radiation as the X-ray source, enabling spatial resolution up to 2 μm.[297]
Thus, in recent times, in vitro structural analyses in 2D or 3D of small bone samples (typically <2 cm^3) have widely employed μCT scanners. Applications of μCT are found widely in animal studies, typically for characterizing skeletal phenotype in gene knockout [298-300] in osteoporotic[53] or arthritic rodents.[301] μCT 3-D- determined trabecular parameters showed greater percentage changes than those observed with DXA, and also showed better correlation with biomechanical properties. In clinical studies, μCT with a resolution of 20μm^3 was employed to compare iliac crest bone samples from women in pre and post-menopausal states. The postmenopausal samples showed significant changes in 3-D

trabecular structural parameters, including a change from plate like structure to rod like structure; decrease in trabecular thickness and number; and increase in trabecular separation.[302] Evaluation of these 3D bone microstructure parameters has also been used to analyse bone biopsies from patients treated with antiresorptive agents such as oestrogen[303], residronate[304] and anabolic agents, such as PTH.[305] An extensive review of the technical considerations relating to μCT can be found in a previously published article.[306]

Despite its extensive applications as described above, quantification of marrow fat has not been evaluated. For the purpose of this thesis, we applied similar concepts and approaches to define thresholds for different tissues, as in the case of clinical CT, described in an earlier section.

In the validation study, fat depots and bone tissue were chemically stained, and thus were directly visualized with certainty. The range of gray scale attenuation of bone and fat pixels was obtained directly from the images in Slice O Matic. Nevertheless, to reduce effects of image variations and partial volume effects, ten random images of bone and fat depots were analysed, and the pixel gray scale values were plotted on a histogram. The range of values, which best estimated a 95% confidence interval, was chosen to represent the density threshold range of bone and marrow fat for the remainder of the analysis. The gray scale values for blood were assumed to be the values between bone and fat.

Threshold ranges derived from the validation study were used in the second μCT study. This assumption was based on the rationale that both micro CT systems employed equivalent energy settings, and therefore, attenuation values should not significantly differ. Local thresholds were further manually adjusted based on visual inspection of individual pixels.

It should be further noted that the author of this thesis was blinded to group allocation and treatment group allocation in all experimental procedures until the time of statistical analysis. The author was the primary researcher to carry out preliminary image analyses to derive initial

thresholds and the subsequent range of local thresholds. The final range of thresholds was applied to all subsequent analyses. Another blinded evaluator then applied the same thresholds to all subsequent image analyses.

References

1. Raisz L, Rodan G. Pathogenesis of osteoporosis. Endocrinol Metab Clin North Am 2003; 32(1):15–24.

2. Siris E, Miller P, Barrett-Connor E, et al. Identification and Fracture Outcomes of Undiagnosed Low Bone Mineral Density in Postmenopausal Women . Results from the National Osteoporosis Risk Assessment. JAMA. 2001; 286(22):2815–2822.

3. Wilkins C, Birge S. Prevention of osteoporotic fractures in the elderly. Am J Med. 2005; 118(11):1190–1195.

4. 3rd LM, Lane A, Cooper C, et al. Prevalence and incidence of vertebral deformities. Osteoporos Int. 1993; 3(3):113-119.

5. Henry M, Pasco J, Nicholson G, et al. Prevalence of osteoporosis in Australian men and women: Geelong Osteoporosis Study. Med J Aust. 2011; 195(6):321-322.

6. https://www.iofbonehealth.org/site/default/files/PDFs/white_paper_australia-23-06-08.pdf (Accessed 08/2014)

7. Klotzbuecher C, Ross P, Landsman P, et al. Patients with prior fractures have an increased risk of future fractures: a summary of the literature and statistical synthesis. J Bone Miner Res. 2000; 15(4):721–739.

8. Kanis J, Johnell O, Laet CD, et al. A meta-analysis of previous fracture and subsequent fracture risk. Bone. 2004; 35(2):375–382.

9. Center J, Bliuc D, Nguyen T, et al. Risk of subsequent fracture after low-trauma fracture in men and women. JAMA. 2007; 297(4):387-394.

10. Friesendorff M, Besjakov J, Åkesson K. Long-term survival and fracture risk after hip fracture: a 22-year follow-up in women. J Bone Miner Res. 2008; 23(11):1832–1841.

11. Cooper C, Atkinson E, Jacobsen S, et al. Population based study of survival after osteoporotic fractures. Am J Epidemiol. 1993; 137(9):1001–1005.

12. Center J, Nguyen T, Schneider D, et al. Mortality after all major types of osteoporotic fracture in men and women: an observational study. Lancet. 1999; 353(9156):878–882.

13. Magaziner J, Fredman L, Hawkes W, et al. Changes in functional status attributable to hip fracture: a comparison of hip fracture patients to community- dwelling aged. Am J Epidemiol. 2003; 157(11):1023–1031.

14. Haentjens P, Magaziner J, Colón-Emeric C, et al. Meta-analysis: excess mortality after hip fracture among older women and men. Ann Intern Med. 2010; 152(6):380-390.

15. March L, Cameron I, Cumming R, et al. Mortality and morbidity after hip fracture: can evidence based clinical pathways make a difference? J Rheumatol. 2000; 27(9):2227-2231.

16. Sanders K, Nicholoson G, Ugoni A, et al. Health Burden of hip and other fractures in Australia beyond 2000. Projections based on the Geelong Osteoporosis Study. MJA 1999; 170(10):467-470.

17. F. Richard Bringhurst, Marie B. Demay, Stephen M. Krane, Henry M. Kronenberg. Bone and Mineral Metabolism in Health and Disease. http://clinicalgate.com/bone-and-mineral-metabolism-in-health-and-disease/ (Accessed 8/2014)

18. Riggs B, Khosla S, Melton LI. Sex steroids and the construction and conservation of the adult skeleton. Endocr Rev 2002; 23 (3):279–302.

19. Raisz L, Seeman E. Causes of age related bone loss and bone fragility: An alternative view. J Bone Miner Res 2001; 16 (11):1948–1952.

20. Lips P. Vitamin D status and nutrition in Europe and Asia. J Steroid Biochem Mol Biol. 2007; 103 (3-5):620–625.

21. Garn SM, Rohmann CG, Molan P Jr. Relations of development and aging, Chapter 4, 1980: The developmental nature of bone changes during aging. Nutr Rev. 1991; 49(6):176-178.

22. Duque G, Troen B. Understanding the mechanisms of senile osteoporosis: new facts for a major geriatric syndrome. J Am Geriatr Soc. 2008; 56 (5):935–941.

23. Lips P. Vitamin D deficiency and secondary hyperparathyroidism in the elderly: Consequences for bone loss and fractures and therapeutic implications. Endocr Rev 2001; 22 (4):477–501.

24. Eastell R, Yergey A, Vieira N, et al. Interrelationship among vitamin D metabolism, true calcium absorption, parathyroid function, and age in women: evidence of an age-related intestinal resistance to 1, 25-dihydroxyvitamin D action. J Bone Miner Res. 1991; 6 (2):125–132.

25. Ledger G, Burrit M, Kao P, et al. Role of parathyroid hormone in mediating nocturnal and age-related increases in bone resorption. J Clin Endocrinol Metab 1995; 80 (11):3304–3310.

26. Khosla S, Amin S, Orwoll E. Osteoporosis in men. Endocr Rev 2008; 29 (4):441–464.

27. Khosla S. Update in male osteoporosis. J Clin Endocrinol Metab 2010; 95 (1):3–10.

28. Kennel K, Riggs B, Achenbach S, et al. Role of parathyroid hormone in mediating age-related changes in bone resorption in men. Osteoporos Int 2003; 14(8):631–636.

29. Khosla S, Atkinson E, III LM, et al. Effects of age and estrogen status on serum parathyroid hormone levels and biochemical markers of bone turnover in women: a population-based study. J Clin Endocrinol Metab 1997; 82(5):1522–1527.

30. Khosla S, Riggs B. Pathophysiology of age-related bone loss and osteoporosis. Endocrinol Metab Clin N Am 2005 34(4):1015–1030.

31. McCauley L, Tozum T, Kozloff K, et al. Transgenic models of metabolic bone disease: Impact of estrogen receptor deficiency on skeletal metabolism. Connect Tissue Res 2003; 44 Suppl 1:250–263.

32. Hofbauer L, Khosla S, Dunstan C, et al. Estrogen stimulates gene expression and

protein production of osteoprotegerin in human osteoblastic cells. Endocrinology 1999; 140(9):4367–4370.

33. Hughes D, Dai A, Tiffee J, et al. Estrogen promotes apoptosis of murine osteoclasts mediated by TGF-beta. Nat Med. 1996; 2(10):1132-1136.

34. Eghbali-Fatourechi G, Khosla S, Sanyal A, et al. Role of RANK ligand in mediating increased bone resorption in early postmenopausal women. J Clin Invest 2003; 111(8):1221– 1230.

35. Clowes J, Riggs B, Khosla S. The role of the immune system in the pathophysiology of osteoporosis. Immunol Rev. 2005; 208: 207–227.

36. Lundberg P, Boström I, Mukohyama H, et al. Neuro-hormonal control of bone metabolism: vasoactive intestinal peptide stimulates alkaline phosphatase activity and mRNA expression in mouse calvarial osteoblasts as well as calcium accumulation mineralized bone nodules. Regul Pept. 1999; 85(1):47-58.

37. Mitnick MA, Grey A, Masiukiewicz U, et al. Parathyroid hormone induces hepatic production of bioactive interleukin-6 and its soluble receptor. American journal of physiology Endocrinology and metabolism. 2001; 280(3):E405-412.

38. Charatcharoenwitthaya N, Khosla S, Atkinson EJ, et al. Effect of blockade of TNF-alpha and interleukin-1 action on bone resorption in early postmenopausal women. J Bone Miner Res. 2007; 22(5):724-729.

39. Oursler MJ, Pederson L, Fitzpatrick L, et al. Human giant cell tumours of the bone (osteoclastomas) are estrogen target cells. Proc Natl Acad Sci U S A. 1994; 91(12):5227-5231.

40. Perrien DS, Achenbach SJ, Bledsoe SE, et al. Bone turnover across the menopause transition: correlations with inhibins and follicle-stimulating hormone. J Clin Endocrinol Metab. 2006; 91(5):1848-1854.

41. Slemenda CW, Longcope C, Zhou L, et al. Sex steroids and bone mass in older men. Positive associations with serum estrogens and negative associations with androgens. J Clin Invest. 1997; 100(7):1755-1759.

42. Khosla S, Melton LJ, 3rd, Atkinson EJ, et al. Relationship of serum sex steroid levels to longitudinal changes in bone density in young versus elderly men. J Clin Endocrinol Metab. 2001; 86(8):3555-3561.

43. Khosla S, Amin S, Singh RJ, et al. Comparison of sex steroid measurements in men by immunoassay versus mass spectroscopy and relationships with cortical and trabecular volumetric bone mineral density. Osteoporos Int. 2008; 19(10):1465-1471.

44. Mellstrom D, Vandenput L, Mallmin H, et al. Older men with low serum estradiol and high serum SHBG have an increased risk of fractures. J Bone Miner Res. 2008; 23(10):1552-1560.

45. Szulc P, Munoz F, Claustrat B, et al. Bioavailable estradiol may be an important determinant of osteoporosis in men: the MINOS study. J Clin Endocrinol Metab. 2001; 86(1):192-199.

46. Falahati-Nini A, Riggs BL, Atkinson EJ, et al. Relative contributions of testosterone and estrogen in regulating bone resorption and formation in normal elderly men. J Clin Invest. 2000; 106(12):1553-1560.

47. Leder BZ, LeBlanc KM, Schoenfeld DA, et al. Differential effects of androgens and estrogens on bone turnover in normal men. J Clin Endocrinol Metab. 2003; 88(1):204-210.

48. Sanyal A, Hoey KA, Modder UI, et al. Regulation of bone turnover by sex steroids in men. J Bone Miner Res. 2008; 23(5):705-714.

49. LeBlanc ES, Nielson CM, Marshall LM, et al. The effects of serum testosterone, estradiol, and sex hormone binding globulin levels on fracture risk in older men. J Clin Endocrinol Metab. 2009; 94(9):3337-3346.

50. Clarke BL, Khosla S. Physiology of bone loss. Radiol Clin North Am. 2010; 48(3):483-495.

51. Rosen CJ, Bouxsein ML. Mechanisms of disease: is osteoporosis the obesity of bone? Nat Clin Pract Rheumatol. 2006; 2(1):35-43.

52. Perrien DS, Akel NS, Dupont-Versteegden EE, et al. Aging alters the skeletal response to disuse in the rat. Am J Physiol Regul Integr Comp Physiol. 2007; 292(2):R988-996.

53. Duque G, Rivas D, Li W, et al. Age-related bone loss in the LOU/c rat model of healthy ageing. Exp Gerontol. 2009; 44(3):183-189.

54. Verma S, Rajaratnam JH, Denton J, et al. Adipocytic proportion of bone marrow is inversely related to bone formation in osteoporosis. J Clin Pathol. 2002; 55(9):693-698.

55. Meunier P, Aaron J, Edouard C, et al. Osteoporosis and the replacement of cell populations of the marrow by adipose tissue. A quantitative study of 84 iliac bone biopsies. Clin Orthop Relat Res. 1971; 80:147-154.

56. Griffith JF, Yeung DK, Antonio GE, et al. Vertebral bone mineral density, marrow perfusion, and fat content in healthy men and men with osteoporosis: dynamic contrast-enhanced MR imaging and MR spectroscopy. Radiology. 2005; 236(3):945-951.

57. Shen W, Chen J, Punyanitya M, et al. MRI-measured bone marrow adipose tissue is inversely related to DXA-measured bone mineral in Caucasian women. Osteoporos Int. 2007; 18(5):641-647.

58. Justesen J, Stenderup K, Ebbesen EN, et al. Adipocyte tissue volume in bone marrow is increased with aging and in patients with osteoporosis. Biogerontology. 2001; 2(3):165-171.

59. Rosen CJ, Ackert-Bicknell C, Rodriguez JP, et al. Marrow fat and the bone microenvironment: developmental, functional, and pathological implications. Crit Rev

Eukaryot Gene Expr. 2009; 19(2):109-124.

60. Duque G, Rivas D. Alendronate has an anabolic effect on bone through the differentiation of mesenchymal stem cells. J Bone Miner Res. 2007; 22(10):1603-1611.

61. Chamberlain G, Fox J, Ashton B, et al. Concise review: mesenchymal stem cells: their phenotype, differentiation capacity, immunological features, and potential for homing. Stem cells. 2007; 25(11):2739-2749.

62. Zhou S, Greenberger JS, Epperly MW, et al. Age-related intrinsic changes in human bone-marrow-derived mesenchymal stem cells and their differentiation to osteoblasts. Aging cell. 2008; 7(3):335-343.

63. Wang Y, Wan C, Gilbert SR, et al. Oxygen sensing and osteogenesis. Ann N Y Acad Sci. 2007; 1117:1-11.

64. Gimble JM, Zvonic S, Floyd ZE, et al. Playing with bone and fat. J Cell Biochem. 2006; 98(2):251-266.

65. Moerman EJ, Teng K, Lipschitz DA, et al. Aging activates adipogenic and suppresses osteogenic programs in mesenchymal marrow stroma/stem cells: the role of PPAR-γ2 transcription factor and TGF-β/BMP signaling pathways. Aging Cell. 2004; 3(6): 379–389.

66. Hutchison CJ, Worman HJ. A-type lamins: guardians of the soma? Nat Cell Biol. 2004; 6(11):1062-1067.

67. Hutchison CJ, Alvarez-Reyes M, Vaughan OA. Lamins in disease: why do ubiquitously expressed nuclear envelope proteins give rise to tissue-specific disease phenotypes? J Cell Sci. 2001; 114(Pt 1):9-19.

68. Harborth J, Elbashir SM, Bechert K, et al. Identification of essential genes in cultured mammalian cells using small interfering RNAs. J Cell Sci. 2001; 114(Pt 24):4557-4565.

69. Pajerowski JD, Dahl KN, Zhong FL, et al. Physical plasticity of the nucleus in stem cell differentiation. Proc Natl Acad Sci U S A. 2007; 104(40):15619-15624.

70. de Paula Rodrigues GH, das Eiras Tamega I, Duque G, et al. Severe bone changes in a case of Hutchinson-Gilford syndrome. Ann Genet. 2002; 45(3):151-155.

71. Mounkes LC, Kozlov S, Hernandez L, et al. A progeroid syndrome in mice is caused by defects in A-type lamins. Nature. 2003; 423(6937):298-301.

72. Duque G, Rivas D. Age-related changes in lamin A/C expression in the osteoarticular system: laminopathies as a potential new aging mechanism. Mech Ageing Dev. 2006; 127(4):378-383.

73. De Sandre-Giovannoli A, Bernard R, Cau P, et al. Lamin a truncation in Hutchinson-Gilford progeria. Science. 2003; 300(5628):2055.

74. Rivas D, Li W, Akter R, et al. Accelerated features of age-related bone loss in zmpste24 metalloproteinase-deficient mice. J Gerontol A Biol Sci Med Sci. 2009; 64(10):1015-1024.

75. Maurin AC, Chavassieux PM, Frappart L, et al. Influence of mature adipocytes on osteoblast proliferation in human primary cocultures. Bone. 2000; 26(5):485-489.

76. Musacchio E, Priante G, Budakovic A, et al. Effects of unsaturated free fatty acids on adhesion and on gene expression of extracellular matrix macromolecules in human osteoblast-like cell cultures. Connect Tissue Res. 2007; 48(1):34-38.

77. Grey A. Skeletal consequences of thiazolidinedione therapy. Osteoporos Int. 2008; 19(2):129-137.

78. Lazarenko OP, Rzonca SO, Hogue WR, et al. Rosiglitazone induces decreases in bone mass and strength that are reminiscent of aged bone. Endocrinology. 2007; 148(6):2669-2680.

79. Wan Y, Chong LW, Evans RM. PPAR-gamma regulates osteoclastogenesis in mice. Nat Med. 2007; 13(12):1496-1503.

80. Akune T, Ogata N, Hoshi K, et al. Insulin receptor substrate-2 maintains predominance of anabolic function over catabolic function of osteoblasts. J Cell Biol. 2002; 159(1):147-156.

81. Botolin S, McCabe LR. Inhibition of PPARgamma prevents type I diabetic bone marrow

adiposity but not bone loss. J Cell Physiol. 2006; 209(3):967-976.

82. Yu WH, Li FG, Chen XY, et al. PPARgamma suppression inhibits adipogenesis but does not promote osteogenesis of human mesenchymal stem cells. Int J Biochem cell Biol. 2012; 44(2):377-384.

83. Ferguson VL, Ayers RA, Bateman TA, et al. Bone development and age-related bone loss in male C57BL/6J mice. Bone. 2003; 33(3):387-398.

84. Duque G, Li W, Vidal C, et al. Pharmacological inhibition of PPARgamma increases osteoblastogenesis and bone mass in male C57BL/6 mice. J Bone Miner Res. 2013; 28(3):639-648.

85. Albala C, Yáñez M, Devoto E, et al. Obesity as a protective factor for postmenopausal osteoporosis. Int J Obes Relat Metab Disord. 1996; 20(11):1027-1032.

86. Reid IR. Relationships among body mass, its components, and bone. Bone. 2002; 31(5):547-555.

87. Felson DT, Zhang Y, Hannan MT, et al. Effects of weight and body mass index on bone mineral density in men and women: the Framingham study. J Bone Miner Res. 1993; 8(5):567-573.

88. Marcus R, Greendale G, Blunt BA, et al. Correlates of bone mineral density in the postmenopausal estrogen/progestin interventions trial. J Bone Miner Res. 1994; 9(9):1467-1476.

89. Chen Z, Lohman TG, Stini WA, et al. Fat or lean tissue mass: which one is the major determinant of bone mineral mass in healthy postmenopausal women? J Bone Miner Res. 1997; 12(1):144-151.

90. Ravn P, Cizza G, Bjarnason NH, et al. Low body mass index is an important risk factor for low bone mass and increased bone loss in early postmenopausal women. Early Postmenopausal Intervention Cohort (EPIC) study group. J Bone Miner Res. 1999; 14(9):1622-7.

91. Reid IR, Plank LD, Evans MC. Fat mass is an important determinant of whole body

bone density in premenopausal women but not in men. J Clin Endocrinol Metab. 1992; 75(3):779-82.

92. Reid IR, Ames R, Evans MC, et al. Determinants of total body and regional bone mineral density in normal postmenopausal women--a key role for fat mass. J Clin Endocrinol Metab. 1992; 75(1):45-51.

93. Khosla S, Atkinson EJ, Riggs BL, et al. Relationship between body composition and bone mass in women. J Bone Miner Res. 1996; 11(6):857-63.

94. Pluijm SM, Visser M, Smit JH, et al. Determinants of bone mineral density in older men and women: body composition as mediator. J Bone Miner Res. 2001; 16(11):2142-51.

95. El Hage R, Jacob C, Moussa E, et al. Relative importance of lean mass and fat mass on bone mineral density in a group of Lebanese postmenopausal women. J Clin Densitom. 2011; 14(3):326-31.

96. Reid IR, Ames RW, Evans MC, et al. Determinants of the rate of bone loss in normal postmenopausal women. J Clin Endocrinol Metab. 1994; 79(4):950-4.

97. Hsu YH, Venners SA, Terwedow HA, et al. Relation of body composition, fat mass, and serum lipids to osteoporotic fractures and bone mineral density in Chinese men and women. Am J Clin Nutr. 2006; 83(1):146-54.

98. Blum M, Harris SS, Must A, et al. Leptin, body composition and bone mineral density in premenopausal women. Calcif Tissue Int. 2003; 73(1):27-32.

99. Janicka A, Wren TA, Sanchez MM, et al. Fat mass is not beneficial to bone in adolescents and young adults. J Clin Endocrinol Metab. 2007; 92(1):143-7.

100. Zhao LJ, Liu YJ, Liu PY, et al. Relationship of obesity with osteoporosis. Clin Endocrinol Metab. 2007; 92(5):1640-6.

101. Reid IR, Legge M, Stapleton JP, et al. Regular exercise dissociates fat mass and bone density in premenopausal women J Clin Endocrinol Metab. 1995; 80(6):1764-8.

102. de Gregório LH, Lacativa PG, Melazzi AC, et al. Glucocorticoid-induced osteoporosis. Arq Bras Endocrinol Metabol. 2006; 50(4):793-801.

103. Livingstone DE, Jones GC, Smith K, et al. Understanding the role of glucocorticoids in obesity: tissue-specific alterations of corticosterone metabolism in obese Zucker rats. Endocrinology. 2000; 141(2):560-3.

104. Zhao LJ, Jiang H, Papasian CJ, et al. Correlation of obesity and osteoporosis: effect of fat mass on the determination of osteoporosis J Bone Miner Res. 2008;23(1):17-29.

105. Lindsay R, Cosman F, Herrington BS, et al. Bone mass and body composition in normal women. J Bone Miner Res. 1992; 7(1):55-63.

106. Glauber HS, Vollmer WM, Nevitt MC, et al. Body weight versus body fat distribution, adiposity, and frame size as predictors of bone density. J Clin Endocrinol Metab. 1995; 80(4):1118-1123.

107. Considine RV, Sinha MK, Heiman ML, et al. Serum immunoreactive-leptin concentrations in normal-weight and obese humans. N Engl J Med. 1996; 334(5):292-295.

108. Thomas T, Gori F, Khosla S, et al. Leptin acts on human marrow stromal cells to enhance differentiation to osteoblasts and to inhibit differentiation to adipocytes. Endocrinology. 1999; 140(4):1630-1638.

109. Ducy P, Amling M, Takeda S, et al. Leptin inhibits bone formation through a hypothalamic relay: a central control of bone mass. Cell. 2000; 100(2):197-207.

110. Wolff I, van Croonenborg JJ, Kemper HC, et al. The effect of exercise training programs on bone mass: a meta-analysis of published controlled trials in pre- and postmenopausal women. Osteoporos Int. 1999;9(1):1-12

111. Shi Y, Yadav VK, Suda N, et al. Dissociation of the neuronal regulation of bone mass and energy metabolism by leptin in vivo. Proc Natl Acad Sci U S A. 2008; 105(51):20529-20533.

112. Rosen CJ, Donahue LR, Hunter SJ. Insulin-like growth factors and bone: the osteoporosis connection. Proc Soc Exp Biol Med. 1994; 206(2):83-102.

113. Boonen S, Mohan S, Dequeker J, et al. Down-regulation of the serum stimulatory components of the insulin-like growth factor (IGF) system (IGF-I, IGF-II, IGF binding protein [BP]-3, and IGFBP-5) in age-related (type II) femoral neck osteoporosis. J Bone Miner Res. 1999; 14(12):2150-8.

114. Seeman E. From density to structure: growing up and growing old on the surfaces of bone. J Bone Miner Res. 1997; 12(4):509-521.

115. Riggs BL, Melton LJ, 3rd. Involutional osteoporosis. N Engl J Med. 1986; 314(26):1676-1686.

116. Modder UI, Achenbach SJ, Amin S, et al. Relation of serum serotonin levels to bone density and structural parameters in women. J Bone Miner Res. 2010; 25(2):415-422.

117. Weinreb M, Rodan GA, Thompson DD. Osteopenia in the immobilized rat hind limb is associated with increased bone resorption and decreased bone formation. Bone. 1989; 10(3):187-194.

118. Duque G, Li W, Yeo LS, et al. Attenuated anabolic response to exercise in lamin A/C haploinsufficient mice. Bone. 2011; 49(3):412-418.

119. Leichter I, Simkin A, Margulies JY, et al. Gain in mass density of bone following strenuous physical activity. J Orthop Res. 1989; 7(1):86-90.

120. Marie PJ, Hott M, Launay JM, et al. In vitro production of cytokines by bone surface-derived osteoblastic cells in normal and osteoporotic postmenopausal women: relationship with cell proliferation. J Clin Endocrinol Metab. 1993; 77(3):824-830.

121. Amin S, Riggs BL, Melton LJ, 3rd, et al. High serum IGFBP-2 is predictive of increased bone turnover in aging men and women. J Bone Miner Res. 2007; 22(6):799-807.

122. Kneissel M. The promise of sclerostin inhibition for the treatment of osteoporosis. IBMS BoneKEy. 2009; 6:259–264.

123. Balemans W, Ebeling M, Patel N, et al. Increased bone density in sclerosteosis is due to the deficiency of a novel secreted protein (SOST). Hum Mol Genet. 2001; 10(5):537-543.

124. Balemans W, Patel N, Ebeling M, et al. Identification of a 52 kb deletion downstream of the SOST gene in patients with van Buchem disease. J Med Genet. 2002; 39(2):91-97.

125. Li X, Ominsky MS, Niu QT, et al. Targeted deletion of the sclerostin gene in mice results in increased bone formation and bone strength. J Bone Miner Res. 2008; 23(6):860- 869.

126. Li X, Ominsky MS, Warmington KS, et al. Sclerostin antibody treatment increases bone formation, bone mass, and bone strength in a rat model of postmenopausal osteoporosis. J Bone Miner Res. 2009; 24(4):578-588.

127. Lane NE, Silverman SL. Anabolic therapies. Curr Osteoporos Rep. 2010; 8 (1): 23-27.

128. Lin C, Jiang X, Dai Z, et al. Sclerostin mediates bone response to mechanical unloading through antagonizing Wnt/beta-catenin signaling. J Bone Miner Res. 2009; 24(10):1651-1661.

129. Eisman JA, Bone HG, Hosking DJ, et al. Odanacatib in the treatment of postmenopausal women with low bone mineral density: three-year continued therapy and resolution of effect. J Bone Miner Res. 2011; 26(2):242-251.

130. Langdahl B, Binkley N, Bone H, et al. Odanacatib in the treatment of postmenopausal women with low bone mineral density: five years of continued therapy in a phase 2 study. J Bone Miner Res. 2012; 27(11):2251-2258.

131. Brixen, K., Chapurlat, R., Cheung, A, et al. Bone Density, turnover, and estimated strength in postmenopausal women treated with odanacatib: a randomized trial. J Clin Endocrinol Metab. 2013; 98 (2): 571–580.

132. Engelke K, Fuerst T, Dardzinski B, et al. Odanacatib treatment affects trabecular and cortical bone in the femur of postmenopausal women: results of a two-year placebo-controlled

trial. J Bone Miner Res. 2015; 30(1):30-38.

133. Cheung AM, Majumdar S, Brixen K, et al. Effects of odanacatib on the radius and tibia of postmenopausal women: improvements in bone geometry, microarchitecture, and estimated bone strength. J Bone Miner Res. 2014; 29(8):1786-1794.

134. Bone HG, Dempster DW, Eisman JA, et al. Odanacatib for the treatment of postmenopausal osteoporosis: development history and design and participant characteristics of LOFT, the Long-Term Odanacatib Fracture Trial. Osteoporos Int. 2015; 26(2):699-712.

135. Chapurlat RD. Odanacatib: a review of its potential in the management of osteoporosis in postmenopausal women. Ther Adv Musculoskelet Dis. 2015; 7(3):103–109.

136. Saag KGAP, Benhamou CL, Gilchrist N, et al. Efficacy of odanacatib in postmenopausal women with osteoporosis: subgroup analyses of data from the phase 3 long-term odanacatib fracture trial (LOFT). American Society for Bone and Mineral Research Annual Meeting, 2015; Abstract 1144.

137. Langdahl BDT, Keaveny T, Engelke K, et al. Effect of odanacatib on bone density and estimated bone strength in postmenopausal women: a CT-based sub-study of the phase 3 Long-Term Odanacatib Fracture Trial (LOFT). American Society for Bone and Mineral Research Annual Meeting, 2015; Abstract 1056.

138. McClung MR, Papapoulos S, Saag KG, et al. 2016 Odanacatib efficacy and safety in postmenopausal women with osteoporosis: 5-year data from the extension of the phase 3 Long-Term Odanacatib Fracture Trial (LOFT). American Society for Bone and Mineral Research Annual Meeting, Atlanta, Georgia, 2016.

139. McClung MLB, Papapoulos S, Saag KG, et al. Odanacatib anti-fracture efficacy and safety in postmenopausal women with osteoporosis: results from the phase III Long-Term Odanacatib Fracture Trial (LOFT). American Society for Bone and Mineral Research Annual Meeting, 2014; Abstract 1147.

140. Papapoulos S, McClung MR, Langdahl B, et al. Safety of odanacatib in postmenopausal women with osteoporosis: 5-year data from the extension of the phase 3 Long-Term Odanacatib Fracture Trial (LOFT). American Society for Bone and Mineral Research Annual Meeting, Atlanta, Georgia, 2016.

141. Papapoulos SMM, Langdahl B, Saag KG, et al. Safety and tolerability of odanacatib therapy in postmenopausal women with osteoporosis: results from the phase III Long-Term Odanacatib Fracture Trial (LOFT). American Society for Bone and Mineral Research Annual Meeting, 2014; Abstract 1148

142. O'Donoghue M, Cavallari I, Bonaca M, et al. The Long-Term Odanacatib Fracture Trial (LOFT): cardiovascular safety results. American Society for Bone and Mineral Research Annual Meeting, Atlanta, Georgia, 2016.

143. Ton FN, Gunawardene SC, Lee H, et al. Effects of low-dose prednisone on bone metabolism. J Bone Miner Res 2005; 20 (3):464–470.

144. Weinstein RS, Jilka RL, Parfitt AM, et al. Inhibition of osteoblastogenesis and promotion of apoptosis of osteoblasts and osteocytes by glucocorticoids. Potential mechanisms of their deleterious effects on bone. J Clin Invest 1998; 102 (2):274–82.

145. Ito S, Suzuki N, Kato S, et al. Glucocorticoids induce the differentiation of a mesenchymal progenitor cell line, ROB-C26 into adipocytes and osteoblasts, but fail to induce terminal osteoblast differentiation. Bone 2007; 40(1):84–92.

146. O'Brien CA, Jia D, Plotkin LI, et al. Glucocorticoids act directly on osteoblasts and osteocytes to induce their apoptosis and reduce bone formation and strength. Endocrinology 2004; 145(4):1835–41.

147. Ohnaka K, Tanabe M, Kawate H, et al. Glucocorticoid suppresses the canocical Wnt signal in cultured human osteoblasts. Biochem Biophys Res Commun 2005; 329(1):177–81.

148. Canalis E, Mazziotti G, Giustina A, et al. Glucocorticoid-induced osteoporosis:

pathophysiology and therapy. Osteoporos Int 2007; 18(10):1319–1328.

149. Rozman C, Feliu E, Berga L, et al. Age-related variations of fat tissue fraction in normal human bone marrow depend both on size and number of adipocytes: a stereological study. Exp Hematol. 1989; 17(1):34–37.

150. Griffith JF, Yeung DK, Ma H, et al. Bone marrow fat content in the elderly: a reversal of sex difference seen in younger subjects. J Magn Reson Imaging. 2012; 36(1):225–230.

151. Roldan-Valadez E, Pina-Jimenez C, Favila R, et al. Gender and age groups interactions in the quantification of bone marrow fat content in lumbar spine using 3TMR spectroscopy: a multivariate analysis of covariance (MANCOVA). Eur J Radiol. 2013; 82911):e697–702.

152.

153. Minaire P, Edouard C, Arlot M, Meunier PJ. Marrow changes in paraplegic patients. Calcif Tissue Int 1984; 36 (3):338–340.

154. Bredella MA, Fazeli PK, Miller KK, et al. Increased bone marrow fat in anorexia nervosa. J Clin Endocrinol Metab. 2009; 94(6):2129– 2136.

155. Bredella MA, Torriani M, Ghomi RH, et al. Vertebral bone marrow fat is positively associated with visceral fat and inversely associated with IGF-1 in obese women. *Obesity*. 2011; 19(1):49–53.

156. Yeung DKW, Griffith JF, Antonio GE, Lee FKH, Woo J, Leung PC. Osteoporosis is associated with increased marrow fat content and decreased marrow fat unsaturation: a proton MR spectroscopy study. *J Magn Reson Imaging*. 2005; 22(2):279–285.

157. Duque G. As a matter of fat: new perspectives on the Understanding of age-related bone loss. BoneKEy-Osteovision 2007; 4(4):129–140.

158. Lecka-Czernik B, Moerman EJ, Grant DF, et al. Divergent effects of selective peroxisome proliferator-activated receptor-gamma2 ligands on adipocyte versus osteoblast differentiation. Endocrinology. 2002; 143 (6):2376–2384.

159. Gimble, JM. Marrow Stromal Adipocytes. In: Beresford, J.; Owen, M., editors. Marrow stromal cell culture. Cambridge: Cambridge University Press; 1998.

160. Nuttall ME, Gimble JM. Controlling the balance between osteoblastogenesis and adipogenesis and the consequent therapeutic implications. Curr Opin Pharmacol. 2004; 4(3):290–294.

161. Corre J, Planat-Benard V, Corberand JX, et al. Human bone marrow adipocytes support complete myeloid and lymphoid differentiation from human CD34 cells. Br J Haematol 2004; 127(3):344–347.

162. Troen BR. The role of cathepsin K in normal bone resorption. Drug News Perspect. 2004; 17(1):19-28.

163. Yasuda Y, Kaleta J, Bromme D. The role of cathepsins in osteoporosis and arthritis: rationale for the design of new therapeutics. Adv Drug Deliv Rev. 2005; 57(7):973-993.

164. Motyckova G, Fisher DE. Pycnodysostosis: role and regulation of cathepsin K in osteoclast function and human disease. Curr Mol Med. 2002; 2(5):407-421.

165. Shalhoub V, Faust J, Boyle WJ, et al. Osteoprotegerin and osteoprotegerin ligand effects on osteoclast formation from human peripheral blood mononuclear cell precursors. J Cell Biochem. 1999; 72(2):251-261.

166. Troen BR. The regulation of cathepsin K gene expression. Ann N Y Acad Sci. 2006; 1068:165-172.

167. Stoch SA, Zajic S, Stone J, et al. Effect of the cathepsin K inhibitor odanacatib on bone resorption biomarkers in healthy postmenopausal women: two double-blind, randomized, placebo-controlled phase I studies. Clin Pharmacol Ther. 2009; 86(2):175-182.

168. Unger RH. Lipotoxic diseases. Annu Rev Med. 2002; 53:319–336.

169. Kusminski CM, Shetty S, Orci L, et al. Diabetes and apoptosis: lipotoxicity. Apoptosis. 2009; 14(12):1484–1495.

170. Unger RH, Zhou YT. Lipotoxicity of beta-cells in obesity and in other causes of fatty acid spillover. Diabetes. 2001; 50 Suppl 1:S118-121.

171. Griffith JF, Yeung DK, Ahuja AT, et al. A study of bone marrow and subcutaneous fatty acid composition in subjects of varying bone mineral density. Bone. 2009; 44(6):1092-1096.

172. Vande Berg BC, Malghem J, Lecouvet FE, et al. Magnetic resonance imaging of normal bone marrow. Eur Radiol. 1998; 8(8):1327-1334.

173. Tavassoli M. Differential response of bone marrow and extramedullary adipose cells to starvation. Experientia. 1974; 30(4):424-425.

174. Bathija A, Davis S, Trubowitz S. Bone marrow adipose tissue: response to acute starvation. Am J Hematol. 1979; 6(3):191-198.

175. Ecklund K, Vajapeyam S, Feldman HA, et al. Bone marrow changes in adolescent girls with anorexia nervosa. J Bone Miner Res. 2010; 25(2):298-304.

176. Gasparrini M, Rivas D, Elbaz A, et al. Differential expression of cytokines in subcutaneous and marrow fat of aging C57BL/6J mice. Exp Gerontol. 2009; 44(9):613-618.

177. Ross SE, Hemati N, Longo KA, et al. Inhibition of adipogenesis by Wnt signaling. Science. 2000; 289(5481):950-953.

178. Tontonoz P, Hu E, Graves RA, et al. mPPAR gamma 2: tissue-specific regulator of an adipocyte enhancer. Genes Dev. 1994; 8(10):1224-1234.

179. Bennett CN, Ross SE, Longo KA, et al. Regulation of Wnt signaling during adipogenesis. J Biol Chem. 2002; 277(34):30998-31004.

180. Zipori D. The stem state: mesenchymal plasticity as a paradigm. Curr Stem Cell Res Ther. 2006; 1(1):95-102.

181. Rosen ED, Walkey CJ, Puigserver P, et al. Transcriptional regulation of adipogenesis. Genes Dev. 2000; 14(11):1293-1307.

182. Rosen ED, MacDougald OA. Adipocyte differentiation from the inside out. Nat Rev Mol

Cell Biol. 2006; 7(12):885-896.

183. Clarke SL, Robinson CE, Gimble JM. CAAT/enhancer binding proteins directly modulate transcription from the peroxisome proliferator-activated receptor gamma 2 promoter. Biochem Biophys Res Commun. 1997; 240(1):99-103.

184. Saladin R, Fajas L, Dana S, et al. Differential regulation of peroxisome proliferator activated receptor gamma1 (PPARgamma1) and PPARgamma2 messenger RNA expression in the early stages of adipogenesis. Cell Growth & Differentiation: the Molecular Biology Journal of the American Association for Cancer Research. 1999; 10(1):43-48.

185. Fajas L, Fruchart JC, Auwerx J. Transcriptional control of adipogenesis. Curr Opin Cell Biol. 1998; 10(2):165-173.

186. Yeh WC, Cao Z, Classon M, et al. Cascade regulation of terminal adipocyte differentiation by three members of the C/EBP family of leucine zipper proteins. Genes Dev. 1995; 9(2):168-181.

187. Wu Z, Rosen ED, Brun R, et al. Cross-regulation of C/EBP alpha and PPAR gamma controls the transcriptional pathway of adipogenesis and insulin sensitivity. Mol Cell. 1999; 3(2):151-158.

188. Centrella M, Horowitz MC, Wozney JM, et al. Transforming growth factor-beta gene family members and bone. Endocr Rev. 1994; 15(1):27-39.

189. Massagué J, Cheifetz S, Endo T, et al. Type beta transforming growth factor is an inhibitor of myogenic differentiation. Proc Natl Acad Sci U S A. 1986; 83(21): 8206–8210.

190. Ignotz RA, Massagué J. Type beta transforming growth factor controls the adipogenic differentiation of 3T3 fibroblasts. Proc Natl Acad Sci U S A. 1985; 82(24): 8530–8534.

191. Choy L, Skillington J, Derynck R. Roles of autocrine TGF-beta receptor and Smad signaling in adipocyte differentiation. J Cell Biol. 2000; 149(3):667-682.

192. Heldin CH, Miyazono K, ten Dijke P. TGF-beta signalling from cell membrane to

nucleus through SMAD proteins. Nature. 1997; 390(6659):465-471.

193. Massagué J, Wotton D. Transcriptional control by the TGF-beta/Smad signaling system. EMBO J. 2000; 19(8):1745-1754.

194. Itoh S, Itoh F, Goumans MJ, et al. Signaling of transforming growth factor-beta family members through Smad proteins. Eur J Biochem. 2000; 267(24):6954-6967.

195. Choy, L., Derynck, R. Transforming growth factor-beta inhibits adipocyte differentiation by Smad3 interacting with CCAAT/enhancer-binding protein (C/EBP) and repressing C/EBP transactivation function. J Biol Chem. 2003; 278(11):9609-9619.

196. Tzameli I, Fang H, Ollero M, et al. Regulated production of a peroxisome proliferator-activated receptor-gamma ligand during an early phase of adipocyte differentiation in 3T3-L1 adipocytes. J Biol Chem. 2004; 279(34):36093-36102.

197. Rzonca SO, Suva LJ, Gaddy D, et al. Bone is a target for the antidiabetic compound rosiglitazone. Endocrinology. 2004; 145(1):401-406.

198. Werner AL, Travaglini MT. A review of rosiglitazone in type 2 diabetes mellitus. Pharmacotherapy. 2001; 21(9):1082-1099.

199. Fontaine C, Cousin W, Plaisant M, et al. Hedgehog signaling alters adipocyte maturation of human mesenchymal stem cells. Stem cells. 2008; 26(4):1037- 1046.

200. Ross DA, Rao PK, Kadesch T. Dual roles for the Notch target gene Hes-1 in the differentiation of 3T3-L1 preadipocytes. Mol Cell Biol. 2004; 24(8):3505- 3513.

201. Richardson RL, Hausman GJ, Gaskins HR. Effect of transforming growth factor-beta on insulin-like growth factor 1- and dexamethasone-induced proliferation and differentiation in primary cultures of pig preadipocytes. Acta Anat (Basel). 1992; 145(4):321-326.

202. Choy L, Derynck R. Transforming growth factor-beta inhibits adipocyte differentiation by Smad3 interacting with CCAAT/enhancer-binding protein (C/EBP) and repressing C/EBP transactivation function. J Biol Chem. 2003; 278(11):9609-9619.

203. Hata K, Nishimura R, Ikeda F, et al. Differential roles of Smad1 and p38 kinase in regulation of peroxisome proliferator-activating receptor gamma during bone morphogenetic protein 2-induced adipogenesis. Mol Biol Cell. 2003; 14(2):545-555.

204. Carrel AL, Allen DB. Effects of growth hormone on adipose tissue. J Pediatr Endocrinol Metab. 2000; 13 Suppl 2:1003-1009.

205. Huang G, Zheng Q, Sun J, et al. Stabilization of cellular properties and differentiation mutilpotential of human mesenchymal stem cells transduced with hTERT gene in a long-term culture. J Cell Biochem. 2008; 103(4):1256-1269.

206. Kobune M, Kato J, Chiba H, et al. Telomerized human bone marrow-derived cell clones maintain the phenotype of hematopoietic-supporting osteoblastic and myofibroblastic stromal cells after long-term culture. Exp Hematol. 2005; 33(12):1544-1553.

207. Rauner M, Sipos W, Goettsch C, et al. Inhibition of lamin A/C attenuates osteoblast differentiation and enhances RANKL-dependent osteoclastogenesis. J Bone Miner Res. 2009; 24(1):78-86.

208. Varela I, Pereira S, Ugalde AP, et al. Combined treatment with statins and aminobisphosphonates extends longevity in a mouse model of human premature aging. Nat Med. 2008; 14(7):767-772.

209. Kita K, Kawai K, Hirohata K. Changes in bone marrow blood flow with aging. J Orthop Re.1987; 5(4):569-575.

210. Elbaz A, Rivas D, Duque G. Effect of estrogens on bone marrow adipogenesis and Sirt1 in aging C57BL/6J mice. Biogerontology. 2009; 10(6):747-755.

211. Fehrer C, Lepperdinger G. Mesenchymal stem cell aging. Exp Gerontol. 2005; 40(12):926-930.

212. Fink T, Abildtrup L, Fogd K, et al. Induction of adipocyte-like phenotype in human mesenchymal stem cells by hypoxia. Stem Cells. 2004; 22(7):1346-1355.

213. Park HJ, Della-Fera MA, Hausman DB, et al. Genistein inhibits differentiation of primary human adipocytes. J Nutr Biochem. 2009; 20(2):140-148.

214. Syed FA, Oursler MJ, Hefferanm TE, et al. Effects of estrogen therapy on bone marrow adipocytes in postmenopausal osteoporotic women. Osteoporos Int. 2008; 19(9):1323-1330.

215. Chan GK, Duque G. Age-related bone loss: old bone, new facts. Gerontology. 2002; 48(2):62-71.

216. Muruganandan S, Roman AA, Sinal CJ. Adipocyte differentiation of bone marrow-derived mesenchymal stem cells: cross talk with the osteoblastogenic program. Cell Mol Life Sci. 2009; 66(2):236-253.

217. Beresford JN, Bennett JH, Devlin C, et al. Evidence for an inverse relationship between the differentiation of adipocytic and osteogenic cells in rat marrow stromal cell cultures. J Cell Sci. 1992; 102 (Pt 2):341-351.

218. Dorheim MA, Sullivan M, Dandapani V, et al. Osteoblastic gene expression during adipogenesis in hematopoietic supporting murine bone marrow stromal cells. J Cell Physiol. 1993; 154(2):317-328.

219. Gimble JM, Morgan C, Kelly K, et al. Bone morphogenetic proteins inhibit adipocyte differentiation by bone marrow stromal cells. J Cell Biochem. 1995; 58(3):393-402.

220. Kawai K, Tamaki A, Hirohata K. Steroid-induced accumulation of lipid in the osteocytes of the rabbit femoral head. A histochemical and electron microscopic study. J Bone Joint Surg Am. 1985;67(5):755-763

221. Sheng H, Sheng CJ, Cheng XY, et al. Pathomorphological changes of bone marrow adipocytes in process of steroid-associated osteonecrosis. Int J Clin Exp Pathol. 2013; 6(6):1046-1050.

222. Martin RB, Chow BD, Lucas PA. Bone marrow fat content in relation to bone remodeling and serum chemistry in intact and ovariectomized dogs. Calcif Tissue Internat. 1990;

46(3):189-194.

223. Martin RB, Zissimos SL. Relationships between marrow fat and bone turnover in ovariectomized and intact rats. Bone. 1991; 12(2):123-131.

224. Kirkland JL, Tchkonia T, Pirtskhalava T, et al. Adipogenesis and aging: does aging make fat go MAD? Exp Gerontol. 2002; 37(6):757-767.

225. Mary L. Bouxsein. Bone quality: where do we go from here? Osteoporos Int 2003; 14 (Suppl 5): S118–S127.

226. Seeman E. Bone quality. Osteoporos Int. 2003; 14 (Suppl 5): S3–S7.

227. Bennett JH, Joyner JT, Triffitt JT, et al. Adipocytic cells cultured from marrow have osteogenic potential. J Cell Sci. 1991; 99 (1):131–139.

228. Houghton A, Oyajobi BO, Foster GA, et al. Immortalization of human marrow stromal cells by retroviral transduction with a temperature sensitive oncogene. Identification of bipotential precursor cells capable of directed differentiation to either an osteoblast or adipocyte phenotype. Bone 1998; 22(1):7–16.

229. Hirano T, Iwasaki K. Bone marrow plays a role in bone metabolism: histomorphometry of iliac bone in postmenopausal women. Calcif Tissue Int. 1992; 51(5):348-351.

230. Burkhardt R, Kettner G, Bohm W, et al. Changes in trabecular bone, hematopoiesis and bone marrow vessels in aplastic anemia, primary osteoporosis, and old age: a comparative histomorphometric study. Bone. 1987; 8(3):157-164.

231. Cohen A, Dempster DW, Stein EM, Nickolas TL, Zhou H, McMahon DJ, Muller R, Kohler T, Zwahlen A, Lappe JM, et al. Increased marrow adiposity in premenopausal women with idiopathic osteoporosis. J Clin Endocrinol Metab. 2012; 97:2782–2791.

232. Adams JE. Quantitative computed tomography. Eur J Radiol. 2009; 71(3):415–424.

233. Engelke K, Libanati C, Fuerst T, et al. Advanced CT based in vivo methods for the assessment of bone density, structure, and strength. Curr Osteoporos Rep. 2013; 11(3):246-255.

234. Faulkner KG, von Stetten E, Miller P. Discordance in patient classification using T-scores. J Clin Densitom. 1999; 2(3):343-350.

235. Bergot C, Laval-Jeantet AM, Hutchinson K, et al. A comparison of spinal quantitative computed tomography with dual energy X-ray absorptiometry in European women with vertebral and nonvertebral fractures. Calcif Tissue Int. 2001; 68(2):74-82.

236. Carballido-Gamio J, Nicolella DP. Computational Anatomy in the Study of Bone Structure. Curr Osteoporos Rep. 2013; 11:237-245.

237. Rantalainen T, Nikander R, Heinonen A, et al. Differential effects of exercise on tibial shaft marrow density in young female athletes. J Clin Endocrinol Metab. 2013; 98(5):2037–2044.

238. Gibbs JC, Brown ZM, Wong AK, et al. Measuring Marrow Density and Area Using Peripheral Quantitative Computed Tomography at the Tibia: Precision in Young and Older Adults and Individuals With Spinal Cord Injury. J Clin Densitom. 2017 Mar 27. pii: S1094-6950(16)30258-X. doi: 10.1016/j.jocd.2017.02.002. [Epub ahead of print]

239. Treece GM, Gee AH, Mayhew PM, et al. High resolution cortical bone thickness measurement from clinical CT data. Med Image Anal. 2010; 14(3):276-290.

240. Pickhardt PJ, Lee LJ, Munoz Del RA, et al. Simultaneous screening for osteoporosis at CT colonography: bone mineral density assessment using MDCT attenuation techniques compared with the DXA reference standard. J Bone Miner Res. 2011 26(9):2194–21203.

241. Romme EAPM, Murchison JT, Phang KFP, et al. Bone Attenuation on Routine Chest CT Correlates With Bone Mineral Density on DXA in Patients With COPD. J Bone Miner Res. 2012; 27(11):2338-2343.

242. Emohare O, Cagan A, Morgan R, et al. The use of computed tomography attenuation to evaluate osteoporosis following acute fractures of the thoracic and lumbar vertebra. Geriatr Orthop Surg Rehabil. 2014; 5(2):50-55.

243. Pickhardt PJ, Dustin Pooler B, Lauder T, et al. Opportunistic Screening for Osteoporosis Using Abdominal Computed Tomography Scans Obtained for Other Indications. Ann Intern Med. 2013; 158 (8):588-595.

244. Goodsitt MM, Rosenthal DI. Quantitative computed tomography scanning for measurement of bone and bone marrow fat content. A comparison of single- and dual-energy techniques using a solid synthetic phantom. Invest Radiol. 1987; 22(10):799-810.

245. Rosenthal DI, Mayo-Smith W, Goodsitt MM, et al. Bone and bone marrow changes in Gaucher's disease: evaluation with quantitative CT. Radiology. 1989; 170 (1 part 1):143-146.

246. Rosenthal DI, Barton NW, McKusick KA, et al. Quantitative imaging of Gaucher disease. Radiology. 1992; 185(3):841-845.

247. Mayo-Smith W, Rosenthal DI, Goodsitt MM, et al. Intravertebral fat measurement with quantitative CT in patients with Cushing disease and anorexia nervosa. Radiology. 1989; 170(3 Pt 1):835-838.

248. Di Iorgi N, Rosol M, Mittelman SD, et al. Reciprocal relation between marrow adiposity and the amount of bone in the axial and appendicular skeleton of young adults. J Clin Endocrinol Metab. 2008; 93(6):2281-2286.

249. Genant HK, Engelke K, Prevrhal S. Advanced CT bone imaging in osteoporosis. Rheumatology (Oxford). 2008; 47 Suppl 4:iv9-16.

250. Muller R, Koller B, Hildebrand T, et al. Resolution dependency of microstructural properties of cancellous bone based on three-dimensional mu-tomography. Technol Health Care. 1996; 4(1):113-119.

251. Burghardt AJ, Pialat JB, Kazakia GJ, et al. Multicenter precision of cortical and trabecular bone quality measures assessed by high-resolution peripheral quantitative computed tomography. J Bone Miner Res. 2013; 28(3):524-536.

252. Boutroy S, Bouxsein ML, Munoz F, et al. In vivo assessment of trabecular bone

microarchitecture by high-resolution peripheral quantitative computed tomography. J Clin Endocrinol Metab. 2005; 90(12):6508-6515.

253. Khosla S, Riggs BL, Atkinson EJ, et al. Effects of sex and age on bone microstructure at the ultra-distal radius: a population-based noninvasive in vivo assessment. J Bone Miner Res. 2006; 21(1):124-131.

254. Khosla S, Melton LJ, 3rd, Achenbach SJ, et al. Hormonal and biochemical determinants of trabecular microstructure at the ultra-distal radius in women and men. J Clin Endocrinol Metab. 2006; 91(3):885-891.

255. Sornay-Rendu E, Boutroy S, Munoz F, et al. Alterations of cortical and trabecular architecture are associated with fractures in postmenopausal women, partially independent of decreased BMD measured by DXA: the OFELY study. J Bone Miner Res. 2007; 22(3):425- 433.

256. Sornay-Rendu E, Cabrera-Bravo JL, Boutroy S, et al. Severity of vertebral fractures is associated with alterations of cortical architecture in postmenopausal women. J Bone Miner Res. 2009; 24(4):737-743.

257. Szulc P, Boutroy S, Vilayphiou N, et al. Cross-sectional analysis of the association between fragility fractures and bone microarchitecture in older men: the STRAMBO study. J Bone Miner Res. 2011; 26(6):1358-1367.

258. Vilayphiou N, Boutroy S, Szulc P, et al. Finite element analysis performed on radius and tibia HR-pQCT images and fragility fractures at all sites in men. J Bone Miner Res. 2011; 26(5):965-973.

259. MacNeil JA, Boyd SK. Load distribution and the predictive power of morphological indices in the distal radius and tibia by high resolution peripheral quantitative computed tomography. Bone. 2007; 41(1):129-137.

260. Schneider W, Bortfeld T, Schlegel W. Correlation between CT numbers and tissue parameters needed for Monte Carlo simulations of clinical dose distributions. Phys Med Biol.

2000; 45 (2):459–478.

261. Goodsitt MM, Hoover P, Veldee MS, et al. The composition of bone marrow for a dual-energy quantitative computed tomography technique. a cadaver and computer simulation study. Invest Radiol. 1994; 29 (7):695–704.

262. Genant HK, Jiang Y. Advanced imaging assessment of bone quality. Ann N Y Acad Sci. 2006; 1068:410-428.

263. Yang J, Pham SM, Crabbe DL. High-resolution Micro-CT evaluation of mid- to long-term effects of estrogen deficiency on rat trabecular bone. Acad Radiol. 2003; 10(10):1153-1158.

264. Ito M, Nishida A, Aoyagi K, et al. Effects of risedronate on trabecular microstructure and biomechanical properties in ovariectomized rat tibia. Osteoporos Int. 2005; 16(9):1042-1048.

265. Xiang A, Kanematsu M, Kumar S, et al. Changes in micro-CT 3D bone parameters reflect effects of a potent cathepsin K inhibitor (SB-553484) on bone resorption and cortical bone formation in ovariectomized mice. Bone. 2007; 40(5):1231-1237.

266. Washimi Y, Ito M, Morishima Y, et al. Effect of combined human-PTH (1-34) and calcitonin treatment in ovariectomized rats. Bone. 2007; 41(5):786-793.

267. Dempster DW, Cosman F, Kurland ES, et al. Effects of daily treatment with parathyroid hormone on bone microarchitecture and turnover in patients with osteoporosis: a paired biopsy study. J Bone Miner Res. 2001; 16(10):1846-1853.

268. Dufresne TE, Chmielewski PA, Manhart MD, et al. Risedronate preserves bone architecture in early postmenopausal women in 1 year as measured by three-dimensional microcomputed tomography. Calcif Tissue Int. 2003; 73(5):423-432.

269. Borah B, Dufresne TE, Chmielewski PA, et al. Risedronate preserves bone architecture in postmenopausal women with osteoporosis as measured by three-dimensional microcomputed tomography. Bone. 2004; 34(4):736-746.

270. Fox J, Miller MA, Recker RR, et al. Treatment of postmenopausal osteoporotic women with parathyroid hormone 1-84 for 18 months increases cancellous bone formation and improves cancellous architecture: a study of iliac crest biopsies using histomorphometry and micro computed tomography. J Musculoskelet Neuronal Interact. 2005; 5(4):356-357.

271. Arlot ME, Jiang Y, Genant HK, et al. Histomorphometric and micro CT analysis of bone biopsies from postmenopausal osteoporotic women treated with strontium ranelate. J Bone Miner Res. 2008; 23(2):215-222.

272. Kalpakcioglu BB, Morshed S, Engelke K, et al. Advanced imaging of bone macrostructure and microstructure in bone fragility and fracture repair. J Bone Joint Surg Am. 2008; 90 Suppl 1:68-78.

273. Berger A. Magnetic resonance imaging. BMJ. 2002; 324(7328):35.

274. Griffith JF, Yeung DK, Antonio GE, et al. Vertebral marrow fat content and diffusion and perfusion indexes in women with varying bone density: MR evaluation. Radiology. 2006; 241(3):831-838.

275. Tang GY, Lv ZW, Tang RB, et al. Evaluation of MR spectroscopy and diffusion-weighted MRI in detecting bone marrow changes in postmenopausal women with osteoporosis. Clin Radiol. 2010; 65(5):377-381.

276. Li X, Kuo D, Schafer AL, et al. Quantification of vertebral bone marrow fat content using 3 Tesla MR spectroscopy: reproducibility, vertebral variation, and applications in osteoporosis. Journal of magnetic resonance imaging: JMRI. 2011; 33(4):974-979.

277. Schellinger D, Lin CS, Fertikh D, et al. Normal lumbar vertebrae: anatomic, age, and sex variance in subjects at proton MR spectroscopy--initial experience. Radiology. 2000; 215(3):910-916.

278. Wehrli FW, Hopkins JA, Hwang SN, et al. Cross-sectional study of osteopenia with quantitative MR imaging and bone densitometry. Radiology. 2000; 217(2):527-538.

279. Schellinger D, Lin CS, Hatipoglu HG, et al. Potential value of vertebral proton MR spectroscopy in determining bone weakness. AJNR Am J Neuroradiol. 2001; 22(8):1620- 1627.

280. Kugel H, Jung C, Schulte O, et al. Age- and sex-specific differences in the 1H- spectrum of vertebral bone marrow. J Magn Reson Imaging. 2001; 13(2):263-268.

281. Yeung D, JF Griffith, Antonio G, et al. Osteoporosis is associated with increased marrow fat content and decreased marrow fat unsaturation: a proton MR spectroscopy study. J Magn Reson Imaging. 2005; 22(2):279–228.

282. Shen W, Chen J, Gantz M, et al. MRI-measured pelvic bone marrow adipose tissue is inversely related to DXA-measured bone mineral in younger and older adults. Eur J Clin Nutr. 2012; 66(9):983-988.

283. Karampinos DC, Ruschke, S, Dieckmeyer M, et al. Quantitative MRI and spectroscopy of bone marrow. J. Magn. Reson. Imaging. 2018; 47 (2):332–353.

284. Shen W, Scherzer R, Gantz M, et al. Relationship between MRI-Measured Bone Marrow Adipose Tissue and Hip and Spine Bone Mineral Density in African-American and Caucasian Participants: The CARDIA Study. J Clin Endocrinol Metab. 2012; 97(4): 1337–1346.

285. Shen W, Gong X, Weiss J, et al. Comparison among T1-weighted magnetic resonance imaging, modified dixon method, and magnetic resonance spectroscopy in measuring bone marrow fat. J Obes. 2013; 2013:298675. doi: 10.1155/2013/298675. Epub 2013 Mar 31.

286. Blake GM, Fogelman I. Role of dual-energy X-ray absorptiometry in the diagnosis and treatment of osteoporosis. J Clin Densitom. 2007; 10(1):102-110.

287. Hounsfield GN. Computed medical imaging. Science. 1980; 210(4465):22-28.

288. Woodard HQ, White DR. Bone models for use in radiotherapy dosimetry. Br J Radiol. 1982; 55(652):277-282.

289. White DR, Woodard HQ, Hammond SM. Average soft-tissue and bone models for use in radiation dosimetry. Br J Radiol. 1987; 60(717):907-913.

290. Moore SG, Dawson KL. Red and yellow marrow in the femur: age-related changes in appearance at MR imaging. Radiology. 1990; 175(1):219-223.

291. Vande Berg BC, Lecouvet FE, Moysan P, et al. MR assessment of red marrow distribution and composition in the proximal femur: correlation with clinical and laboratory parameters. Skeletal Radiol. 1997; 26(10):589-596.

292. Helms CA, Cann CE, Brunelle FO, et al. Detection of bone-marrow metastases using quantitative computed tomography. Radiology. 1981; 140(3):745-750.

293. Vogler JB, 3rd, Murphy WA. Bone marrow imaging. Radiology. 1988; 168(3):679- 693.

294. Despres JP. Abdominal obesity as important component of insulin-resistance syndrome. Nutrition. 1993; 9(5):452-459.

295. Pascot A, Lemieux S, Lemieux I, et al. Age-related increase in visceral adipose tissue and body fat and the metabolic risk profile of premenopausal women. Diabetes Care. 1999; 22(9):1471-1478.

296. Goodpaster BH, Krishnaswami S, Harris TB, et al. Obesity, regional body fat distribution, and the metabolic syndrome in older men and women. Arch Intern Med. 2005; 165(7):777-783.

297. Johnson KT, Harmsen WS, Limburg PJ, et al. Visceral fat analysis at CT colonography. Acad Radiol. 2006; 13(8):963-968.

298. Bonse U, Busch F, Gunnewig O, et al. 3D computed X-ray tomography of human cancellous bone at 8 microns spatial and 10(-4) energy resolution. Bone Miner. 1994; 25(1):25-38.

299. Bergo MO, Gavino B, Ross J, et al. Zmpste24 deficiency in mice causes spontaneous bone fractures, muscle weakness, and a prelamin A processing defect. Proceedings of the National Academy of Sciences of the United States of America. 2002; 99(20):13049-13054.

300. Takeshita S, Namba N, Zhao JJ, et al. SHIP-deficient mice are severely osteoporotic due

to increased numbers of hyper-resorptive osteoclasts. Nat Med. 2002; 8(9):943- 949.

301. Roemer FW, Mohr A, Guermazi A, et al. Phenotypic characterization of skeletal abnormalities of Osteopotentia mutant mice by micro-CT: a descriptive approach with emphasis on reconstruction techniques. Skeletal radiology. 2011; 40(8):1073-1078.

302. Lee YS, Heo EA, Jun HY, et al. Articular cartilage imaging by the use of phase-contrast tomography in a collagen-induced arthritis mouse model. Academic radiology. 2010; 17(2):244-250.

303. Jiang Y, Zhao J, Recker RR, et al. Longitudinal changes between premenopausal and postmenopausal in three-dimensional trabecular microstructural characteristics of human iliac crest bone biopsies. J Bone Miner Res. 2000; 15(S1):S184 (S1):S184.

304. Zhao J, Jiang Y, Vedi S, et al. Longitudinal changes in three-dimensional trabecular microarchitecture of paired iliac crest bone biopsies before and after estrogen replacement therapy in postmenopausal women. J Bone Miner Res. 2002; 17:S208.

305. Borah B, Dufresne TE, Ritman EL, et al. Long-term risedronate treatment normalizes mineralization and continues to preserve trabecular architecture: sequential triple biopsy studies with micro-computed tomography. Bone. 2006; 39(2):345-352.

306. Dempster DW, Cosman F, Kerland E, et al. Two- and three-dimensional structural analysis of paired biopsies from osteoporotic patients before and after treatment with parathyroid hormone. J Bone Miner Res. 2000; 15:S194.

307. Jiang Y, Zhao J, Liao EY, et al. Application of micro-CT assessment of 3-D bone microstructure in preclinical and clinical studies. Journal of bone and mineral metabolism. 2005; 23 Suppl: 122-131.

Chapter 3: Validation of non-invasive quantification of marrow fat in aging LOU rats

Presented as published in the journal ***Experimental Gerontology***

Experimental Gerontology 46 (2011) 435–440

Contents lists available at ScienceDirect

Experimental Gerontology

Journal homepage: www.elsevier. com/ locate/ expgero

3.0 Validation of noninvasive quantification of bone marrow fat volume with microCT in aging rats

Oddom Demontiero, Wei Li, Emma Thembani, Gustavo Duque *

Ageing Bone Research Program, Sydney Medical School-Nepean, The University of Sydney, PO Box 63, Penrith, NSW, 2751, Australia

a r t i c l e i n f o

Article history:
Received 8 December 2010
Received in revised form 5 January 2011
Accepted 12 January 2011
Available online 20 January 2011

Section Editor: Dr. Christiaan Leeuwenburgh

Keywords:
Marrow fat
MicroCT
Aging
Osteoporosis
Reliability

A b s t r a c t

Marrow fat infiltration is one ofthehallmarks of age-related bone loss. This fat infiltration has been quantified by invasive and noninvasive methods. However, the validity of the noninvasive methods has not been correlated with a gold standard. In this study we aim to validate the usefulness of marrowfat quantification by correlating micro CT (μCT) images with histology analysis. Fat volume (FV) and bone volume (BV) of distal femora of young (4 months) and old (27 months) Louvain/c (LOU) rats (n= 22) were quantified by histology and compared with μCT images analyzed by an image analysis software (SliceOMatic).

We found that for SliceOMatic/μCT the intra-rater reliability for duplicate measurements was 0.94 ($p < 0.001$) and the inter-rater reliability for FV/BV ratio in young and old rats was 98% and 99% respectively. Both methods showed a significant increase (~ 2 fold) in the FV/BV ratio in the old rats as compared with their young counterparts ($p < 0.001$). A significantly higher correlation ($r2 = 0.85$) in the old rats was found between our noninvasive method and histology. Furthermore, our noninvasive method showed good agreement with histology.

In conclusion, noninvasive quantification of FV/BV ratio using an image analysis software is as reliable as histology for identifying age related marrow fat changes with high inter and intra-rater reliability. These findings provide a new noninvasive method for quantifying marrow fat, which is useful and can be tested not only in animals but also in human studies.

3.1 Introduction

Osteoporosis and its most devastating sequelae, fractures, is a rising global health, economic and social burden. Thus the early detection and treatment of individuals at risk of fractures is a priority before the fragility fracture cascade sets in. Bone Mineral Density (BMD) and Dual Energy X-ray Absorptiometry (DXA) have long been the recommended fracture surrogate and non-invasive tool respectively that estimate fracture risk. However, there is evidence that BMD alone, as defined by the World Health Organization (WHO), does not reliably predict fractures (Marshall et al., 1996), does not identify the majority who are at moderate risk (Pasco et al., 2006), and is limited for monitoring the effect of drug therapy (Delmas and Seeman, 2004). This has led to the development of clinical tools for predicting fracture risks such as the WHO Fracture Risk Assessment Tool (FRAX) (Kanis et al., 2005) and the Garvan fracture risk calculator (Nguyen et al., 2007). However, the validity of a purely clinical tool to predict fractures is still controversial (Leslie and Hans, 2009) and its accuracy may be limited by differences between cohorts (Sandhu et al., 2010).

In recent years it is increasingly recognized that trabecular microarchitecture confers bone its strength (Seeman and Delmas, 2006) and hence may explain the discrepancy between BMD and fracture risk (Delmas and Seeman, 2004). Several non-invasive methods [e.g. magnetic resonance imaging (MRI), and computed tomography (CT) scan] have been used to assess the microarchitecture of the different components of bone (Brandi, 2009). However despite their usefulness, there are other components of bone microarchitecture that have not been fully assessed. One of them is the presence of increasing levels of marrow fat (Burkhardt et al., 1987). In contrast to menopausal bone loss, age-related bone loss is not only associated with high levels of bone resorption, but also with increased adipogenesis (Rozman et al., 1989) and reduced osteoblas- togenesis (Zhou et al., 2008), which affects bone mass. Biopsy studies have shown significant increase in marrow fat with age (Tanaka and Inoue, 1976), as well as an inverse relationship between fat volume (FV) and bone volume that was independent of sex and correlated with the changes seen in people with osteoporosis (Justesen et al., 2001).

Currently there are few non-invasive methods that have quantified marrow fat in humans. Among them, magnetic resonance imaging (MRI) has been the main modality showing increased marrow fat in older subjects (Schellinger et al., 2001) and in osteoporotic individuals (Yeung et al., 2005). However the

* Corresponding author at: Ageing Bone Research Program, Sydney Medical School-Nepean, The University of Sydney, PO Box 63 Penrith NSW 2751, Australia. Tel.: +61 2 4734 4278; fax: +61 2 4734 2614.
E-mail address: gduque@med.usyd.edu.au (G. Duque).

0531-5565/$ - see front matter © 2011 Elsevier Inc. All rights reserved.
doi:10.1016/j.exger.2011.01.001

correlations between MRI and BMD by DXA have been inconsistent and were limited to the vertebrae (Griffith et al., 2005; Schellinger et al., 2004; Shen et al., 2007). Furthermore, although studies using MRI suggest that the degree of marrow adiposity may be a better predictor of bone loss and thus could be used as a surrogate for fracture risk (Schellinger et al., 2004), the lack of histology correlation limits the validity of this conclusion. Due to these reasons and other technical limitations (e.g. metallic prosthesis), a reliable alternative method to quantify fat infiltration is still required. With the emerging use of high resolution imaging methods to assess bone microarchitecture, such as peripheral quantitative CT (pQCT) in humans and microCT (μCT) in bone samples, the development of new image analysis methods to quantify marrow fat could offer an alternative to MRI. In this study, we aimed to validate a new method of non-invasive quantification of bone marrow fat by correlating μCT image analyses with the gold standard (histology) in aging rats. We expect that this new method will facilitate marrow fat quantification in animal and human studies looking at the mechanisms of age-related bone loss and senile osteoporosis.

3.2 Materials and methods

3.2.1 Animals

Twenty-two young mature (4-month-old, n= 12) and old (27- month-old, n= 10) male Louvain/c/rqrv (LOU) rats were studied. Male rats were selected due to their significantly higher levels of marrow fat infiltration as compared with old female LOU rats (Duque et al., 2009). Rats were obtained from the Aging LOU Rat Colony Infrastructure of the Quebec Network for Research on Aging (RQRV; www.rqrv.com). The rats were killed by rapid decapitation in block design fashion. Their bones were rapidly dissected and fixed. All animal protocols were approved by the Animal Care Committee of Centre Hospitaliere de l'Universite de Montreal Research Center in compliance with guidelines of the Canadian Council for Animal Care.

3.2.2 Quantitative radiologic imaging

μCT was performed, using a modification of previously published methods (Duque et al., 2009) on the left femur keeping soft tissues and after overnight fixation in 4% paraformaldehyde. A Skyscan 1172 instrument (Skyscan, Antwerp, Belgium) equipped with a 1.3 Mp camera was used to capture 2D serial cross-sections (axial and coronal), which were used to reconstruct 2- and 3-dimensional images for the quantification of the bone volume (BV) (cortical and trabecular) in the distal metaphysis.

Analyses of the bone microarchitecture were carried out in a region of interest (ROI), which was defined as the cancellous bone compartment beginning 0.6 mm proximal to the most proximal point of the growth plate and extending proximally 1.0 mm, corresponding to approximately 1.55 mm thick region of the distal femora. Topographic images of the bone were acquired with a rotation of 0.9° between each picture and at energy settings of 100 kV and 98 μA. The segmentation of the image was made by a global threshold and a voxel size of 21.90 × 21.90 × 21.90 μm. The same threshold setting was used for all the samples.

3.2.3 μCT image analysis

Tomovision SliceOMatic 4.3 Rev-6i software (Tomovision, Montreal, QC, Canada) was used to analyze the images. This software has been validated against chemical analysis (Janssen et al., 2000) and other image analysis methods (Mitsiopoulos et al., 1998) and has been used as a reference standard method for comparisons of newer
methods for adipose tissue quantification (Demerath et al., 2007; Bonekamp et al., 2008).

Two trained observers carried out the image analysis. The image data were saved as Tagged Image File (TIFF) format. Adequate grayscale thresholds were determined by calculating the average of 20 quantifications per representative area for bone and fat in the images obtained from soft and bone tissue and applying the concept of multiple thresholds as previously described (Kuhn et al., 1990). All adipose and bone tissue pixels within the bone were measured. The calculated thresholds were: bone (blue) >100, bone marrow fat (yellow) -200 to +40, hematopoietic tissue 40-60 (Fig. 1). described (Duque et al., 2009; Richard et al., 2005). Images were captured using a Nikon Eclipse E100 microscope (Nikon Instruments Inc.,Melville,NY,USA)equippedwithaRetiga1300camera(Qimaging, Burnaby, British Columbia, Canada) and the primary histomorpho- metric data obtained using Bioquant Nova Prime image analysis software (Bioquant Image Analysis Corp., Nashville, Tennessee).

For quantification of BV and FV, three coronal image sections were selected from each rat. Since the same femur was used in subsequent histology analysis, coronal sections were selected to closely match the histology sections anatomically. Regions of interest representing the whole axial section of the femur were created as previously described. Bone (cortical and trabecular), marrow fat and hematopoietic tissue were tagged blue, yellow and red respectively using the program's 'Region growing/painting' mode. Within the 'Region growing/painting' control panel, the upper threshold and lower threshold for each tissue were set to a value within the range as determined by the average pixel intensity of bone, marrow fat and hematopoietic tissue respectively. Each consecutive slice and each series of images were tagged using the same region growing procedure. Tagged images resulting from the 'Region growing/painting mode' were then manually inspected and edited as needed using the 'Edit' mode to

exclude image artifacts and to tag the relevant tissue not previously tagged. BV and FV in mm^3 were calculated from these respective tagged areas using the SliceOMatic TAG Surface/Volume tool in edit mode. Finally, the FV/BV ratio was calculated and expressed in percentage.

3.2.4 Intra- and inter-observer reliability

Two observers independently analyzed a total of sixty six μCT femoral slices (three coronal per rat). In addition, the observers performed the segmentations on two separate occasions 3 months apart. Both observers were blinded to the results obtained earlier.

3.2.5 Histology and histomorphometry

After μCT analysis was completed, the femora were processed for plastic embedding. For histomorphometric analyses of FV and BV, femora were embedded in polymethylmethacrylate (MMA) or a mixture of 50% MMA and 50% glycolmethacrylate (GMA). Serial 4- to 6-μm sections of the MMA-embedded tissues were left unstained or stained with von Kossa. Serial 4-μm sections cut on a Leica RM 2155 rotary microtome (Leica Microsystems, Richmond Hill, Ontario, Canada) were deplastified in three changes of 2-methyoxyethyl acetate and 3 changes of acetone for 10 minute each, rehydrated in sequential concentrations of ethanol and maintained in PBS before staining as described previously (Valverde-Franco et al., 2006). FV was quantified using undecalcified, von-Kossa stained sections as previously described (Richard et al., 2005). Briefly, marrow fat (adipocytes) appears as distinct, translucent, yellow ellipsoids in the marrow cavity. A uniform number of fields were read in all sections, starting three fields from the left end of the bone section and three fields from the top endocortical surface. Any disruption in adipocyte shape would generate the exclusion of the field. All measures were done in a tissue volume area corresponding to 0.62 mm^2 and analyzed at 40× magnification using the Bioquant Image Analysis Software.

BV was quantified in von-Kossa stained sections as previously

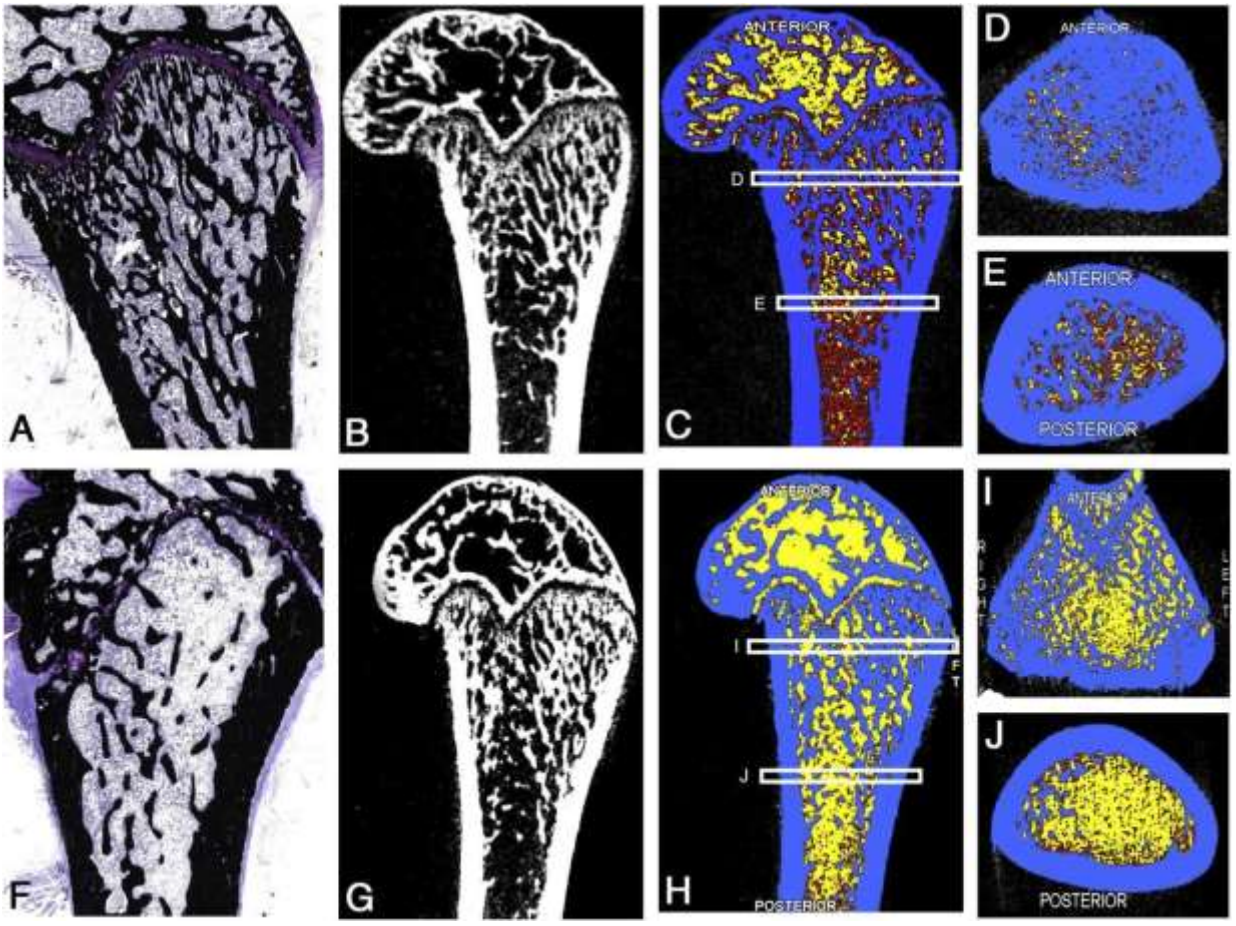

Fig. 1. Comparison between fat volume/bone volume in histology and μCT image analysis in aging LOU rats. Bone micro architecture by histology analysis in young (A) and old (F) bones as compared with bone volume (BV, blue) and fat volume (FV, yellow) labeling using SliceOMatic analysis of μCT sections (B and G) obtained from the same young (C-E) and old (H-J) rats. In agreement with fat identification using histological analysis (A and F) μCT labeling shows higher levels of FV and low levels of BV in old rats (H-J) as compared to young rats (C-E).

Nomenclature and abbreviations conform to those recommended by the American Society for Bone and Mineral Research (Parfitt et al., 1987). Three independent examiners analyzed the histological sections.

3.2.6 Statistical analysis

Means and standard error of the mean (SEM) were used to describe the study sample. Intra- and inter-rater reliability was conducted using the intra-class correlation coefficient (ICC). In the intra-observer analyses, two measurements of the primary rater were compared. In the inter-observer analysis, the mean of the primary raters' results was compared to the mean of a second rater. Finally, to assess the correlation between the micro CT and histology variables, linear regression analysis was used with a p value <0.05 considered as significant. A Bland-Altman plot was used to determine the agreement between our non-invasive method and histology.

3.3 Results

3.3.1 Invasive and non-invasive identification of marrow fat in young and old LOU rats

Fig. 1 illustrates both bone micro architecture by histology analysis in young (A) and old (F) bone as compared with BV and FV labeling using SliceOMatic analysis of μCT sections obtained from the same femur in young (B, C-E) and old (G, H-J) male LOU rats. In agreement with fat identification using histological analysis (A and F), μCT

labeling shows higher levels of FV in old rats (H-J) as compared to young rats (C-E).

3.3.2 Intra- and inter-rater reliability

For SliceOMatic/μCT the intra-rater reliability for duplicate measurements was 0.94 (p b 0.001). The agreement between FV/BV in young and old rats identified by SliceOMatic was 98% and 99% respectively (Table 1).

3.3.3 Age-related changes and SliceOMatic validity

In agreement with previous histology reports (Duque et al., 2009), SliceOMatic identified an age-related increase in FV and a significant decrease in BV on the older group (Fig. 2A, p b 0.01). Both methods showed a significant level of correlation when age-related changes in FV and BV were quantified (Fig. 2B) with a significantly higher correlation (r^2 0.85) in the old animals. In both, histology and SliceOMatic, FV/BV ratio significantly increased in old vs. young rats

Table 1
Reliability of method between independent examiners.

Fat volume/bone volume	(N)	Reader 1 mean		Reader 2 mean	SD	
	ICC Young (4 m)			22	0.23	
	0.24	0.02	0.98			
Old (27 m)	22	0.41		0.45	0.03	0.99

SD − standard deviation.
ICC − interclass correlation coefficient.

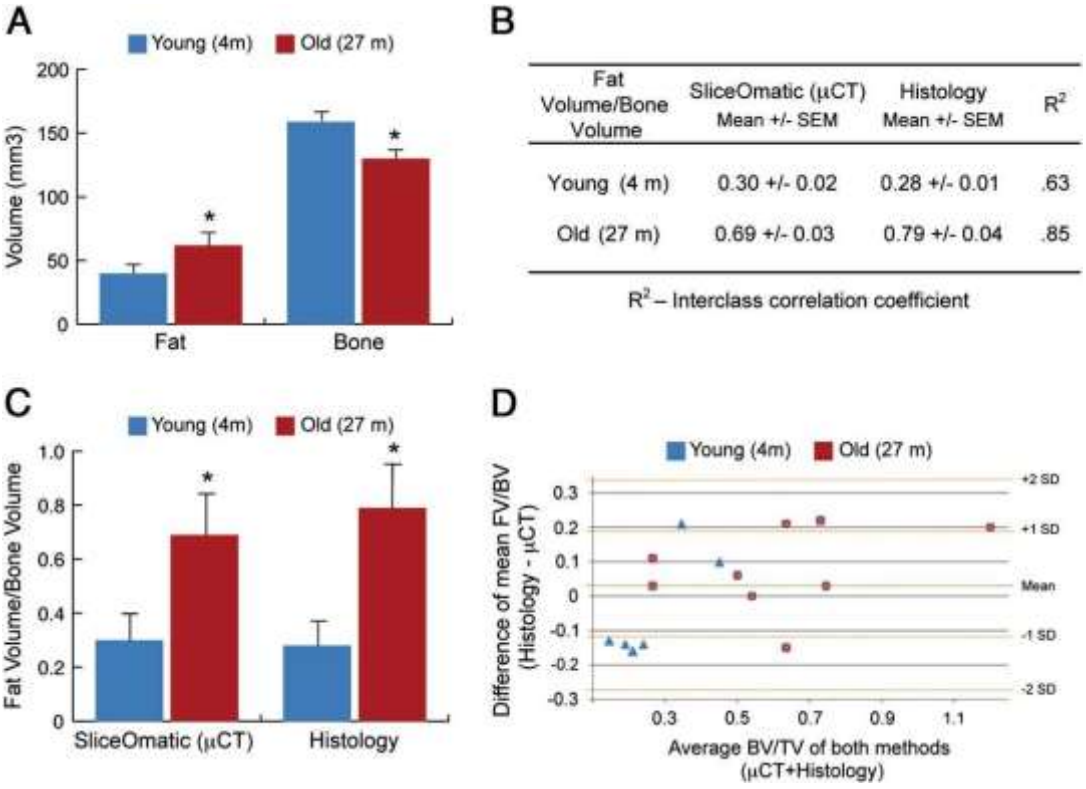

Fig. 2. Age-related changes in fat and bone volume in young (4 m) vs. old (27 m) LOU rats. (A) Bone and fat volumes were quantified in μCT images using SliceOMatic. The figure shows an age-related increase in fat volumes with a concomitant significant decrease in bone volume in old rats as compared with the younger group. *p b 0.001 for the comparison between young and old rats. (B) Correlation between volumes quantified by μCT vs. histology is shown in panel B (table). The correlation between both methods was significantly higher in the older rats. Panel C shows a significant difference in FV/BV ratio between young and old rats (n= 22), which was similar in both methods. Results represent mean ± standard error of the mean (SEM) after analysis of three different ROIs in two bone sections per rat by two independent observers. *p b 0.001 for the comparison between young and old rats. (D) Bland–Altman plot analysis showed a good level of agreement between both methods. The agreement was stronger when quantifying FV and BV in the older rats.

(Fig. 2C, p b 0001). Both methods (histology and SliceOMatic) showed a significant increase (~ 2 fold) in the FV/BV ratio in the old rats as compared with their young counterparts (Fig. 2C, p b 0001).

3.3.4 Agreement between SliceOMatic and histology

Using a Bland–Altman plot, Micro CT image analysis method demonstrated good agreement with histology (Fig. 2D). All volume ratios calculated by both methods lie within ±2 SD from the mean volume ratio difference.

3.4 Discussion

In this study we successfully correlated image and histology analysis of the marrow fat/bone relationship in the aging skeleton. We validated anon-invasive method of FVquantification with μCT images using well-established imaging software. Consistent with previous invasive studies (Justesen et al., 2001; Verma et al., 2002) and with our own previous report in this same model (Duque et al., 2009), our noninvasive quantification indicates that FV increases and BV decreases with age in this animal model. In addition, our non-invasive method shows a high intra- and inter-rater reliability for duplicate measurements, demonstrates high correlation and good agreement with the gold standard when quantifying age-related changes in marrow fatinfiltration.

Biopsy studies with animal models (Duque et al., 2009) and humans (Verma et al., 2002; Meunier et al., 1971) have demonstrated a significant increase in FV and a parallel decline in BV in aging bone.

Studies looking at age-related changes in bone mineral structure in both an invasive and non-invasive manner have shown a high level of

correlation and reliability (Muller et al., 1996; Schmidt et al., 2003). In contrast, despite growing interest in the role of bone marrow adipocytes in the pathogenesis of osteoporosis, noninvasive studies quantifying marrow fat are mostly limited to MRI (Griffith et al., 2005; Shen et al., 2007) and have not been correlated with histology.

In this study we correlated μCT analysis of marrow fat with histology in bones obtained from aging rats. μCT has been used to quantify visceral adipose tissue in animal models (Luu et al., 2009; Judex et al., 2010), however its usefulness in marrow fat quantification remains unknown.

Considering that the aging human skeleton is characterized by low bone mass arising from a reduction in bone formation, uncompensated bone resorption, and an increase in bone marrow adipogenesis (Zhou et al., 2008; Justesen et al., 2001), an animal model that exhibits similar physiological changes is ideal for the study and evaluation of bone changes with aging. We therefore used aging LOU rats as they have been shown to be a good model of healthy aging due to their longevity, absence of obesity and systemic pathologies that may confound skeletal changes that occur with aging (Alliot et al., 2002). Furthermore, their bone phenotype, showing the hallmarks of senile osteoporosis, has recently been characterized (Duque et al., 2009).

To correlate between invasive and non-invasive methods, we compared histology and image analysis of FV/BV in aging LOU rats using the SliceOMatic imaging software. This software is a validated, reference standard, and non-invasive tool to measure adipose tissue (Demerath et al., 2007; Bonekamp et al., 2008), which has not been previously tested in bone. In our analyses, hematopoietic volume was not considered due to its inconsistent relationship with other volumes (Ogawa et al., 2000; Hirano and Iwasaki, 1992) and its variability with age (Burkhardt et al., 1987). Therefore, in this study the ratio FV/BV is

chosen because these parameters have been widely assessed in biopsy specimens and their relationship with age has shown better consistency (Justesen et al., 2001; Verma et al., 2002).

The validity of this method is demonstrated by the high inter- and intra-rater reliability, high correlation with histology quantification and good agreement with the gold standard. Although this method still requires validation in human bone images, the clinical applicability of noninvasive quantification of marrow fat is on the horizon considering the emergence of new imaging methods, such as pQCT in bone (Burghardt et al., 2010; Liu et al., 2010; Nishiyama et al., 2010), which provides better and more accurate information on bone microarchitecture and therefore could increase the usefulness of this image analysis method.

However, there were limitations in this study that must be addressed. One difficulty is that there is no established reference range of gray scale threshold (GLI) values for marrow fat that can be used to determine the region of interest from which volumes were calculated. The different threshold ranges obtained by the average of 20 quantifications per representative areas in 66 images may have a degree of error that is not quantifiable. However our concept of multiple thresholds is similar to an earlier study (Kuhn et al., 1990), which used different thresholds for different tissues in the analysis of μCT images and was shown to be accurate compared with histology. Another limitation is that, as in histology sections, the volumes calculated from the images are not 3D volumes but an average of the total volume of three cross sections, thus the true volume may be significantly underestimated.

1. Conclusion

In conclusion, non-invasive quantification of FV/BV ratio using image analysis software is a useful and reliable tool to quantify one of the hallmarks of age-related bone loss and senile osteoporosis. The fact that this method is comparable to histology for identifying age related changes in marrow adiposity assures the use of this noninvasive method for aging bone research in the near future.

Acknowledgements

This study was supported by a project grant from the Australian National Health and Medical Research Council (NHMRC, Grant # 632767) and by an operating grant from the Nepean Medical Research Foundation. A/Prof. Duque and Dr Li hold Fellowships from the University of Sydney Medical Research Foundation. Dr Demontiero holds a scholarship from The Rebecca Cooper Medical Research Foundation. The authors are deeply grateful to the members of the Quebec Network for Research in Aging for providing us with samples from their LOU rat colony.

3.5 References

Alliot, J., Boghossian, S., Jourdan, D., Veyrat-Durebex, C., Pickering, G., Meynial-Denis, D., Gaumet, N., 2002. The LOU/c/jall rat as an animal model of healthy aging? J. Gerontol. Biol. Sci. Med. Sci. 57A, B312–B320.

Bonekamp, S., Ghosh, P., Crawford, S., Solga, S., Horska, A., Brancati, F., Diehl, A., Smith, S., Clark, J., 2008. Quantitative comparison and evaluation of software packages for assessment of abdominal adipose tissue distribution by magnetic resonance imaging. Int. J. Obes. 32, 100–111.

Brandi, M., 2009. Microarchitecture, the key to bone quality. Rheumatology 48, iv3–iv8.

Burghardt, A.J., Kazakia, G.J., Sode, M., Papp, A.E., Link, T.M., Majumdar, S., 2010. A longitudinal HR-pQCT study of alendronate treatment in post-menopausal women with low bone density: relations between density, cortical and trabecular microarchitecture, biomechanics, and bone turnover. J. Bone Miner. Res. June [Epub ahead of print].

Burkhardt, R., Kettner, G., Bohm, W., Schmidmeier, M., Schlag, R., Frisch, B., Mallmann, B., Eisenmenger, W., Gilg, T., 1987. Changes in trabecular bone, hematopoiesis and bone marrow vessels in aplastic anemia, primary osteoporosis, and old age: a comparative histomorphometric study. Bone 8, 157–164.

Delmas, P., Seeman, E., 2004. Changes in bone mineral density explain little of the reduction in vertebral or nonvertebral fracture risk with anti-resorptive therapy. Bone 34, 599–604.

Demerath, E., Ritter, K., Couch, W., Rogers, N., Moreno, G., Choh, A., Lee, M., Remsberg, K., Czerwinski, S., Chumlea, W., Siervogel, R., Towne, B., 2007. Validity of a new automated software program for visceral adipose tissue estimation. Int. J. Obes. 31, 285–291.

Duque, G., Rivas, D., Wei, L., Ailian, L., Henderson, J., Ferland, G., Gaudreau, P., 2009. Accelerated bone loss in the LOU/c rat model of healthy ageing. Exp. Gerontol. 44, 183–189.

Griffith, J., Yeung, D., Antonio, G., Lee, F., Hong, A., Wong, S., Lau, E., Leung, P.C., 2005. Vertebral bone mineral density, marrow perfusion, and fat content in healthy men and men with osteoporosis: dynamic contrast-enhanced MR imaging and MR spectroscopy. Radiology 236, 945–951.

Hirano, T., Iwasaki, K., 1992. Bone marrow plays a role in bone metabolism: histomorphometry of iliac bone in postmenopausal women. Calcif. Tissue Int. 51, 348–351.

Janssen, I., Heymsfield, S., Baumgartner, R., Ross, R., 2000. Estimation of skeletal muscle mass by bioelectrical impedance analysis. J. Appl. Physiol. 89, 465–471.

Judex, S., Luu, Y.K., Ozcivici, E., Adler, B., Lublinsky, S., Rubin, C.T., 2010. Quantification of adiposity in small rodents using micro-CT. Methods 50, 14–19.

Justesen, J., Stenderup, K., Ebbesen, E., Mosekilde, L., Steiniche, T., Kassem, M., 2001. Adipocyte tissue volume in bone marrow is increased with aging and in patients with osteoporosis. Biogerontology 2, 165–171.

Kanis, J., Borgstrom, F., Laet, C., Johansson, H., Johnell, O., Jonnson, B., Oden, A., Zethraeus, N., Pfleger, B., Khaltaev, N., 2005. Assessment of fracture risk. Osteoporos. Int. 16, 581–588.

Kuhn, J.L., Goldstein, S.A., Feldkamp, L.A., Goulet, R.W., Jesion, G., 1990. Evaluation of a microcomputed tomography system to study trabecular bone structure. J. Orthop. Res. 8, 833–842.

Leslie, W., Hans, D., 2009. Commentary on lumpers and splitters: the FRAX debate continues. J. Bone Miner. Res. 24, 1789–1792.

Liu, X.S., Cohen, A., Shane, E., Yin, P.T., Stein, E.M., Rogers, H., Kokolus, S.L., McMahon, D.J., Lappe, J.M., Recker, R.R., Lang, T., Guo, E., 2010. Bone density, geometry, microstructure and stiffness: relationships between peripheral and central skeletal sites assessed by DXA, HR-pQCT, and cQCT in premenopausal women. J. Bone Miner. Res. 9999 Published Online: 30 April.

Luu, Y.K., Lublinsky, S., Ozcivici, E., Capilla, E., Pessin, J.E., Rubin, C.T., Judex, S., 2009. In vivo quantification of subcutaneous and visceral adiposity by micro-computed tomography in a small animal model. Med. Eng. Phys. 31, 34-41.

Marshall, D., Johnell, O., Wedel, H., 1996. Meta-analysis of how well measures ofbone mineral density predict occurrence of osteoporotic fractures. B. M. J. 312, 1254–1259.

Meunier, P., Aaron, J., Edouard, C., Vignon, G., 1971. Osteoporosis and the replacement of cell populations in the marrow by adipose tissue. A quantitative study of 84 iliac bone biopsies. Clin. Orthop. Relat. Res. 80, 147–154.

Mitsiopoulos, N., Baumgartner, R., Heymsfield, S., Lyons, W., Gallagher, D., Ross, R., 1998. Cadaver validation of skeletal muscle measurement by magnetic resonance imaging and computerized tomography. J. Appl. Physiol. 85, 115–122.

Muller, R., Hahn, M., Vogel, M., Delling, G., Ruegsegger, P., 1996. Morphometric analysis of noninvasively assessed bone biopsies: comparison of high-resolution computed tomography and histologic sections. Bone 18, 215–220.

Nguyen, N., Frost, S., Center, J., Eisman, J., Nguyen, T., 2007. Development of a nomogram for individualizing hip fracture risk in men and women. Osteoporos. Int. 18, 1109-1117.

Nishiyama, K.K., Macdonald, H.M., Buie, H.R., Hanley, D.A., Boyd, S.K., 2010. Postmenopausal women with osteopenia have higher cortical porosity and thinner cortices at the distal radius and tibia than women with normal aBMD: an in vivo HR-pQCT study. J. Bone Miner. Res. 25,882–890.

Ogawa, T., Kitagawa, M., Hirokawa, K., 2000. Age-related changes of human bone marrow: a histometric estimation of proliferative cells, apoptic cells, T cells, B cells, and macrophages. Mech. Ageing Dev. 117, 57–68.

Parfitt, A., Drezner, M., Glorieux, F., Kanis, J., Malluche, H., Meunier, P., Ott, S., Recker, R., 1987. Bone histomorphometry: standardization of nomenclature, symbols and units.
J. Bone Miner. Res. 2, 595–610.

Pasco, J., Seeman, E., Henry, M., Merriman, E., Nicholson, G., Kotowicz, M., 2006. The population burden of fractures originates in women with osteopenia, not osteoporosis. Osteoporos. Int. 17, 1404-1409.

Richard, S., Torabi, N., Franco, G., Tremblay, G., Chen, T., Vogel, G., Morel, M., Cléroux, P., Forget, R., Komarova, S., Tremblay, M., Li, W., Li, A., Gao, Y., Henderson, J., 2005. Ablation of the Sam68 RNA binding protein protects mice from age-related bone loss. PLoS Genet. 1, e74.

Rozman, C., Feliu, E., Berga, L., Reverter, J., Climent, C., Ferran, M., 1989. Age related variations of fat tissue fraction in normal human bone marrow depend on both size and number of adipocytes: a stereological study. Exp. Hematol. 17, 34- 37.

Sandhu, S.K., Nguyen, N.D., Center, J.R., Pocock, N.A., Eisman, J.A., Nguyen, T.V., 2010. Prognosis of fracture: evaluation of predictive accuracy of the FRAX™ algorithm and Garvan nomogram. Osteoporos. Int. 21, 863-871.

Schellinger, D., Lin, C., Hatipoglu, H., Fertikh, D., 2001. Potential value of vertebral proton MR spectroscopy in determining bone weakness. AJNR Am. J. Neuroradiol. 22, 1620–1627.

Schellinger, D., Lin, C., Lim, J., Hatipoglu, H., Pezzulo, J., Singer, A., 2004. Bone marrow fat and bone mineral density on proton MR spectroscopy and dual-energy x-ray absorptiometry: their ratio as a new indicator of bone weakening. AJR Am. J. Roentgenol. 183, 1761–1765.

Schmidt, C., Priemel, M., Kohler, T., Weusten, A., Muller, R., Amling, M., Eckstein, F., 2003. Precision and accuracy of peripheral quantitative computed tomography (pQCT) in the mouse skeleton compared with histology and microcomputed tomography (μCT). J. Bone Miner. Res. 18, 1486–1496.

Seeman, E., Delmas, P.D., 2006. Bone quality − the material and structural basis of bone strength and fragility. N. Engl. J. Med. 354, 2250–2261.

Shen, W., Chen, J., Punyanitya, M., Shapses, S., Heshka, S., Heymsfield, S., 2007. MRI measured bone marrow adipose tissue is inversely related to DXA-measured bone mineral in Caucasian women. Osteoporos. Int. 18, 641–647.

Tanaka, Y., Inoue, T., 1976. Fatty marrow in the vertebrae a parameter for haematopoietic activity in the aged. J. Gerontol. 31, 527–532.

Valverde-Franco, G., Binette, J.S., Li, W., Wang, H., Chai, S., Laflamme, F., Tran-Khanh, N., Quenneville, E., Meijers, T., Poole, A., Mort, J., Buschmann, M.D., Henderson, J., 2006. Defects in articular cartilage metabolism and early arthritis in fibroblast growth factor receptor 3 deficient mice. Hum. Mol. Genet. 15, 1783–1792.

Verma, S., Rajaratnam, J., Denton, J., Hoyland, J., Byers, R., 2002. Adipocytic proportion of bone marrow is inversely related to bone formation in osteoporosis. J. Clin. Pathol. 55, 693–698.

Yeung, D., Griffith, J., Antonio, G., Lee, F., Woo, J., Leung, P., 2005. Osteoporosis is associated with increased marrow fat content and decreased marrow fat unsaturation: a proton MR spectroscopy study. J. Magn. Reson. Imaging 22, 279–285.

Zhou, S., Greenberger, J., Epperly, M., Goff, J., Adler, C., LeBoff, M., Glowacki, J., 2008. Age related intrinsic changes in human bone-marrow-derived mesenchymal stem cells and their differentiation to osteoblasts. Aging Cell 7, 335–343.

4.0 Chapter 4: The effect of Dietary Fatty Acids on Bone Marrow Fat in a Murine Model of Senile Osteoporosis

Abstract:

Ageing induces high levels of marrow fat infiltration, which has a deleterious effect on bone mass. In contrast, dietary fatty acids may exert protective effects on bone. In this study, we aimed to analyse the changes in bone parameters and fat distribution induced by different dietary fatty acids in a mice model of senile osteoporosis.

4.1 Introduction

Although excess adiposity is detrimental to bone, evident by the negative association with bone mass and positive correlation with bone fractures,[1-4] it has been postulated that fatty acid quality may be the real determining factor. The quality is determined in turn by the origin of the fatty acids; the structure of the fatty acids; the relative concentration and the metabolic context in which the fatty acids are present.[5] Indeed, fatty acids in one group may be beneficial, while another group may be detrimental to bone.[6] Data from *in vivo* and *in vitro* studies have shown that saturated fatty acids (SFAs) or omega−6 poly-unsaturated fatty acids (ω-6 PUFAs) induce bone loss, while omega−3 poly-unsaturated fatty acids (ω-3 PUFAs) are believed to protect bone health.[7-14] However, mechanisms underlying the impact fat intake has in bone changes remain quite controversial, and with numerous fatty acids present in the human diet, the mechanisms of action are complex and far from being well understood (Fig. 1).[5]

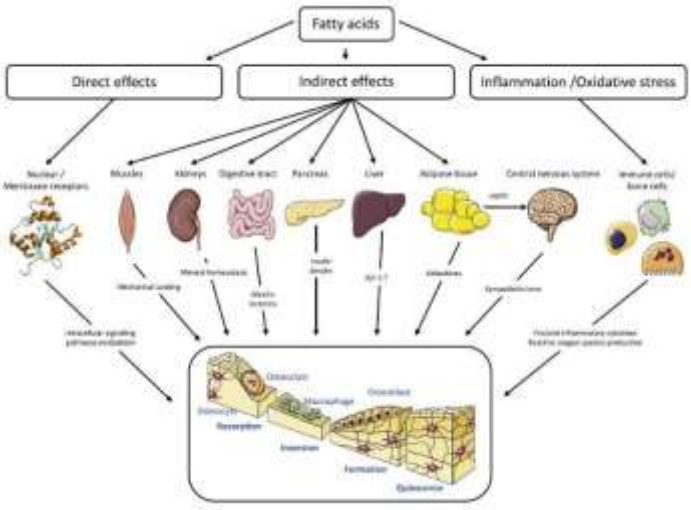

Figure 1. *Fatty acids and bone remodelling relationships: overview. This figure summarizes how fatty acids may impact bone remodelling either directly or indirectly.*[5]

The mechanisms by which PUFAs affect bone are complex. However, it is considered to involve the modulation of a number of molecular signalling pathways and fatty acid metabolites, including prostaglandins; resolvins and protectins; cytokines and growth factors. With respect to ω-3 PUFAs, it modulates bone metabolism by releasing less prostaglandin E2 (PGE2), reducing receptor-activated nuclear kappa-β ligand (RANKL); modulating the concentration of proinflammatory cytokines; stimulating production and release of IGF1; and enhances calcium retention in bone;[11, 15] whereas, ω-6 PUFAs induce osteoclastic activity by attenuating OPG/RANKL gene expression in osteoblasts and stimulate MSC to differentiate into adipocytes, which ultimately results in a decreased production of osteoblasts.[16]

In general, the metabolites of these two types of PUFAs seem to carry out opposing physiological processes. Eicosanoids derived from ω-6 have predominantly proinflammatory actions and in contrast, those produced by ω-3 have anti-inflammatory actions.[16, 17] In addition, metabolites of ω-6 and ω-3 fatty acids act on progenitor cells of osteoblast and adipocytes.[16] Either the fatty acids themselves or their metabolites can trigger the shift from osteoblastogenesis to adipogenesis[18] by the binding Peroxisome Proliferator-Activated Receptors (PPARs).[19, 20] In a co-culture model of primary human cells, the

presence of mature adipocytes induced a significant inhibition of osteoblastic cell proliferation. This effect appeared to be mediated by fatty acids released by the adipocytes-mainly docosahexaenoic acid (22:6 (n-3); DHA) and arachidonic acid (20:4 (n-6); AA).[21]

To date, animal studies showing the impact of fatty acids on bone have correlated fatty acid profile with bone tissue indices and indices of calcium metabolism. Some studies quantified bone formation, bone resorption markers and markers of calcium metabolism.[22-26] These studies showed a positive association between higher n-3 PUFA levels and trabecular surface and tissue level bone formation rates[22]; Serum biomarkers of bone formation (R^2 of 0.51 to 0.34)[23]; and increased intestinal calcium absorption (mg/24 h), calcium balance (mg/24 h) and bone calcium (mg/g bone ash).[26] Some quantified bone morphology, such as areas and cross-sectional moment of inertia[25, 27] and others, have measured BMD[28] and bone mineral content.[25, 29, 30] Studies looking at bone strength outcomes showed low n-6/n-3 PUFA ratio in the femur was negatively correlated with bone mineral content (BMC) (r=-.57, P=.01) and peak load at femur midpoint (r=-.53, P=.02) and femur neck (r=-.52, P=.02). Moreover, long-chain n-3 PUFA, eicosapentaenoic acid and docosahexaenoic acid also significantly and positively correlated with BMC and peak load.[29]

Only one study examined the direct effects of fatty acid on adipocytes.[18]This study showed that when cells from osteoblastic lineage are grown in free fatty acids enriched medium (palmitic and linoleic acids), they develop such features as lipid vesicles in the cytoplasm resembling adipocyte. It also showed increased expression of aP2, a late adipocytic differentiation marker gene, in both preadipocytes and osteoblastic cells.

However, a direct relationship between dietary free fatty acids concentration and the amount of marrow fat have not been described. Given the integral role of adipocytes within the bone marrow milieu, and the demonstrated relationship between amount of

marrow fat, age, bone quality and importance of dietary interventions in osteoporosis, there is a need to examine effects of dietary lipids on marrow fat. Determining the amount of marrow fat induced by different dietary lipids is important, as dietary interventions are an important part of osteoporosis management.

This is the first study to quantify marrow fat, and the first to employ a non-invasive imaging based technique. In addition, previous studies did not use animal models that mimic senile osteoporosis physiologically. In this study, senescence-accelerated prone mice (SAMP8) were used to mimic senile osteoporosis, as this model features sarcopenia and osteoporosis, and it is consistent with clinical features associated with older and ageing adults. Senescence accelerated mice-Resistant 1 (SAMR1) were used as normal ageing controls.

Thus, following on from the known relationship between fatty acid and skeletal effects, and the relationship between ageing bone and adipogenesis so far, this study's objective was to evaluate marrow adiposity induced by different dietary fatty acids in a mouse model of age related osteoporosis. We hypothesise that over 10 months, a sunflower diet (low in n-3 PUFA) will be associated with an increase in marrow fat tissue volume in all mice, other than the mice on the control diet. The secondary hypotheses are

- The increase in marrow fat volume will be greater in osteoporotic mice (SAMP 8) than non-osteoporotic mice (SAMR1)
- The effects of sunflower will be altered by the changes in proportion of ω6 and ω3 fatty acids.

4.2 Materials and methods

The present study was part of a larger study that was designed to evaluate *"the impact of fatty acid quality on the age related evolution of the locomotor system and to understand*

which ageing mechanisms are involved."[31]

Two-month-old senescence accelerated P8 (SAMP8) mice and their SAMR1 normal controls were allocated into 4 different groups (n=20/group) and administered the following diets:

- Standard "growth"
- "Sunflower" (high ω6/ω3 ratio)
- Borage (high γ linoleic acid)
- "Fish" (high in long ω3).

Mice were fed ad-libitum for 10 months, and then euthanized for bone and fat investigation using pathology and micro-CT technologies. CT scan images were analysed by Tomovision SliceOMatic 4.3 Rev-6i software (Tomovision, Montreal, QC, Canada). Images were blind-assessed by two evaluators. One hundred slices of the region of interest were selected for each mouse. A total of 8000 CT scan sections were analysed. Total tissue volume, marrow fat volume and bone volume were determined and compared between different dietary groups.

4.2.1 Ethics

The institution's animal welfare committee approved all animal procedures. All procedures complied with the National Research Council's guidelines for the care and use of laboratory animals. Animals were housed in the animal laboratory of the INRA Research Centre for Human Nutrition (http://www1.clermont.inra.fr/unh/telechargementinternet /ienplaquette.pdf). A controlled environment housed the animals for the duration of the study (12:12 h light–dark cycle, 20–22 °C, 50–60% relative humidity; 5 mice per plastic cage with free access to water). Animals were delivered to the facility 1 month before the study for acclimatization to the local animal environment. When the protocol ended, blood was drawn on

anesthetized animals. Then, animals were sacrificed by IP injection of lethal dose of pentobarbital sodium (0.1 ml/g of body weight — CEVA Santé Animale, Libourne, France) and tissues were harvested, frozen and stocked prior to investigation.

4.2.2 Animals

One- month -old female Senescence accelerated mouse-Prone 8 (SAMP8) and Senescence accelerated mouse-Resistant 1 (SAMR1) derived from AKR/J strain were obtained from INRA-Dijon (UMR INRAENESAD Flaveur, Vision et Comportement du consommateur, 21065 Dijon Cedex, France). As an acclimatization period, they were provided with free access to a standard growth diet for a month. Subsequently, SAMR1 and SAMP8 animals were randomly allocated into different groups and submitted to different diets ad libitum for 10 months (Fig. 2), after ensuring that daily food intake was not modified significantly by diet enrichment. Randomization was conducted using a computer-generated random numbers program (http://www.graphpad.com/quickcalcs/index.cfm).

The experimental procedure was conducted with a total of 20 mice per group to allow data analysis on at least 12 mice per group at the end of the protocol. Thus, 40 SAMR1 were randomized into the standard growth diet or sunflower diet group, and 80 SAMP 8 mice were randomized into one of the four groups as depicted in Figure 2. Further, the experimental protocol was designed not to exceed 10 months, to avoid a dramatic increase in SAMP8 mortality, which is observed from 12 months of age.[32]

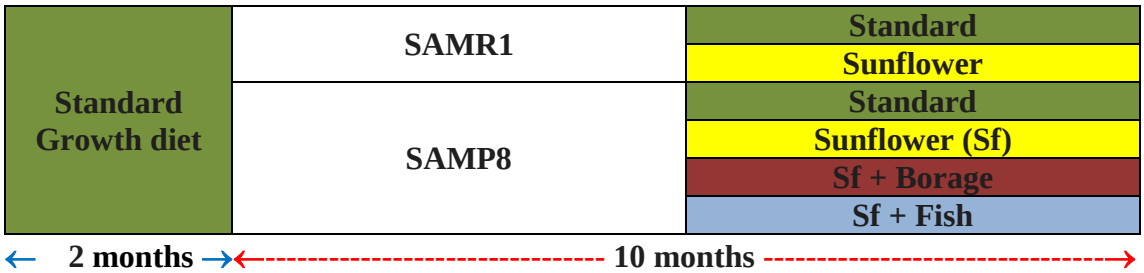

Figure 2. Schema of diet regimen

4.2.3 Diets

Diets were purchased from INRA (Jouy-en-Josas, France) or Harlan (Ganat France). Adjustments were made to all diets to ensure they had similar caloric values (Δb5%). SamR1 mice received either the control diet, standard growth diet (Harlan Teklad Global 2019) or a sunflower oil based diet with a high ω6/ω3 Polyunsaturated Fatty Acid (PUFA) ratio (Tables 1 and 2). In parallel, SamP8 mice were fed either a standard growth diet (Harlan Teklad Global 2019), a sunflower oil based diet or an enriched sunflower oil based diet with varying fatty acid composition (Table 1). To examine the effects of γ-Linolenic acid (18:3 ω6; GLA) enrichment, Borage was used; and to test the effect of lowering ω6/ω3 ratios (by providing Eicosapentaenoic acid (20:5 ω3; EPA) and Docosohexaenoic (22:6 ω3; DHA)), fish oils were used.

4.2.4 Bone morphological analysis

An eXplore CT 120 scanner (GE Healthcare, Canada) was used to conduct bone morphological analysis. Frozen femoras, cleaned of soft tissues, were scanned. Three hundred and sixty degree images are acquired in 1° increments, collected in a single complete gantry rotation, with a 20ms exposure/ view and X-ray energy settings of 100 kV and 50 mA. A built in modified cone beam algorithm was used to reconstruct CT images with isotropic voxels of 0.045×0.045×0.045 mm3. CT scans were analysed using SliceOmatic (Tomovision™, Montreal,

Canada). Images were blind-assessed by two evaluators. Images were manually visually inspected, and selected to avoid artefacts and poor quality. The axial slice representing the centre of the femur (starting 0.1 mm proximally from the growth plate and extending a further 0.32 mm in the proximal direction) was determined manually and was used as the reference slice. Fifty regions of interest were selected from both sides of the central axial slice, totalling one hundred axial slices of femur being selected as the region of interest for each mouse. A total of 8000 CT scan sections were analysed across all mice. Using our previously validated approach,[33] bone and marrow tissue (blood and fat) were manually assessed and the range of gray-scale density levels were determined. The thresholds obtained in the validation study were converted to equivalent gray scale values for the device used in this study. Subsequently, to isolate bone, marrow fat and blood tissue respectively, the following thresholds were applied: bone ≥1901, -750 ≤ marrow fat ≤450 and 451≤ blood ≤ 1900 (Fig. 3). In primary analysis, bone marrow fat volumes were then calculated using an automated algorithm in SliceOmatic. For secondary analyses, bone volumes and blood volumes were also calculated.

Ingredient (g/100 g diet)	Standard diet (Harlan 2019)	Sunflower based diet	Borage enriched diet	Fish enriched diet
Wheat starch	55.24	59.14	56.79	56.79
Casein	19.00	19.20	19.20	19.20
Sucrose	4.16	4.16	4.16	4.16
Fiber cellulose	3.60	3.50	3.50	3.50
DL méthionine	3.30	0.30	0.30	0.30
Choline bitartrate	0.20	0.20	0.20	0.20
Mineral mix	3.50	2.50	2.50	2.50
Vitamin mix	1.00	1.00	1.00	1.00
Sunflower oil	0.00	5.45	5.62	6.73
Canola oil	0.00	2.73	3.37	3.37
Borage oil	0.00	0.00	2.79	0.00
Fish oil	0.00	0.00	0.00	1.68
Oleisol oil	0.00	1.82	0.57	0.57
Soybean oil	10.00	0.00	0.00	0.00
Energy (cal)	420	428	440	440

Table 1. Diet formulations.

Fatty acids	Standard diet (Harlan 2019)	Sunflower based diet	Borage enriched diet	Fish enriched diet
12:0	0.71	0.00	0.00	0.00
14:0	0.15	0.05	0.05	0.09
15:0	0.00	0.00	0.00	0.00
16:0	11.35	5.11	6.58	5.03
17:0	0.00	0.02	0.01	0.01
18:0	3.24	2.75	2.89	2.97
19:0	0.00	0.00	0.00	0.00
20:0	0.25	0.19	0.16	0.16
22:0	0.08	0.24	0.12	0.12
Total SFA	15.78	8.36	9.81	8.38
16:1	0.15	0.08	0.14	0.19
18:1 n−9	23.4	46.89	36.84	37.77
18:1 n−7	0.00	0.00	0.21	0.52
20:1	0.54	0.34	1.17	0.73
22:1	0.05	0.00	0.54	0.00
24:1	0.00	0.00	0.34	0.00
Total MUFA	24.14	47.31	39.24	39.21
18:2 n−6	54.23	42.04	43.40	40.51
18:3 n−6	0.00	0.00	5.19	0.00
20:4 n−6	0.00	0.00	0.00	0.31
Total PUFA ω-6	54.23	42.04	48.59	40.82
18:3 n−3	5.93	2.29	2.35	2.38
18:4 n−3	0.01	0.00	0.00	0.52
20:4 n−3	0.00	0.00	0.00	0.32
20:5 n−3	0.00	0.00	0.00	6.35
21:5 n−3	0.00	0.00	0.00	0.22
22:5 n−3	0.00	0.00	0.00	0.31
22:6 n−3	0.00	0.00	0.00	1.50
Total PUFA ω-3	5.94	2.29	2.35	11.60
Total PUFA	60.16	44.33	50.94	52.4
LA/ALA	9.14	18.35	18.46	17.02
n−6/n−3	9.13	18.35	20.67	3.52
Total percent	100.00	100.00	100.00	100.00

Table 2. Diets' fatty acid composition (% of total fatty acids).

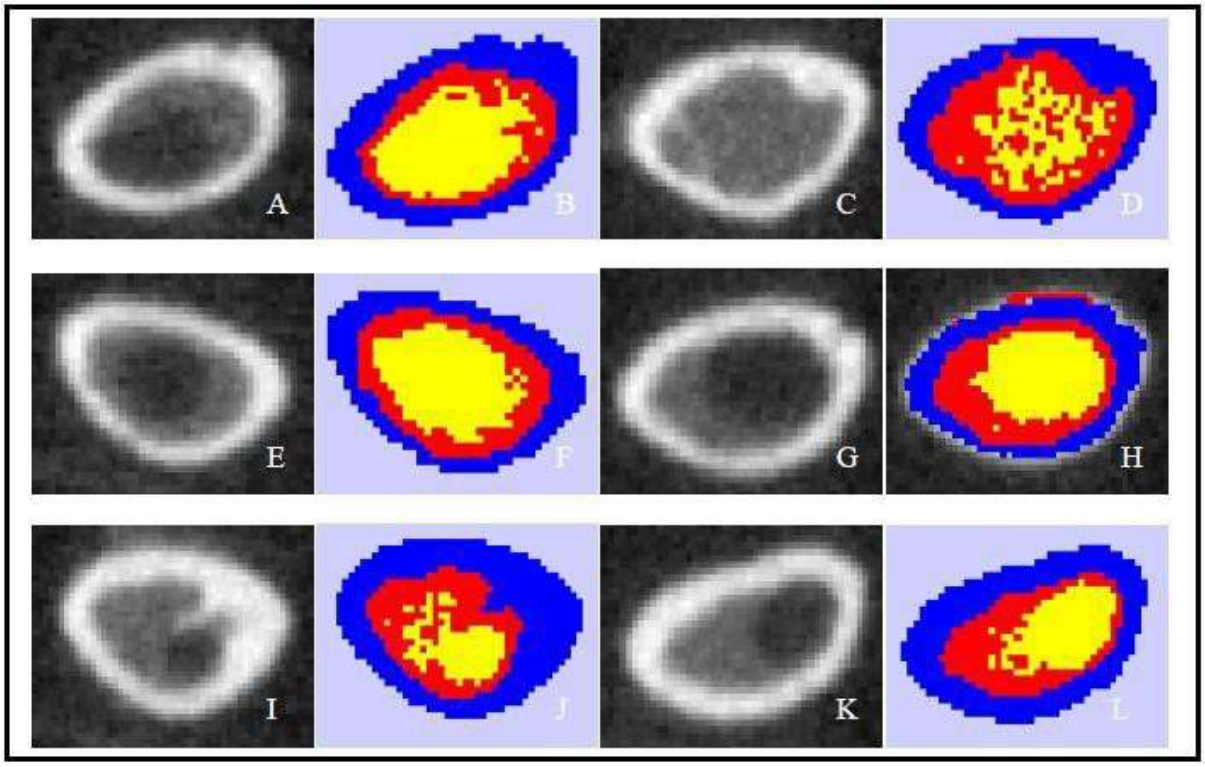

Figure 3. SAMR1 on Growth diet (A&B) and Sunflower diet (C&D). SAMP8 on Growth diet (E&F), Sunflower diet (G&H), Fish diet (I&J), and Borage diet (K&L).

4.2.5 Data Analysis

Data on all variables are expressed as group means ± standard deviations. An initial analysis comparing marrow fat volumes and bone volumes of SAMR1 and SAMP8 mice on a standard growth diet was carried out using independent t tests. This was to show how well the SAMP8 mice phenotype represented the progeria model. Similarly, independent t tests were used to compare the effects of a sunflower diet on marrow fat volumes inSAMR1 mice (standard growth diet vs sun flower diet), and separately in SAMP8 mice (standard growth diet vs sun flower diet). Real differences in marrow fat volumes between all four groups on a sunflower diet were then compared (SAMR1 on standard growth diet and sunflower diet; and SAMP8 on standard growth and sunflower diet) using ANOVA. Finally, the rescue or depressing effects of a fish enhanced diet and

Borage enhanced diet respectively were examined by analysing differences between SAMP8 groups on different diets using ANOVA and Tukeys post hoc tests (IBM SPSS version 20.1). In all of the analyses, P <0.05 was considered to be statistically significant.

4.3 Results

4.3.1 SAMP8 mice as a progeria model

Under a growth diet, SAMP8 mice exhibited lower mean fat volume and higher mean bone volume (Fig. 4A & 4B respectively) - however, these differences to SAMR1 mice were not statistically significant. Similarly, fat volume to bone volume ratio and fat volume fraction overall did not differ significantly between the mice (Fig 4E and 4C respectively) - however, SAMP8 mice on a growth diet showed higher bone volume fraction of 6%, which was significant (Fig 4D).

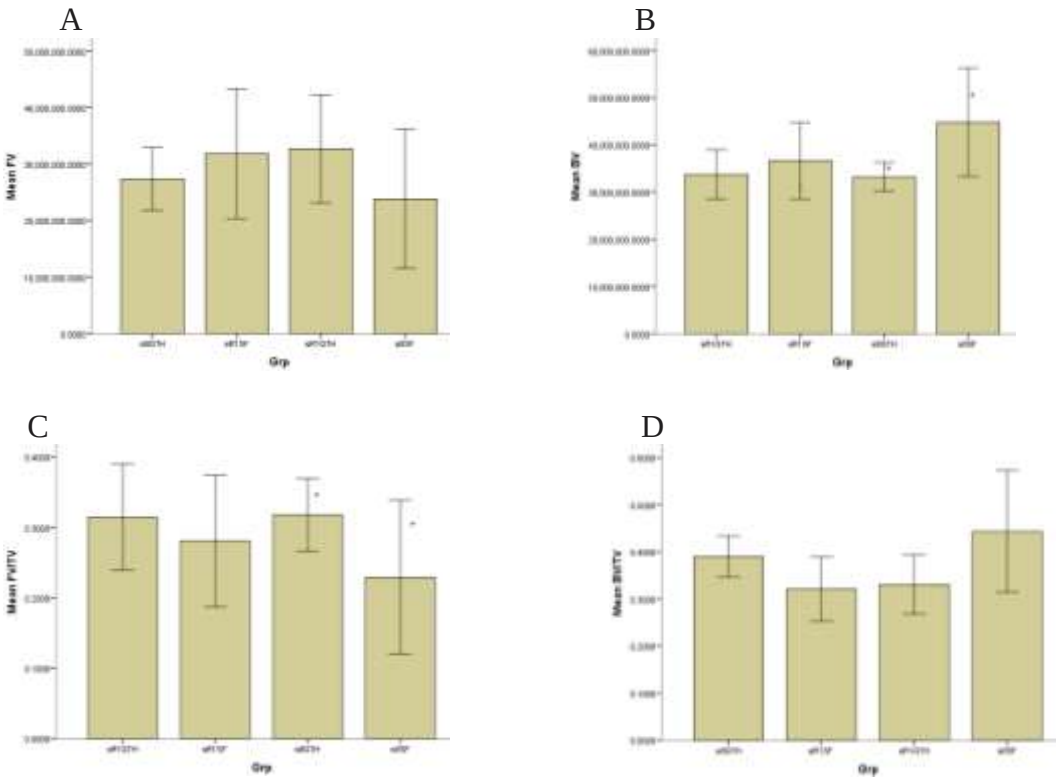

E

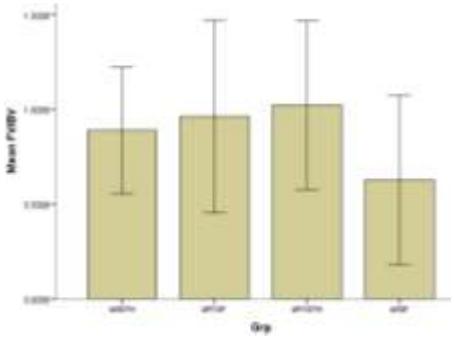

Figure 4. [A] Mean marrow fat volume (Mean FV), [B] Mean bone volume (Mean BV), [C] Mean percentage of fat volume as a proportion of total tissue volume (TV) (Mean FV/TV), [D] Mean percentage of bone volume as a proportion of total tissue volume (Mean BV/TV) and [E] Mean ratio of fat volume to bone volume (Mean FV/BV) in SAMR1 (sR1) and SAMP8 (s8) mice on growth diet (GRTH) and sunflower diet (SF). Significant different groups are marked with * as analysed by Independent Student t Test ($p < 0.05$).

4.3.2 Sunflower diet and marrow fat volumes

When SAMP8 mice were fed s sunflower diet, there was an increase in mean bone volume (24% ± 8%) and a reduction in fat fraction (9% ± 3.5%), compared to SAMP8 on a growth diet (Figs 4B, & 4C respectively). Although mean fat volume reduced (23% ± 10%), fat to bone volume ratio decreased, and bone volume fraction increased (5% ± 4%), these did not reach statistical significance (Figs. 4A, 4E &4D respectively). In contrast, the effects of a sunflower based diet on SAMR1 mice were not statistically significantly different from the effects of a standard growth diet on SAMR1 mice on all skeletal variables (Figs.4A-4E).

4.3.3 Fatty acid enriched diets (Borage [ω-6] and Fish oil [ω-3]) and marrow fat volumes

We then set out to analyse the effects of a sunflower oil based diet and other diets that modulate the fatty acid composition of Borage and fish. Borage oil was used to test the effect of a γ- Linolenic acid (18:3 ω6; GLA) enrichment, and fish oil was used to test the effect of a reduced

ω6/ω3 ratio, by enriching ω-3 content with Eicosapentaenoic acid (20:5 ω3; EPA) and Docosohexaenoic (22:6 ω3; DHA). A one-way between groups analysis of variance was conducted to explore the impact of this variation in dietary fatty acids on marrow fat and bone volumes. There were statistically significant differences in the mean bone volume [F (3, 23.7) = 10, p = .000], fat to bone volume ratio [F (3, 22.8) = 3.6, p = .03] and fat volume fraction [F (3, 23.2) = 6.1, p = .003] between the groups, as determined by a Welch test (Figs 5B, 5C & 5D respectively).

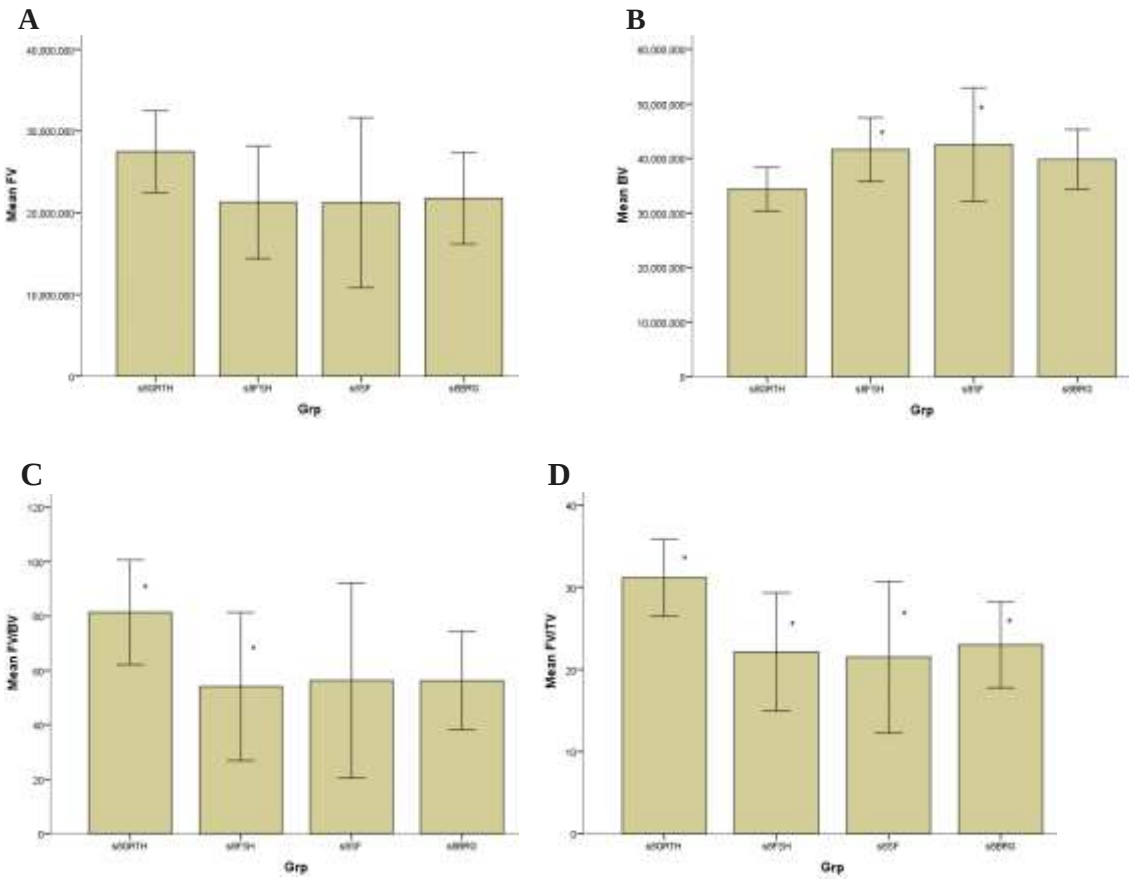

E

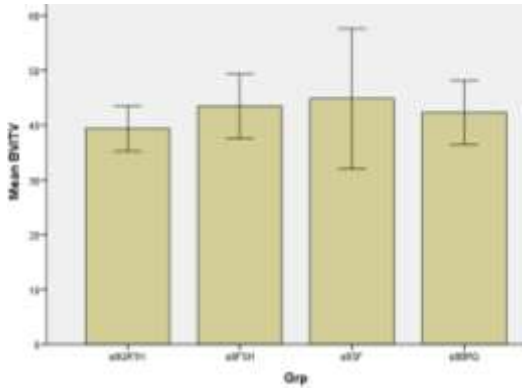

Figure 5. Comparisons of skeletal parameters in SAMP8 mice on standard growth diet (GRTH), sunflower diet (SF), Borage (BRG) and Fish diet (FSH). [A]: Mean Bone Volume (BV) in μm^3, [B] Mean Fat Volume (FV) in μm^3, [C] Mean ratio of fat volume to bone volume (Mean FV/BV), [D] Mean percentage of fat volume as a proportion of total tissue volume (Mean FV/TV), and [E] Mean percentage of bone volume as a proportion of total tissue volume (Mean BV/TV). Significant group differences are marked with * as analysed by ANOVA ($p < 0.05$).

Post-hoc comparisons using the Games-Howell test indicated that the mean bone volumes of SAMP8 mice on the sunflower and fish diet were 34% ± 10.5% and 25% ± 5% higher, compared to SAMP8 mice on the standard diet (Fig 5B). Although the mean bone volume in the borage group was 13.5% ± 9% higher than the standard diet, this was not statistically significant. Fat volume to bone volume ratio was lowered by 29.5 points in the fish diet group, and was statistically significant (Fig 5C). The borage and sunflower diets also lowered the ratio by 24 and 22 points respectively, but were not statistically significant from the growth diet. Fat volume fractions were significantly reduced by both the fish and borage diets by 9.5% ± 2.3% and 7.3% ± 2.1% respectively (Fig 5D). Interestingly, the sunflower diet also reduced fat volume fraction (8.8% ± 3.6%), but the effect did not reach statistical significance. Similarly, despite decreases in mean fat volume by 14% ± 15%, 19% ± 8.5% and 22% ± 8.4% in the sunflower, borage and fish diet groups respectively, these values were not statistically significant (Fig 5B). Likewise, non-statistically significant increases in bone volume fractions of 5% ± 4%, 3% ± 2% and 4% ± 2% in the sunflower, borage and fish diets respectively, (Fig 5E) compared to growth diet, were also

seen.

The sunflower diet protected bone health through positive effects on bone volume and marrow fat fraction. Significantly increasing ω-3 fatty acids in the diet (Fish) maintained positive effects on bone volume, but further lowered fat fraction and fat to bone volume ratio. In addition, increasing ω-6 fatty acids in the diet (Borage) reduces fat fraction, but at the expense of attenuation of bone volume. Dietary regulation of bone mass by sunflower, borage and fish oils is independent of an effect on marrow fat volume, being most likely associated with their direct effect on other bone cells or by regulating fat-secreted factors. Due to their bone-protective effect, sunflower and fish diet could constitute a new nutritional strategy to prevent age-related bone loss in the near future.

4.4 Discussion

In this study, we showed that in an osteoporotic bone microenvironment, a sunflower diet had no significant effect on fat volumes and most bone indices. Enriching the diet with ω-3 fatty acids reduced fat fraction and fat to bone volume ratio, and maintained mean bone volume. On the other hand, increasing the proportion of ω-6 fatty acids reduced fat fraction, but did not affect other marrow fat volume indices and bone indices.

Based on previous animal studies, our first hypothesis was that a sunflower diet containing less total ω6, less total ω3 fatty acids and a high ω6:ω3 fatty acid ratio compared to a standard diet, would be detrimental to bone health and thereby would increase marrow fat. Our findings were, however, the opposite. In fact, when SAMP8 mice diet changed from the standard growth diet to the sunflower based diet, there was a significant reduction in fat tissue fraction (9.7%, p=.001) and an increase in mean bone volume (24%, p =.004). These results

differ from previous animal studies, which showed that a higher ω-6 to ω-3 fatty acids ratio is detrimental to bone health, and higher ω-3 fatty acids or lower ω-6 to ω-3 ratios are conducive to healthy bones.[34, 35]

However, many previous studies have not utilized similar animal models of senile osteoporosis, so comparisons are difficult. Past studies have included young chicks,[22] ovariectomized rats[36] and male rats.[23-26] Previous studies also did not directly measure the amount of adipose tissue or bone tissue, but markers of bone formation and resorption. In one study, young chicks fed a semi-purified diet containing soybean oil high in ω-6 PUFA demonstrated a lower rate of bone formation compared with other chicks given a low dietary ratio of n-6/n-3 fatty acids.[22] In this study, bone ash weight, morphometry and serum alkaline phosphatase were used to determine the effects on bone. Another study compared ovariectomized rats, fed one of four dietary conditions-

- Normal diet
- Low calcium diet (1.5 mg/day)
- EPA-enriched diet (160 mg/day/kg),
- EPA-enriched and low calcium diet.[36]

Bone weight, serum alkaline phosphatase activity and bone strength were the indices to confirm effects of EPA. The results showed that EPA enriched diets were able to prevent the reduction in bone mass (as measured directly by weight) and bone strength, caused by calcium deficiency. Similarly, Claassen et al[26] examined the effects of PFAs, specifically different ratios of ω6:ω3, on calcium balance and indices of bone mineralisation. Here, male Sprague-Dawley rats were fed diets supplemented with linolenic acid (GLA, n-6) and eicoapentaenioc acid (EPA, n-3) in the ratios 3:1, 1:1 and 1:3. Rats fed diets high in (ω-3) or low (n-6)/ (n-3) ratios

displayed higher levels of serum alkaline phosphatase isoenzymes activities, including the bone-specific isoenzyme (BALP).

The ω6:ω3 ratios in these studies ranged from 2[22,24] to 3[23,26] and others varied from lower[25] to slightly higher.[27-30] In our study, ω6:ω3 ratio in the sunflower diet was 18, and the standard growth diet's ratio was 9. These ratios are much higher than the dietary ratios in previous studies that show detrimental effect. However, the sunflower diet in this study has less of the fatty acids that negatively impact bone (half the amount of saturated fatty acids and 12% less total PUFA ω-6). Whether this has an impact on the net outcome of marrow fat and bone volume indices is uncertain, and further studies would need to be done to clarify this.

Our results suggest that more complex interactions are perhaps at play in this model. Is it possible that in the setting of age related osteoporotic marrow microenvironment, the combination of low levels of saturated fatty acids and moderate level of total PUFA ω-6 have independent and positive skeletal effects, augmenting the positive effects of total PUFA and total PUFA ω-3 levels, and thereby negating the negative effects of a high ω6/ω3 ratio? This question cannot be answered by the current study and has not been investigated in previous studies. Furthermore, considering the fact that mean BV increased significantly with a smaller increase in bone volume fraction, whereas FV fraction decreased significantly with a proportionately large reduction in mean fat volume, could it be that essential fatty acids act on bone marrow cells independently and preferentially on adipogenesis over osteoblastogenesis?

It is well recognized that mechanisms of age related bone loss are different to those in menopause related bone loss, and it is plausible that fatty acids behave differently in different bone marrow microenvironments. This is supported by the observation in some human studies of senile osteoporosis, that higher ω-3 in take was not associated with higher BMD,[37,39]or that higher ω-6:ω-3 ratios were not associated with lower BMD.[38,39] In fact, there have been human studies showing that

moderately higher dietary ratios of ω- 6:ω-3 maintained or enhanced bone health.

In one study involving pre- and postmenopausal women, supplementation with ω-6 to ω-3 fatty acids in a ratio of 10:1, combined with calcium, had equivalent effect on bone and bone markers compared to calcium alone.[40] In this randomized clinical trial, 85 healthy premenopausal women (aged 25±40 years, n= 43) and postmenopausal women (aged 50±65, n=42) with normal BMI (18-32) and normal BMD at baseline were allocated either to a diet supplement containing both γ-linolenic acid and eicosapentaenoic acid (in proportions thought to be optimal for bone tissue) in addition to calcium 1.0 gm daily (treatment group), or a usual diet with 1.0 gm calcium only (control group). After 12 months of supplementation, a 1% increase in BMD was observed with both treatment and control groups in premenopausal women, but these increases were not statistically significantly different. Among postmenopausal women, although a decrease in BMD was observed within both groups, there was no significant difference with these changes between the groups. With bone turnover markers, urinary markers of bone resorption (N-telopeptide and hydroxyproline) did not change significantly within groups among the premenopausal women. There were significant decreases in the serum markers of bone formation (osteocalcin and bone-specific alkaline phosphatase). On the other hand, there were significant increases in parathyroid hormone in the treatment group and significant increases in serum Ca in both treatment and control groups, but there were no significant differences between the treatment and control groups for any of these changes. In comparison, markers for bone formation and bone resorption fell in both treatment and control groups among the postmenopausal women, and most of these within-group changes were highly significant. However, there were no significant differences between the treatment and control groups for any of these changes.

Whereas, in another study, a similar supplementation given to postmenopausal women with low bone mass preserved BMD at the spine and increased BMD at the femoral neck compared to

bone loss in the placebo group.[41] Sixty-five women (mean age 79.5) with a diet low in calcium were randomly assigned to γ-linolenic acid (GLA) + eicosapentaenoic acid (EPA) + 600 mg/day calcium carbonate, or coconut oil placebo capsules + 600 mg/day calcium carbonate. Markers of bone turnover and BMD were measured at baseline and at 18 months. Twenty-one patients were continued on treatment for a second period of 18 months, after which BMD (36 months) was measured again. At 18 months, osteocalcin and deoxypyridinoline levels fell significantly in both groups. Lumbar spine BMD did not change in the treatment group, but decreased 3.2% in the placebo group; whereas, femoral BMD increased 1.3% in the treatment group, but decreased 2.1% in the placebo group. Over the second period of 18 months, lumbar spine BMD increased 3.1% in patients who remained on active treatment, and 2.3% in patients who switched from placebo to active treatment; whereas, femoral BMD in the latter group showed an increased 4.7%. Similar responses were also found in younger men and women on a mediteranean diet high in monosaturated fat.[42] Monounsaturated fatty acids containing olive oil, withω−6 and ω−3 PUFAs in a ratio of ≈10:1, was positively associated with bone mass.

Currently, which of these marrow variables is the overriding factor that determines the final bone outcome in a senile osteoporosis animal model remains unknown. Thus, determining which combinations of specific total levels or specific thresholds of saturated fatty acids, PUFA ω-3, PUFA ω-6 and ω-6/ω-3 ratios ultimately affect the skeletal outcome would be the next step in future studies. Concurrently, measuring ex vivo prostaglandin E2 production and IGF-1 and evaluating the correlations between these mediators and dietary fatty acid levels would also assist in answering this question.

Next, we set out to determine the effects of varying fatty acids proportions on marrow fat volume and bone volume. Our results are interesting for two reasons. Firstly, in this mice model of senile osteoporosis, moderate levels of total ω-6 and relatively high ω-6:ω-3 ratios

demonstrated positive bone effects, as reflected in the enhancement in mean bone volume over other variables, suggesting a predominant effect via the osteoblastic pathway. Secondly, for each essential fatty acid, there may be a threshold, at which point, opposite effects on osteoblasts and adipocytes are seen- that is to say that fatty acids are capable of dual actions. These hypotheses will need to be tested in future studies.

In our study, holding further increasing the total ω-6 level and thus ω6:ω-3 ratio with borage resulted in an increase in fat volume fraction and reductions in mean bone volume and bone volume fraction. This suggests that elevated levels of ω-6 and ω-6: ω-3 ratios beyond moderate levels in a sunflower diet are detrimental to bone health through activation of adipogenesis. We did not measure adipocyte numbers and sizes, and adipokines in this study, but an increase in these parameters would be supportive. In contrast, dramatically increasing total ω-3 and correspondingly decreasing ω-6:ω3 ratios further reduced mean fat volume and fat volume fraction with attenuation of mean bone volume and bone volume fraction. The mechanism underlying this outcome is uncertain. Examining for inhibition of adipogenesis at the cellular level concurrently would support the possibility that there is a preferential inhibition of adipogenesis as the mechanism.

Thus, overall, the results suggest that both EFAs act on both pathways concurrently but that at highly elevated levels, ω-3 preferentially inhibits adipogenesis and ω-6 stimulates adipogenesis. Furthermore, absolute levels of essential fatty acids seem to be primary determinants of net skeletal outcomes and the ratios are secondary determinants.

Although previous studies have assessed bone outcomes using different indices to our study, as previously stated, some animal studies have reported conflicting results in line with our findings. One study exploring the effects of different ω-6 to ω-3 essential fatty acids ratios showed that a low ω-6 to ω-3 fatty acids (3:1) dietary ratio did not have a statistically significant

effect on bone in growing rats,[26] whilst another study showed that lowering the ω-6:ω-3 ratio from 9:1 to 4.5:1, while SFA and MUFA were held constant, altered the fatty acid profile, but did not affect bone mass in rapidly growing piglets.[30] Similarly, in a short study of 9 weeks, although reducing the (n-6):(n-3) FA ratio using (n-3) PUFA decreased ex vivo PGE2 secretion from bone, bone mass was not affected.[25] Another study showed that although the activity of bone-specific alkaline phosphatase and formation rate were higher in rats fed diets with high amounts of (n-3) FAs and a (n-6):(n-3) ratio of 1.2, osteocalcin was not affected.[23] In fact, significantly increasing ω-3 has been shown to have either no effect or an adverse effect in some human studies. In a 12-week n-3 PUFA supplement study, a 150% increase in n-3 PUFA concentration compared with baseline by the end of the period was not associated with reduction in bone resorption.[43] Similarly, in longer studies, n-3 PUFA supplementation for 24 weeks was not associated with bone turnover markers,[44] and n-3 PUFA supplementation for 12 months or more was found to have no influence on BMD.[40, 45] In fact, in rapidly growing rabbits, 10% fish oil supplementation (ω-6 : ω-3 [1:21]) combined with a modest amount of supplemental vitamin E, affected the skeleton negatively.[27]

In addition to the possibility that these EFAs may have dual actions depending on their levels and the bone microenvironment, three other observations are important to consider that may explain the results of our study. It has been shown that resultant plasma GLA (metabolites of ω-6): EPA (metabolites of ω-3) does not reflect dietary supplementation of GLA: EPA, and that ω-3 EFAs accumulate to a higher percentage in tissues than ω-6.[26, 40] Secondly, bone marrow acid profiles of fatty acids in various animal studies are not known. This is important, as although the lipid content of dietary treatments significantly influence and is reflected in the fatty acid profile of the bone marrow, absolute levels and ratios differ from dietary proportions. In one study[46], a ratio of ω-6/ω-3 fatty acids in the diet showed negative correlation with the concentrations of EPA

and DHA in bone marrow and in fact there were significant differences in the levels of EPA and total ω-3 PUFA between male and female rabbits. Compared to males, female rabbits had significantly higher concentrations. This finding contradicts another study, where relative to female mice, male mice were observed to have higher EPA and total ω-3 PUFA levels in the femur.[29] These results in animal studies suggest that ω-6 supplementation does not substantially inhibit the ω-3 pathway, and that the relationship between dietary essential fatty acid profiles and corresponding absolute levels and ratios of essential fatty acids in plasma and bone marrow may differ significantly, and thus affect bone differently dependent on sex and life stages of the animals. Notably, we did not measure bone tissue or marrow fatty acid profiles. Nor did we analyse the differences in male versus female mice. These additional analyses would provide further insight into the complicated fatty acid interactions.

It is plausible that not only the plasma ratio of ω-6:ω-3 in our sunflower group may be significantly lower than the dietary ratio of 18.35:1, but also that the plasma levels of ω-6 fatty acid derivatives may be quite low, and the levels of ω-3 may be higher, therefore resulting in a net positive effect on bone. In future studies, it would be relevant to measure plasma level and bone marrow tissue levels of essential fatty acids to determine any metabolic relationships between different fatty acids, bone markers and indices.

In summary, the effects of EFAs on skeletal metabolism remain complex. Fatty acids of both ω-6 and ω-3 origin may give rise to many different metabolites with various effects on bone.[5] The balance between omega-6 and omega-3 (n-3) PUFA can benefit bone modelling,[34] and for the first time we demonstrated the possibility of "duality of fatty acids" using a model of senile osteoporosis that mimics clinical features of ageing in humans. On one hand, sunflower and fish oil are protective of bone loss, while on the other hand, borage with higher ω-6 fatty acids is less protective of bone health. However, the optimal combinations of absolute levels of individual fatty acids and ratios

remain to be determined. There is also a need to determine which tissue levels (dietary, serum or bone marrow) best predict skeletal outcomes. Indeed, there are many questions that remain unanswered, such as what is the volume of distribution of ω3 and ω6 fatty acids? Do they enter bone readily and are able to access marrow? At what concentrations do they exist in the marrow? Further studies are required to delineate the components responsible for skeletal outcomes, and overall biological effects utilizing a similar model of senile osteoporosis.

4.5 References

1. Blum M, Harris SS, Must A, et al. Leptin, body composition and bone mineral density in premenopausal women. Calcif Tissue Int. 2003; 73(1):27-32.

2. De Laet C, Kanis JA, Oden A, et al. Body mass index as a predictor of fracture risk: a meta-analysis. Osteoporos Int. 2005; 16(11):1330-1338.

3. Hsu YH, Venners SA, Terwedow HA, et al. Relation of body composition, fat mass, and serum lipids to osteoporotic fractures and bone mineral density in Chinese men and women. Am J Clin Nutr. 2006; 83(1):146-154.

4. Zhao LJ, Liu YJ, Liu PY, et al. Relationship of obesity with osteoporosis. J Clin Endocrinol Metab. 2007; 92(5):1640-1646.

5. Wauquier F, Leotoing L, Philippe C, et al. Pros and cons of fatty acids in bone biology. Prog Lipid Res. 2015; 58:121-145.

6. Raisz LG, Alander CB, Simmons HA. Effects of prostaglandin E3 and

eicosapentaenoic acid on rat bone in organ culture. Prostaglandins. 1989; 37(5):615-625.

7. Corwin RL. Effects of dietary fats on bone health in advanced age. Prostaglandins Leukot Essent Fatty Acids. 2003; 68(6):379-386.

8. Albertazzi P, Coupland K. Polyunsaturated fatty acids. Is there a role in postmenopausal osteoporosis prevention? Maturitas. 2002; 42(1):13-22.

9. Fernandes G, Lawrence R, Sun D. Protective role of n-3 lipids and soy protein in osteoporosis. Prostaglandins Leukot Essent Fatty Acids. 2003; 68(6):361-372.

10. Kim Y, Ilich JZ. Implications of dietary alpha-linolenic acid in bone health. Nutrition. 2011; 27(11-12):1101-1107.

11. Kruger MC, Coetzee M, Haag M, et al. Long-chain polyunsaturated fatty acids: selected mechanisms of action on bone. Prog Lipid Res. 2010; 49(4):438-449.

12. Poulsen RC, Moughan PJ, Kruger MC. Long-chain polyunsaturated fatty acids and the regulation of bone metabolism. Exp Biol Med (Maywood). 2007; 232(10):1275-1288.

13. Salari P, Rezaie A, Larijani B, et al. A systematic review of the impact of n-3 fatty acids in bone health and osteoporosis. Med Sci Monit. 2008; 14(3):RA37-44.

14. Watkins BA, Li Y, Lippman HE, et al. Modulatory effect of omega-3 polyunsaturated fatty acids on osteoblast function and bone metabolism. Prostaglandins Leukot Essent Fatty Acids. 2003; 68(6):387-398.

15. Griel AE, Kris-Etherton PM, Hilpert KF, et al. An increase in dietary n-3 fatty acids decreases a marker of bone resorption in humans. Nutr J. 2007; 6:2.

16. Casado-Diaz A, Santiago-Mora R, Dorado G, et al. The omega-6 arachidonic fatty acid, but not the omega-3 fatty acids, inhibits osteoblastogenesis and induces adipogenesis of human mesenchymal stem cells: potential implication in osteoporosis. Osteoporos Int. 2013; 24(5):1647- 1661.

17. Schmitz G, Ecker J. The opposing effects of n-3 and n-6 fatty acids. Prog Lipid Res. 2008; 47(2):147-155.

18. Diascro DD, Jr., Vogel RL, Johnson TE, et al. High fatty acid content in rabbit serum is responsible for the differentiation of osteoblasts into adipocyte-like cells. J Bone Miner Res.1998; 13(1):96-106.

19. Maurin AC, Chavassieux PM, Meunier PJ. Expression of PPARgamma and beta/delta in human primary osteoblastic cells: influence of polyunsaturated fatty acids. Calcif Tissue Int. 2005; 76(5):385-392.

20. Hihi AK, Michalik L, Wahli W. PPARs: transcriptional effectors of fatty acids and their derivatives. Cell Mol Life Sci. 2002; 59(5):790-798.

21. Maurin AC, Chavassieux PM, Frappart L, et al. Influence of mature adipocytes on osteoblast proliferation in human primary cocultures. Bone. 2000; 26(5):485-489.

22. Watkins BA, Shen CL, Allen KG, Seifert MF. Dietary (n-3) and (n-6) polyunsaturates and acetylsalicylic acid alter ex vivo PGE2 biosynthesis, tissue IGF-I levels, and bone morphometry in chicks. J Bone Miner Res. 1996; 11(9):1321-32.

23. Watkins BA, Li Y, Allen KG, et al. Dietary ratio of (n-6)/ (n-3) polyunsaturated fatty acids alters the fatty acid composition of bone compartments and biomarkers of bone formation in rats. J Nutr. 2000; 130(9):2274-2284.

24. Li Y, Seifert MF, Ney DM, Grahn M, Grant AL, Allen KG, Watkins BA. Dietary conjugated linoleic acids alter serum IGF-I and IGF binding protein concentrations and reduce bone formation in rats fed (n-6) or (n-3) fatty acids. J Bone Miner Res. 1999; 14(7):1153-1162.

25. Mollard RC, Gillam ME, Wood TM et al. (n-3) fatty acids reduce the release of prostaglandin E2 from bone but do not affect bone mass in obese (fa/fa) and lean Zucker rats. J Nutr. 2005; 135(3):499-504.

26. Claassen N, Coetzer H, Steinmann CM, et al. The effect of different n-6/n-3 essential fatty acid ratios on calcium balance and bone in rats. Prostaglandins Leukot Essent Fatty Acids. 1995; 53(1):13-19.

27. Judex S, Wohl GR, Wolff RB, et al. Dietary fish oil supplementation adversely affects cortical bone morphology and biomechanics in growing rabbits. Calcif Tissue Int. 2000; 66(6):443-448.

28. Sun, D.Krishnan, A.Zaman, K.Lawrence, R.Bhattacharya, A. Fernandes, G. Dietary n-3 fatty acids decrease osteoclastogenesis and loss of bone mass in ovariectomized mice. J Bone Miner Res 2003; 18(7); 1206-1216.

29. Lau BY, Ward WE, Kang JX, et al. Femur EPA and DHA are correlated with femur biomechanical strength in young fat-1 mice. J Nutr Biochem. 2009; 20(6):453-461.

30. Weiler HA, Fitzpatrick-Wong S. Dietary long-chain polyunsaturated fatty acids minimize dexamethasone-induced reductions in arachidonic acid status but not bone mineral content in piglets. Pediatr Res. 2002; 51(3):282-289.

31. Wauquier F, Barquissau V, Leotoing L, et al. Borage and fish oils lifelong supplementation decreases inflammation and improves bone health in a murine model of senile osteoporosis. Bone. 2012; 50(2):553-561.

32. Lo WC, Chiou JF, Gelovani JG, et al. Transplantation of embryonic fibroblasts treated with platelet-rich plasma induces osteogenesis in SAMP8 mice monitored by molecular imaging. J Nucl Med. 2009; 50(5):765-773.

33. Demontiero O, Li W, Thembani E, et al. Validation of noninvasive quantification of bone marrow fat volume with microCT in aging rats. Exp Gerontol. 2011; 46(6):435-440.

34. Watkins BA, Li Y, Lippman HE, et al. Omega-3 polyunsaturated fatty acids and skeletal health. Exp Biol Med (Maywood). 2001; 226(6):485-497.

35. Simopoulos AP. Evolutionary aspects of omega-3 fatty acids in the food supply. Prostaglandins Leukot Essent Fatty Acids. 1999; 60(5-6):421-9.

36. Sakaguchi K, Morita I, Murota S. Eicosapentaenoic acid inhibits bone loss due to ovariectomy in rats. Prostaglandins Leukot Essent Fatty Acids. 1994; 50(2):81-4.

37. Farina EK, Kiel DP, Roubenoff R, et al. Protective effects of fish intake and interactive effects of long-chain polyunsaturated fatty acid intakes on hip bone mineral density in older adults: the Framingham Osteoporosis Study. Am J Clin Nutr. 2011; 93(5):1142-1151.

38. Weiss LA, Barrett-Connor E, von Muhlen D. Ratio of n-6 to n-3 fatty acids and bone mineral density in older adults: the Rancho Bernardo Study. Am J Clin Nutr. 2005; 81(4):934-938.

39. Suzuki T, Yoshida H, Hashimoto T, et al. Case-control study of risk factors for hip fractures in the Japanese elderly by a Mediterranean Osteoporosis Study (MEDOS) questionnaire. Bone. 1997; 21(5):461-464.

40. Bassey EJ, Littlewood JJ, Rothwell MC, et al. Lack of effect of supplementation with essential fatty acids on bone mineral density in healthy pre- and postmenopausal women: two randomized controlled trials of Efacal v. calcium alone. Br J of Nutr. 2000; 83(6):629-635.

41. Kruger MC, Coetzer H, deWinter R, et al. Calcium, gamma-linolenic acid and eicosapentaenoic acid supplementation in senile osteoporosis. Aging Clin. Exp. Res. 1998; 10 (5), 385–394.

42. Trichopoulou A, Georgiou E, Bassiakos Y, et al. Energy intake and monounsaturated fat in relation to bone mineral density among women and men in Greece. Preventive medicine. 1997; 26(3):395-400.

43. Appleton KM, Fraser WD, Rogers PJ, et al. Supplementation with a low-moderate dose of n-3 long-chain PUFA has no short-term effect on bone resorption in human adults. Br J Nutr. 2011; 105(8):1145-1149.

44. Trebble TM, Stroud MA, Wootton SA, et al. High-dose fish oil and antioxidants in Crohn's disease and the response of bone turnover: a randomised controlled trial. Br J Nutr. 2005; 94(2):253-261.

45. Dodin S, Lemay A, Jacques H, et al. The effects of flaxseed dietary supplement on lipid profile, bone mineral density, and symptoms in menopausal women: a randomized, double-blind, wheat germ placebo-controlled clinical trial. J Clin Endocrinol Metab. 2005; 90(3):1390-1397.

46. Alnouri DM, El-Din MF, Al-Khalifa AS. The effect of long-term supplementation with different dietary omega-6/omega-3 ratios on mineral content and ex vivo prostaglandin E2 release in bone of growing rabbits. Nutr Res Pract. 2014; 8(4):360-367.

5.0 Chapter 5: Anatomical Differences in Marrow Fat in a Cohort of Older Men: Correlation with Body Composition and Calciotropic Hormones.

Abstract

A number of MRI studies have shown higher marrow fat concentrations with ageing and osteoporosis, but the nature of the relationship between marrow fat tissue and bone tissue; clinical surrogates of bone mass and strength; and calciotropic hormones at specific skeletal sites have not been previously examined. We conducted a cross sectional study looking at these relationships using clinical CTs and the image analysis software, Tomovision Slice O Matic 4.3 Rev-6i software (Tomovision, Montreal, QC, Canada), to quantify marrow fat and bone tissue.
One hundred and twenty male subjects (mean age: 67.7 ± 6) underwent CT imaging of the lumbar spine and both proximal femurs, and a complete physical examination. In addition to anthropometric parameters, full serum biochemistry panels and BMD via DXA were measured. CT axial slices of L2, L3, left and right proximal femur, neck of femur, and trochanteric regions were analysed, and fat volumes and bone volumes quantified.

5.1. Introduction

Senile osteoporosis is associated with increased marrow fat infiltration, which affects bone mass and quality. An inverse relationship between marrow fat and bone mass has been demonstrated at a cellular level[1] and at macroscopic level using magnetic resonance imaging (MRI).[2, 3] MRI studies have shown both a linear increase in marrow fat content with ageing, and a higher fat concentration

in osteoporotic individuals.[4, 5]

Indeed, MRI has been the predominant non-invasive modality of marrow fat evaluation. Many studies have demonstrated vertebral marrow fat and its relationship with age,[3-4,6]sex[4,7-8,10] and disease states.[7-12,14] However, few have evaluated marrow fat in the femur and peripheral skeleton,[13,15-16] and because marrow fat values are location dependent, with variations within regions- for example, marrow fat significantly increases from L1 to L4[12] - whether the inverse relationship between marrow fat and bone holds true at these sites remains to be determined. Given that osteoporotic fractures at these nonvertebral sites are also associated with significant morbidity and mortality, in particular hip fractures, it would seem pertinent to examine marrow fat distribution in the regions of the proximal femur, namely the trochanteric and neck of femur. Although MRI quantification of marrow fat is considered the gold standard method of noninvasively quantifying marrow fat, the method by which marrow fat is quantified is not standardized. With the most common MRI technique used to quantify marrow fat, magnetic resonance spectroscopy (1H-MRS), a single voxel is placed in the region of interest, and based on the water proton peak and saturated lipid proton peak, marrow fat is calculated as a percentage, rather than a total volume. Marrow fat content is then reported either as a lipid/ water ratio or as a fat fraction (calculated as lipid/ (lipid + water). Thus, the quantity of fat reported can be variable and comparisons between studies may be challenging. Similarly, there are some limitations with T1-weight MRI. It is semi-quantitative, and may also have errors due to partial volume effects.[17] However, the main limitation at this time is that MR assessment of marrow fat is not performed clinically due to its availability and cost.

Over the last decade, the investigations into the role of marrow fat in osteoporosis and other related bone conditions have intensified. Studies examining the relationship between marrow fat and markers associated with bone metabolism, including vitamin D, PTH, markers of bone

formation and resorption, and disease states such as diabetes, are gaining attention. With regards to vitamin D, its protective effect on bone by directly influencing osteoblastogenesis is well established. Mechanistic studies have shown that it stimulates osteoblastogenesis by enhancing MSC differentiation to osteoblasts,[18,19]but less data is available on its effects on adipogenesis. Cell culture studies showed that preadipocytes treated with $1,25(OH)_2D$ inhibit adipognensis[20] through inhibition of C/EBPα and PPARγ, with nuclear vitamin D(3) receptor (VDR) and PPARγ acting synergistically to inhibit adipogenesis.[21] This is also supported by animal studies- for example, in one study, 4-month old SAM-P/6 mice were treated with $1,25(OH)_2D_3$ (18pmol/24 h) or vehicle for 6 weeks. Initially, the investigators found that with ageing, the levels of PPARgamma2 expression increase in bone marrow of SAM-P/6 ($P<0.001$). However, when the changes in the expression of PPARgamma2 were measured by semi-quantitative reverse transcription-polymerase chain reactions and immunofluorescence, a significant reduction of PPARgamma2-expressing cells in 1,25(OH)(2)D(3)-treated (32% +/-6) as compared to vehicle (76% +/-5) treated mice ($p<0.01$) was found. Human studies quantifying marrow fat have not investigated this relationship to support the findings from invitro and animal studies. Our study, to date, is the first to explore this relationship using clinical CT.

In a similar vein, human studies examining PTH's effect on adipogenesis are lacking. In vitro studies have shown that it may have a role in directing the fate of MSCs. When the PTH/PTHrP receptor (PTH1R) in mesenchymal stem cells was deleted, low bone formation, increased bone resorption and high bone marrow adipose tissue (BMAT) resulted. Bone marrow adipocytes traced to Prx1, expressed classic adipogenic markers and high receptor activator of nuclear factor kappa B ligand (RankL) expression.[22] Translational work showing an increase in marrow adipose tissue volume would support in vitro findings; however, only one study has measured the amount of marrow fat tissue. Paired bone biopsies from 7 males in a small randomized

trial of PTH for male idiopathic osteoporosis found a 27% reduction in adipocyte number at 18 months in men treated with PTH.[23] The size of the adipocytes did not change, however, the trial was not powered for change in marrow fat cell volume or number.

In contrast, changes in marrow fat associated with diabetes have been explored mechanistically and in animal studies. Bone loss and increases in BMAT have been consistently demonstrated in mice with induced diabetes[24-27] and they have shown that the effect of diabetes may be location dependent. In a control versus diabetic BALB/c mice (males and females) study, increased marrow adiposity was evident in diabetic femurs and calvaria, but not in vertebrae. Human studies, on the other hand, have not shown such consistent relationships between marrow adiposity and diabetes status, and the observed changes have been smaller and less certain. The largest study to date to examine BMAT changes in type 1 diabetics did not show a significant difference with their nondiabetic counterparts. This study was cross-sectional and enrolled 30 young women with T1DM, with a median age of 22 years, a mean BMI of 25 kg/m^2, and average haemoglobin A1c of 9.8 %.[14] Median L3 marrow fat fraction by 1H-MRS was 4.8% higher in T1DM subjects compared to healthy controls ($p = 0.20$), and the proximal tibia demonstrated lower apparent bone volume/total volume; apparent trabecular number; and greater apparent trabecular spacing.

Another cross-sectional study also showed that marrow fat levels were similar between T1DM participants and controls.[28] Eight T1DM men and women, with mean HbA1c at 7.7 % and an average age of 37 years and 40 years respectively, were compared with age and BMI-matched controls. Marrow fat levels at L4 vertebra, distal femur and proximal tibia were similar between the groups. Furthermore, there was no correlation between marrow fat and HbA1c, or disease duration in those with T1DM.

More relevant to this thesis, marrow fat in subjects with T2DM was found to be significantly

higher than those without diabetes. In the Osteoporotic Fracture in Men Study (largest marrow fat study in T2DM), 156 men aged 74–96 years of whom 24 % had T2DM, had lumbar spine marrow fat measured by 1H-MRS.[29] T2DM was associated with higher marrow fat (59 %) compared with controls (55 %, $p = 0.03$), independently of age.

Two other studies reported conflicting results, however. In one study, 26 postmenopausal women without osteoporosis (13 with T2DM and 13 age- and BMI-matched controls) had L1–L3 marrow fat measured by 1H-MRS. The women with T2DM had a mean age of 59 years, BMI of 27 kg/m2 and HbA1c at 7.6 %. Marrow fat content at L1-L3 was higher in women with T2DM (69.3 %) compared with the controls (67.5 %, $p = 0.31$).[30]More importantly, within the T2DM women group, those with higher HbA1c had higher marrow fat levels ($r = 0.83$, $p < 0.01$).

In the other study, 69 diabetic and non-diabetic postmenopausal women, with and without a history of fragility fracture, had L1–L3 marrow fat content quantified by 1HMRS.[31] T2DM women without a fracture had an HbA1c of 7.6%, and those T2DM women with a fracture had a mean HbA1c of 7.8%. After adjustment for age, race, and spinal BMD by QCT, vertebral marrow fat content did not correlate with diabetes status ($\beta = 0.02$, $p = 0.27$).

Another study examined the prediabetes stage, and showed potential association between marrow fat and dysglycaemia. Thirty women had L3 vertebral fat content measured by 1H-MRS.[32] Eleven women, who had pre diabetes, had a mean HbA1c of 5.5%, a mean age of 47.8 years and BMI of 25.5 kg/m^2. Analysis of the entire cohort showed a positive association between marrow fat and HbA1c and fasting blood glucose, but not with insulin level or the homeostatic model assessment of insulin resistance (HOMAIR). Thus, overall the role of marrow fat and diabetes need further work.

A similar scenario exists with metabolic and inflammatory markers. Although a large body of work exists in the literature describing the associations between these markers and marrow fat,

this is the first study to examine the relationships with an older cohort. In addition, clinical computed tomography (CT) has not been employed to quantify marrow fat in this manner, or to explore the relationship between marrow fat and known clinical surrogates of bone mass and strength.

Thus, this cross sectional study aims to (1) quantify marrow fat in different regions of the skeleton of older men utilizing CT images and a validated image analysis tool, (2) to examine the relationship of marrow fat in these regions of interest with age, bone mineral density (BMD), PTH, vitamin D status and diabetes status and (3) to examine associations and correlations of marrow fat in different skeletal regions with selected markers of bone metabolism.

5.2 Subjects and Methods

5.2.1 Subjects

This is a sub study of a clinical trial investigating the *"relationship between visceral adipose tissue and metabolic syndrome".* Details of recruitment and procedures have been described previously.[33] In brief, a total of 120 men (60 Chinese, 60 Indian) aged 60 and over were recruited through health check fairs in the community. For this thesis, the whole original cohort of participants is included in the analysis. Where results of particular tests are not available, analysis is carried out on the available number pf patients and investigations. Participants were consecutively recruited from community-based health fairs, based on eligibility and willingness to participate. Informed consent was obtained from all the subjects. Every attempt was made to recruit those who were apparently healthy and who were not on any medication for hypertension, hypercholesterolemia or diabetes. However, given the demographics of the locale where recruitment was taking place, some Indians who were taking these medications were recruited. This was not surprising, as it has been

shown that compared to Chinese, diabetes, hypertension and dyslipidaemia were more prevalent amongIndians.[34,35]Investigators of the original study interviewed subjects directly to collect data on their health background. Medical histories of smoking habits, alcohol consumption, exercise habits, diabetes, hypertension, hyperlipidaemia, ischemic heart disease and family history of diabetes or hypertension were documented. Fracture history was not available.

Subjects on antiviral/ anti-obesity/ corticosteroids / anti-osteoporosis drugs, previous abdominal surgery, previous cancer, any investigational drugs for the past 3 months or excessive weight loss (45% body weight) over the last 3 months were excluded from the study.
All subjects had anthropometric measurements recorded, and included height to the nearest millimetre, and with subjects wearing light clothing and no shoes, weight in kilograms was measured by electronic weighing scales (seca 220 - seca deutschland, Hamburg, Germany). Body mass index (BMI) was calculated as per convention, weight divided by the square of the height (kilograms per meter squared).

5.2.2 Biochemical analysis

Blood lipid profiles, insulin and glucose were drawn in the fasting state (overnight fast of at least 10 hours) for all subjects. The glucose oxidase method, which had an interassay CV of 3.3% (Beckman Coulter, Inc., Brea, CA, USA), was used to measure plasma glucose level. The 1-step immunoenzymatic assay, which had an interassay CV approximately 1.6 to 1.7% (Beckman), was used to measure total cholesterol, high-density lipoprotein cholesterol (HDL-c) and triglyceride (TG). Low-density lipoprotein cholesterol (LDL-c) was calculated by Friedewald's equation. Insulin resistance was calculated as fasting serum insulin (mUml/1) x fasting plasma glucose (mmol/1)/22.5- consistent with the homeostasis model assessment. Insulin resistance (HOMA-IR); leptin; resistin and another adipokines; plus adiponectin were measured with commercially available

kits (Linco Research, Inc., St Charles, MO, USA).A "*highly sensitive near infrared particle immunoassay rate technology",* which had an intra- and inter-assay CV of 1.3% and 4.1% (Beckman Coulter, Inc.), was used to measure high-sensitivity C-reactive protein levels. Interleukin-6 was measured by ELISA (in commercially available kits Linco Research, Inc.).

Total body fat mass was measured with a fan beam DEXA densitometer (Delphi W; Hologic, Inc., Waltham, MA) in array mode and was analysed with the manufacturer's software- the coefficients of variation for these measurements reportedly range from 1.2 to 5%.[36]

5.2.3 CT abdomen

Imaging of the abdomen and pelvis was conducted using a 64-slice multi-detector CT scanner (Somatom Definition, Siemens AG, Erlangen, Germany). For trans axial views, subjects were in the supine position and scanning was done with a 35x35-cm field of view, starting at the dome of the diaphragm and down towards the inferior aspect of the pelvis. Scans were non-contrast, but enhanced employing scan parameters of kVp (120); effective mAs (210); slice collimation 0.6 mm; slice width 5.0 mm; pitch factor 1.4 and increment 5.0mm were acquired. The 1mm sections at zero gap intervals were reconstructed from the thin-slice raw data.

One research assistant performed all image analyses and was supervised by a radiologist. The 2D CT image data sets were saved in DICOM format and onto compact discs. These images were analysed with the commercial image analysis software, Tomovision Slice O Matic 4.3 Rev-6i (Tomovision, Montreal, QC, Canada).

5.2.4 Slice-O-Matic imaging analysis

5.2.4.1 Anatomical Regions of interest

Axial slices of L2, L3, left neck of femur, left trochanteric region, right neck of femur and right trochanteric region were selected for analysis. Subjects with fractures or prosthesis in the regions of interest are excluded from the analysis. Each region of interest was identified in the following manner for each subject. The most distinct and easily recognized vertebral landmark, S1 (the first bone of the sacrum), was first identified by scrolling down the set of images. Scrolling through the axial slices proximally, the intervertebral cartilage is next identified. This is the cartilage that sits between S1 and L5 and thus, the first vertebra visualized after this cartilage is L5. This procedure is repeated to identify the next vertebral body, L4, which is followed by the next vertebrae, and so on until L3 and L2 are identified. Similar procedures were followed to identify the proximal femur, and the neck of femur and trochanteric regions were defined manually on an image-by- image basis, as depicted in Figure 1.

Each set of axial CT scan images of each anatomical region of interest was further examined for adequate quality for inclusion. Presence of artefacts and other poor image quality features rendered the slice not suitable, and were excluded, as described in the methodology section of this thesis. Ultimately, three contiguous axial slices of L2 and L3, five contiguous slices of the left neck of femur and trochanter were selected for each subject. The centre slice is determined by the total number of slices divided by 2, and contiguous slices are taken from either side of the centre slice.

5.2.4.2 Thresholds for bone, blood and marrow fat tissue

CT numbers express the measure of the linear attenuation of the x-ray beam through the medium in that space, and are defined as cm^{-1},which are then converted to Hounsfield units (HU) by calibration against an air, bone and water phantom (HU), using the linear attenuation coefficient of water (HU =0) and air (HU= -1000). Previous published works have correlated

mass densities and elemental weights of human tissues with CT numbers in Hounsfield units. CT numbers for adipose tissue fell between a range of negative values (-20 to -60) and soft tissues are situated within the range of −100 and +100 Hounsfield units, whereas the CT numbers of the skeletal tissues take values from 100 up to 1524.[37-40]

Invariably, CT numbers for bone marrow also fell in a range. Calculated CT numbers for yellow marrow, red marrow, yellow and red marrow mixture of 1:1 and whole blood were -49, 11, - 22 and 56 respectively.[13] Furthermore, it has been noted that *in vivo* studies have shown variable normal distribution and proportions of both yellow and red marrow depending on age, bone and site[41, 42]. In addition, CT images of marrow from different regions within a bone have different appearances and absolute Hounsfield values are location dependent.[10]For example, Hounsfield values in the adult metaphyseal and epiphyseal regions are generally positive, sometimes approaching 100 HU; whereas, in the diaphyses of the long bones, the marrow reaches its adult pattern by 15 years of age, when it is mostly comprised of fat, and it has generally negative Hounsfield values in the order of -100 HU.[43]

Thus, for the purpose of this study, the final threshold ranges of attenuation for the regions of interest, namely bone, marrow fat and haemopoietic tissue, were determined in three steps:

- Automated segmentation;
- Manual editing of segmented regions to capture additional tissue, plus manual segmentation to capture regions not captured during step 1;
- Manual segmentation in zoom mode to capture pixels which were visually similar to those captured in the first two steps, but which have not been captured in the first 2 steps.

Step 1: The axial slice was opened in the region growing mode function. Initial CT Hounsfield values for bone, marrow fat and haematopoietic volume, based on previous published

studies described above, were set using the thresholding function (Fig. 2A). The initial ranges ≥ 100, 11 to 99 and ≤ 10 for bone, blood and marrow fat respectively were inserted in the range bar. For the purpose of quantification of volumes, each depot was assigned the following colours arbitrarily: marrow fat (yellow), bone (blue) and blood volume (red) (Fig. 2B)

Step 2: The threshold ranges for the region of interest from step 1 were set in the range bar again, and a painting mode of segmentation was selected. The region of interested was "painted" manually by moving the cursor over the region repeatedly to capture all pixels within the region (Fig. 2B).

Step 3: The region of interest was visually inspected. Areas that appear similar to those already painted were assumed to have the same CT numbers, and were painted manually over one pixel or more at a time (Fig. 2C).

These steps were carried out for each region of interest, and one region of interest at a time. However, the final threshold ranges used for quantification of volumes of the regions of interest for the whole study were derived through a similar process to previous techniques for delineating tissues of overlapping densities with an image histogram.[44] The steps above were repeated for 3 axial slices at L3 from 10 different subjects selected randomly from within the study cohort. Results were plotted on a histogram and the range of CT number values which best approximated the 95% confidence interval was chosen for the final quantification process. Thus, the following resultant CT number thresholds for bone (trabecular 130-600, cortical > 601), marrow fat ≤ 20, and 21 ≥ and blood (≤ 129) were applied throughout the remainder of the thesis.

5.2.4.3 Volume quantifications

Before volume quantifications were carried out, each region of interest was coloured using steps 1 and 2 as above. Once all regions were coloured in, the volume function was selected and

computations of the segmented ROIs were achieved automatically through a built in algorithm (Fig. 2D).

Regions of interest (ROIs) describing the whole axial cross sections of the proximal femur were created through the steps described above, and the respective areas were measured. All adipose and bone tissue pixels within the bone were measured by a blind examiner (Fig. 3).

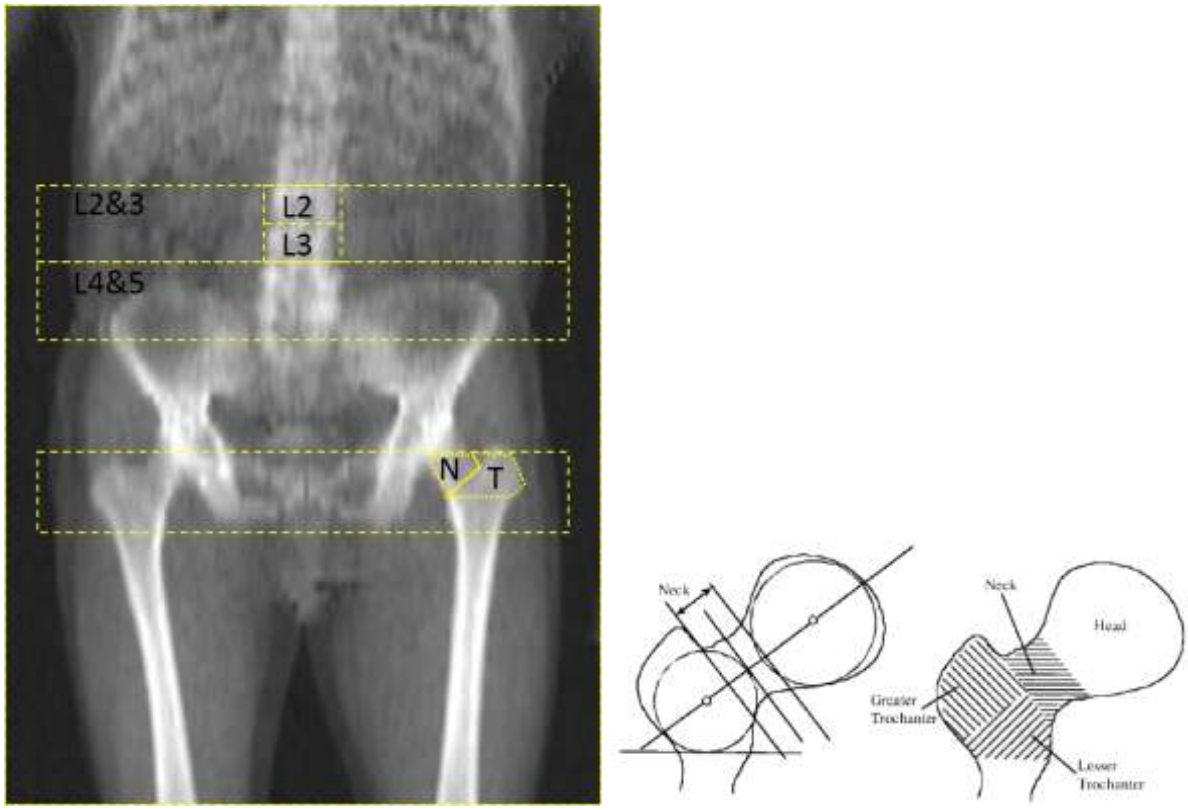

Fig 1. ROI selection for lumbar levels and the process of dividing the femur into head, neck, greater trochanteric, and lesser trochanteric regions for which the mean was calculated for all output parameters. The regions analysed were the femoral neck, trochanteric (greater trochanter plus lesser trochanter) and proximal femur (all regions combined).

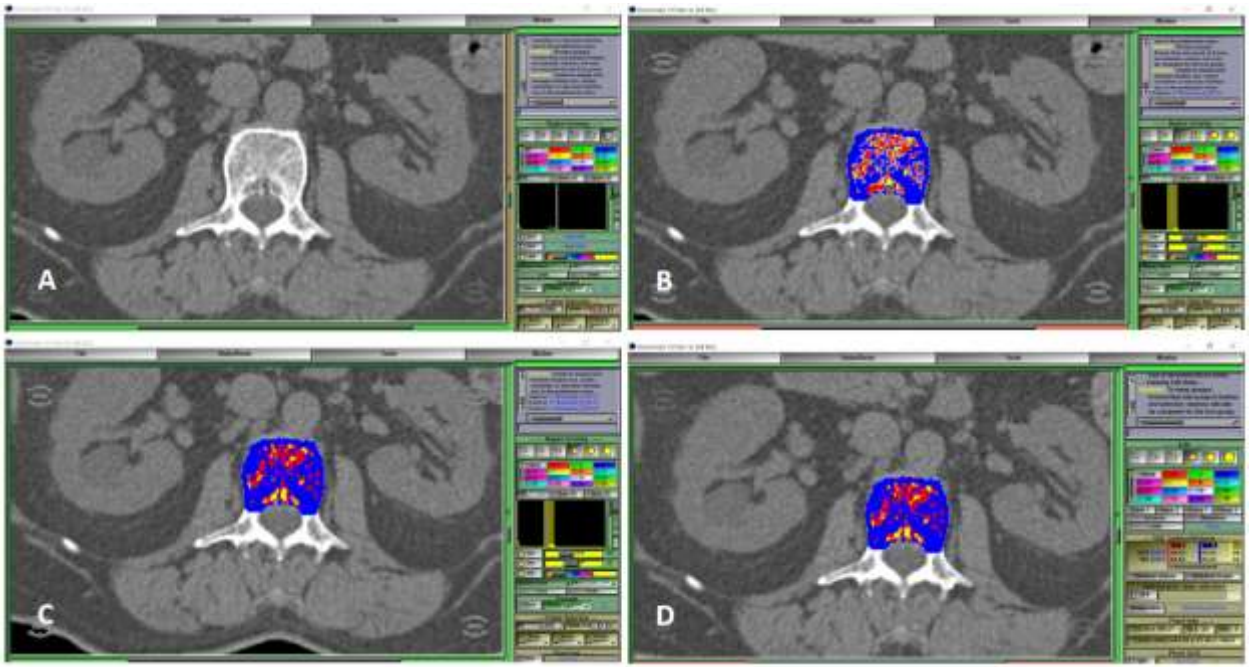

Fig 2 (A-D) CT image analysis of bone using SliceOmatic. (A) Image opened, arbitrary colours chosen to represent ROIs and initial thresholds entered for ROI. (B) Autosegmentation of ROIS (C) Thresholds of the signal intensity for bone (blue) fat (yellow) and bone marrow (red) were manually adjusted by visual inspection of individual pixels (D) Volume was quantified once all regions coloured.

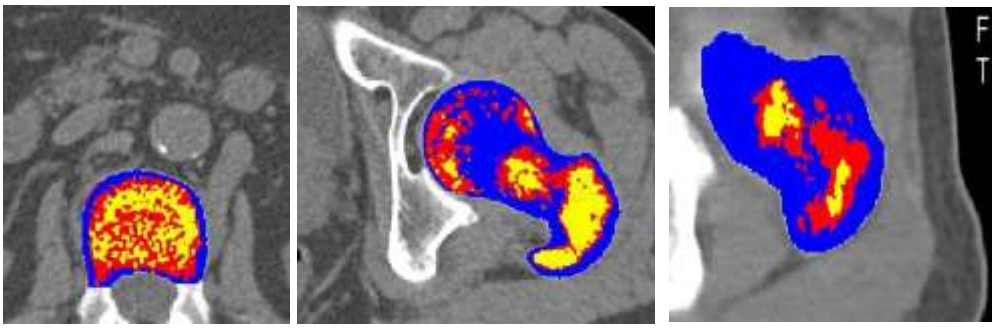

Fig 3. Bone image analysis showing high levels of marrow fat (yellow) compared with low levels of bone (blue) and bone marrow (red).

5.2.5 Statistical analyses

Various scatter plots were used to visually confirm linearity of associations.

Pearson's and Spearman's correlations (for normally and abnormally distributed or ordinal variables, respectively) were used to investigate the association between regional fat volumes and fat volume/bone ratios with age; BMI; diabetes status; PTH; vitamin D; markers of bone resorption; and formation and inflammatory mediators. Partial correlation was used to assess the independent

associations between variables after adjusting for confounders. Where the results remained unchanged, only unadjusted correlations are presented to aid simplicity.

The linearity of the correlations was checked visually using scatter plots. The IBM SPSS statistics for Windows, Version 20.0 (Armonk, NY; IBM Corp.) was used for the analyses. Variables were expressed as mean ± SD or median (interquartile range). *P*-values ≤ 0.05 were considered as significant.

5.3 Results

5.3.1 Baseline characteristics

One hundred and twenty men (mean age ± SD = 67.5 ± 5.5; range: 60-87) fulfilled the inclusion criteria. Forty eight subjects had DXA reports available. The anthropometric, body composition and blood biochemistry profiles of the patients are presented in Table 1.

Morphometric and bone density characteristics	
Variables	***Mean (SD)***
Age **(years)**	67.5 (5.5)
BMI **(kg/m^2)**	24.6 (4.2)
Height **(cm)**	164.7 (6.4)
Lumbar spine BMD **(g/cm^2)**	1.01 (0.136)
T-score	0.143 (1.179)
Z-Score	0.958 (1.225)
Fem Neck BMD **(g/cm^2)**	0.764 (0.092)
T-score	-1.180 (0.729)
Z-Score	0.306 (0.790)
Biochemistry results	
Analyte	***Median (IQR)***
Vitamin D **(µg/L)**	22.4 (19.9, 27)
Parathyroid Hormone **(pmol/L)**	3.8 (3.4,4.3)
Serum albumin **(g/L)**	39 (37, 40)
IFN gamma **(IU/ml)**	18.2 (10.2-28.6)
IL-6 **(IU/mL)**	4.6 (2.6, 5.6)
TNF alpha **(ng/mL)**	3.14 (2.7, 3.9)

OPG **(ng/mL)**	1.4 (0, 5.8)
RANKL **(ng/mL)**	58.4 (47.5, 83.5)
Osteopontin **(µg/L)**	4.4 (2.8, 7.7)
Resistin **(ng/ml)**	7.4 (5.7, 10.4)
IGF1 **(ng/mL)**	116.6 (101.1, 145.7)
Leptin **(µg/L)**	4 (3.3, 6.5)
Adiponectin **(ng/mL)**	6040 (4368, 7364)
Osteocalcin **(ng/mL)**	15 (12, 16)
CTX **(mg/L)**	0.26 (0.22, 0.36)
Glucose **(mmol/L)**	5.2 (4.9, 5.4)

Table 1. Demographic, Clinical, Body Composition and Serological Characteristics of Participants (mean ± SD). BMI: Body mass index; IFN: Interferon; IL: Interleukin; OPG: Osteoprotegerin; RANKL: Receptor activator of nuclear factor kappa-B ligand; IGF: Insulin-like growth factor 1; CTX: Collagen type 1 cross-linked C-telopeptide.

5.3.2 Distribution of marrow fat at ROIs with age

Examining marrow adiposity in the neck of the femur, the trochanteric region and L2 and L3 vertebrae with increasing age, showed characteristic associations. With each decade from the age of 60, there was a corresponding increase in mean volumes of marrow fat in the neck of the femur, trochanteric region, proximal femur and the lumbar vertebrae (Figures 4A [i-v]). Inversely, the corresponding bone volumes in these skeletal sites decreased with increasing age (Figures 4B [i-v]).The marrow fat to bone ratio in these anatomical sites increased with increasing age (Figures 4C [i-vii]), however, the greatest proportion of fat volume increase occurred within the trochanteric region of the proximal femur (Figure 4C [iv-vii]).

i ii iii

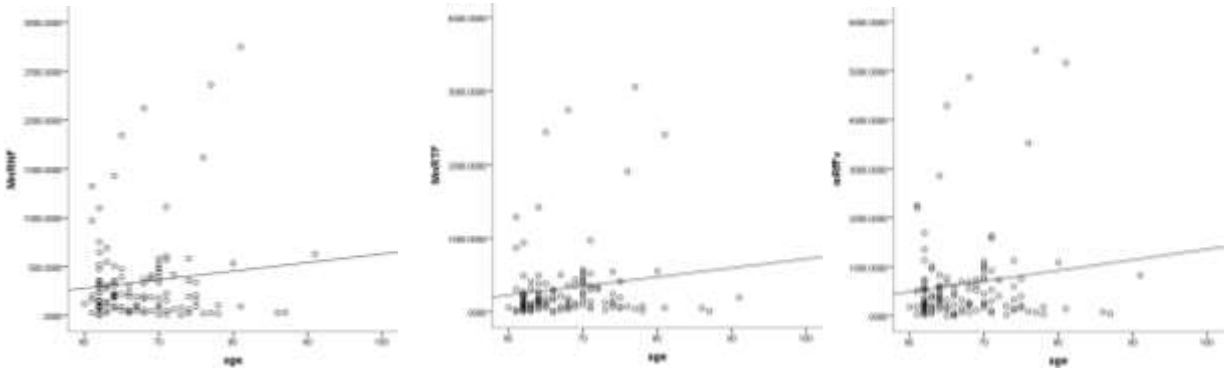

iv v

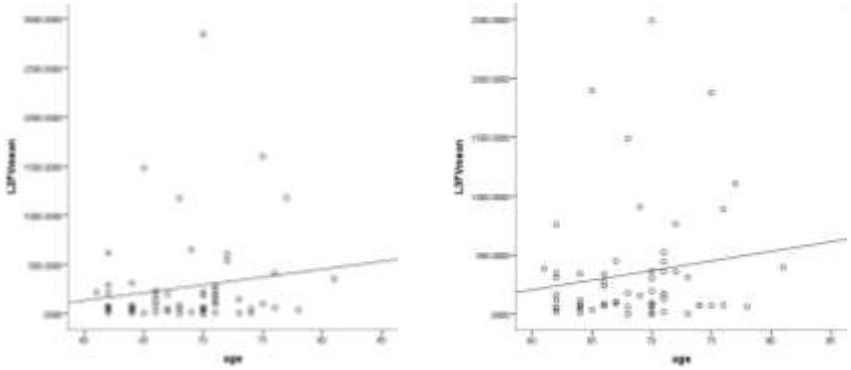

Figure 4A. Increasing age is associated with increasing absolute fat volumes in the neck (i) trochanteric (ii), proximal femur (iii), L2 (iv) and L3 vertebra (v).

i ii

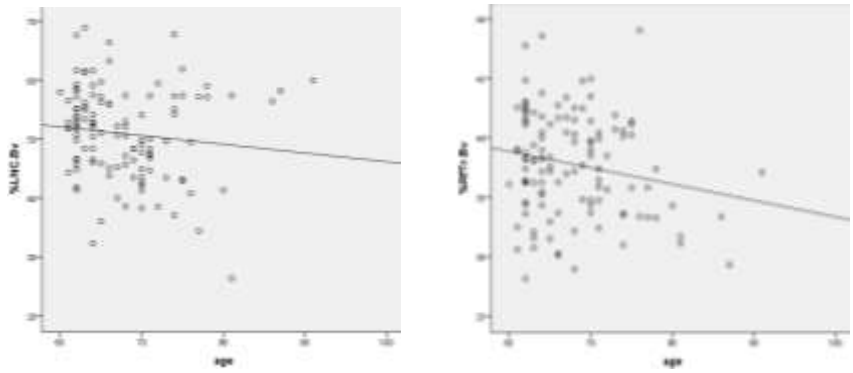

iii iv

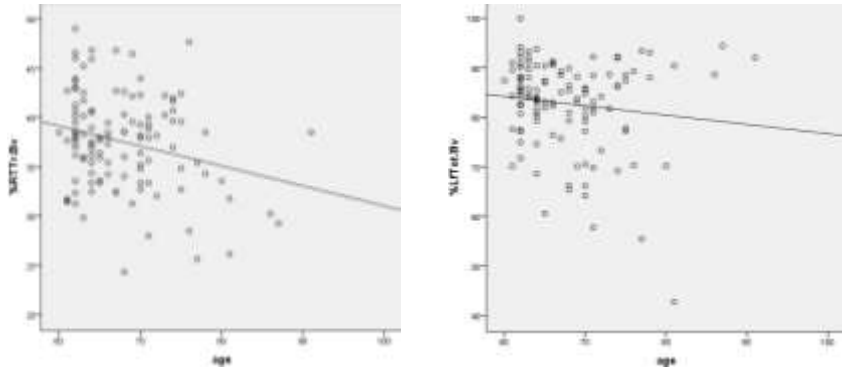

Figure 4B. Increasing age is associated with decreasing bone volume fraction in the neck (i), trochanteric region (ii), proximal femur trabecular volume fraction (iii) and total bone volume fraction (iv).

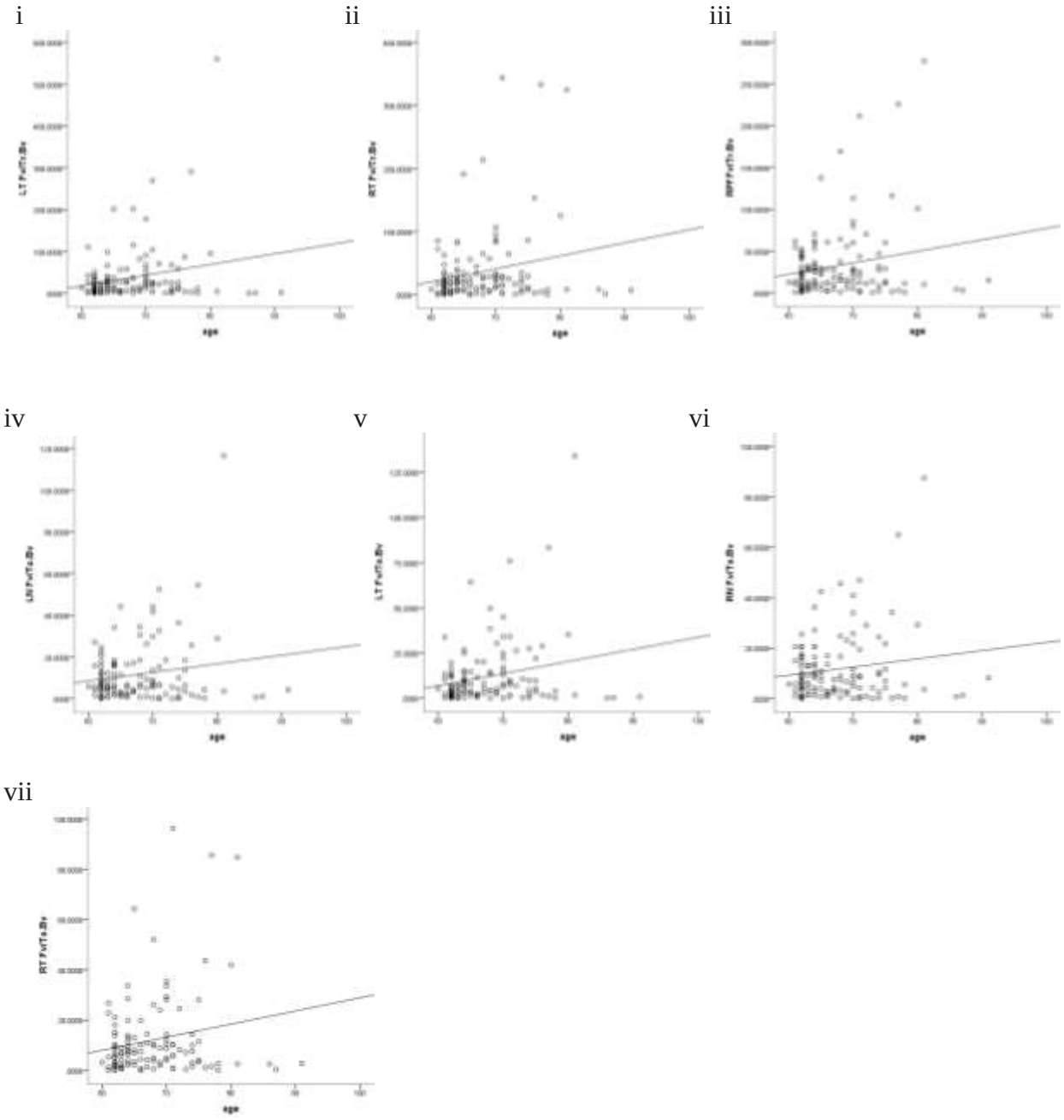

Figure 4C. Marrow fat to bone ratio increases in all sites as a fraction of trabecular bone volume in trochanteric regions (i) and (ii), in proximal femur (iii) and as a fraction of total bone volume in the neck [(iv), (vi)] and trochanteric regions [(v), (vii)]. Within the same region, the proportions of fat increase in trochanteric regions are greater than the neck regions (v) vs. (iv) and (vii) vs. (vi).

5.3.3 Associations of ROI fat volume with age, BMI, vitamin D status and glucose

Interestingly, age was the only clinical parameter that significantly correlated with marrow fat volume indices in the hip ROIs, but the inverse relationship between marrow fat and

bone with increasing age was most consistent in the trochanteric regions (Table 2). Other clinical factors, such as BMI, diabetes status and vitamin D levels did not correlate with fat/bone volume ratios in the proximal femur ROIs. However, glucose levels highly correlated with all indices of marrow adiposity in both lumbar vertebrae.

Variable	Left trochanteric	Left proximal femur	Right trochanteric	Right proximal femur	L2	L3
Fv	NS	NS	NS	NS	.6**	.5**
Fv/Tr.Bv	0.2*	0.2*	0.2*	0.2*	.6**	.3**
Fv/To.Bv	0.2*	0.2*	0.2*	NS	.6**	.3**
Fv/T v	0.2*	NS	NS	NS	.5**	.3**

Table 2. Correlations between mean fat volume (FV), ratio of fat volume to trabecular bone volume (Fv/Tr.Bv), ratio of fat volume to total bone volume (Fv/To.Bv), ratio of fat volume to the total tissue volume (Fv/Tv) and clinical parameters. * Pearson's correlation is significant at the 0.05 level (2-tailed). ** Pearson's correlation is significant at the 0.001 level (2-tailed). Correlations at the trochanteric and proximal femur regions only were found for age and correlations found only in L2 and L3 for glucose. No correlations found for BMI and Vitamin D at all ROIs.

In multiple linear regression analyses using age; diabetes status; mean fasting glucose levels; BMI and vitamin D status as independent variables, age was the main associating factor with fat/bone volume ratios in trochanteric regions of the femur. BMI and diabetes status were associated with marrow fat volume in the right trochanteric, but not the left (Table 3A). Interestingly, mean fasting glucose levels or diabetic states strongly correlated with marrow adiposity indices in the lumbar vertebrae (Table 3B).

Variable	Left Trochanter		Right Trochanter			Right proximal femur	
	Fv/Tr.Bv	Fv/To.Bv	Fv	Fv/Tr.Bv	Fv/To.Bv	Fv/Tr.Bv#	Fv
Age	2.5*	0.7*		2.1*	.5*	1.4*	
BMI			.2*				.4*
Diabetes			-.4*				

Table 3A. Multivariate regression analyses for the prediction of fat volumes indices in the right proximal femur and sub regions. Unstandardized β values and level of significance indicated where correlation reaches significance. *Correlation is significant at the 0.05 level (2-tailed). Vit D was in all models but did not contribute to overall significance of the models.

Variables	L2			L3		
	FV	L2FV%	Fv/Bv	FV	L3FV%	Fv/Bv
Age	NS					
BMI	NS					
Vit D	NS					
Diabetes status/Glucose	1226**	77**	0.8**	979**	NS	

Table 3B. Multivariate regression analyses for the prediction of fat volumes indices of the lumbar vertebrae. Unstandardized β values and level of significance indicated where correlation reaches significance. **Correlation is significant at the 0.001 level (2-tailed).
*Correlation is significant at the 0.05 level (2-tailed). NS denotes not statistically significant.

5.3.4 Associations of fat volume with bone volume and BMD

All proximal femoral ROIs showed a strong negative correlation between MAT and bone volume (BV/TV). This negative correlation was weaker for the L2 and L3 vertebral ROIs (Table 4). There was also a consistent negative association between MAT vs DXA-derived BMD of femoral neck and total hip (Table 4).

5.3.5 Associations of fat volume with inflammatory cytokines, insulin resistance indicators and bone biomarkers

There was no association between marrow fat volume fraction (MAT) and insulin resistance, indicators or hormones involved in the metabolism of glucose and fat in any ROI (Table 5). No consistent associations were detected for any MAT ROIs with any of the tested inflammatory mediators, except a weak negative association between L2 and L3 MAT with IL-6 (Table 5).
No associations between fat volumes vs. hormones and bone biomarkers ($R<0.147$, $p>0.238$) were found.

	Lt neck MAT%	Rt neck MAT%	Lt troch. MAT%	Rt troch. MAT%	Lt prox hip MAT%	Rt prox hip MAT%	L2 MAT%	L3 MAT%
Lt neck BV/TV%	**-0.964**	**-0.892**	**-0.896**	**-0.850**	**-0.942**	**-0.893**	**-0.333 (0.012)**	**-0.330 (0.013)**
Rt neck BV/TV%	**-0.884**	**-0.963**	**-0.840**	**-0.883**	**-0.870**	**-0.946**	**-0.376 (0.004)**	**-0.346 (0.009)**
Lt troch. BV/TV%	**-0.880**	**-0.836**	**-0.966**	**-0.906**	**-0.953**	**-0.892**	**-0.372 (0.005)**	**-0.347 (0.009)**
Rt troch. BV/TV%	**-0.841**	**-0.886**	**-0.906**	**-0.967**	**-0.893**	**-0.950**	**-0.424**	**-0.386 (0.003)**
Lt Ttl hip BV/TV% (	**-0.925**	**-0.865**	**-0.953**	**-0.894**	**-0.969**	**-0.900**	**-0.362 (0.006)**	**-0.347 (0.009)**
Rt Ttl hip BV/TV% (	**-0.884**	**-0.947**	**-0.893**	**-0.947**	**-0.903**	**-0.972**	**-0.409**	**-0.374 (0.009)**
L2 BV/TV (n=60)	**-0.398 (0.002)**	**-0.336 (0.010)**	**-0.348 (0.008)**	**-0.317 (0.015)**	**-0.375 (0.004)**	**-0.3433 0.011**	-0.240 (0.090)	-0.213 (0.138)
L3 BV/TV% (n=60)	**-0.471**	**-0.409**	**-0.440**	**-0.397 (0.002)**	**-0.460**	**-0.410**	**-0.274 (0.052)**	-0.264 (0.06)
Lt neck BMD (g/cm^2, n=40)	**-0.370 (0.031)**	-0.276 (0.115)	**-0.340 (0.049)**	-0.284 (0.103)	**-0.364 (0.035)**	-0.295 (0.090)	-0.282 (0.23)	-0.262 (0.27)
Lt Ttl hip BMD (g/cm^2, n=40)	**-0.368 (0.032)**	-0.274 (0.117)	-0.322 (0.063)	-0.302 (0.082)	**-0.355 (0.040)**	-0.305 (0.079)	-0.105 (0.57)	-0.031 (0.87)
LS BMD (g/cm^2, N=40)	-0.161 (0.28)	-0.177 (0.23)	-0.001 (0.99)	-0.106 (0.43)	-0.083 (0.57)	-0.168 (0.23)	-0.22 (0.92)	-0.09 (0.62)

Table 4: Correlations between MAT and BV/TV at several ROIs. Significant associations have been highlighted in bold and p-values ≤0.001 have not been displayed. Rt: right, Lt: left; prox: proximal; L2 and L3: second and third lumbar vertebra; BV/TV: bone volume fraction; MAT: FV/TV; troch: trochanteric

	Adiponectin (ng/mL)	Leptin (µg/L)	Insulin (µU/mL)	HOMA-IR	CRP (mg/L)	IL-1α (pg/mL)	IL-6 (IU/mL)	TNF-α (ng/mL)
Lt troch. MAT% (n=96)	-0.051 (0.627)	-.12 (0.248)	0.034 (0.748)	0.025 (0.807)	-0.128 (0.22)	-0.014 (0.894)	**0.242 (0.019)**	-0.014 (0.892)
Rt troch. MAT% (n=96)	-0.002 (0.985)	0.151 (0.145)	-0.131 (0.21)	-0.083 (0.428)	0.027 (0.796)	0.069 (0.511)	0.054 (0.603)	-0.105 (0.316)
Lt Ttl hip MAT% (n=96)	-0.065 (0.532)	-0.12 (0.249)	0.014 (0.891)	0.007 (0.943)	-0.143 (0.17)	0.019 (0.856)	**0.221 (0.032)**	0.021 (0.839)
Rt Ttl hip MAT% (n=96)	0.003 (0.975)	0.135 (0.193)	-0.146 (0.159)	-0.106 (0.308)	0.016 (0.875)	0.036 (0.731)	0.024 (0.819)	-0.132 (0.204)
L2 MAT% (n=57)	-0.169 (0.208)	0.252 (0.059)	0.116 (0.39)	0.11 (0.414)	.075 (0.578)	-0.185 (0.167)	**-0.286 (0.031)**	-0.217 (0.105)
L3 MAT% (n=57)	-0.123 (0.363)	0.204 (0.127)	0.088 (0.517)	0.076 (0.575)	0.147 (0.276)	-0.194 (0.148)	**-0.318 (0.016)**	-0.204 (0.128)

Table 5: Associations between metabolic and inflammatory markers and fat volumes at different ROIs. Significant associations are in bold and p-values ≤0.001 have not been displayed. Rt: right, Lt: left; Ttl: total; L2, L3: second and third lumbar vertebra, respectively; marrow fat volume fraction=MAT; troch: trochanteric

Results showed a corresponding increase in mean volumes of marrow fat in the neck of the femur, trochanteric region, proximal femur and the lumbar vertebrae with increasing age. The change in the trochanteric region was the greatest. Conversely, bone volumes at these sites decreased with increasing age. Age, glucose levels and some serum markers of bone turnover correlated with marrow adiposity in some skeletal sites and not others. Age was associated with fat volume indices in trochanteric regions and the proximal femur, whilst mean fasting glucose levels or diabetic states were strongly associated with marrow adiposity indices in the lumbar vertebrae.

Significant differences in fat to bone volume rations were evident between age, vitamin D levels and BMI subgroups, but not diabetes status or T Score status subgroups. In conclusion, this study demonstrated some associations between marrow adiposity and clinical parameters not previously identified. Findings from this study warrant further investigations to clarify the relationships.

5.4 Discussion

As quantified by CT scans, we found that in this cohort of older men, marrow adiposity in proximal femora and lumbar vertebrae increased with ageing. Concurrently, bone volume decreased with increasing age, however, the inverse relationship between marrow fat and bone at these sites is consistently significant only in the trochanteric regions and proximal femora. An association between age and marrow fat in L2 and L3 was not detected.

In contrast, associations between BMI, vitamin D and marrow fat were not detected at all ROIs, including the lumbar vertebrae. Glucose was associated in marrow fat L2 and L3 only. Similarly, the correlations between markers of bone turnover, adipocyte activity and inflammatory mediators with marrow fat volume indices were either absent or inconsistent.

5.4.1 Regional marrow fat depots and age

In the whole study population, we found increased marrow fat with increasing age, which was similar to findings from previous studies with MRI[4, 45-47] and histology.[48] Similar to previous MRI studies, we also found an inverse relationship between marrow fat and bone with increasing age;[49, 50] however, this is limited to the regions of the proximal femur. This significant finding in the proximal femur, neck and trochanteric regions, compared to the lumbar vertebrae, may

explain a higher incidence of hip fractures, compared to clinical vertebral fractures in some of the older population.[51]

The lack of a significant inverse relationship in the lumbar vertebrae may relate to the smaller sample size, smaller age range of the study population and technical errors in its quantification. Nevertheless, as far as we know, this is the first study to show (1) a persistent and significant inverse relationship in the trochanteric region and proximal femora (2) that age was independently associated with marrow adiposity in the neck, trochanteric and proximal femur regions and (3) such relationships using clinical CT.

Although we confirmed the changes in marrow fat and the inverse relationship between fat and bone with increasing age, we were not able to show statistically significant differences in marrow fat indices between older men (>65) and younger men (<65) [result of analyses in appendix]. The mean marrow fat volumes were greater in the older age group (≥ 65) compared to the younger age group (< 65), but the difference was not significant. Possible explanations for this result include:

- The small sample size did not have enough spread of ages to reflect the difference
- Variations in skeletal sites lend to errors in quantification and
- The increment in marrow fat in the vertebrae of men beyond 60 years is slow and small, and thus, the difference is small and not significantly different.

Indeed, a recent MRI study seems to support the last possibility. The study showed that male vertebral marrow fat deposition differed from females, in that it tends to rise steadily throughout life with this gradual trend continuing into later years.[52] It also showed the difference in vertebral marrow fat content between men in the age range of 61-90 to be small, and not significantly different.

5.4.2 Relationship with BMD

Although fat fraction and other ratios of fat to bone volume indices were inversely and highly associated, we found inconsistent relationships between these indices and their corresponding BMD derived by DEXA. Only the left femoral neck fat fraction correlated with left femoral neck BMD and total hip BMD. Lumbar spine fat fraction and volume ratios at both L2 and L3 did not correlate with BMD.

The findings at the lumbar spine were not surprising, given the findings by Griffith et al[52] and another study that examined vertebral BMF at L1–L4 measured with MR spectroscopy; and BMD of the hip and spine with quantitative computed tomography and DXA scans.[53] This cross sectional study involved a cohort of older women and men with a mean age of 79, and found an inverse association between vertebral marrow fat and BMD in older men compared to women, that was not statistically significant.

One reason that may explain our finding of no statistically significant inverse relationship relates to our sample. Our study population consisted of men only from 2 ethnic backgrounds (Chinese and Indian); and the spread of age was not even and adequate in size. All these deficiencies may lead to small differences being seen within the group. This is consistent with a recent study by Griffith et al[52] in which an inverse relationship between BMD and vertebral marrow fat was not evident and diminished with increasing years. In fact, the association between BMF and BMD in this cohort only became significant when the analysis included both men and women. In contrast, there was a significant inverse relationship between vertebral marrow fat and lumbar spine BMD throughout the 61-90 age range for women. It should be noted that other studies using non-invasive imaging methods to assess BMF, which have reported a significant inverse association between BMF and BMD, have involved study populations consisting largely of pre and postmenopausal women, with and without men.[2, 3, 54] Future studies would need to

consider a wider age range and each age range should be of adequate size. Furthermore, it may be rather informative to study men and women separately.

A similar result is seen when we compared subjects with osteopaenia and subjects with normal BMD by DEXA. Previous studies showed significantly elevated marrow fat content in osteoporotic and osteopaenic subjects, compared to normal subjects;[1, 55, 56] whereas, even though our result demonstrated the inverse relationship, it did not reach significance. However, it should be noted that most of these studies combined pre- and postmenopausal women and men in the analyses. Only one study examining a cohort of older men specifically showed significantly elevated vertebral marrow fat content in osteoporotic and osteopaenic subjects, compared to normal subjects.[57] In addition, one study, which measured vertebral marrow fat fraction with MR spectroscopy and BMD by DEXA in a group of 68 healthy men and women [mean age, 50.7 years], found no significant correlation between vertebral marrow fat fraction and BMD.[68]

Furthermore, it remains to be seen whether the relationship between marrow fat and BMD in sub regions of the proximal femur follows what is seen in the vertebrae. To our knowledge, our study is the first to examine this relationship at different regions of the hip individually. However, our result of a significant association found at the femoral neck needs further clarification through adequately powered studies in the future. Such studies would need to examine these relationships stratified by age, sex and ethnicity.

5.4.3 Marrow fat and BMI

Our study did not find correlations between marrow adiposity and BMI consistent with previous studies, which have also not found an association between BMI and adipocyte tissue volume.[55] We then examined the relationship more closely by dividing the cohort based on BMI, and compared subjects with normal BMI and those with higher BMI (≥ 25) [appendix-chapter 5;

table 2).We found no significant differences with all the marrow fat indices in the regions of the proximal femur and spine, however, those with higher BMIs overall had greater marrow adiposity in terms of mean fat volume and fat/bone ratios, which is consistent with some of the existing literature.

Our result is not unexpected, given that previous studies have shown conflicting results, and have compared normal BMI vs. obesity range BMIs compared to our study. The BMI range in our study population lies in the normal to overweight and thus, may be too narrow to show a difference. Results from previous studies have been conflicting, with some showing negative correlations between BMI and pelvic and hip marrow fat but no correlation with vertebral marrow fat,[59, 60] and some showed no correlations.[55,61] In contrast, marrow fat in L4 and the femur, and BMI were inversely related consistently in patients with anorexia nervosa.[64] We were not able to confirm this in our study, as only two subjects had BMIs fitting the criteria.

5.4.4 Marrow fat and Vitamin D

Overall, we did not find correlations between vitamin D levels and marrow adiposity. We further compared subjects based on their vitamin D status, and found that subjects with vitamin D levels of 21ng/ml or higher, compared to lower vitamin D levels had significantly higher marrow adiposity in some trochanteric and proximal femur regions [appendix-chapter 5, table 3]. This seemed to go against known mechanisms of vitamin D inhibition of adipogenesis;[63, 64] however, it must be noted that in this study the mean level of vitamin D for the higher vitamin D group is only 25ng/ml or 62 nmol/L (and with normal PTH levels) which, in the older population, may not be optimal to shift the balance in favour of osteoblastogenesis over adipogenesis. Indeed, this is consistent with some studies, which did not show correlations between vitamin D status, BMD, bone turnover markers or prevalence of fractures.[65]

5.4.5 Marrow fat and diabetes

We found a strong positive association between mean fasting glucose and absolute fat volume and fat/bone volume ratio in the lumbar vertebrae. In fact, glucose accounts for up to almost 40% of the variation in fat volume indices in this region, and is associated with marrow adiposity in the lumbar vertebrae independent of age, vitamin D levels and BMI.

To our knowledge, the relationship between glucose and marrow fat has not been explored, although bone turnover markers and diabetes/glucose have been examined. Given inconclusive data, showing significantly lower osteocalcin and CTX levels in diabetes,[66] further studies examining the effects of glucose on marrow fat may be reasonable.

Comparing diabetics versus nondiabetics, our study showed no significant differences in the mean fat volume in regions of the proximal femur, in agreement with a recent study.[33] However, overall, diabetic subjects seemed to accumulate greater marrow adiposity, most prominently in the lumbar spine, especially at L3. This finding in the spine is consistent with a study that compared vertebral bone marrow fat content, quantified with MR spectroscopy, between postmenopausal women with and without type 2 diabetes mellitus (T2DM).[67] This study demonstrated higher vertebral marrow adiposity in diabetic subjects compared to nondiabetics, and showed significant correlations of mean vertebral fat content with HbA1c in the diabetic group ($r = 0.825$; $P < 0.05$). We also found high correlations between vertebral marrow fat indices and fasting glucose levels, and diabetes status in the whole study population (appendix- chapter 5; Table 4).

5.4.6 Marrow fat and markers of bone turnover and adipocyte activity

The final aim of our study was to examine relationships between marrow fat indices in the regions of the femur and spine with blood biomarkers. We did not find significant correlations

between regional marrow fat volume indices and bone biomarkers, metabolic and most inflammatory markers. It is physiologically plausible that, similar to the conflicting data on the association between leptin and BMD,[68 - 70] that these markers may exert different effects on the bones of different subjects depending on bone tissue, skeletal region, loading, sex and/or signalling pathways.

Regarding inflammation, it has been shown that MAT-released palmitate induces a pro-inflammatory response.[71] Interestingly, in our subjects, the associations between IL-6 and marrow fat in femoral and vertebral ROIs had opposite trends (positive and negative associations, respectively), and other inflammatory factors in the bloodstream did not show associations with marrow fat volumes, thus suggesting that the pro-inflammatory role of marrow fat is site-dependent; a hypothesis that should be tested in future human studies.

5.4.7 Study limitations

This study has some limitations relating to the quantification technique and the study design. Two technical aspects of CT need to be discussed for the appropriate interpretation of our results. First, there was the occurrence of beam hardening, which is a relatively common type of artifact seen in CT. In this phenomenon, greater attenuation of lower-energy photons occur as the polychromatic x x-ray beam passes through the tissues, compared to higher energy photons which may not attenuate. This potentially gives rise to false information about the composition and density of tissues, especially when applying the technique of global thresholding to delineate tissues based on their relative intensities. Thus, in effect, the degree of marrow fat in the cavity of long bones may be underestimated, and it is likely that these errors reduced the strength of the association between bone and fat findings in our study.

Secondly, the much finer size/thickness of the trabeculae greatly exceeded the limited spatial

resolution of CT, and thus, limited the accuracy when measuring cancellous bone density. Furthermore, the finer the trabeculae, the greater the influence from marrow fat, giving rise to volume averaging errors. A similar scenario arises when deriving the Hounsfield threshold range, delineating marrow fat from haemopoietic tissue. Ultimately, pixel density averaging errors will influence volume calculation. The degree of this error remains to be determined in future studies.

Another limitation is the cross sectional design. Further investigations, including longitudinal studies, will be needed to confirm the associations. However, the relatively large number of subjects; quantification of separate sub regions of the proximal femur; and limiting the cohort to older men are the strengths of this study.

In summary, using clinical CT and quantifying marrow fat contents as volumes and volume ratios, we were able to confirm relationships between marrow adiposity and clinical parameters, relevant to the pathophysiology of osteoporosis. Our results are consistent with other imaging modalities, which are considered gold standards for assessing marrow fat. The findings also suggest that this technique may be applicable in future clinical studies.

5.5 References

1. Verma S, Rajaratnam JH, Denton J, et al. Adipocytic proportion of bone marrow is inversely related to bone formation in osteoporosis. J Clin Pathol. 2002; 55(9):693-698.

2. Shen W, Chen J, Gantz M, et al. MRI-measured pelvic bone marrow adipose tissue is inversely related to DXA-measured bone mineral in younger and older adults. Eur J Clin Nutr. 2012;

66(9):983-988.

3. Griffith JF, Yeung DK, Antonio GE, et al. Vertebral marrow fat content and diffusion and perfusion indexes in women with varying bone density: MR evaluation. Radiology. 2006; 241(3):831-838.

4. Schellinger D, Lin CS, Fertikh D, et al. Normal lumbar vertebrae: anatomic, age, and sex variance in subjects at proton MR spectroscopy--initial experience. Radiology. 2000; 215(3):910-916.

5. Wehrli FW, Hopkins JA, Hwang SN, et al. Cross-sectional study of osteopenia with quantitative MR imaging and bone densitometry. Radiology. 2000; 217(2):527-538.

6. Griffith JF, Yeung DK, Antonio GE, et al. Vertebral bone mineral density, marrow perfusion, and fat content in healthy men and men with osteoporosis: dynamic contrast-enhanced MR imaging and MR spectroscopy, Radiology. 2005; 236 (3); 945–951.

7. Griffith JF, Yeung DK, Antonio GE, et al. Vertebral marrow fat content and diffusion and perfusion indexes in women with varying bone density: MR evaluation, Radiology. 2006; 241 (3); 831–838.

8. Yeung DK, Griffith JF, Antonio GE, et al. Osteoporosis is associated with increased marrow fat content and decreased marrow fat unsaturation: a proton MR spectroscopy study. J. Magn. Reson. Imaging. 2005; 22 (2); 279–285.

9. Tang GY, Lv ZW, Tang RB, et al. Evaluation of MR spectroscopy and diffusion-weighted MRI in detecting bone marrow changes in postmenopausal women with osteoporosis. Clin. Radiol. 2010; 65 (5); 377–381.

10. Sheu Y, Amati F, Schwartz AV, et al; Osteoporotic Fractures in Men (MrOS) Research Group. Vertebral bone marrow fat, bone mineral density and diabetes: The Osteoporotic Fractures in Men (MrOS) study. Bone. 2017; 97:299-305.

11. Yu EW, Greenblatt L, Eajazi A, et al. Marrow adipose tissue composition in adults with morbid obesity. Bone. 2017; 97:38-42.

12. Li X, Kuo D, Schafer AL, et al. Quantification of vertebral bone marrow fat content using 3 Tesla MR spectroscopy: reproducibility, vertebral variation, and applications in osteoporosis. J Magn Reson Imaging. 2011; 33(4):974–979.

13. Griffith JF, Yeung DK, Leung JC, et al. Prediction of bone loss in elderly female subjects by MR perfusion imaging and spectroscopy. Eur Radiol. 2011; 21(6):1160–1169.

14. Abdalrahaman N, McComb C, Foster JE, et al. Deficits in trabecular bone microarchitecture in young women with type 1 diabetes mellitus. J Bone Miner Res. 2015; 30(8):1386–9133.

15. Slade JM, Coe LM, Meyer RA, et al. Human bone marrow adiposity is linked with serum lipid levels not T1-diabetes. J Diabetes Complications. 2012; 26(1):1–9.

16. Di Pietro G, Capuani S, Manenti G,et al. Bone Marrow Lipid Profiles from Peripheral Skeleton as Potential Biomarkers for Osteoporosis: A 1H-MR Spectroscopy Study. Acad Radiol. 2016; 23(3):273-283.

17. Schwartz AV. Marrow fat and bone: review of clinical findings. Front Endocrinol (Lausanne). 2015; 6:40

18. Liu P, Oyajobi BO, Russell RG, et al. Regulation of osteogenic differentiation of human bone marrow stromal cells: interaction between transforming growth factor-beta and 1,25(OH)(2) vitamin D(3) In vitro. Calcif Tissue Int. 1999; 65(2):173-180.

19. Zhou S, LeBoff MS, Glowacki.J. Vitamin D Metabolism and Action in Human Bone Marrow Stromal Cells. Endocrinology. 2010; 151(1): 14–22

20. Mutt SJ, Hypponen E, Saarnio J, et al. Vitamin D and adipose tissue-more than storage. Front Physiol (2014) 5:228.10.3389/fphys.2014.00228

21. Sakuma T, Miyamoto T, Jiang W, et al. Inhibition of peroxisome proliferator-activated

receptor alpha signaling by vitamin D receptor. Biochem Biophys Res Commun. 2003; 312(2):513–519.

22. Fan Y, Hanai JI, Le PT, et al. Parathyroid Hormone Directs Bone Marrow Mesenchymal Cell Fate. Cell Metab. 2017; 25(3):661-672.

23. Dempster DW, Cosman F, Kurland ES, et al. Effects of daily treatment with parathyroid hormone on bone microarchitecture and turnover in patients with osteoporosis: a paired biopsy study. J Bone Miner Res. 2001; 16(10):1846-1853.

24. Botolin S, McCabe SLR. Bone loss and increased bone adiposity in spontaneous and pharmacologically induced diabetic mice. Endocrinology. 2007; 148 (1); 198–205.

25. Krings A, Rahman S, Huang S, et al. Bone marrow fat has brown adipose tissue characteristics, which are attenuated with aging and diabetes. Bone. 2012; 50 (2); 546–552.

26. Botolin S, Faugere MC, Malluche H,et al. Increased bone adiposity and peroxisomal proliferator-activated receptor-gamma2 expression in type I diabetic mice, Endocrinology. 2005; 146 (8); 3622–3631.

27. Devlin MJ, Van Vliet M, Motyl K, et al. Early-onset type 2 diabetes impairs skeletal acquisition in the male TALLYHO/JngJ mouse. Endocrinology. 2014; 155(10):3806–3816.

28. Slade JM, Coe LM, Meyer RA, et al.. Human bone marrow adiposity is linked with serum lipid levels not T1-diabetes. J Diabetes Complications. 2012; 26(1):1–9.

29. Sheu Y, Schwartz AV, Amati F, Goodpaster BH, Li X, Bauer DC, et al. Bone marrow adiposity is elevated in older men with type 2 diabetes. Diabetes. 2012; 61:A367.

30. Baum T, Yap SP, Karampinos DC, et al. Does vertebral bone marrow fat content correlate with abdominal adipose tissue, lumbar spine bone mineral density, and blood biomarkers in women with type 2 diabetes mellitus? J Magn Reson Imaging. 2012; 35(1):117–124.

31. Patsch JM, Li X, Baum T, et al. Bone marrow fat composition as a novel imaging biomarker

in postmenopausal women with prevalent fragility fractures. J Bone Miner Res. 2013; 28(8):1721–1728.

32. de Paula FJ, de Araujo IM, Carvalho AL, et al. The relationship of fat distribution and insulin resistance with lumbar spine bone mass in women. PLoS ONE. 2015; 10(6):e0129764.

33. Ng AC, Wai DC, Tai ES, et al. Visceral adipose tissue, but not waist circumference is a better measure of metabolic risk in Singaporean Chinese and Indian men. Nutr Diabetes. 2012; 2(8):e38.

34. Yeo KK, Tai BC, Heng D, et al. Ethnicity modifies the association between diabetes mellitus and ischaemic heart disease in Chinese, Malays and Asian Indians living in Singapore. Diabetologia. 2006; 49(12):2866-2873.

35. Sabanayagam C, Lim SC, Wong TY, et al. Ethnic disparities in prevalence and impact of risk factors of chronic kidney disease. Nephrol Dial Transplant. 2010; 25(8):2564-2570.

36. Aasen G, Fagertun H, Halse J. Body composition analysis by dual X-ray absorptiometry: in vivo and in vitro comparison of three different fan-beam instruments. Scand J Clin Lab Invest. 2006; 66(8):659-666.

37. Hounsfield G N. Computed medical imaging. Science. 1980; 210(4465):22-28.

38. Woodard HQ, White DR. Bone models for use in radiotherapy dosimetry. Br J Radiol. 1982; 55(652):277-282.

39. White DR, Woodard HQ, Hammond SM. Average soft-tissue and bone models for use in radiation dosimetry. Br J Radiol. 1987; 60(717):907-913.

40. Schneider W, Bortfeld T, Schlegel W. Correlation between CT numbers and tissue parameters needed for Monte Carlo simulations of clinical dose distributions. Phys Med Biol. 2000; 45(2):459-478.

41. Moore SG, Dawson KL. Red and yellow marrow in the femur: age-related changes in

appearance at MR imaging. Radiology. 1990; 175(1):219-223.

42. Vande Berg BC, Lecouvet FE, Moysan P, et al. MR assessment of red marrow distribution and composition in the proximal femur: correlation with clinical and laboratory parameters. Skeletal Radiol. 1997; 26(10):589-596.

43. Helms CA, Cann CE, Brunelle FO, et al. Detection of bone-marrow metastases using quantitative computed tomography. Radiology. 1981; 140(3):745-750.

44. Despres JP. Abdominal obesity as important component of insulin-resistance syndrome. Nutrition. 1993; 9(5):452-459.

45. Dooms GC, Fisher MR, Hricak H, et al. Bone marrow imaging: magnetic resonance studies related to age and sex. Radiology. 1985; 155(2):429-432.

46. De Bisschop E, Luypaert R, Louis O, et al. Fat fraction of lumbar bone marrow using in vivo proton nuclear magnetic resonance spectroscopy. Bone. 1993; 14(2):133-136.

47. Kugel H, Jung C, Schulte O, et al. Age- and sex-specific differences in the 1H- spectrum of vertebral bone marrow. J Magn Reson Imaging. 2001; 13(2):263-268.

48. Rozman C, Feliu E, Berga L, et al. Age-related variations of fat tissue fraction in normal human bone marrow depend both on size and number of adipocytes: a stereological study. Exp Hematol. 1989; 17(1):34-37.

49. Di Iorgi N, Mo AO, Grimm K, et al. Bone acquisition in healthy young females is reciprocally related to marrow adiposity. J Clin Endocrinol Metab. 2010; 95(6):2977-2982.

50. Wren TA, Chung SA, Dorey FJ, et al. Bone marrow fat is inversely related to cortical bone in young and old subjects. J Clin Endocrinol Metab. 2011; 96(3):782-786.

51. Bow CH, Cheung E, Cheung CL, et al. Ethnic difference of clinical vertebral fracture risk. Osteoporos Int. 2012; 23(3):879-885.

52. Griffith JF, Yeung DK, Ma HT, et al. Bone marrow fat content in the elderly: a reversal of sex difference seen in younger subjects. J Magn Reson Imaging. 2012; 36(1):225- 230.

53. Schwartz AV, Sigurdsson S, Hue TF, et al. Vertebral bone marrow fat associated with lower trabecular BMD and prevalent vertebral fracture in older adults. J Clin Endocrinol Metab. 2013; 98(6):2294-2300.

54. Li X, Kuo D, Schafer AL, et al. Quantification of vertebral bone marrow fat content using 3 Tesla MR Spectroscopy: reproducibility, vertebral variation, and applications in osteoporosis. Journal of magnetic resonance imaging: JMRI. 2011; 33(4):974-979.

55. Justesen J, Stenderup K, Ebbesen EN, et al. Adipocyte tissue volume in bone marrow is increased with aging and in patients with osteoporosis. Biogerontology. 2001; 2(3):165- 171.

56. Yeung DK, Griffith JF, Antonio GE, et al. Osteoporosis is associated with increased marrow fat content and decreased marrow fat unsaturation: a proton MR spectroscopy study. J Magn Reson Imaging. 2005; 22(2):279-285.

57. Griffith JF, Yeung DK, Antonio GE, et al. Vertebral bone mineral density, marrow perfusion, and fat content in healthy men and men with osteoporosis: dynamic contrast- enhanced MR imaging and MR spectroscopy. Radiology. 2005; 236(3):945-951.

58. Youn I, Lee H, Kim J. Correlation between Vertebral Marrow Fat Fraction Measured Using Dixon Quantitative Chemical Shift MRI and BMD Value on Dual-energy X-ray Absorptiometry. JKSMRM 2012; 161(1):16-24.

59. Shen W, Scherzer R, Gantz M, et al. Relationship between MRI-measured bone marrow adipose tissue and hip and spine bone mineral density in African-American and Caucasian participants: the CARDIA study. J Clin Endocrinol Metab. 2012; 97(4):1337-1346.

60. Shen W, Chen J, Gantz M, et al. Ethnic and sex differences in bone marrow adipose tissue and bone mineral density relationship. Osteoporos Int. 2012; 23(9):2293-2301.

61. Bredella MA, Torriani M, Ghomi RH, et al. Vertebral bone marrow fat is positively associated with visceral fat and inversely associated with IGF-1 in obese women. Obesity. 2011; 19(1):49-53.

62. Bredella MA, Fazeli PK, Miller KK, et al. Increased bone marrow fat in anorexia nervosa. J Clin Endocrinol Metab. 2009; 94(6):2129-2136.

63. Kelly KA, Gimble JM. 1, 25-Dihydroxy vitamin D3 inhibits adipocyte differentiation and gene expression in murine bone marrow stromal cell clones and primary cultures. Endocrinology. 1998; 139(5):2622-2628.

64. Wood RJ. Vitamin D and adipogenesis: new molecular insights. Nutr Rev. 2008; 66(1):40-46.

65. Garnero P, Munoz F, Sornay-Rendu E, et al. Associations of vitamin D status with bone mineral density, bone turnover, bone loss and fracture risk in healthy postmenopausal women. The OFELY study. Bone. 2007; 40(3):716-722.

66. Starup-Linde J, Eriksen SA, Lykkeboe S, et al. Biochemical markers of bone turnover in diabetes patients--a meta-analysis, and a methodological study on the effects of glucose on bone markers. Osteoporos Int. 2014; 25(6):1697-1708.

67. Baum T, Yap SP, Karampinos DC, et al. Does vertebral bone marrow fat content correlate with abdominal adipose tissue, lumbar spine bone mineral density, and blood biomarkers in women with type 2 diabetes mellitus? J Magn Reson Imaging. 2012; 35(1):117- 124.

68. Di Monaco M, Vallero F, Di Monaco R, et al. Fat body mass, leptin and femur bone mineral density in hip-fractured women. J Endocrinol Invest. 2003; 26(12):1180-1185.

69. Ruhl CE, Everhart JE. Relationship of serum leptin concentration with bone mineral density in the United States population. J Bone Miner Res. 2002; 17(10):1896-1903.

70. Sato M, Takeda N, Sarui H, et al. Association between serum leptin concentrations and bone

mineral density, and biochemical markers of bone turnover in adult men. J Clin Endocrinol Metab. 2001; 86(11):5273-5276.

71. Gillet C, Spruyt D, Rigutto S, et al. Oleate Abrogates Palmitate-Induced Lipotoxicity and Proinflammatory Response in Human Bone Marrow-Derived Mesenchymal Stem Cells and Osteoblastic Cells. Endocrinology. 2015; 156(11):4081-4093.

6.0 Chapter 6: Effects of Calcium-Vitamin D3 and Exercise on Marrow fat in Older Men: An 18-Month Randomized Controlled Trial

6.1 Introduction

Exercise has long been the recommended alternate approach for improving bone density, by increasing and/or retarding bone loss during the older years.[1] A number of meta-analyses have evaluated the effects of exercise on FN and LS BMD in adults.[2-19] Physical activity, in general, has shown a significant effect on BMD at the lumbar spine (ES 0.8745, $p < .05$), but not on forearm and femoral bone mass.[2] In postmenopausal women, impact and non-impact exercise increased FN and LS BMD, ranging from 0.7% to 1.6%;[3, 7] high-intensity resistance exercise had a small statistically significant benefit in LS BMD,[13] whereas walking only shows a non-statistically significant benefit in FN and LS BMD in another meta-analysis.[14] Mixed exercise programs, consisting of impact loading activity with resistance training, benefited FN BMD and total hip BMD, but not LS.[15] Low-impact and resistance exercise studies observed increases in LS and FN BMD in older adults,[18] but a more recent Cochrane systematic review reported a small statistically significant BMD increase in LS only with joint and/or ground reaction force exercise.[16] Nevertheless, the most effective type of exercise intervention on bone mineral density (BMD) for the neck of the femur appears to be non-weight bearing high force exercise, such as progressive resistance strength training for the lower limbs, and the most effective intervention for BMD at the spine was a combination exercise program.[16] An updated meta-analysis, which also included randomized controlled trials with exercise intervention ≥ 24 weeks; subjects not participating in any type of recent exercise and unpublished studies in any language[17] confirmed

small, statistically significant improvements in BMD for both FN and LS.

In men, an earlier meta-analysis showed positive effects of exercise on BMD at the femur and lumbar spine.[8] However, a recent meta-analysis, which included randomized controlled exercise trials ≥ 24 weeks, only showed a moderate statistically significant improvement at the FN and a small trend towards statistical improvement at the LS.[20]

As for calcium and/or vitamin D supplementation, each one independently or both combined, have demonstrated beneficial effects on bone in older men[21, 22] and women.[23-25] Calcium, combined with weight bearing exercise, increased BMD in post-menopausal women.[26] The mechanisms that may explain the effects of exercise on bone have been investigated in mice studies. Positive effects of exercise have been shown on bone strength and bone formation.[27, 28] Bone volume and osteoblast numbers significantly increased in mice subjected to climbing exercise, while marrow adipocyte volumes and numbers decreased in control mice.[29-31] Even with low intensity mechanical loading signals (intensity well below the level that would arise during walking), Rubin et al[32] showed that C57BL/6J mice subjected to brief, daily high-frequency mechanical signals for 15 weeks showed inhibition of adipogenesis by up to 27%. In another mice study, endurance exercise-trained animals had significantly less total fat in their marrow cavities than sedentary control animals.[33] Exercise has also been shown to prevent accumulation of marrow adipose tissue in mice fed a high fat diet.[34]

There is physiological and clinical rationale to examine the effects of exercise on marrow adiposity given the link between marrow adiposity and bone density[35-37] and osteoporosis,[38] and the inverse relationship between osteoblastogenesis and adipogenesis.[39, 40] There is in vitro evidence that mechanical loading down regulate peroxisome proliferator activated receptor gamma in bone marrow stromal cells, favouring osteoblastogenesis over adipogenesis,[41, 42] and exercise has been shown to mitigate the impact of PPARγ agonists on bone and marrow health.[43]

Furthermore, human studies quantifying marrow fat in response to exercise is lacking. In one study, healthy young men were subjected to head-down tilt bed rest for 60 days and resistance exercises, with or without whole body vibration, and this was shown to prevent vertebral marrow fat accumulation quantified by MRI.[44] In contrast, the effects of Calcium and Vitamin D alone, or in combination on marrow fat, have not been explored. Whether they have suppressive effects on marrow fat whilst increasing bone mass remain unknown. Indeed, what effects they have on marrow fat when combined with exercise has not been examined. Thus, the objectives for this study are to

- Determine marrow fat response to calcium, calcium-vitamin D_3, exercise and exercise supplemented with calcium-vitamin D_3 by quantifying the amount of marrow fat
- Assess whether calcium-vitaminD_3 fortified milk could enhance the effects of exercise on bone marrow fat and indeed whether these effects are neutral, additive or opposing in nature.

Here we report the effects seen with bone volume and marrow fat volume using our described marrow fat quantification method.

6.2 Materials and Methods

Note that this is an ancillary study of a larger study, whose original objective was to assess whether calcium-vitamin D(3) fortified milk could enhance the effects of exercise on bone strength, structure, and mineral density in middle-aged and older men. The methodology for this study has been described in detail previously.[45] Here a summary is presented.

6.2.1 Study design

The study was an ancillary analysis of an 18-month factorial 2x2 RCT, which was conducted over a 3 year period, from February 2003 to February 2006. There were 4 groups to which 180 subjects were randomized. Group 1 (n =45) received exercise, combined with fortified milk; Group 2 (n = 46) was exposed to exercise only; Group 3 (n =45) received fortified milk only and group 4 (n =44) was the control group. Stratification of subjects, based on age under 65 or 65 and older, in addition to the amount of calcium consumed in the diet (< 800 or ≥ 800 mg/d), was carried out before randomization.

6.2.2 Participants

The study took place in Geelong, a regional city of south-western Victoria (38˚ south latitude) with a population of around 220,000. Healthy men aged 50–79 yrs., who were living in the community, were recruited.

Exclusion criteria included:

- Taking any calcium-vitamin D supplement in the previous 12 months
- Undertaken resistance training in the preceding 12 months and/or within the last 6 months have participated in weight bearing activities that are high-impact, and for more than half an hour in duration, three times per week
- Body mass index (BMI) of >35 kg/m2
- Any previous osteoporotic fracture
- Any medical condition or taking any medication known to affect bone metabolism
- Lactose intolerance
- Current drinker of > 4standard alcoholic drinks daily
- Current smokers

- Any chronic condition limiting the ability to participate in and comply with the trial.

6.2.3 Screening and randomization

Four hundred and fifty-one men were pre-screened, with 296 suitable to have a dual energy x-ray absorptiometry (DXA) scan. Men with an average aBMD that is normal or less (*i.e.*, total hip or femoral neck T-score -2.4 SD to +0.4) were included (n =180). Using a computer- generated randomization of study numbers, 180 subjects were allocated to one of the four groups. The researchers were blinded to the randomization, and subsequent allocation of subjects into groups and interventions. Subjects were not blinded to interventions.

All eligible subjects were medically cleared by their local physicians, to ensure they did not have any medical conditions that exercise would be harmful for, *"based on the American College of Sports Medicine (ACSM) guidelines."*[46]

The Deakin University Human Ethics Committee and Barwon Health Human Research Ethics Committee approved the study, and all study participants signed their written consent. The trial was registered on the 22nd of August 2017, and the trial ID is ACTRN12617001224314.

6.2.4 Interventions

6.2.4.1 Exercise program

The exercise program was conducted in 4 leisure facilities in the community, and for the duration of the study, certified exercise trainers supervised exercise training. Subjects performed exercise training for 3 non-consecutive sessions per week (no longer than three days apart between each session) with each session lasting 60–75 minutes. Three types of activities formed the basis of the exercise program:

- Stationary cycling, and stretching for 5- to 10-min for warming-up and cooling-down
- 6- 8 moderate- to high-intensity progressive resistance training exercises
- Three moderate impact weight-bearing exercises.

Table 1 illustrates the exercise schedule. The high intensity progressive resistance training involved combining upper and lower body machine, and free weights with core strength exercises.

All subjects performed exercises in a slow and controlled manner for the first 12 months. In the remaining 6 months, the program focused on high-velocity power-based training (rapid concentric muscle contractions). Compliance with the exercise program was determined by an exercise card system. Each subject was required to 'sign in' for each session by the gymnasium staff, and the completed exercise cards were verified daily by the trainers and returned to the research staff monthly. Recording of adverse events and injuries was done by the trainer who was supervising the exercise session at the time.

Study Period		Exercise	Intensity
Month	Week		
1-6	1-12	Progressive resistance training 3 sets of 15–20 repetitions of: Squats (or leg press), lunges, hip abduction/adduction, latissimus dorsa pull down (or seated row), back extension, and a combination of abdominal and core stability exercises. Moderate-impact weight-bearing exercises Single and double foot landings, bench stepping, and jumping off 15- and 30-cm benches.	 50–60% of one repetition maximum (1-RM) strength for each resistance exercise 3 sets of 10 repetitions:

	13-24	Progressive resistance training 2 sets of 8–12 repetitions of: Squats (or leg press), lunges, hip abduction/adduction, latissimus dorsa pull down (or seated row), back extension, and a combination of abdominal and core stability exercises. Moderate-impact weight-bearing exercises Single and double foot landings, bench stepping, and jumping off 15- and 30-cm benches.	<u>Week 13-16</u> 1) a warm-up set at 60–65% 1-RM 2) a single training set at 60–70% 1-RM <u>Week 17-24</u> 1) a warm-up set at 60–65% 1-RM 2) a single training set at 80–85% 1-RM 3 sets of 10 repetitions
7-18		Progressive resistance training 2 sets of 8–12 repetitions of: Squats (or leg press), lunges, hip abduction/adduction, latissimus dorsa pull down (or seated row), back extension, and a combination of abdominal and core stability exercises. Moderate-impact weight-bearing exercises Single and double foot landings, bench stepping, and jumping off 15- and 30-cm benches.	<u>Week 1-4 of 12 week cycle</u> 1) a warm-up set at 60–65% 1-RM 2) a single training set at 60–70% 1-RM <u>Week 5-12 of 12 week cycle</u> 1) a warm-up set at 60–65% 1-RM 2) a single training set at 80–85% 1-RM 3 sets of 10 repetitions:

Table 1. Exercise program Schedule. The high intensity progressive resistance training involved combining upper and lower body machine and free weights with core strength exercises. The weight bearing exercises were interspersed between the resistance training exercises. Repetitions

progressively increased to a maximum of 20 and varied in magnitude, rate, and distribution (direction) by either increasing the height of jumps and/or by introducing more complex movement patterns. Peak vertical ground reaction forces (GRFs) for these exercises varied from 1.5 to 9.7 times body weight (BW).

6.2.4.2 Calcium-vitamin D3

Calcium and vitamin D was provided as a low fat (~1%) ultra-high temperature milk supplement (Murray Goulburn Cooperative, Brunswick, Australia). Approximately 500 mg calcium and 400IU vitamin D3 were contained in each 200ml milk carton. Subjects allocated to the fortified milk consumed 400ml/d (2 x 200 ml packs). This provided approximately 1000mg of elemental calcium and 800IU vitamin D supplement daily, meeting the recommendation of the Australian Osteoporosis Guideline.[47] For the duration of the study, per 100 ml (for 6 cartons), the average (±SD) amount of calcium and VitaminD3 levels were 247 ± 17 mg and 190 ± 26 IU respectively.

6.2.5 Measurements

6.2.5.1 Anthropometry, diet, and physical activity measurements

A stadiometer was used to measure height and a digital scale was used to measure weight. A food diary, recording 3 days of oral intake (two non-consecutive weekdays and one weekend day), was used for the assessment of nutritional status. Recordings at baseline, 12 and 18 months were analysed with the Foodworks nutrient analysis software program (Xyris Software, Brisbane, Queensland, Australia).

The CHAMPS Activity Questionnaire, a validated tool for measuring the physical activity in older adults,[48]was used to assess habitual weight bearing activities that occurred outside of the exercise intervention period (approximate hours per week); and medication use- calcium and

Vitamin D included. At each visit, the responses to the questionnaire were confirmed by a face-to -face interview.

6.2.5.2 Bone mineral density and bone volumes

Lumbar spine (L1–L4) and proximal femur BMD were measured by DXA (Prodigy, GE Lunar Corp., Madison, WI, with analysis software version 8.10.027). A Philips Mx8000 CT scanner (Philips Mx8000 Quad CT scanner, Philips Medical Systems, The Netherlands) was used for the quantitative computed tomography (QCT) scans of the mid-femur, mid-tibia and lumbar spine (L1-L3). The scan settings were 120 kVp and 50–100 mAs. Axial sections through the mid-portion of L1–L3, the left femoral and tibial mid-shafts were obtained as a series of four 2.5-mm slices. Scout scans were performed to assess femur and tibia length. The mid-point of a line drawn from the midpoint of the intercondylar notch to the midpoint of the superior rim of the femoral neck was the mid femur. Similarly, the mid-point of a line drawn from the tip of the medial intercondylar tubercle to the mid-point of the interarticular surface was the mid tibia.

Each subject was scanned simultaneously with a bone equivalent calibration phantom, containing fluid dipotassium hydrogen phosphate (K2HPO4) of different concentrations (50, 100, 150, 250 mg/ cm^3), air and water.

Total bone, haemopoietic and marrow fat volumes were assessed in the mid-femur, mid-tibia and lumbar spine (L1-L3) using the Tomovision SliceOMatic 4.3 Rev-6i software (Tomovision, Montreal, QC, Canada). The thresholds used to quantify each of the volume parameters have been described in chapter 3 of this thesis. The same thresholds were used for all sites and with refinement of initial thresholds.

Twenty axial sections per subject, with four axial slices per anatomical area, were

analysed. Mean volumes of bone (trabecular and cortical), blood and fat were calculated as absolute volume (μm^3 or mm^3), and as percentages of the total tissue volume. Ratios of fat volume to bone volume were calculated using absolute volumes, and changes in these tissues over time (12 and 18 months) were calculated as absolute volume changes and percentage changes. Quantifications of marrow fat with Slice O Matic were conducted by the author of this thesis, along with an assistant (estimated to be ~20% of the total number of scans). Both assessors were blind to group allocations. The images, which were identified only with the subject's ID number, were analysed first. For the tabulation of results, subject IDs were then matched to a master file, identifying their group allocations. These results were then used for statistical analysis.

6.2.6 Statistical analysis

Statistical analyses were conducted using IBM SPSS Statistics for Windows, Version 20.0. (Armonk, NY: IBM Corp.). Characteristics at baseline and after 18 months between the groups were compared using repeated measures ANOVA. Mixed design ANOVA was used to test for an interaction between exercise and calcium-vitamin D_3, and if no significant interactions were detected, the main effects of exercise (exercise with fortified milk and exercise alone *vs.* fortified milk and control) and calcium-vitaminD_3 fortified milk (exercise with fortified milk and fortified milk *vs.* exercise and controls) were examined. Analysis was carried out separately for the mid femur, mid tibia, L1, L2 and L3.

Changes were expressed either as absolute changes or as percentage changes from the baseline. Between group differences were calculated by subtracting within-group changes from the baseline values in each group for each variable. All data were analysed based on an intention to treat. All data were presented as means ± SD or 95% confidence interval (CI), unless otherwise stated. Significance is at $p = .05$ with ANOVA, unless otherwise stated.

6.2.7 Study attrition and adherence

The withdrawal rate for the whole study was 4.4% (8 out of 180 or 2 from each group). On average, 63% (95% CI: 57, 69) adhered to the exercise program and 90% (95% CI, 87, 93) adhered to the fortified milk. The adherence rate did not differ between the two exercise groups, and similarly, between the two fortified milk groups, no difference in adherence was evident. The exercise program was not associated with any adverse events or serious injuries.

6.3 Results

The effects of interventions on diet, physical activity, and changes in hormonal measures were detailed in the results of the original study.[45] In summary, subjects in the fortified milk group, on average, consumed 688 to 721 mg/d of calcium and 17 to 18 mg/d of vitamin D more in their diet than their non-fortified milk counterparts (all $P < 0.001$). There was an increase of 8.4 ng/ml in serum 25(OH) D levels after 12 months seen in the fortified milk group, on average, relative to the non-fortified milk groups ($P <0.001$), but not after 18 months. Conversely, after 12 months, both exercise and fortified milk did not affect serum PTH, but after 18 months PTH decreased significantly in the exercise groups compared to non-exercise groups ($P <0.05$). Otherwise, there were no demonstrable effects of exercise on any other hormonal measures, and for the duration of the study, there were no changes in habitual activity levels in any of the four groups.

6.3.1 Baseline characteristics

As shown in Table 2, the baseline characteristics did not differ among the four groups. The average dietary calcium intakes of the men in each group ranged from 911 to 1064 mg/d, but 58% had a calcium intake below the Australian recommended dietary intake (RDI) of 1000 mg/d for men aged 50 to 70 yr. Mean baseline serum 25(OH)D levels averaged 34.5 ± 14.4 ng/ml across the groups; no participants had severe vitamin D deficiency [25(OH)D <5 ng/ml]; one participant had moderate deficiency [25(OH)D 5–10 ng/ml] and 17 participants (9.4%) had mild deficiency [25(OH)D 10–20 ng/ml].

Characteristic	**Ex + milk (n = 45)**	**Exercise (n = 46)**	**Milk (n = 45)**	**Control (n = 44)**
Age, yr.	61.7 ± 7.6	60.7 ± 7.1	61.7 ± 7.7	59.9 ± 7.4
Height, cm	174.3 ± 6.3	174.2 ± 6.6	174.4 ± 5.8	175.0 ± 6.6
Weight, kg	83.2 ± 11.9	85.2 ± 10.9	84.1 ± 9.8	81.9 ± 10.7
BMI, kg/m^2	27.4 ± 3.7	28.1 ± 3.3	27.7 ± 3.3	26.7 ± 2.9
Diet				
Energy intake, kJ/d	9694 ± 2149	9884 ± 1948	9761 ± 1717	10199 ± 2201
Protein intake, g/kg/d	1.26 ± 0.32	1.32 ± 0.32	1.23 ± 0.28	1.33 ± 0.31

Characteristic	Ex + milk (n = 45)	Exercise (n = 46)	Milk (n = 45)	Control (n = 44)
Calcium intake, mg/d	911 ± 360	1064 ± 449	1039 ± 455	996 ± 293
Vitamin D intake, μg/d	1.2 ± 2.1	0.8 ± 1.1	1.4 ± 3.0	0.7 ± 1.0
Physical activity				
Weight-bearing activity, h/wk	3.7 ± 3.9	3.6 ± 3.4	3.3 ± 3.8	3.4 ± 4.1

Table 2. Baseline characteristics of the study participants. All values are mean ± SD. BMI, body mass index.

As shown in Table 3, at baseline, marrow fat volumes of the mid femur, mid tibia and lumbar vertebrae 1-3 did not differ significantly between the four groups. Bone volumes also did not differ significantly between the four groups at base line (Appendix-Table 2). Fat volume makes up about 12% of total marrow cavity volume in the mid femur. In comparison, the mid tibia showed slightly lower fat volumes (Table 3), and bone volume was slightly higher (Appendix-Table 3).

In the lumbar vertebrae (Appendix-Tables 4-6), blood volumes were four fold higher than the femur and the tibia, ranging from 18% to 26%, whilst bone volumes were lower, ranging from 67% to 78%. On the other hand, marrow fat volume demonstrated greater variability, averaging under 2% in L1, a little over 2% in L3, rising to an average of 16% in L2 (Table 3). Within each group (Table 4), the haemopoietic, bone and fat volumes, expressed as percentages of the total marrow cavity volume, were not significantly different between lumbar vertebrae 1 to 3. This was the case with absolute volumes of haemopoietic and fat volume between L1, 2 and L3.

There was a significant difference in absolute bone and total marrow cavity volumes at baseline between the lumbar vertebrae, however. Interestingly, the ratios of fat to bone volumes did not differ significantly between the three vertebrae at baseline.

Characteristic	Ex+milk (n _ 45)	Exercise (n _ 46)	Milk (n _ 45)	Control (n _ 44)	Main effects	
					Exercise	Milk
Mid Femur Fv , mm^3						
Baseline	218 ± 87	232 ± 97	217 ± 81	231 ± 86		
Change at 18 months	-3 ± 18	5 ± 23	4 ± 11	3 ± 22	-3 (-3, 9)	-3.8 (-10,2)
%Fv						
Baseline	11.9 ± 4.0	12.5 ± 5.0	11.9 ± 3.7	12.4 ± 3.9		
Change at 18 months	**-.42 ± .83[a]**	.03 ± 1.28	**.11 ± .67[a]**	.12 ± 1.11	**-.3 (-.6, 0.0)[a]**	-.3 (.0,.6)
Fv/Bv						
Baseline	.15 ± .09	.16 ± .10	.14 ± .08	.15 ± .05		
Change at 18 months	$-5x10^{-3} \pm 1x10^{-3}$	$1x10^{-3} \pm 2x10^{-3}$	$1x10^{-3} \pm 9x10^{-3}$	$2x10^{-3} \pm 1.5x10^{-3}$	$2x10^{-4}$ ($2x10^{-4}$,$-6x10^{-4}$)	$-2x10^{-4}$ ($-6x10^{-4}$,$2x10^{-4}$)
Mid Tibia						
Fv						
Baseline	147 ± 71	157 ± 71	133 ± 66	135 ± 72		
Change at 18 months	-1 ± 19	-8 ± 11	-2 ± 10	-6 ± 15	.2 (-4, 5)	**-6 (-10 , -1)[a]**
%Fv						
Baseline	9.3 ± 3.7	10.2 ± 4.3	9.0 ± 4.3	8.8 ± 4.1		
Change at 18 months	-.05 ± 1.09	-.50 ± .63	-.15 ± .64	-.40 ± .90	.02 (-.3,.3)	**-.3 (-.6 , -.1)[b]**
Fv/Bv						
Baseline	.11 ± .05	.12 ± .06	.11 ± .06	.10 ± .05		
Change at 18 months	$-5x10^{-4} \pm 1x10^{-3}$	$-6x10^{-4} \pm 8x10^{-4}$	$-2x10^{-4} \pm 8x10^{-4}$	$-5x10^{-4} \pm 1x10^{-3}$	$2x10^{-4}$ ($-3x10^{-3}$, $3x10^{-3}$)	**$-4x10^{-3}$ ($-9x10^{-4}$, $8x10^{-3}$)[a]**
L2						
Fv						
Baseline	102 ± 139	100 ± 106	72 ± 66	75 ± 68		
Change at 18 months	-1 ± 100	5 ± 50	**14 ± 41[a]**	4 ± 27	7(-12,27)	2 (-27, 18)
%Fv						
Baseline	19.5 ± 27.2	18.6 ± 20.9	12.9 ± 11.9	14.1 ± 12.5		
Change at 18 months	$8x10^{-5} \pm 2x10^{-2}$	$3x10^{-4} \pm 9x10^{-3}$	**$2x10^{-3} \pm 7x10^{-3}$[a]**	$2x10^{-3} \pm 7x10^{-3}$	$2x10^{-5}$ ($-2x10^{-3}$,$6x10^{-3}$	$3x10^{-5}$ (-.04, .04)
Fv/Bv						
Baseline	.03 ± .05	.03 ±.04	.02 ± .02	.22 ± .22		
Change at 18 months	$2x10^{-4} \pm .30$	$8x10^{-4} \pm .20$	**$4x10^{-3} \pm .01$[a]**	$2x10^{-3} \pm .01$	$29x10^{-4}$ ($-32, 91)x10^{-4}$	$5x10^{-4}$ ($-7x10^{-3}$, $6x10^{-3}$)
L3						
Fv						
Baseline	130 ± 183	123 ± 115	145 ± 224	122 ± 98		
Change at 18 months	-20 ± 59	11 ± 52	-20 ± 215	4 ± 43	5 (-32, 43)	-28 (-65, 9)
%Fv						
Baseline	2.2 ± 2.2	2.1 ± 2.2	2.4 ± 3.5	2.1 ± 1.6		
Change at 18 months	-.3 ± 1.0	.1 ± .9	-.3 ± 3.4	.1 ± .7	-.03 (-.05, .1)	-.1 (-.1 , 0)
Fv/Bv						
Baseline	.03 ± .05	.03 ± .03	.04 ± .05	.03 ± .02		
Change at 18 months	$-4.8x10^{-3} \pm 1x10^{-3}$	$1.5x10^{-3} \pm 1.4x10^{-2}$	$-4.4x10^{-3} \pm 4.8x10^{-2}$	$1.1x10^{-3} \pm 1.1x10^{-2}$	$-1x10^{-4}$ ($-9x10^{-4}$, $8x10^{-3}$)	$-5x10^{-2}$ ($-.01$, $3x10^{-2}$)

Table 3. Mean baseline marrow fat volume values (±SD) and percentage unadjusted changes (95% CI) from baseline within each group and the mean differences (95% CI) between the exercise and calcium-vitamin D3 fortified milk groups (main effects). **[a] p ≤.05, [b] p< .01**.

Group	Mean Volume ± SD (95% CI)	L1	L2	L3	p
Control	Fv	87 ± 79	75 ± 68	122 ± 98	.07
	%Fv	1.9 ± 1.7	1.5 ± 1.3	2.1 ± 1.6	.3
	Fv/Bv	.027 ± .026	.022 ± .022	.030 ± .024	.4
Ca only	Fv	70 ± 79	72 ± 66	145 ± 224	.4
	%Fv	1.4 ± 1.4	1.4 ±1.3	2.4 ± 3.6	.9
	Fv/Bv	.022 ± .024	.021 ± .019	.036 ± .051	.9
Ex only	Fv	89 ± 100	100 ± 106	123 ± 115	.4
	%Fv	188.0 ± 216.7	196.3 ±213.3	214.3 ± 202.0	.9
	Fv/Bv	.029 ± .038	.030 ± .036	.032 ±.034	.9
Ex + Ca	Fv	100 ± 138	102 ± 139	130 ± 183	.7
	%Fv	21.4 ± 29.1	20.4 ± 26.9	23.0 ± 29.5	.9
	Fv/Bv	.032 ± .048	.031± .047	.034 ± .050	.9

Table 4. Within groups comparisons of lumbar vertebrae at baseline. Fv (fat volume) and %Fv of total volume. Fv/Bv is ratio of mean absolute fat volume to mean absolute bone volume. # and * are significance at .05 level with Robust test equality of means or ANOVA respectively.

6.3.2 Changes in marrow fat volume indices

There were no significant exercise-by-calcium-vitamin D3 interactions for any marrow fat volume measurements (mean absolute fat volume, fat volume fraction and Fv/Bv) in the mid femur, mid tibia or lumbar vertebrae 2 and 3. For these regions of interest, we are reporting on the main effects of exercise (exercise + calcium and exercise alone vs. calcium and control) and calcium supplement (exercise + calcium and calcium alone vs. exercise

alone and controls) (Table 3 and Fig 1). After 18 months, exercise resulted in a small, but statistically significant, reduction in percentage of marrow fat volume in the mid femur [0.3% (95% CI, 0, 0.6)], relative to no exercise. There were no other beneficial effects of exercise on any marrow fat measurements in other skeletal regions (Table 3 and Fig. 1). In contrast, supplementation with the fortified milk had a significant effect on marrow fat measurements in the mid tibia, relative to those assigned to the non-supplemented group. Significant reductions were seen in mean fat volume (-6 (-10, -1), $p < .05$), percentage fat volume (-0.3 (-0.6, -0.1), $p < .01$), and marrow fat volume to bone volume ratio ($-4x10^{-3}$ ($-9x10^{-4}$, $8x10^{-3}$, $p < .05$) (Table 3).

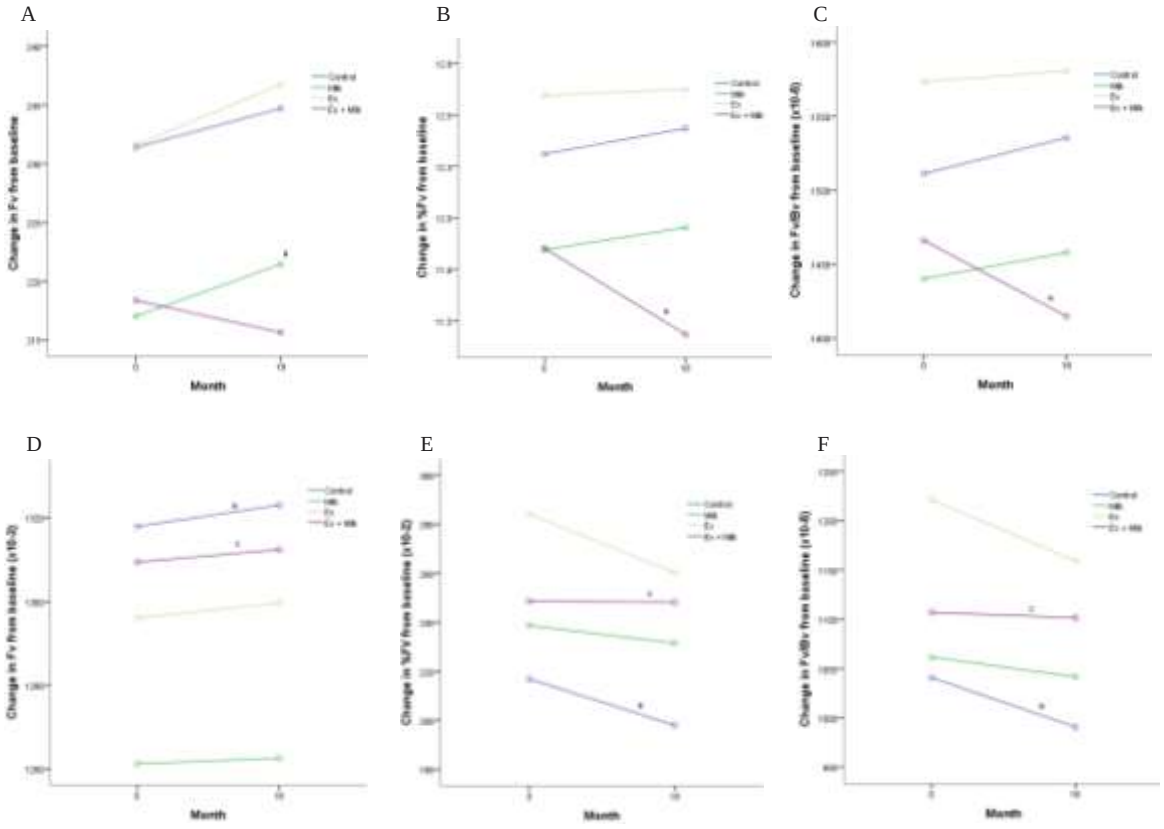

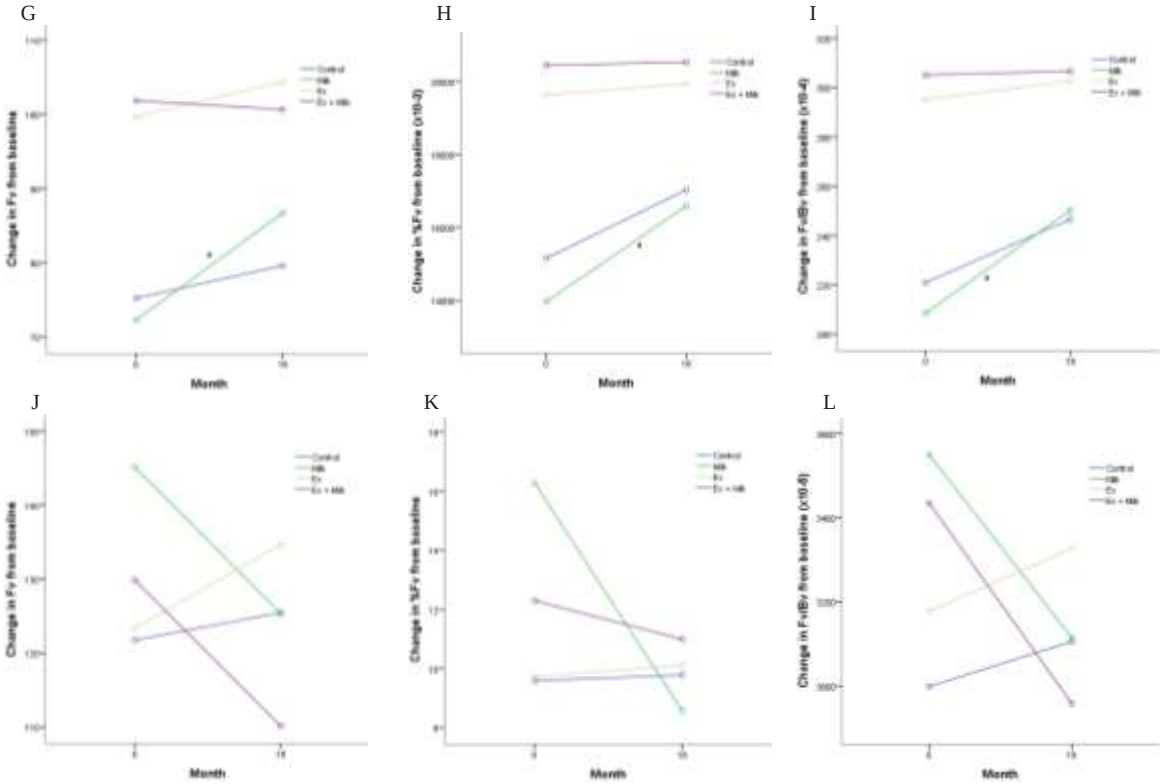

Figure 1. Mean unadjusted changes from baseline of mean fat volume, percentage fat volume and Fat to Bone Volume ratio (Fv/bv) respectively in mid femur (A-C), in mid tibia (D-F), L2 (G-I) and in L3 (J-L) according to treatment group. No exercise-by-calcium/vitamin D3 interactions were detected. a, $P \leq 0.05$; b, $P \leq 0.01$; c, $P \leq 0.001$ for Exercise + milk, Exercise, milk > controls. d, $P \leq 0.01$ for main effect of exercise *vs.* no exercise.

However, there were significant time group interactions in L1, F (3,139) = 4.6, p = .004, F (3,139) = 3.5, p = .02, F (3,139) = 4.1, p = .008 for Fv, %Fv and Fv/Bv respectively. Statistically significant exercise-by-calcium-vitamin D3 interaction was evident for all marrow fat volume measurements in L1 (Figure 2A-C). In following up this interaction, there was an indication that there was no significance difference between the groups at baseline and at 18 months. However, the exercise with the fortified milk group showed reduction in absolute fat volume (29mm^3), percentage of fat volume (3.5%) and reduction in Fv/Bv ratio.

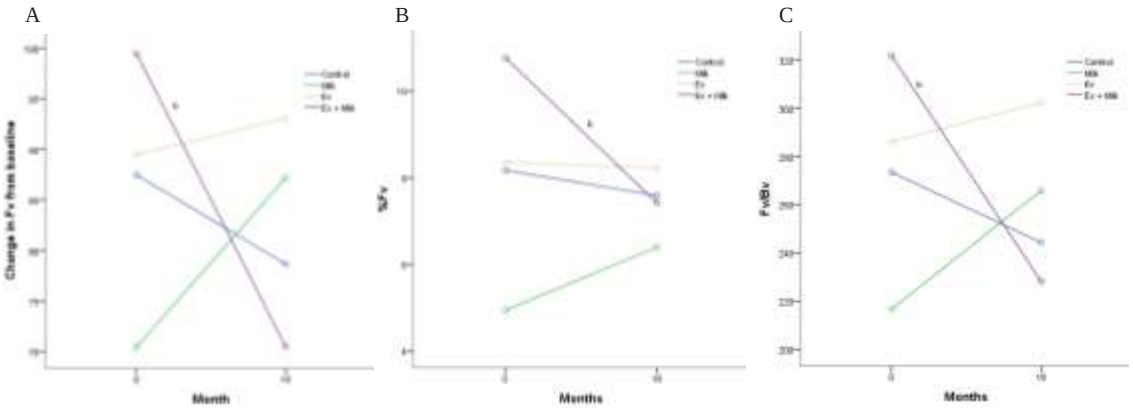

Figure 2. Exercise-by-calcium-vitamin D3 interaction in Lumbar vertebrae 1. b $p < .01$ for change in Fv, %Fv and Fv/Bv over time in Exercise + Milk supplement group.

6.4 Discussion

The result of this 2 by 2 factorial design RCT showed that resistance training and weight bearing exercises, combined with vitamin D/calcium supplements, produced inconsistent and variable effects on marrow fat in different skeletal regions of middle-aged and older men who were healthy and living in the community. Our first aim was to determine the response of marrow fat to calcium/vitamin D, exercise and the combination of the two. Calcium, as a single intervention (Table 2), increased fat volume in the lumbar vertebrae (L1 and L2), and exercise alone significantly reduced fat volume in the mid tibia only.

The second objective was to determine the effects of the combination of exercise and calcium/vitamin D3. The main findings suggest a positive interaction between calcium and exercise, such that this combination attenuates marrow fat volume over time. When exercise was combined with calcium (Table2 and Figure 1), the positive effects on bone volume were observed, as fat volume was reduced in the mid femur and L1 and L3.

However, it is uncertain why the effects differ greatly between different regions. Significant reductions in fat were seen in the mid femur and the first lumbar spine, but no

significant effects were seen in other areas. A number of possibilities may explain these variabilities. Firstly, skeletal loading is greatest in the mid femur and the spine, and hence, effects are maximal. These two regions contain the most adipocyte volume in the normal state, and thus, any interventions that affect this compartment will likely be associated with greater change comparatively.

Another factor that may contribute to the variable responses seen at these skeletal regions, and the lack of more definitive bone and marrow fat response overall, is the calcium intake and serum 25(OH) D levels at baseline. In this study, across all groups, the mean dietary calcium intake ranged from 911-1064 mg/d and serum 25(OH)D levels ranged between 34 and36 ng/ml.[45] These daily dietary calcium intakes approximated the current recommendation for Australian men under 70 years of 1000 mg/d., [49] and similarly, the 'optimal' serum 25(OH)D threshold of 30 ng/ml that confers musculoskeletal benefit[50] is lower than the baseline 25(OH)D across the four groups. Thus, it was expected that further supplementation of calcium and vitamin D beyond the baseline dietary intake for these men would not result in significant differences between exercise alone and exercise plus calcium. Nevertheless, the findings of this study indicated that overall, exercise and calcium do benefit skeletal health, even if the effects are not consistent throughout all skeletal regions.

Given the close relationship between BMD and marrow adiposity, it is not surprising to see inconsistencies paralleling the inconsistent findings of effects of resistance exercise on BMD in prior studies. In premenopausal women, efficacy on lumbar spine and femoral neck BMD ranges from negative effect,[51] no effect at either site, [11] positive effect on lumbar BMD only,[52] to positive effects at both sites.[53] Differences in types of exercise, exercise prescription in terms of intensity, duration and frequency, most likely account for the conflicting results seen with these studies. Studies in middle age men showed shorter duration resistance training increased femoral neck BMD, but no

other proximal femoral regions, lumbar spine or total body BMD.[54, 55] Similarly, in a study of an older cohort, 64-75 year old men undergoing 16 weeks of resistance training, only Ward's triangle BMD increased from baseline. Whole-body, lumbar spine, and femoral neck BMD were unchanged.[56] However, a small study examining the effect of 6 months of whole-body resistive training (RT) on regional BMD in a cohort of younger and older men and women showed a significant increase in BMD at the femoral neck, ward's triangle and greater trochanter BMD overall, but no change in L2-L4 spine BMD.[57]

Longer duration of resistance training in an older cohort of 60-80 year olds also did not show significant BMD responses. After 10 months, although increases in dynamic muscle strength, muscle size, and functional capacity were evident, there were no changes in bone mineral density or content in the lumbar spine, proximal femur or whole body.[58]

Studies of resistance training alone, or in combination with other interventions in postmenopausal women, have also reported disparate results.[58-66] Nine months of resistance training maintained lumbar spine BMD, but did not benefit the proximal femur or distal wrist site.[63] In a longer study of more than 12 months, resistance training in 60-80 year old women did not produce positive changes in bone mineral density or content;[58] and similarly, no significant increase in BMD of (L2-L4), femoral neck, Ward's triangle, and greater trochanter were found with a shorter intense training regime in another study.[66]

It is not certain why there are differences between these findings and those of the present study, but differences in exercise types, exercise duration and different loading force at each skeletal site (despite the same exercise regime) may be important factors. Furthermore, studies examining marrow adiposity as an endpoint of exercise effect is lacking; even studies examining correlates of marrow adiposity as endpoints of exercise is rare.

Nevertheless, from a clinical perspective, this study shows that incorporating calcium into

a multi-component exercise program, consisting of resistance training and impact weight bearing, provides the most benefits to bone health. The changes in marrow content indices are greatest and most significant in this combined group.

The strengths of the original randomized controlled study lies in the factorial trial design, with relatively long-term follow-up, and high participant retention and adherence rate.[45]Also, as far as we are aware, although our study uses secondary analysis, it is the first to examine changes with marrow fat in response to exercise.

However, the interpretations of the results of our study are limited by a number of factors. This is a secondary analysis study, and the objectives were to explore marrow fat responses and generate hypotheses for future studies. The original study was not powered to detect differences in marrow fat changes, and furthermore, the impact of these interventions on marrow fat are largely unknown.

Also, the analyses in this study were not prespecified in the original trial; the power is low; and inherent bias is unavoidable.

In addition, before any firm conclusions can be reached, this technique of quantifying marrow fat with clinical CT needs to be validated in humans. It is likely the uncertainties in the accuracy and sensitivity of this technique more than likely contributed to the inconsistent findings in the quantification of marrow fat. Furthermore, currently it is not known which aspect of marrow adiposity is the most suitable surrogate for the clinical outcome. Whether the mean absolute volume in a region of interest; the percentage of marrow fat over the total tissue volume; or, indeed, the ratio of marrow fat to bone volume serves as the marker, remains to be determined.

In addition, the subjects included in the study were ‘young’ older men with a mean age of only 62; healthy; community-dwelling; not osteoporotic; had adequate dietary calcium intake and optimal serum 25(OH) D levels. Thus, the effects seen in this population may underestimate the effects

that may be seen in older populations with osteosarcopaenia who have significantly higher fracture risk.

Nevertheless, there are both clinical and technical considerations arising from the findings of this study. Although the findings from this study are in keeping with current evidence, the accuracy and reliability of this technique has not been established. A future study comparing it to MRI- a technique that is currently considered the gold standard imaging technique to quantify marrow fat- is needed. A study we envisage in the future would involve a cohort of subjects from a wide spectrum of ages and both sexes. MRI would be used to quantify fat fraction, along with clinical CT. From this study, the percentage of fat volume seems to be most sensitive to intervention, and hence, could be the best variable to compare with fat fraction calculated by MRI. Hence, a 2x2 factorial RCT with similar intervention protocol would help to elucidate further the effect of exercise on marrow fat, and validate this CT method of quantification.

In conclusion, the results of this secondary analysis study showed that a community based exercise program, consisting of progressive resistance training and weight-bearing impact exercise, had inconsistent and variable effects on marrow fat indices. Further study examining the impact of exercise on marrow fat indices using both MRI and CT are warranted.

6.5 References

1. Snow-Harter C, Marcus R. Exercise, bone mineral density, and osteoporosis. Exer Sport Sci Rev. 1991; 19:351-388.

2. Berard A, Bravo G, Gauthier P. Meta-analysis of the effectiveness of physical activity for the prevention of bone loss in postmenopausal women. Osteoporos Int. 1997; 7(4):331-337.

3. Kelley GA. Exercise and regional bone mineral density in postmenopausal women: a meta-analytic review of randomized trials. Am J Phys Med Rehabil. 1998; 77(1):76-87.

4. Kelley G. Aerobic exercise and lumbar spine bone mineral density in postmenopausal women: a meta-analysis. J Am Geriatr Soc. 1998; 46(2):143-152.

5. Kelley GA. Aerobic exercise and bone density at the hip in postmenopausal women: a meta-analysis. Prev Med. 1998; 27(6):798-807.

6. Wolff I, van Croonenborg JJ, Kemper HC, et al. The effect of exercise training programs on bone mass: a meta-analysis of published controlled trials in pre- and postmenopausal women. Osteoporos Int. 1999; 9(1):1-12.

7. Wallace BA, Cumming RG. Systematic review of randomized trials of the effect of exercise on bone mass in pre- and postmenopausal women. Calcif Tissue Int. 2000; 67(1):10-18.

8. Kelley GA, Kelley KS, Tran ZV. Exercise and bone mineral density in men: a meta-analysis. J Appl Physiol. 2000; 88(5):1730-1736.

9. Kelley GA, Kelley KS, Tran ZV. Resistance training and bone mineral density in women: a meta-analysis of controlled trials. Am J Phys Med Rehabil. 2001; 80(1):65-77.

10. Kelley GA, Kelley KS, Tran ZV. Exercise and lumbar spine bone mineral density in postmenopausal women: a meta-analysis of individual patient data. J Gerontol Biol Sci Med Sci. 2002; 57(9):M599-604.

11. Kelley GA, Kelley KS. Efficacy of resistance exercise on lumbar spine and femoral neck bone mineral density in premenopausal women: a meta-analysis of individual patient data. J Womens Health (Larchmt). 2004; 13(3):293-300.

12. Palombaro KM. Effects of walking-only interventions on bone mineral density at various skeletal sites: a meta-analysis. J Geriatr Phys Ther. 2005; 28(3):102-107.

13. Martyn-St James M, Carroll S. High-intensity resistance training and postmenopausal bone loss: a meta-analysis. Osteoporos Int. 2006; 17(8):1225-1240.

14. Martyn-St James M, Carroll S. Meta-analysis of walking for preservation of bone mineral density in postmenopausal women. Bone. 2008; 43(3):521-531.

15. Martyn-St James M, Carroll S. A meta-analysis of impact exercise on postmenopausal bone loss: the case for mixed loading exercise programmes. Br J Sports Med. 2009; 43(12):898-908.

16. Howe TE, Shea B, Dawson LJ, et al. Exercise for preventing and treating osteoporosis in postmenopausal women. Cochrane Database Syst Rev. 2011(7):Cd000333.

17. Kelley GA, Kelley KS, Kohrt WM. Effects of ground and joint reaction force exercise on lumbar spine and femoral neck bone mineral density in postmenopausal women: a meta-analysis of randomized controlled trials. BMC Musculoskelet Disord. 2012; 13:177.

18. Marques EA, Mota J, Carvalho J. Exercise effects on bone mineral density in older adults: a meta-analysis of randomized controlled trials. Age (Dordr). 2012; 34(6):1493-1515.

19. Ma D, Wu L, He Z. Effects of walking on the preservation of bone mineral density in perimenopausal and postmenopausal women: a systematic review and meta-analysis. Menopause. 2013; 20(11):1216-1226.

20. Kelley GA, Kelley KS, Kohrt WM. Exercise and bone mineral density in men: a meta-analysis of randomized controlled trials. Bone. 2013; 53(1):103-111.

21. Daly RM, Bass S, Nowson C. Long-term effects of calcium-vitamin-D3-fortified milk on bone geometry and strength in older men. Bone. 2006; 39(4):946-953.

22. Daly RM, Brown M, Bass S, et al. Calcium- and vitamin D3-fortified milk reduces bone loss at clinically relevant skeletal sites in older men: a 2-year randomized controlled trial. J Bone

Miner Res. 2006; 21(3):397-405.

23. Dawson-Hughes B, Harris SS, Krall EA, et al. Effect of calcium and vitamin D supplementation on bone density in men and women 65 years of age or older. N Engl J Med. 1997; 337(10):670-676.

24. Peacock M, Liu G, Carey M, et al. Effect of calcium or 25OH vitamin D3 dietary supplementation on bone loss at the hip in men and women over the age of 60. J Clin Endocrinol Metab. 2000; 85(9):3011-3019.

25. Zhu K, Devine A, Dick IM, et al. Effects of calcium and vitamin D supplementation on hip bone mineral density and calcium-related analytes in elderly ambulatory Australian women: a five-year randomized controlled trial. J Clin Endocrinol Metab. 2008; 93(3):743-749.

26. Going S, Lohman T, Houtkooper L, et al. Effects of exercise on bone mineral density in calcium-replete postmenopausal women with and without hormone replacement therapy. Osteoporos Int. 2003; 14(8):637-643.

27. Notomi T, Okimoto N, Okazaki Y, et al. Effects of tower climbing exercise on bone mass, strength, and turnover in growing rats. J Bone Miner Res. 2001; 16(1):166-174.

28. Notomi T, Okimoto N, Okazaki Y, et al. Tower climbing exercise started 3 months after ovariectomy recovers bone strength of the femur and lumbar vertebrae in aged osteopenic rats. J Bone Miner Res. 2003; 18(1):140-149.

29. Mori T, Okimoto N, Sakai A, et al. Climbing exercise increases bone mass and trabecular bone turnover through transient regulation of marrow osteogenic and osteoclastogenic potentials in mice. J Bone Miner Res. 2003; 18(11):2002-2009.

30. Menuki K, Mori T, Sakai A, et al. Climbing exercise enhances osteoblast differentiation and inhibits adipogenic differentiation with high expression of PTH/PTHrP receptor in bone marrow cells. Bone. 2008; 43(3):613-620.

31. Sakai A. Morphological analysis of bone dynamics and metabolic bone disease. Effect of loading on bone tissue. Clin Calcium. 2011; 21(4):569-574.

32. Rubin CT, Capilla E, Luu YK, et al. Adipogenesis is inhibited by brief, daily exposure to high-frequency, extremely low-magnitude mechanical signals. Proc Natl Acad Sci U S A. 2007; 104(45):17879-17884.

33. Baker JM, De Lisio M, Parise G. Endurance exercise training promotes medullary hematopoiesis. FASEB J. 2011; 25(12):4348-4357.

34. Styner M, Thompson WR, Galior K, et al. Bone marrow fat accumulation accelerated by high fat diet is suppressed by exercise. Bone. 2014; 64:39-46.

35. Shen W, Chen J, Punyanitya M, et al. MRI-measured bone marrow adipose tissue is inversely related to DXA-measured bone mineral in Caucasian women. Osteoporos Int. 2007; 18(5):641-647.

36. Shen W, Chen J, Punyanitya M, et al. MRI-measured bone marrow adipose tissue is inversely related to DXA-measured bone mineral in Caucasian women. Osteoporos Int. 2007; 18(5):641-647.

37. Shen W, Chen J, Gantz M, et al. MRI-measured pelvic bone marrow adipose tissue is inversely related to DXA-measured bone mineral in younger and older adults. Eur J Clin Nutr. 2012; 66(9):983-988.

38. Wehrli FW, Hopkins JA, Hwang SN, et al. Cross-sectional study of osteopenia with quantitative MR imaging and bone densitometry. Radiology. 2000; 217(2):527-538.

39. Justesen J, Stenderup K, Ebbesen EN, et al. Adipocyte tissue volume in bone marrow is increased with aging and in patients with osteoporosis. Biogerontology. 2001; 2(3):165-171.

40. Justesen J, Stenderup K, Eriksen EF, et al. Maintenance of osteoblastic and adipocytic differentiation potential with age and osteoporosis in human marrow stromal cell cultures.

Calcif Tissue Int. 2002; 71(1):36-44.

41. David V, Martin A, Lafage-Proust MH, et al. Mechanical loading down-regulates peroxisome proliferator-activated receptor gamma in bone marrow stromal cells and favors osteoblastogenesis at the expense of adipogenesis. Endocrinology. 2007; 148(5):2553-2562.

42. Luu YK, Pessin JE, Judex S, et al. Mechanical Signals As a Non-Invasive Means to Influence Mesenchymal Stem Cell Fate, Promoting Bone and Suppressing the Fat Phenotype. BoneKEy Osteovision. 2009; 6(4):132-149.

43. Styner M, Pagnotti GM, Galior K, et al. Exercise Regulation of Marrow Fat in the Setting of PPARgamma Agonist Treatment in Female C57BL/6 Mice. Endocrinology. 2015; 156(8):2753-2761.

44. Trudel G, Coletta E, Cameron I, et al. Resistive exercises, with or without whole body vibration, prevent vertebral marrow fat accumulation during 60 days of head-down tilt bed rest in men. J Appl Physiol (1985). 2012; 112(11):1824-1831.

45. Kukuljan S, Nowson CA, Sanders KM, et al. Independent and combined effects of calcium-vitamin D3 and exercise on bone structure and strength in older men: an 18-month factorial design randomized controlled trial. J Clin Endocrinol Metab. 2011; 96(4):955-963.

46. American College of Sports Medicine 2000 ACSM Guidelines for exercise testing and prescription. Philadelphia: Lippincott, Williams, and Wilkins.

47. https://www.osteoporosis.org.au/supplementation. Accessed March 2018

48. Stewart AL, Mills KM, King AC, et al. CHAMPS physical activity questionnaire for older adults: outcomes for interventions. Med Sci Sports Exerc. 2001; 33(7):1126-1141.

49. Marie PJ, Hott M, Launay JM, et al. In vitro production of cytokines by bone surface- derived osteoblastic cells in normal and osteoporotic postmenopausal women:

relationship with cell proliferation. J Clin Endocrinol Metab. 1993; 77(3):824-830.

50. Dawson-Hughes B, Mithal A, Bonjour JP, et al. IOF position statement: vitamin D recommendations for older adults. Osteoporos Int. 2010; 21(7):1151-1154.

51. Rockwell JC, Sorensen AM, Baker S, et al. Weight training decreases vertebral bone density in premenopausal women: a prospective study. J Clin Endocrinol Metab. 1990; 71(4):988-993.

52. Gleeson PB, Protas EJ, LeBlanc AD, et al. Effects of weight lifting on bone mineral density in premenopausal women. J Bone Miner Res. 1990;5(2):153-158.

53. Lohman T, Going S, Pamenter R, et al. Effects of resistance training on regional and total bone mineral density in premenopausal women: a randomized prospective study. J Bone Miner Research. 1995; 10(7):1015-1024.

54. Menkes A, Mazel S, Redmond RA, et al. Strength training increases regional bone mineral density and bone remodeling in middle-aged and older men. J Appl Physiol (1985). 1993; 74(5):2478-2484.

55. Ryan AS, Treuth MS, Rubin MA, et al. Effects of strength training on bone mineral density: hormonal and bone turnover relationships. J Appl Physiol (1985). 1994; 77(4):1678-1684.

56. Yarasheski KE, Campbell JA, Kohrt WM. Effect of resistance exercise and growth hormone on bone density in older men. Clin Endocrinol (Oxf). 1997; 47(2):223-229.

57. Ryan AS, Ivey FM, Hurlbut DE, et al. Regional bone mineral density after resistive training in young and older men and women. Scand J Med Sci Sports. 2004; 14(1):16-23.

58. McCartney N, Hicks AL, Martin J, et al. Long-term resistance training in the elderly: effects on dynamic strength, exercise capacity, muscle, and bone. J Gerontol A Biol Sci Med

Sci. 1995; 50(2):B97-104.

59. Dalsky GP, Stocke KS, Ehsani AA, et al. Weight-bearing exercise training and lumbar bone mineral content in postmenopausal women. Ann Intern Med. 1988; 108(6):824-828.

60. Rikli RE, McManis BG. Effects of exercise on bone mineral content in postmenopausal women. Res Q Exerc Sport. 1990; 61(3):243-249.

61. Notelovitz M, Martin D, Tesar R, et al. Estrogen therapy and variable-resistance weight training increase bone mineral in surgically menopausal women. J Bone Miner Res. 1991; 6(6):583-590.

62. Peterson SE, Peterson MD, Raymond G, et al. Muscular strength and bone density with weight training in middle-aged women. Med Sci Sports Exerc. 1991; 23(4):499-504.

63. Pruitt LA, Jackson RD, Bartels RL, et al. Weight-training effects on bone mineral density in early postmenopausal women. J Bone Miner Res. 1992; 7(2):179-185.

64. Svendsen OL, Hassager C, Christiansen C. Effect of an energy-restrictive diet, with or without exercise, on lean tissue mass, resting metabolic rate, cardiovascular risk factors, and bone in overweight postmenopausal women. Am J Med. 1993; 95(2):131- 140.

65. Nelson ME, Fiatarone MA, Morganti CM, et al. Effects of high-intensity strength training on multiple risk factors for osteoporotic fractures. A randomized controlled trial. JAMA. 1994; 272(24):1909-1914.

66. Ryan AS, Treuth MS, Hunter GR, et al. Resistive training maintains bone mineral density in postmenopausal women. Calcif Tissue Int. 1998; 62(4):295-299.

7.0 Chapter 7: Conclusions and Future directions

Marrow fat (i.e. adipocytes) has now been shown to have an active and major role in the pathophysiology of age related bone loss. Yet, its role in clinical applications is scarce. In fact, its quantification in a non-invasive manner is limited exclusively to special MRI techniques, which are mainly seen in research settings.

In the clinical settings, standard MRI is expensive; requires expert interpretation; not readily available and not well tolerated by older people. On the other hand, CT is more accessible, cheaper, well tolerated by older people and is the imaging modality that practicing clinicians are generally more familiar with. A method of quantifying marrow fat that is readily applicable in routine clinical care, such as that with CT, is sorely needed and further exploration of the clinical applications of marrow fat is warranted.

Thus, the aims of this thesis were to demonstrate a new technique of marrow fat quantification involving CT technology, and using these principles combined with established concepts; explore the effects of fatty acids on marrow fat; examine the relationship between marrow fat and clinical surrogates of bone mass, strength and calciotropic hormones; and assess the effects of exercise, calcium and vitamin D on marrow fat.

We achieved the first aim by demonstrating that marrow fat can be quantified reliably from µCT images using an image analysis software, Slice O Matic version 4.1 (Tomovision), and compared it to the gold standard method of histology. In the study "*Validation of non-invasive quantification of marrow fat in aging LOU rats,"* volumes of bone, fat and haemopoietic tissue in the femoral and tibial marrow cavity of young and old LOU rats were quantified with both methods and the results compared. Marrow fat indices quantified from µCT images with Slice O Matic showed high levels of agreement with corresponding indices quantified by histology.

Furthermore, our results, showing an increase in fat volume with corresponding decrease in bone volume with increasing age, were consistent with previous findings utilising MRI and histological methods, thus confirming the potential of our technique for applications in future clinical studies. To our knowledge, this was the first study to quantify fat using μCT images and imaging software, and the first study to validate a non-invasive quantification technique with a gold standard invasive method. The novel aspect of our technique lies in the use of density values of tissues directly obtained from the CT images to compute volumes of interest. No conversions to other units through complicated algorithms or sophisticated procedures to alter the resolution of the images were involved. The implication from this is that clinical application in the future is achievable.

Limitations exist however. Given that this validation study was conducted with a specific μCT scanner and images were obtained at specific energy settings, the thresholds used in the study can only be applied to a similar device scanning at similar energy levels. Changes in scanning parameters would require validation in the particular experiment cohort. Another limiting factor is observer error in the visual identification of fat depots in regions affected by partial volume effects. Marrow fat may be under quantified in areas adjacent to bone structures or over quantified in areas adjacent to lower density mediums, such as air. The size of this margin of error is uncertain and not within the scope of this body of work. However, we estimate that the thresholds which we have validated may be applicable to different μCT scanners, but with similar scanning settings.

Thus, in our next study, "*The effect of Dietary Fatty Acids on Bone Marrow Fat in a Murine Model of Senile Osteoporosis"*, we applied our technique to explore a topic of clinical relevance to osteoporosis. We examined the effects of fatty acids on marrow fat with a murine model of senile osteoporosis (SAMP8). Consistent with previous studies, our results suggested

that ω-3 and ω-6 fatty acids largely act independently. However, in contrast to previous findings, the net effect on bone is influenced by the interactions of not only ω-3 level, ω-6 level and ω-6: ω-3 ratio, but also saturated fatty acid levels, total PUFAs, and the bone microenvironment itself. In fact, in an osteoporotic bone microenvironment, a sunflower diet (high ω-6: ω-3 ratio) exerts a protective effect on bone, compared to a neutral effect on a non-osteoporotic bone microenvironment Decreasing this ratio by more than four fold through enriching the ω-3 fraction five fold with a fish diet maintained protective effect on bone through a reduction in marrow fat volume. Increasing total ω-6 PUFA, and thus raising ω-6: ω-3 with borage led to negative trends on bone health (reduced bone tissue volume with increasing fat tissue volume) consistent with previous literature.

Overall, the results from our study highlighted the complexity of the actions of fatty acids. To clarify our results, future studies ideally should adopt a similar animal model. In addition, it would be informative to measure levels of individual fatty acids in the diet and in different tissues (serum and bone marrow) in order to determine the optimal combinations and proportions to achieve heathy bones. Significantly, this study paves the way for future studies to explore other nutritional elements that may benefit bone health that have not been possible to study in the past due to inability to measure marrow elements non-invasively. However, the findings from this study need further clarification. In addition, the technique needs validation, as a number of assumptions have been made, such as the application of the same thresholds in different scanners with similar setings. The main assumptions made in the study need to be verified in a repeat experiment with multiple measurements using different scanners, plus their dedicated phantoms and different energy settings need to be compared. Reliability and margin of error also need to be determined.

We then moved forward from animals to humans. In the study *"Anatomical Differences in Marrow Fat in a Cohort of Older Men: Correlation with Body Composition and Calciotropic*

Hormones", we employed clinical CT to quantify marrow fat and explored the relationship between marrow fat; clinical surrogates of bone mass and strength; and calciotropic hormones in a population of community-dwelling older men from Singapore. Different Hounsfield units ascribed to different tissues, as used in day –to- day clinical settings, were used to compute marrow fat, bone and haemopoietic volumes.

Our results showed that marrow adiposity increased and bone volume decreased in the proximal femora and lumbar vertebrae with ageing. Interestingly, the inverse relationship between marrow fat and bone in these sites is consistently significant only in the trochanteric regions and proximal femora. Other significant findings include: age was mainly associated with marrow adiposity in the trochanteric regions, whereas fasting glucose was mainly associated with marrow adiposity in the lumbar vertebrae; and vertebral marrow fat indices highly correlated with fasting glucose levels and diabetes status in the whole study population. Consistent with this, diabetic subjects had higher vertebral marrow adiposity (mean marrow fat volume and Fv/Bv) compared to nondiabetics, and vertebral fat content highly correlated with HbA1c in this group. As for the calciotropic hormones, higher vitamin D levels were associated with greater marrow adiposity in the proximal femora and lumbar vertebrae and, although not statistically significant, higher BMIs tended to be associated with higher adiposity indices. Marrow fat volume indices correlated positively with cytokines involved in bone resorption (RANKL, leptin, resistin, IL6 and TNFα) and negatively with those involved in bone formation (PTH, IFNλ, osteopontin, and IGF1).

As far as we are aware, this is the first study using clinical CT to examine relationships between these clinical risk factors and marrow fat. The findings are significant, and warrant future prospective studies to confirm the associations. More importantly, a number of these results are consistent with previous studies utilising gold standard modalities, such as MRI and histology. This indicates that our technique may be applicable in future clinical studies. However, this

method requires validation in humans, and its accuracy need to be compared with MRI methods. Another important clinical issue in the field of osteoporosis is the effect of exercise on bone macro and micro architecture. Although the effects of exercise, calcium and vitamin D on bone density have been well examined, their effects on bone marrow fat have had little attention. In our final study "*Effects of Exercise and calcium on Bone marrow Contents – A randomised Control Trial",* we explored the effects of these interventions on marrow fat indices in a cohort of healthy older men.

The results showed that within a multicomponent strategy to improve bone health, combined resistance and weight bearing exercises alone increased bone volumes in the mid femur and decreased fat volumes in some lumbar vertebrae, but had no effect in the mid tibia. Conversely, calcium/vitamin D3 alone reduced fat volumes and improved the fat to bone volumes ratio in the mid tibia only. However, these interventions interacted to primarily affect marrow haematopoiesis in the mid femur and marrow fat volume changes in the lumbar vertebrae, but no effect was seen in the mid tibia. Despite limited interactions between the interventions, the results from this study suggest that as a stand -alone intervention, the combined strategy (exercise plus calcium/vitaminD3) had the most widespread positive effects on bone marrow health. It increased bone volumes and reduced fat volumes in the mid femur and lumbar vertebrae. Exercise alone was the next most beneficial, with bone volume increases in all skeletal regions, but fat volume attenuation in the mid tibia only.

The results for bone tissue parameters were consistent with existing literature, but the results for marrow fat were modest. This was not surprising, given that the study was not powered to detect marrow fat indices as primary outcomes. Nevertheless, a larger similarly designed RCT to further elucidate this relationship is needed to confirm the effects.

7.1 Going forward

With the exception of the validation study in chapter 3, the remaining bodies of work consist of secondary analyses, addressing gaps in our knowledge of osteoporosis. Although the findings from secondary analyses are far from conclusive, they serve as important starting points for a number of hypotheses to address in future studies. However, due to the limitation of translatability between micro CT and clinical CT, the first step is to validate clinical CT as a tool to quantify bone marrow fat in humans.

As identified in the body of the thesis, the limitation with our technique is the lack of validation against a gold standard non-invasive method. Since we used Hounsfield tissue densities in the calculations of the bone marrow tissues, the only area of uncertainties are the true densities of tissues in areas affected by partial volume effects, such as the interface between cortical and trabecular bone; the interface between thin trabeculae bone and haemopoietic tissue; and the interface between haemopoietic tissue and adipose tissue. A study quantifying fat fraction using MRI spectroscopy, compared to quantification using clinical CT and an image software analysis, may be able to resolve this uncertainty to an extent, and determine the reliability and margin of error with this method.

The cohort should consist of a wide range of ages, as well as involve healthy men and women. The exclusion criteria would include conditions that may influence bone turnover, such as osteoporosis, malignant bone disease and other metabolic bone diseases. Conditions that are associated with changes to bone marrow fat- such as anorexia, diabetes, and steroid therapy- should also be excluded. From the technical aspect, CT calibrations have to be rigorously performed using a number of phantoms, covering air, water, bone and bone marrow of different densities according to proportions of red and yellow marrow. The marrow phantoms should cover a range of densities of bone marrow, reflecting different proportions of red and yellow marrow as previously published.

Following this, a precision error study needs to be undertaken to ensure this clinical CT method is of acceptable precision. This can be done with 15 subjects scanned in triplicate or 30 subjects scanned in duplicate according to ISCD recommendation. Finally, the statistical analysis validating the technique needs to be more comprehensive. That is, the interpretations of Bland Altman need to examine additional issues of bias and method error.

Once the validation of clinical CT is achieved, further studies investigating the associations found in this body of work will help address the assumptions and limitations. A study investigating "Bone marrow adiposity in the lumbar spine and proximal femur of older men and women with varying bone densities" can further clarify the inverse relationship between marrow fat and bone in the proximal femur, and whether this is independent of age and sex in older subjects. Another objective is to determine the correlation between BMD and marrow fat indices in these regions. Similarly, extending the findings from the mice free fatty acids study, a study investigating "The effect of dietary fatty acids on bone marrow fat and BMD in older men and postmenopausal women" would help further knowledge in this important area of nutritional intervention in osteoporosis.

Finally, a study to elucidate whether exercise significantly influences marrow fat should be conducted. The design would have adequate power to detect marrow fat changes, and the primary objective is marrow fat volume changes as absolute mean volume change; fat to bone volume ratio change; and fat volume to bone volume ratio changes. The hypothesis for this study would be that "Exercise reduces bone marrow fat in the proximal femur and lumbar spine in postmenopausal women compared to controls without exercise intervention."

In conclusion, this body of work has demonstrated a potential method of marrow fat quantification using computed tomography, and has generated a number of clinically important hypotheses for future clinical studies. Although our technique promises to enable studies

examining a number of osteoporosis clinical risk factors and their relationship with marrow fat, much work remains to validate its accuracy. Nevertheless, this thesis is the beginning of the development of a fat quantification technique that is accessible; feasible; applicable in general clinical settings; and reliable as an opportunistic screening tool.

8.0 Appendix

8.1 Chapter 5

Parameter	Age		Vitamin D		BMI	
	≤ 65 (n=56)	> 65 (n=64)	< 21 (n=52)	≥ 21 (n=68)	< 25 (n=74)	≥ 25 (n=46)
Age (Kg)	63* ± 1	72* ± 5	66 ± 6	69± 5	68 ± 5	68 ± 7
BMI	26 ± 4	25 ± 5	26 ± 5	25 ± 4	23 ± 2	29 ± 5
Vitamin D level (ng/ml)	20* ± 4	23* ± 6	17 ± 3	25 ± 3	23 ± 5*	20 ± 5*
Diabetes	12	12	15	9	10	14
FN T score	-0.92 ± 1 (25)	-1.04 ± 1 (23)	-.79 ± 1.1 (19)	-1.1 ± .9 (29)	-1.1 ± .9 (32)	-.69 ± 1.1 (16)
LS Tscore	.36 ± 1.2 (25)	.04 ± 1.3 (23)	.42 ± 1.2 (19)	.07 ± 1.3 (29)	.22 ± 1.2	.19±1.328
LNF (mm^3)	304 ± 358	353 ± 571	289 ± 306	361 ± 579	334± 502	324± 456
LNBC (mm^3)	2347 ±1535	2084 ±1320	2440±1577	2035 ±1287	2129±1384	2328± 1494
LNBT (mm^3)	1358 ± 848	1343 ± 846	1425 ± 864	1296 ± 830	1324±834	1392± 865
LN Fv/Tr.Bv	26 ± 23	35 ± 50	25 ± 22	35 ± 49	33 ± 45	27 ± 30
LNFv/To.Bv	10 ± 9	14 ± 19	9 ± 8	13 ± 18	13 ± 17	10 ± 12
LN Fv/Tv	7 ± 6	9 ± 10	7 ± 6	9 ±10	9 ± 9	8 ± 8
RNF (mm^3)	339 ± 373	352 ± 5423	318 ± 335	367 ± 549	327 ± 406	377 ± 559
RNBC (mm^3)	2276±1397	2209±1414	2341±1441	2167±1376	2216± 1387	2279 ± 1437
RNBT (mm^3)	1355 ± 808	1321 ± 830	1384 ± 808	1302 ± 827	1325 ± 839	1356 ± 788
RN Fv/Tr.Bv	28 ± 2	35 ± 45	26 ± 22	36 ± 45	33 ± 39	29 ± 34
RNFv/To.Bv	11 ± 9	13 ± 17	10 ± 8	13 ± 16	12 ± 14	11 ± 13
RN Fv/Tv	8 ± 6	9 ± 10	8 ± 6	9 ± 10	9 ± 8	8 ± 8
L2FV (mm^3)	214 ± 363 (n=17)	293 ± 527 (n=43)	97 ± 120 (n=16)	333 ± 549 (n=44)	220 ± 455	420 ± 552
L2FV/Bv	.1 ± .2 (n=17)	.2 ± .4 (n=43)	.1 ± .1 (n=16)	.2 ± .4 (n=44)	.1 ± .3	.3 ±.4
L3FV (mm^3)	283 ± 459 (n=17)	371 ± 520 (n=43)	166 ± 217 (n=16)	411 ± 559 (n=44)	279 ± 429	545 ± 651
L3FV/Bv	.2 ± .3 (n=17)	.2 ± .3 (n=43)	.1 ± .1 (n=16)	.2 ± .3 (n=44)	.1 ± .2*	.3 ± .5*

Table 5A. Comparisons of means of clinical parameters and marrow fat volume indices in the neck of femur regions and lumbar vertebrae between subjects in subgroups according to age, Vitamin D, and BMI. Indices are means □ standard deviations. * Means between the two groups are different and are statistically significant at the 0.05 level (2-tailed). ** Difference is statistically significant at the 0.05 level (2-tailed).

Parameter	Age		Vitamin D		BMI	
	< 65 (56)	≥ 65 (64)	< 21 (n=52)	≥ 21 (n=68)	< 25 (n=74)	≥ 25 (n=46)
LTF (mm^3)	241 ± 396	400 ± 676	233 ± 295	394 ± 698	322 ±496	332± 669
LTBC (mm^3)	125869 ± 918698	2030 ± 1282	138368 ± 963523	1946 ± 1237	96614± 802950	2054± 1323
LTBT (mm^3)	1234 ± 793	1164 ± 790	1306 ± 819	1117 ± 762	1180± 789	1223± 797
LT Fv/Tr.Bv	23 ± 33*	50 ± 88*	23 ± 27*	48 ± 87*	40 ± 75	33 ± 60
LT Fv/To.Bv	8 ± 11*	16 ± 23*	8 ± 9*	15 ± 23*	13 ± 19	11 ± 17
LT Fv/Tv	6 ± 7* (55)	10 ± 12* (63)	6 ± 6* (50)	10 ± 11* (68)	9 ± 10	7 ± 10
RTF (mm^3)	267 ± 416	371 ± 608	255 ± 333	372 ± 632	285 ± 353	381 ± 722
RTBC (mm^3)	1940 ± 1242	1995 ± 1246	2049 ± 1276	1912 ± 1218	1924 ± 1212	2041 ± 1291
RTBT (mm^3)	1193 ± 795	1174 ± 798	1281 ± 847	1111 ± 750	1164 ± 766	1214 ± 843
RT Fv/Tr.Bv	25* ± 32	46* ± 76	25 ± 30	45 ± 74	36 ± 57	38 ± 66
RT Fv/To.Bv	9 ± 11*	15 ± 21*	9 ± 10	14 ± 20	12 ± 16	12 ± 18
RT Fv/Tv	7 ± 7	10 ± 11	7 ± 7	10 ± 11	9 ± 9	8 ± 10
LfFv	535 ± 732	741 ± 1227	502 ± 579	755 ± 1262	638 ± 977	657 ± 1115
Lf Fv/Tr.Bv	24 ± 26	41 ± 64	24 ± 23*	40 ± 62*	36 ± 55	29 ± 42
Lf Fv/ To.Bv	9 ± 9	15 ± 21	9 ± 8*	14 ± 20*	13 ± 18	11 ± 15
Lf Fv/Tv	7* ± 6	10* ± 11	7 ± 6*	10 ± 11*	9 ± 9	8 ± 9
RfFv (mm^3)	596 ± 762	713 ± 1130	551 ± 636	739 ± 1167	596 ± 732	758 ± 1274
Rf Fv/Tr.Bv	26 ± 24	39 ± 56	25 ± 24	39 ± 54	33 ± 43	32 ± 46
Rf Fv/ To.Bv	10 ± 9	134 ± 18	9 ± 9	14 ± 18	12 ± 14	12 ± 16
Rf Fv/Tv	8 ± 6	10 ± 10	7 ± 6	10 ± 10	9 ± 8	8 ± 9

Table 5B. Comparisons of marrow fat volume indices in the trochanteric regions of the femur and proximal femur between subjects in subgroups according to age, Vitamin D, and BMI. Indices are means ± standard deviations. * Means between the two groups are different and are statistically significant at the 0.05 level (2-tailed). ** Difference is statistically significant at the 0.05 level (2-tailed).

8.2 Chapter 6

Parameter	Group (n)	Mean	SD	CI	p
Tv	0 (42)	1851	182	1795-1908	0.8
	1 (41)	1805	186	1746-1864	
	2 (41)	1826	187	1767-1885	
	3 (41)	1825	215	1757-1893	
Hv	0 (42)	91	29	82-100	.04
	1 (41)	88	29	79-97	
	2 (41)	95	35	84-106	
	3 (41)	108	40	95-120	
Bv	0 (42)	1529	131	1488-1569	.7
	1 (41)	1500	134	1458-1542	
	2 (41)	1499	155	1450-1548	
	3 (41)	1499	166	1446-1551	
Fv	0 (42)	231	86	205-258	.8
	1 (41)	217	81	192-243	
	2 (41)	232	97	201-262	
	3 (41)	218	87	191-246	
%Hv	0 (42)	4.8	1.5	4.3-5.3	.02
	1 (41)	4.9	1.6	4.4-5.4	
	2 (41)	5.1	1.7	4.6-5.6	
	3 (41)	5.9	1.9	5.3-6.5	
%Bv	0 (42)	82.8	3.6	81.6-83.9	.5
	1 (41)	83.3	3.2	82.2-84.3	
	2 (41)	82.2	5.2	80.6-83.8	
	3 (41)	82.2	4	80.9-83.5	
%Fv	0 (42)	12.4	3.9	11.2-13.6	.8
	1 (41)	11.9	3.7	10.7-13	
	2 (41)	12.5	5	10.9-14.1	
	3 (41)	11.9	4	10.6-13.1	
Fv/Bv	0 (42)	.15	.05	.13-.17	.8
	1 (41)	.14	.08	.13-.16	
	2 (41)	.16	.1	.13-.18	
	3 (41)	.15	.09	.13-.17	

Table 2. Mid femur baseline volumes: Tv (total volume), Hv (haemopoietic volume), Bv (total bone volume), Fv (fat volume) and as percentages (%Hv, %Bv, %Fv) of total volume. Fv/Bv is ratio of mean absolute fat volume to mean absolute bone volume at baseline. Groups 0 (control), 1 (Calcium supplement only), 2 (Exercise only) and 3 (Exercise plus Calcium supplement). Significance is at p = 0.05.

Parameter	Group (n)	Mean	SD	CI	p
TV	0 (36)	1520	182	1459-1582	.3
	1 (38)	1455	140	1409-1501	
	2 (41)	1511	167	1458-1563	
	3 (34)	1524	203	1453-1595	
Hv	0 (36)	67	24	59-75	.1
	1 (38)	62	21	55-69	
	2 (41)	58	14	54-63	
	3 (34)	68	29	58-78	
Bv	0 (36)	1318	155	1266-1370	.3
	1 (38)	1261	116	1223-1299	
	2 (41)	1296	143	1251-1341	
	3 (34)	1309	150	1257-1318	
Fv	0 (36)	135	72	111-160	.4
	1 (38)	133	66	111-154	
	2 (41)	157	71	134-179	
	3 (34)	147	71	122-172	
%Hv	0 (36)	4.4	1.3	4.0-4.9	.2
	1 (38)	4.1	1.2	3.7-4.5	
	2 (41)	3.9	0.9	3.6-4.2	
	3 (34)	4.5	1.6	3.9-5.0	
%Bv	0 (36)	86.8	4.4	85.3-88.3	.7
	1 (38)	86.8	4.4	85.4-88.2	
	2 (41)	85.9	4.2	84.5-87.2	
	3 (34)	86.2	3.7	84.9-87.5	
%Fv	0 (36)	8.8	4.1	7.4-10.2	.4
	1 (38)	9.0	4.3	7.6-10.4	
	2 (41)	10.2	4.3	8.9-11.6	
	3 (34)	9.3	3.7	8.0-10.6	
Fv/Bv	0 (36)	.104	.054	.086-.122	.5
	1 (38)	.106	.055	.088-.124	
	2 (41)	.122	.057	.104-.140	
	3 (34)	.111	.049	.094-.128	

Table 3. Mid tibia baseline volumes: Tv (total volume), Hv (haemopoietic volume), Bv (total bone volume), Fv (fat volume) and as percentages (%Hv, %Bv, %Fv) of total volume. Fv/Bv is ratio of mean absolute fat volume to mean absolute bone volume at baseline. Groups 0 (control), 1 (Calcium supplement only), 2 (Exercise only) and 3 (Exercise plus Calcium supplement). Significance is at $p = 0.05$.

Parameter	Group (n)	Mean	SD	CI	p
Tv	0 (36)	7701	17555	1761-13641	.07
	1 (33)	4896	725	4638-5153	
	2 (40)	4888	726	4656-5120	
	3 (34)	4540	629	4321-4760	
Hv	0 (36)	4037	17435	-1862-9936	.1
	1 (33)	1334	655	1101-1567	
	2 (40)	1155	656	945-1364	
	3 (34)	972	627	753-1191	
Bv	0 (36)	3577	672	3349-3804	.6
	1 (33)	3491	530	3302-3678	
	2 (40)	3643	650	3436-3851	
	3 (34)	3469	530	3284-3654	
Fv	0 (36)	88	79	61-114	.7
	1 (33)	70	79	43-98	
	2 (40)	89	100	58-121	
	3 (34)	100	138	51-148	
%Hv	0 (36)	25.1	15.9	19.8-30.5	.2
	1 (33)	26.4	11.1	22.5-30.3	
	2 (40)	22.9	11.5	19.2-26.6	
	3 (34)	20.4	11.5	16.4-24.5	
%Bv	0 (36)	73.0	16.2	67.5-78.5	.4
	1 (33)	72.3	11.9	68.1-76.5	
	2 (40)	75.2	12.6	71.2-79.2	
	3 (34)	77.3	12.9	72.8-81.8	
%Fv	0 (36)	1.8	1.8	1.2-2.4	.4
	1 (33)	1.4	1.5	.8-1.9	
	2 (40)	1.8	2.3	1.1-2.5	
	3 (34)	2.2	3.0	1.2-3.3	
Fv/Bv	0 (36)	.027	.026	.018-.036	.7
	1 (33)	.022	.024	.013-.030	
	2 (40)	.029	.038	.017-.041	
	3 (34)	.018	.048	.015-.049	

Table 4. Baseline mean volumes of L1 lumbar vertebrae: Tv (total volume), Hv (haemopoietic volume), Bv (total bone volume), Fv (fat volume) and as percentages (%Hv, %Bv, %Fv) of total volume. Fv/Bv is ratio of mean absolute fat volume to mean absolute bone volume at baseline. Groups 0 (control), 1 (Calcium supplement only), 2 (Exercise only) and 3 (Exercise plus Calcium supplement). Significance is at $p = 0.05$.

Parameter	Group (n)	Mean	SD	CI	p
TV	0 (36)	53334	1378	50536-56132	.1
	1 (33)	55231	7842	52450-58012	
	2 (40)	55202	1344	52482-57921	
	3 (34)	51342	7239	48816-53868	
Hv	0 (36)	1053	598	850-1255	.1
	1 (33)	1335	629	1112-1558	
	2 (40)	1180	654	971-1389	
	3 (34)	969	662	738-1200	
Bv	0 (36)	3789	681	3558-4019	.6
	1 (33)	3679	513	3497-3861	
	2 (40)	3829	640	3624-4034	
	3 (34)	3689	516	3509-3869	
Fv	0 (36)	75	68	52-98	.4*
	1 (33)	72	66	49-96	
	2 (40)	100	106	66-134	
	3 (34)	102	139	53-150	
%Hv	0 (36)	19.3	9.9	15.9-22.6	.1
	1 (33)	23.5	9.6	20.1-26.9	
	2 (40)	20.7	10.3	17.4-24.0	
	3 (34)	18.0	10.7	14.3-21.8	
%Bv	0 (36)	71.5	10.0	68.1-74.9	.2
	1 (33)	67.3	9.6	63.9-70.7	
	2 (40)	70.0	10.4	66.7-73.3	
	3 (34)	72.7	10.9	68.9-76.5	
%Fv	0 (36)	14.1	12.5	9.8-18.3	.4*
	1 (33)	12.9	11.9	8.7-17.2	
	2 (40)	18.6	20.9	11.9-25.3	
	3 (34)	19.5	27.2	10.0-29.0	
Fv/Bv	0 (36)	.221	.221	.015-.030	.5*
	1 (33)	.0208	.019	.014-.028	
	2 (40)	.0295	.036	.018-.041	
	3 (34)	.0305	.047	.014-.047	

Table 5. Baseline volumes for L2 lumbar vertebrae: Tv (total volume), Hv (haemopoietic volume), Bv (total bone volume), Fv (fat volume) and as percentages (%Hv, %Bv, %Fv) of total volume. Fv/Bv is ratio of mean absolute fat volume to mean absolute bone volume at baseline. Groups 0 (control), 1 (Calcium supplement only), 2 (Exercise only) and 3 (Exercise plus Calcium supplement). Significance is at p = 0.05.* Robust tests of Equality of Means.

Parameter	Group (n)	Mean	SD	CI	p
TV	0 (36)	5726	925	5413-6039	.06
	1 (33)	6007	1445	5495-6520	
	2 (40)	5765	872	5486-6044	
	3 (34)	5321	805	5040-5602	
Hv	0 (36)	1286	746	1034-1539	.09
	1 (33)	1548	735	1287-1808	
	2 (40)	1324	735	1089-1559	
	3 (34)	1087	715	838-1337	
Bv	0 (36)	4318	682	4087-4549	.7
	1 (33)	4314	1364	3831-4798	
	2 (40)	4317	685	4098-4536	
	3 (34)	4104	604	3893-4315	
Fv	0 (36)	122	98	89-155	.9
	1 (33)	145	224	66-225	
	2 (40)	123	115	87-160	
	3 (34)	130	183	66-194	
%Hv	0 (36)	21.5	10.8	17.9-25.2	.1
	1 (33)	25.7	10.7	21.9-29.5	
	2 (40)	22.1	10.8	18.6-25.5	
	3 (34)	19.5	10.6	15.8-23.2	
%Bv	0 (36)	76.4	11.8	72.4-80.4	.2
	1 (33)	72.0	11.1	68.1-75.9	
	2 (40)	75.7	12.0	71.9-79.6	
	3 (34)	78.2	12.2	73.9-82.5	
%Fv	0 (36)	2.1	1.6	1.5-2.6	1.0
	1 (33)	2.4	3.5	1.1-3.6	
	2 (40)	2.1	2.2	1.4-2.8	
	3 (34)	2.2	2.2	1.2-3.3	
Fv/Bv	0 (36)	.030	.024	.022-.038	.9
	1 (33)	.036	.051	.018-.053	
	2 (40)	.032	.034	.021-.043	
	3 (34)	.034	.051	.017- .052	

Table 6. Baseline volumes for L3 lumbar vertebrae: Tv (total volume), Hv (haemopoietic volume), Bv (total bone volume), Fv (fat volume) and as percentages (%Hv, %Bv, %Fv) of total volume. Fv/Bv is ratio of mean absolute fat volume to mean absolute bone volume at baseline. Groups 0 (control), 1 (Calcium supplement only), 2 (Exercise only) and 3 (Exercise plus Calcium supplement). Significance is at $p = 0.05$.

Group	Mean Volume ± SD (95% CI)	L1	L2	L3	p
Control	Hv	4037± 17435 (	1053 ± 598 (851-1256)	1286 ± 746 (1034- 1539)	.2[#]
	Bv	3576 ± 672 (3349 – 3804)	3789 ± 681 (3558-4019)	4318 ± 682 (4087 – 4549)	.000
	Fv	87 ± 79 (61-114)	75 ± 68 (52 - 98)	122 ± 98 (89-155)	.07[#]
	Tv	7701 ± 17555 (1761-13641)	4917 ± 763 (4659 – 5175)	5726 ± 925 (5413 – 6039)	.001[#]
	%Hv	25.2 ± 15.9 (19.8- 30.6)	20.8 ± 10.5 (17.3- 24.4)	21.6 ± 10.7 (17.9 -25.2)	.3
	%Bv	72.9 ± 16.2 (67.5- 78.4)	77.7 ± 11.5 (73.8- 81.6)	76.4 ± 11.8 (72.4-80.4)	.3
	%Fv	1.9 ± 1.7 (1.3-2.4)	1.5 ± 1.3 (1.1 – 2.0)	2.1 ± 1.6 (1.5 – 2.6)	.3
	Fv/Bv	.027 ± .026 (.018 -.036)	.022 ± .022 (.015- .030)	.030 ± .024 (.022 - .038)	.4
Ca only	Hv	1334 ± 655 (1102 -1567)	1335 ± 629 (1112 -1558)	1548 – 735 (1287 -1808)	.5
	Bv	3491 ± 530 (3303 -3678)	13351 ± 6290 (11121- 15582)	4314 ± 1364 (3831 -4798)	.008
	Fv	70 ± 79 (43 - 98)	72 ± 66 (49 - 96)	145 ± 224 (66 - 225)	.4
	Tv	4895 ± 726 (4638 -5153)	36793 ± 5130 (34974 -38612)	6007 ±1445 (5495 -6520)	.000
	%Hv	26.4 ± 11.1 (22.5 – 30.3)	25.5 ± 10.3 (21.8 -29.1)	25.6 ± 10.7 (21.8 -29.4)	.9
	%Bv	72.2 ± 11.9 (68.0-76.4)	73.1± 10.9 (69.3 ±77.0)	72.0 ±11.0 (68.14-75.9)	1.0
	%Fv	1.4 ± 1.4 (0.9 - 1.9)	1.4 ±1.3 (1.0 - 1.8)	2.4 ± 3.6 (1.1 - 3.7)	.9
	Fv/Bv	.022 ± .024 (.013 -.030)	.021 ± .019 (.014 -.028)	.036 ± .051 (.018 -.053)	.9
Ex only	Hv	1155 ± 656 (945 -1364)	1180 ± 654 (971 - 1389)	1324 ± 735 (1089 -1559)	.5
	Bv	3643 ± 650 (3436 -3851)	4028 ± 1357 (3594 -4462)	4317 ± 685 (4098 -4536)	.008
	Fv	89 ± 100 (58 - 121)	100 ± 106 (66 - 134)	123 ± 115 (87 - 160)	.4
	Tv	4888 ± 726 (4656 -5120)	5109 ± 777 (4860 -5357)	5765 ± 872 (5486 -6044)	.000
	%Hv	22.9 ± 11.5 (19.2 -26.6)	22.3 ± 10.8 (18.8 -25.8)	22.1 ± 10.8 (18.6 -25.5)	.9

	%Bv	75.2 ±12.5 (71.2 -79.2)	75.7 ± 12.0 (71.9 -79.7)	75.8 ± 11.9 (72.0 -79.6)	1.0
	%Fv	188.0 ± 216.7 (118.7 - 257.3)	196.3 ±213.3 (128.0 - 264.5)	214.3 ± 202.0 (149.7 - 278.9)	.9
	Fv/Bv	.029 ± .038 (.016 -.041)	.030 ± .036 (.018 -.041)	.032 ±.034 (.021 -.043)	.9
Ex + Ca	Hv	972 ± 753 (753- 1191)	969 ± 738 (738 – 1200)	715 ± 838 (838 – 1337)	.7
	Bv	3469 ± 530 (3284 – 3654)	3689 ± 515 (3509 – 3869)	4104 ± 604 (3893 – 4315)	.000
	Fv	100 ± 138 (51 – 148)	102 ± 139 (53 – 150)	130 ± 183 (66 – 194)	.7
	Tv	4540 ± 629 (4321 – 4760)	4760 ± 689 (4520 – 5000)	5321 ± 805 (5040 – 5602)	.000
	%Hv	20.5 ± 11.5 (16.5 – 24.5)	19.3 ± 11.3 (15.4 – 23.3)	19.5 ± 10.7 (15.8 – 23.2)	.9
	%Bv	77.4 ± 12.8 (72.9 -81.8)	78.6 ± 12.7 (74.2 – 83.0)	78.2 ± 12.2 (74.0 – 82.5)	.9
	%Fv	21.4 ± 29.1 (11.2 -31.6)	20.4 ± 26.9 (11.1 – 29.8)	23.0 ± 29.5 (12.7 – 33.3)	.9
	Fv/Bv	.032 ± .048 (.015 - .049)	.031± .047 (.014 - .047)	.034 ± .050 (.017 - .052)	.9

Table 7. Within groups comparisons of lumbar vertebrae at baseline. Tv (total volume), Hv (haemopoietic volume), Bv (total bone volume), Fv (fat volume) and as percentages (%Hv,%Bv, %Fv) of total volume. Fv/Bv is ratio of mean absolute fat volume to mean absolute bone volume. # and * are significance at .05 level with Robust test equality of means or ANOVA respectively.

Parameter	Group (n)	Mean	SD	CI	p
Tv	0 (42)	1858	185	1800 - 1925	.8
	1 (41)	1827	197	1765 - 1889	
	2 (41)	1857	192	1797 - 1918	
	3 (41)	1865	228	1793 - 1937	
Hv	0 (42)*	95	29	86 - 105	.005
	1 (41)$^{\#}$	90	32	80 – 101	

	2 (41)	99	36	87 - 110	
	3 (41)*#	117	42	104 - 131	
Bv	0 (42)	1529	138	1486 - 1572	1.0
	1 (41)	1515	145	1469 - 1561	
	2 (41)	1522	152	1474 - 1570	
	3 (41)	1532	176	1476 - 1587	
Fv	0 (42)	235	86	208 - 262	.7
	1 (41)	221	84	195 - 248	
	2 (41)	237	100	205 - 268	
	3 (41)	216	90	187 - 244	
%Hv	0 (42)*	5.0	1.6	4.6 – 5.5	.01
	1 (41)#	5.0	1.7	4.4 – 5.5	
	2 (41)	5.3	1.5	4.8 – 5.8	
	3 (41)*#	6.2	2.1	5.6-6.9	
%Bv	0 (42)	82.5	3.7	81.3 - 3.6	.7
	1 (41)	83.1	3.3	82.0 – 84.2	
	2 (41)	82.1	5.2	80.5 – 83.8	
	3 (41)	82.3	3.9	81.1 – 83.6	
%Fv	0 (42)	12.5	3.9	11.3 – 13.8	.5
	1 (41)	11.9	3.9	10.7 – 13.2	
	2 (41)	12.7	5.1	11.1 – 14.3	
	3 (41)	11.4	4.3	10.1 – 12.8	
Fv/Bv	0 (42)	.15	.05	.14 - .17	.6

	1 (41)	.15	.05	.13 - .16	
	2 (41)	.16	.07	.13 - .18	
	3 (41)	.14	.06	.12 - .16	
ΔTv	0 (42)	7*	79	-18 - 31	.05
	1 (41)	22	37	10 - 33	
	2 (41)	32	37	20 -43	
	3 (41)	40*	58	22 -58	
ΔHv	0 (42)	4	9	2 - 7	.04
	1 (41)	2*	10	-1 - 6	
	2 (41)	4	14	-1 - 8	
	3 (41)	9*	13	5 - 13	
ΔBv	0 (42)	.1 *	68	-21 - 21	.02
	1 (41)	15	35	4 - 26	
	2 (41)	23	37	11 - 34	
	3 (41)	33*	49	18 - 49	
ΔFv	0 (42)	3	22	-3 - 10	.2
	1 (41)	4	11	1 - 8	
	2 (41)	5	23	-2 - 13	
	3 (41)	-3	18	-8 - 3	
%ΔTv	0 (42)	.005*	.04	-.009 - .018	.05
	1 (41)	.011	.02	.005 - .018	
	2 (41)	.017	.02	.005 - .018	
	3 (41)	.022*	.028	.013 - .030	

%ΔHv	0 (42)	.20	.43	.06 - .33	.1
	1 (41)	.06	.54	-.11 - .23	
	2 (41)	.10	.77	-.14 - .35	
	3 (41)	.39	.73	.16 - .62	
%ΔBv	0 (42)	-.32	1.2	-.71 - .07	.4
	1 (41)	-.16	.52	-.32 - .001	
	2 (41)	-.13	.95	-.43 - .16	
	3 (41)	.03	.69	-.19 - .25	
%ΔFv	0 (42)	.12	1.11	-.23 - .48	.05
	1 (41)	.11*	.67	-.10 - .32	
	2 (41)	.03	1.28	-.37 - .43	
	3 (41)	-.42*	.83	-.68 - -.16	
ΔFv/Bv	0 (42)	.002	.015	-.002 - .007	.05
	1 (41)	.001*	.009	-.001 - .005	
	2 (41)	.001	.017	-.005 - .006	
	3 (41)	-.005*	.011	-.009 - -.002	

Table 8a. Mid femur volumes at 18 months and the changes as absolute changes and percentage changes. Tv (total volume), Hv (haemopoietic volume), Bv (total bone volume), Fv (fat volume) and as percentages (%Hv, %Bv, %Fv) of total volume. Fv/Bv is ratio of mean absolute fat volume to mean absolute bone volume. Changes in absolute total, haemopoietic, bone, fat and fat to bone volume ratios are denoted as ΔTv, ΔHv, ΔBv, ΔFv and ΔFv/Bv respectively. Percentage changes are denoted by %Δ prefixes. # and * are significance at .05 level with Robust test equality of means or ANOVA respectively.

Parameter	Group (n)	Mean	SD	CI	p
TV	0 (36)	1523	182	1462 - 1585	.3
	1 (38)	1455	150	1406 -1504	
	2 (41)	1509	167	1457 - 1562	
	3 (34)	1527	206	1455 - 1599	
Hv	0 (36)	71	28	62 - 80	.2
	1 (38)	62	22	55 - 70	
	2 (41)	61	17	56 - 66	
	3 (34)	68	30	58 - 78	
Bv	0 (36)	1323	160	1269 - 1377	.3
	1 (38)	1263	124	1222 - 1303	
	2 (41)	1300	144	1254 - 1345	
	3 (34)	1312	152	1259 - 1366	
Fv	0 (36)	129	67	106 - 152	.4
	1 (38)	130	64	109 - 151	
	2 (41)	149	71	127 - 171	
	3 (34)	147	72	122 - 172	
%Hv	0 (36)	4.6	1.5	4.1 - 5.1	.3
	1 (38)	4.2	1.4	3.7 - 4.6	
	2 (41)	4.0	1.1	3.7 - 4.4	
	3 (34)	4.5	1.7	3.9 - 5.1	
%Bv	0 (36)	87.0	4.4	85.6 - 88.5	.7
	1 (38)	86.9	4.1	85.5 - 88.3	

	2 (41)	86.1	4.3	84.8 - 87.5	
	3 (34)	86.2	3.8	84.9 - 87.5	
%Fv	0 (36)	8.3	4.0	7.0 - 9.7	.4
	1 (38)	8.8	4.0	7. 5 - 10.1	
	2 (41)	9.8	4.3	8.4 - 11.1	
	3 (34)	9.4	3.7	8.1 - 10.7	
Fv/Bv	0 (36)	.0100	.0051	.0082 – 0.0116	.5
	1 (38)	.0104	.0054	.0087 – 0.0122	
	2 (41)	.0116	.0057	0098 – 0.0134	
	3 (34)	.0110	.0049	.0093 – 0.0127	
ΔTv	0 (36)	2.50	16.43	-3.06 - 8.06	.8
	1 (38)	-.16	26.04	-8.72 - 8.40	
	2 (41)	-1.49	16.08	-6.56 - 3.59	
	3 (34)	2.82	24.78	-5.82 - 11.47	
ΔHv	0 (36)	3.82	947.78	62.11 - 703.48	.1
	1 (38)	70	568.12	-116.74 - 256.74	
	2 (41)	2.75	578.45	92.34 - 457.51	
	3 (34)	.32	832.05	-258.49 - 322.14	
ΔBv	0 (36)	5.1	15.0	5.2 - 1018.46	.8
	1 (38)	1.3	24.1	-6.58.38 - 925.49	
	2 (41)	3.6	12.9	-.50.51 - 762.71	
	3 (34)	3.0	17.4	-3.08.94 - 907.17	
ΔFv	0 (36)	-6.41	15.19	-11.6 - -1.3	.08

	1 (38)	-2.22	9.95	-5.5 – 1.0	
	2 (41)	-7.80	10.55	-11.1 - -4.5	
	3 (34)	-.5	19.4	-7.2 – 6.3	
%ΔTv	0 (36)	.18	1.07	- .19 - .54	.8
	1 (38)	-.06	1.90	- .69 – .56	
	2 (41)	-.09	1.06	- .42 - .24	
	3 (34)	.18	1.56	- .37 - .72	
%ΔHv	0 (36)	.24	.66	.02 – .47	
	1 (38)	.04	.38	-.08 - .17	.1
	2 (41)	18	.37	.07 – .30	
	3 (34)	.37	.52	- .18 - .19	
%ΔBv	0 (36)	.16	.46	.39 – .32	
	1 (38)	.11	.48	-.05 – .27	.2
	2 (41)	.32	.64	.12 – .52	
	3 (34)	.04	.70	-.20 – .29	
%ΔFv	0 (36)	-.40	.90	-.71 - -.10	.06
	1 (38)	-.15	.64	-.36 - .06	
	2 (41)	-.50	63	-.70 - -.30	
	3 (34)	-.05	. 1.09	-.43 - .33	
ΔFv/Bv	0 (36)	-.0005	.0012	-.00090 - -.0001	.08
	1 (38)	-.0002	.00079	-.00046 - .000059	
	2 (41)	-.0006	.00081	-.0009 - - .00036	
	3 (34)	-.00005	.0014	-.00054 – .00043	

Table 8b. Mid tibia volumes at 18 months and the changes as absolute changes and percentage changes. Tv (total volume), Hv (haemopoietic volume), Bv (total bone volume), Fv (fat volume) and as percentages (%Hv, %Bv, %Fv) of total volume. Fv/Bv is ratio of mean absolute fat volume to mean absolute bone volume. Changes in absolute total, haemopoietic, bone, fat and fat to bone volume ratios are denoted as ΔTv, ΔHv, ΔBv, ΔFv and ΔFv/Bv respectively. Percentage changes are denoted by %Δ prefixes. # and * are significance at .05 level with Robust test equality of means or ANOVA respectively.

Parameter	Group (n)	Mean	SD	CI	p
TV	0 (36)	4765	742	4514 - 5017	.1
	1 (33)	4921	718	4667 - 5176	
	2 (40)	4853	772	4606 - 5100	
	3 (34)	4522	631	4301 - 4742	
Hv	0 (36)	1065	611	858 - 1272	.005
	1 (33)	1286	666	1050 - 1522	
	2 (40)	1096	620	898 - 1294	
	3 (34)	880	627	661 - 1098	
Bv	0 (36)	3622	693	3388 - 3857	.4
	1 (33)	3548	528	3361 - 3735	
	2 (40)	3664	661	3453 - 3875	
	3 (34)	3571	572	3372 - 3771	
Fv	0 (36)	79	62	58 - 100	.7
	1 (33)	87	99	52 - 122	
	2 (40)	93	119	55 - 131	
	3 (34)	71	93	38 - 103	
%Hv	0 (36)	21.8	11.3	18.0 - 25.6	.01
	1 (33)	25.2	11.1	21.2 - 29.1	
	2 (40)	21.9	10.9	18.5 - 25.4	
	3 (34)	18.7	11.4	14.8 - 22.7	
%Bv	0 (36)	76.5	12.2	72.4 - 80.7	.7
	1 (33)	73.1	12.2	68.8 - 77.4	
	2 (40)	76.2	12.3	72.2 - 80.1	
	3 (34)	79.9	12.7	75.5 - 84.3	

%Fv	0 (36)	1.67	1.4	1.2 - 2.1	.5
	1 (33)	1.70	1.91	1.0 - 2.4	
	2 (40)	1.85	2.48	1.1 - 2.6	
	3 (34)	1.41	1.86	.8 - 2.1	
Fv/Bv	0 (36)	.0244	.0221	.0170 - .0319	.6
	1 (33)	.0266	.0307	.0157 - .0375	
	2 (40)	.0302	.0453	.0158 - .0447	
	3 (34)	.0228	.0342	.0109 - .0348	
ΔTv	0 (36)	-29	176	-89 - 30	.05
	1 (33)	26	100	-9 - 61	
	2 (40)	-35	214	-103 - 34	
	3 (34)	-19	226	-98 - 60	
ΔHv	0 (36)	-30	176	-89 – 30	.04
	1 (33)	-48	173	-110 - 13	
	2 (40)	-59	166	-112 - -6	
	3 (34)	-92	201	-163 - -22	
ΔBv	0 (36)	45	196	-21 – 112	.02
	1 (33)	58	154	3 – 112	
	2 (40)	21	274	-67 – 108	
	3 (34)	102	188	37 - 168	
ΔFv	0 (36)	-89	50	-26 - 8	.2
	1 (33)	17	41	22 - 31	
	2 (40)	4	42	-10 - 17	
	3 (34)	-29	74	-55 - -3	
%ΔTv	0 (36)	-.03	.163	-.08 - .0282	.05

	1 (33)	.006	.02	-.0009 - .0129	
	2 (40)	-.008	.046	-.0228 - .0069	
	3 (34)	-.003	.051	-.0207 - 0.0147	
%ΔHv	0 (36)	-3.42	16.16	-8.89 - 2.05	.1
	1 (33)	-1.13	3.04	-2.21 - -.06	
	2 (40)	-1.02	3.33	-2.09 - .04	
	3 (34)	-1.86	3.79	-3.18 - -.54	
%ΔBv	0 (36)	3.61	16.19	-1.86 - 9.09	.4
	1 (33)	.80	3.50	-.44 - 2.04	
	2 (40)	.96	3.75	-.24 - 2.15	
	3 (34)	2.49	3.65	1.22 - 3.76	
%ΔFv	0 (36)	-.20	1.04	-.55 - .16	.05
	1 (33)	.33	.79	.05 - .61	
	2 (40)	.06	.89	-.22 - .35	
	3 (34)	-.63	1.58	-1.19 - .08	
ΔFv/Bv	0 (36)	-0.0029	.0148	-0.0079 - 0.0021	.05
	1 (33)	0.0049	.0137	.0001 - 0.0098	
	2 (40)	0.0016	.0153	-0.0033 - 0.0065	
	3 (34)	-0.0093	.0254	-0.0182 - -0.0005	

Table 8c. 1st Lumbar vertebrae (L1) volumes at 18 months and the changes as absolute changes and percentage changes. Tv (total volume), Hv (haemopoietic volume), Bv (total bone volume), Fv (fat volume) and as percentages (%Hv, %Bv, %Fv) of total volume. Fv/Bv is ratio of mean absolute fat volume to mean absolute bone volume. Changes in absolute total, haemopoietic, bone, fat and fat to bone volume ratios are denoted as ΔTv, ΔHv, ΔBv, ΔFv and ΔFv/Bv respectively. Percentage changes are denoted by %Δ prefixes. # and * are significance at .05 level with Robust test equality of means or ANOVA respectively.

Parameter	Group (n)	Mean	SD	CI		p
TV	0 (36)	479594.19	109189.49	442649.79	516538.60	.1
	1 (33)	510801.70	72433.07	485118.04	536485.35	
	2 (40)	511639.93	78771.49	486447.58	536832.27	
	3 (34)	471979.56	71041.88	447191.87	496767.25	
Hv	0 (36)	106909.94	58770.71	87024.80	126795.09	.06
	1 (33)	129214.55	67261.29	105364.73	153064.36	
	2 (40)	110154.15	63520.72	89839.24	130469.06	
	3 (34)	86199.09	65669.79	63285.81	109112.36	
Bv	0 (36)	364722.72	90489.08	334105.62	395339.82	.4
	1 (33)	372916.67	53955.21	353784.98	392048.35	
	2 (40)	391048.38	64626.94	370379.67	411717.08	
	3 (34)	375716.18	57567.13	355630.05	395802.30	
Fv	0 (36)	7961.56	6674.72	5703.15	10219.96	.8
	1 (33)	8670.52	9467.51	5313.48	12027.55	
	2 (40)	10437.33	13095.85	6249.07	14625.58	
	3 (34)	10064.29	15347.79	4709.20	15419.39	
%Hv	0 (36)	221952.72	101870.00	187484.87	256420.57	.07
	1 (33)	244723.70	109469.12	205907.63	283539.76	
	2 (40)	207641.18	105003.01	174059.58	241222.77	
	3 (34)	172860.15	113683.73	133194.02	212526.28	
%Bv	0 (36)	761013.56	110200.18	723727.18	798299.93	.1
	1 (33)	738680.91	118017.33	696833.78	780528.04	
	2 (40)	772415.50	119948.85	734054.00	810777.00	
	3 (34)	806609.29	129283.20	761500.25	851718.34	

%Fv	0 (36)	17033.72	13181.99	12573.58	21493.87	.8
	1 (33)	16595.39	17316.55	10455.21	22735.58	
	2 (40)	19943.20	24553.78	12090.52	27795.88	
	3 (34)	20530.47	30920.96	9741.64	31319.30	
Fv/Bv	0 (36)	246.61	214.35	174.08	319.14	.8
	1 (33)	250.36	275.54	152.66	348.07	
	2 (40)	302.75	422.49	167.63	437.87	
	3 (34)	306.74	503.46	131.07	482.40	
ΔTv	0 (36)	-12105.64	76038.08	-37833.22	13621.95	.5
	1 (33)	2124.36	15919.18	-3520.33	7769.06	
	2 (40)	749.95	15506.99	-4209.43	5709.33	
	3 (34)	-4026.26	31820.74	-15129.05	7076.52	
ΔHv	0 (36)	15.94	231.94	-62.53	94.42	.06
	1 (33)	-43.00	164.85	-101.46	15.46	
	2 (40)	-78.65	162.52	-130.63	-26.67	
	3 (34)	-107.41	229.18	-187.38	-27.45	
ΔBv	0 (36)	-141.50	794.40	-410.29	127.29	.01
	1 (33)	49.91	207.75	-23.76	123.57	
	2 (40)	81.33	177.74	24.48	138.17	
	3 (34)	68.24	293.07	-34.02	170.49	
ΔFv	0 (36)	4.42	26.68	-4.61	13.45	.8
	1 (33)	14.33	40.54	-.04	28.71	
	2 (40)	4.73	50.28	-11.36	20.81	
	3 (34)	-1.15	100.32	-36.15	33.86	
%ΔTv	0 (36)	-255.19	1662.95	-817.86	307.47	.5

	1 (33)	50.24	322.34	-64.06	164.54	
	2 (40)	17.28	295.44	-77.21	111.76	
	3 (34)	-68.18	652.69	-295.91	159.56	
%ΔHv	0 (36)	13752.28	76587.11	-12161.07	39665.63	.1
	1 (33)	-9897.67	30962.91	-20876.64	1081.31	
	2 (40)	-15257.35	29100.02	-24563.99	-5950.71	
	3 (34)	-20520.06	40605.58	-34688.02	-6352.10	
%ΔBv	0 (36)	-15625.31	82561.23	-43560.01	12309.40	.02
	1 (33)	7269.18	33662.28	-4666.95	19205.31	
	2 (40)	14939.90	33912.10	4094.28	25785.52	
	3 (34)	20437.09	43966.92	5096.30	35777.87	
%ΔFv	0 (36)	1873.06	7394.99	-629.05	4375.16	.8
	1 (33)	2628.61	7021.53	138.88	5118.34	
	2 (40)	317.58	9576.90	-2745.27	3380.42	
	3 (34)	83.09	20898.93	-7208.89	7375.07	
ΔFv/Bv	0 (36)	25.67	118.81	-14.53	65.87	.8
	1 (33)	41.94	120.48	-.78	84.66	
	2 (40)	7.53	151.68	-40.99	56.04	
	3 (34)	1.44	306.77	-105.60	108.48	

Table 8d. 2nd Lumbar vertebrae (L2) volumes at 18 months and the changes as absolute changes and percentage changes. Tv (total volume), Hv (haemopoietic volume), Bv (total bone volume), Fv (fat volume) and as percentages (%Hv, %Bv, %Fv) of total volume. Fv/Bv is ratio of mean absolute fat volume to mean absolute bone volume. Changes in absolute total, haemopoietic, bone, fat and fat to bone volume ratios are denoted as ΔTv, ΔHv, ΔBv, ΔFv and ΔFv/Bv respectively. Percentage changes are denoted by %Δ prefixes. # and * are significance at .05 level with Robust test equality of means or ANOVA respectively.

Parameter	Group (n)	Mean	SD	CI	p
TV	0 (36)	5663	898	53589 - 5966	.03
	1 (33)	5846	803	5561 - 6131	
	2 (40)	5863	892	5578 - 6149	
	3 (34)	5329	748	5068 - 5590	
Hv	0 (36)	1258	697	1023 - 1494	.05
	1 (33)	1481	751	1215 - 1747	
	2 (40)	1297	711	1069 - 1524	
	3 (34)	996	700	752 - 1240	
Bv	0 (36)	4279	664	4054 - 4504	.5
	1 (33)	4240	593	4030 - 4450	
	2 (40)	4432	686	4213 - 4652	
	3 (34)	4223	628	4004 - 4442	
Fv	0 (36)	125	102	91 - 160	.9
	1 (33)	125	131	789 - 172	
	2 (40)	135	138	91 - 179	
	3 (34)	110	152	57 - 163	
%Hv	0 (36)	21	10	18 - 25	.07
	1 (33)	25	11	21 - 28	
	2 (40)	21	10	18 - 25	
	3 (34)	17.82	11	14 - 22	
%Bv	0 (36)	76	11	73 - 80	.1
	1 (33)	73	12	69 - 77	
	2 (40)	76	12	73 - 80	
	3 (34)	80	12	76 - 84	

%Fv	0 (36)	2.1	1.6	1.6 - 2.7	.9
	1 (33)	2.1	2.0	1.4 - 2.9	
	2 (40)	2.2	2.2	1.5 - 2.9	
	3 (34)	1.9	2.7	.9 - 2.8	
Fv/Bv	0 (36)	.0311	.0258	.0223 - .0398	.9
	1 (33)	.0311	.0313	.0200 - .0422	
	2 (40)	.0333	.0385	.0210 - .0456	
	3 (34)	.0296	.0457	.0136 - .0455	
ΔTv	0 (36)	-63	259	-151 - 24	.5
	1 (33)	-161	1079	-544 - 221	
	2 (40)	98	249	19 - 178	
	3 (34)	8	344	-112 - 128	
ΔHv	0 (36)	-28	292	-127 - 71	.5
	1 (33)	-67	151	-121 - -13	
	2 (40)	-28	172	-83 - 27	
	3 (34)	-91	231	-172 - -10	
ΔBv	0 (36)	-39	381	-168 - 90	.4
	1 (33)	-74	1103	-465 - 317	
	2 (40)	115	296	20 - 209	
	3 (34)	119	296	15 - 222	
ΔFv	0 (36)	4	43	-11 - 18	.5
	1 (33)	-20	215	-96 - 56	
	2 (40)	11	52	-5 - 28	
	3 (34)	-20	59	-40 - .7	
%ΔTv	0 (36)	-.63	2.6	-1.5 - .2	.5

	1 (33)	-1.6	10.8	-5.4 - 2.2	
	2 (40)	1.0	2.5	.2 - 1.8	
	3 (34)	.1	3.4	-1.1 - 1.3	
%ΔHv	0 (36)	-.2	4.8	-1.8 - 1.5	.4
	1 (33)	-1.0	3.4	-2.3 - .2	
	2 (40)	-.8	2.9	-1.7 - .1	
	3 (34)	-1.7	3.8	-3.0 - -.4	
%ΔBv	0 (36)	.07	5.2	-1.7 - 1.8	.3
	1 (33)	1.4	4.5	-.3 - 3.0	
	2 (40)	.7	3.3	-.4 - 1.8	
	3 (34)	2.0	3.8	.7 - 3.3	
%ΔFv	0 (36)	.1	.7	-.1 - .3	.6
	1 (33)	-.3	3.4	-1.5 - .9	
	2 (40)	.1	.9	-.2 - .4	
	3 (34)	-.3	1.0	-.7 - .02	
ΔFv/Bv	0 (36)	.0011	.0113	-.0028 - .00490	.6
	1 (33)	-.0044	.0481	-.0214 - 0.0127	
	2 (40)	.0015	.0139	-.0030 - .0059	
	3 (34)	-.0048	.0154	-.0101 - .0006	

Table 8e. 3rd Lumbar vertebrae (L3) volumes at 18 months and the changes as absolute changes and percentage changes. Tv (total volume), Hv (haemopoietic volume), Bv (total bone volume), Fv (fat volume) and as percentages (%Hv, %Bv, %Fv) of total volume. Fv/Bv is ratio of mean absolute fat volume to mean absolute bone volume. Changes in absolute total, haemopoietic, bone, fat and fat to bone volume ratios are denoted as ΔTv, ΔHv, ΔBv, ΔFv and ΔFv/Bv respectively. Percentage changes are denoted by %Δ prefixes. # and * are significance at .05 level with Robust test equality of means or ANOVA respectively.